Biology and Physics Science
ISBN: 978-0-9886890-7-7

Human Biophysics

Volobuev Andrey Nikolaevich

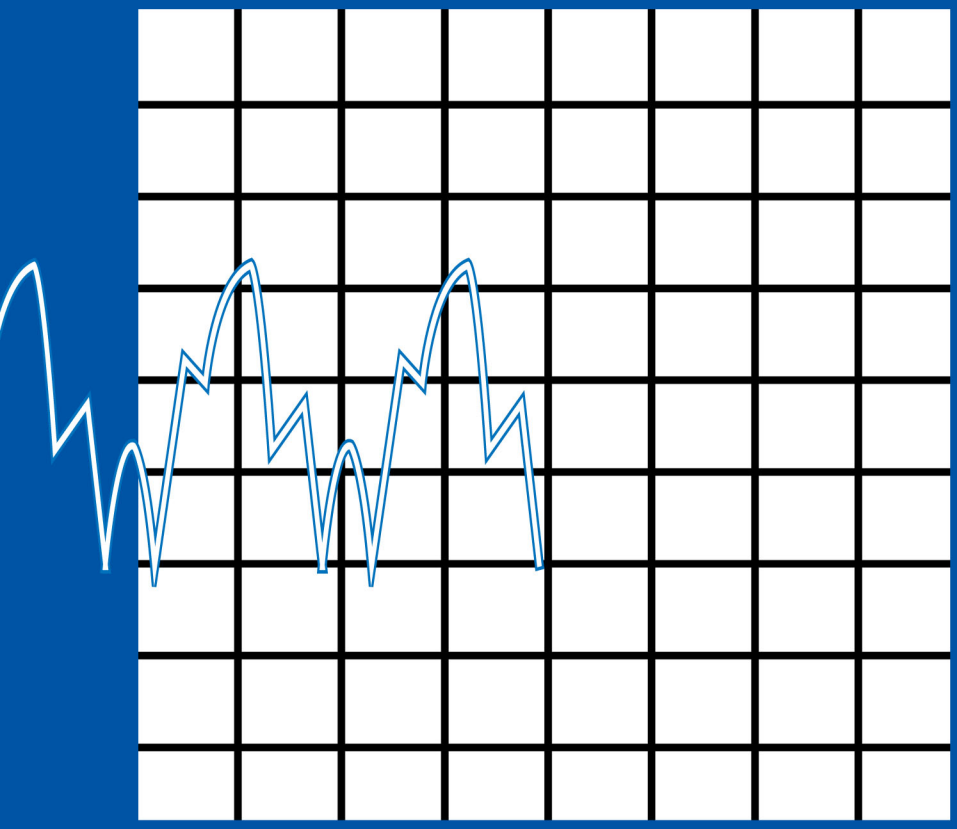

Edited by: Dr. S. M. H. Jahan & M. M. Rashid

Academic and Scientific Publishing
www.acascipub.com

Biology and Physics Science
ISBN: 978-0-9886890-7-7
Available online at www.acascipub.com
Date: 01.02.2014
Pages: 01-204

Human Biophysics

Volobuev Andrey Nikolaevich

E-mail: volobuev47@yandex.ru

Edited by: Dr. S. M. Hemayet Jahan and M. M. Rashid

Academic and Scientific Publishing

www.acascipub.com

Summary

In this book, stated a series of well-known biophysical theories considering a few fundamental questions related with biophysical problems in human body. Here expressed with illustration of different potential biophysical theories and its functioning, such as, occurrence of the resting potential on a cell membrane, the Hodgkin – Huxley theory on the action potential propagation, the theory of active muscular contraction as well. Alongside with it development of the author are submitted also: inductance-capacitor model of the excitable tissue on the basis of which the nonlinear equation for action potential is written down, also quantum character of ions carry through a membrane, cardiac electrogenesis is investigated. New aspects of the high-frequency electromagnetic field influence on tissue of the organism is shown, laws of the impulse current influence on tissue, etc. are investigated. Some new approaches to functioning acoustical and visual analyzers are considered. On the basis of the separate analysis of family trees and a population with use of the new form of the Hardy - Weinberg law the series of mathematical genetics problems is solved.

This book could be useful to the doctors, scientific researchers in the medicine area, to students of medical faculties and everyone who are interested in the human biophysics.

Authors Biography

Volobuev Andrey Nikolaevich 1947 of birth. Has graduated from the Moscow (Russia) Higer Technical School name N. E. Bauman in 1971 on specialty "Heat physics", postgraduate study at MHTS name N. E. Bauman in 1976. Cand. Tech. Sci. since 1978. Dr. Tech. Sci. since 1994, maintain dissertation in Latvian Scientific Research Institute of Traumatology and Orthopaedics on specialty “Biomechanics”. On chair of Medical and Biological Physics of the Samara State Medical University works since 1981. Since 1994 was a post of the professor of chair. Since 1996 is head of chair of Medical and Biological Physics. Is the author more than 350 scientific publications, including 9 monographies, 16 patents. Repeatedly acted at various medical scientific conferences. Is the member of European Physical Society No 019115. Area of scientific interests: biophysics, neuroprocesses, hemodynamics, interaction of electromagnetic radiation with substance, hydrodynamics.

Introduction

Chapter 1. Resting Potential

Chapter 2. Action Potential

Chapter 3. Mechanics of muscular contraction

Chapter 4. Surface biopotentials. Electrocardiography

Chapter 5. Influence on organism by the high-frequency electromagnetic field

Chapter 6. Influence by the low-frequency impulse electric current on organism

Chapter 7. Acoustic analyzer

Chapter 8. The visual analyzer

Chapter 9. Mathematical genetics

Introduction

Biophysical function in human body and its related questions are representing big interest in medicine, pharmacology and biology. They allow understand the laws of functioning of the human body and a society as a whole. Now possession of biophysical methods are used in patient research which necessary criterion of the doctor qualification.

The biophysical approach to research of the human always found a plenty of followers. Feature of the given approach is application of exact methods to object which up to the end is not investigated by us and cannot be investigated essentially since this object is not created by the man. If we find out, for example, the reasons of malfunctions in the technical device we usually know how this device functions, there is design documentation. For debugging in the device the malfunction is necessary to find out. For this purpose we compare units of the device with the design documentation and we find where there is a discrepancy. Further we debug in particular we replace faulty unit and the device again starts to function normally.

At treatment of the human the situation is completely other. The human is not product created by the man and the design documentation to him is not present. Certainly the long studying of the human body has led to that basically anatomy and physiology of the human now are investigated enough. However it is basically. Therefore, applying at diseases various medical products, carrying out surgical intervention, applying various physiotherapeutic procedures we can be never sure that our actions will be successful, and reaction of the patient will be completely predicted. Though the big experience available at mankind allows to treat many illnesses successfully.

The biophysics is a synthesis of biology and physics. However methodologies of these sciences are rather various. Classical biology it is basically descriptive science. Its main tools are supervision, experiment (including statistical processing) and classification of the received knowledge.

Absolutely other situation is in physics. Still Greek scientist Aristotle (384 - 322 BC) in the book "Physics" wrote: "We then are sure in knowledge of any thing when we find out its first reasons the first beginnings and we decompose it down to elements". Physics studying any rather complex phenomenon decompose it to separate components allocate the main simple components and apply physical laws to these components of the general phenomenon.

With biological organism to do the given procedure there is difficultly. To find out simple components of biological structure rather difficultly but it is even more difficult to be convinced that it is a simple component. For example, before discovery of DNA molecule as most complicated genetic structure it was represented that it is simple the certain acid which is taking place in chromosomes. Therefore the basic methodical reception of physics the division of the phenomenon into simple components in biology operates badly.

There is other feature of physics: wide application of the functional mathematical analysis, first of all the various differential equations. However here again in biology the certain complexity is observed. It is connected by that the phenomena in biology usually have essentially nonlinear character. Therefore, even if it is possible to write down any differential equation describing the biological phenomenon to solve analytically this equation frequently it is not obviously possible. It complicates the analysis of the biological phenomenon.

However, despite of all these difficulties in biophysics and in particular human biophysics there are many very important and valuable achievements. One of vivid examples this creation by the Dutch scientist W. Einthoven of electrocardiography bases for what in 1924 he has received the Nobel Prize.

Biophysics it is developing science. Though each step in it is given by the big work and the expenses, undoubtedly many important problems facing to mankind can be solved apparently basically within the framework of this science, for example, a problem of oncology.

Biophysics is science too big that it was possible to state it completely in one-volume edition. Submitted on consideration of the reader the book is not the regular textbook on biophysics. The given monograph in many respects reflects interests and preferences of the author. But too it is far from being completely. The author many power and time has spent for research of vascular system and such disease as the primary arterial hypertension. There is book Volobuev A.N., Koshev V.I., Petrov E.S. Biophysical Principles of Hemodynamics. New York: Nova Science Publishers, Inc. 2010 which is devoted to these questions.

However the author took part in many researches on biophysics which have found the reflection in the given monograph. For the reader will present interest electrodynamical questions of functioning of the human organism. Thus in the book are stated as the standard theories, so developed by the author, for example the inductance-capacitor theory of the excitable biotissue. All positions of this theory for a long time are published in known journals. This theory is well-known to biophysicists. But the author has counted necessary a regular statement of the given theory in monograph the comparison of the inductance-capacitor theory of the excitable biotissue with standard. Questions of influence of electromagnetic field on the organism, electrocardiography, electrostimulation and many other touched in the book will be interesting to the reader.

For specialists will present interest the sections devoted to analyzers: ear and eye.

Important and interesting the chapter “Mathematical genetics” is represented. It is completely special section of biophysics. The mathematical genetics enables to understand those or other phenomena in the human organism, to explain and predict development of human community both from the point of view of people health, and from the point of view of social processes. It allows understand the purposes and problems of human community for improvement of the life.

In the book the author tried to depart only medical problems connected to treatment of the man. Obviously, in the book “Human Biophysics” it is hardly completely feasible. The more the biophysical knowledge of the human organism, first of all, is necessary for struggle against various diseases. However, in spite of the fact that the author more than 30 years works at medical university he is convinced that biophysical research of the human organism and his treatment for those or other diseases these are different though and the interconnected problems. But to leave completely from pathological processes in the organism in the monograph it was not possible. Apparently, it is impossible. Any disease can be examined as some experiment which the nature carries out above the organism of the man. The problem of biophysics except the finding of treatment methods is also necessity to understand that this experiment gives in the knowledge of the organism functioning.

The author hopes that the book will be useful to biophysicists, doctors, students of medical faculties.

Chapter 1. Resting Potential

1.1. Membranes of cells

In 30th years of XIX century, the German botanist Matthias Jacob Schleiden (1804-1881) and biologist Theodor Schvann (1810-1882) have established a cellular structure of all plants and animals.

Inside of a cell in gelatinous mass of cytoplasm are:

- the nucleus, where with the help of DNA (deoxyribonucleic acid) molecules contain the information on a structure, properties of a cell and all organism as a whole is written down,
- mitochondrias - original energy stations in which there is a processing of the energy and formed in energy ATP (adenosine triphosphate) at "combustion" of food,
- Golgi apparatus - with which help is carried out sorting, modifies and transportation of proteins,
- Endoplasmic reticulum are using for transporting intercellular substances and other organelles in cell body.

For carrying out of the functions the cell as the whole, it is separated from an environment by a plasmatic (cellular) membrane.

1.1.1. Membrane functions

1. The membranes create border between a cell and environment, between organelles of a cell and other cytoplasm. Membranes share a cell on separate compartments.
2. Through membranes there is a passive transport of substances. Membranes provide active transport of substances in a direction opposite to a gradient of electrochemical potential, see paragraph 1.2.
3. Into mitochondrial membranes of the basic bioenergy processes are located.
4. On membranes there is a generation of biopotentials. Propagation of a nervous impulse it is membranes process.
5. The reception occurs with participation of membranes: mechanical, acoustic, olfactory, flavouring, visual, etc.

1.1.2. Membranes structure

Biological membranes will consist of phospholipids molecules, proteins, water and inorganic components [1]. In membranes there are also other versions lipid molecules: sphingolipids, glycolipids, and also cholesterol.

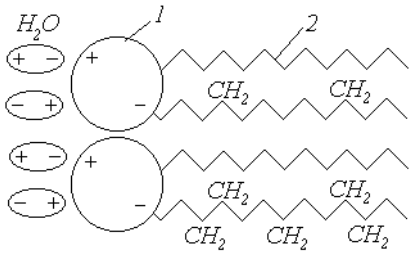

Fig. 1.1.

Basis (matrix) of a membrane there are phospholipids molecules with molecular mass approximately 740, fig. 1.1. These molecules have the lengthened form. The head of a molecule 1 having phosphatic group is polar, therefore it hydrophilic. Thereof the head of phospholipids molecules well contacts with dipole molecule of water (H_2O). Two carbohydrate chains are attached to a head of phospholipids molecule. This so-called the tail of a molecule possesses properties of fats and, hence, hydrophobic. Therefore phospholipids molecule has amphipathic character.

In a water solution there are phospholipids molecule spontaneously arrange (self-assembly), forming a double layer, fig. 1.2. The hydrophilic head settle down on the sides of a double layer directed to water, and hydrophobic tails are directed to the middle of a membrane (to each other) and displace there from molecules of water. Such structure has smaller energy, than a chaotic position of molecules.

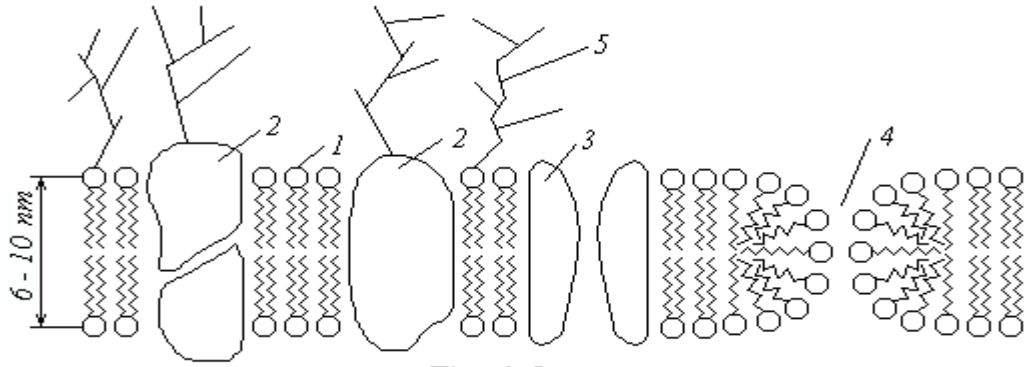

Fig. 1.2.

Thickness of a membrane is 6-10 *nm*.

In phospholipids double layer 1 are integrated membrane proteins 2 and 3, playing a various role: transport channels 3, various ATPases, receptors, proteins providing synthesis ATP, transport of protons, intercellular interaction, etc. Molecular mass of proteins usually some hundred thousand *u.* At near of the peripheral proteins membrane (in figure are not shown), constrained with a membrane by the van der Waals forces or ionic interaction is concentrate.

Outside the membrane is covered with the branched layer of the polysaccharides 5 by thickness 10-20 *nm* - so-called glycocalyx. The polysaccharides covalent bonded with membrane glycoproteins and glycolipids.

Membrane is the semipermeable structure, i.e. it is permeable for one particles and not permeable for others particles.

1.1.3. Membrane dynamics

On the structure the biomembrane is semiotic liquid crystal, however, it is not stiffened film. It is similar to «the storming sea» on which surface rush, rotate and collide proteins "ships" [2]. Such thermal movement of molecules along a membrane refers as lateral diffusion. Average speed of the phospholipid molecules along membrane surface is $V \approx 5\,\frac{\mu m}{s}$. Phospholipid molecule rotates with the big speed about the axis. It is kind of thermal movement. The period of rotation is $T \approx 3 \cdot 10^{-9}\ s$. This rotation stabilizes a membrane due to gyroscopic effect which consists in preservation in space of an axis direction of a rotating body.

The temperature of phase transition of the membrane bilayer from a liquid state to the solid state approximately corresponds to the temperature of the man body, therefore on some sites the membrane is in a solid state that gives to it some rigidity. Lateral diffusion and rotation of the phospholipid molecules is only in the field of a liquid phase of a membrane.

Transition of phospholipid molecules on the one side membranes on another practically does not happen at artificial bilayer lipid membranes since change of an axis rotation direction of phospholipid needs rather big energy, but it transition is significant in natural biomembranes. This process for phospholipids refers as "flip-flop". In the erythrocytes approximately half of all lipid molecules overturned with transition in other layer for 20-30 *mines*. Turn of phospholipids with transition from one layer in another occurs in the area of a membrane where the solid phase is replaced on liquid phase. In these areas speed of rotation of phospholipid molecule is not yet great. Therefore the gyroscopic effect, aspiring to keep a direction of an axis of a molecule rotation, it is shown insignificantly. It allows a molecule to turn over.

At proteins this process is connected to antiport. For example, ADP/ATP translocase (ADP/ATP carrier), turning in inner mitochondrial membrane on 180^0, transfers ATP from inner mitochondrial space where ATP is synthesized, outside, and ADP on the contrary inside of mitochondria. The toxic vegetative glycoside - atractyloside (ATR) inhibit action of ADP/ATP carrier.

1.1.4. Membrane pathology

Pathologies of membranes are very various [77]. We shall consider one of them.

Fig. 1.3.

The phospholipid molecule of a membrane has two hydrocarbonic tails. However, for example, under action of enzyme phospholipases A2 which is present at poisons of bees and some snakes, one tail can torn away off, fig. 1.3. The molecule from cylindrical becomes conic. Such molecules refer to lysolecithins.

In structure of a membrane these molecules form porous, as against channels, have no selective permeability. For example, on fig. 1.2 it is shown porous 4. At occurrence of porous the membrane loses barrier properties. It results in increase of membrane permeability for ions of sodium and some other ions or to full destruction of cells. For example, at stings of bees and some snakes, due to formation lysolecithins, it is observed haemolysis of erythrocytes.

Permeability for all ions at formation porous in a membrane become equal. Resting potential, see 1.5.4, it is reduced. The mitochondria cannot synthesize ATP, nervous cells cannot transfer a nervous impulse. Similar processes occur at virus and bacterial infections, influence ionizing radiations, etc.

1.2. Electrochemical potential on cellular membrane

The energy which enters into an organism together with food goes basically on heart formation, i.e. maintenance of a body temperature at a constant level. But thermal energy at constant temperature (this situation is observed in an organism) according to 2-nd law of thermodynamics cannot be used for mechanical work.

The membrane is the semipermeable border of a cell. As particles (ions, molecules) can be transferred from the one side membranes to another the cell is open thermodynamic system. At the transition of particles from the one side membranes on another the Gibbs free energy of system *G* changes.

Gibbs free energy it is a measure of work, except for mechanical work which can be accomplished by system in isobaric-isothermal process. Such conditions are usually take place in organism.

The organism is physical and chemical system since in a basis of its functioning physical and chemical processes lay.

In physic-chemical systems with the semipermeable membranes the change of Gibbs free energy ΔG at carry of unit of substance ($1\,kg,\quad 1\,mol$, 1 particle) through a membrane it is convenient to describe with the help of change of electrochemical potential $\Delta\bar{\mu}$ on both sides of a membrane:

$$\Delta G = m\Delta\bar{\mu}, \qquad (1.1)$$

where *m* is the mass of transferable substance through a membrane.

As well as for any potential, owing to uncertainty of a reading level, for electrochemical potential change matters only.

In the organism there are basically the processes having isobaric-isothermal character. Under these conditions the part of energy of food through set of intermediate reactions is reserved as macroerg's bonds of ATP (adenosine triphosphate) molecules. It also is Gibbs free energy.

The Gibbs free energy ΔG of ATP molecules is used by an organism, for example, for mechanical work by means of muscle fibres reduction, see chapter 3, carry of substances through semipermeable membrane of cells against electrochemical potential, maintenance of gradients of concentration of particles and potential on membranes of cells due to active transport of substances and for other organism needs. Thus there is hydrolysis ATP according to reaction:

$$ATP + H_2O \rightarrow ADP + P + \Delta G, \qquad (1.2)$$

where ADP is the adenosine diphosphate, *P* - inorganic phosphate (phosphoric acid H_3PO_4), $\Delta G = -30\ \frac{kJ}{mol}$ ATP. The sign a minus specifies that accomplishment of positive work results in reduction of Gibbs free energy of the system containing ATP (organism).

Let's consider the carry of 1 *mol* of substances ($m = 1\,mol$) through semipermeable membrane, fig. 1.4. Let on both sides of a membrane due to the carry there is a difference of concentration of this substance C_1 and C_2, a difference of electric potentials φ_1 and φ_2, a difference of chemical potentials μ_1 and μ_2.

Change of the Gibbs free at change of the mass of system on unit (usually on one mol) refers to as chemical potential:

$$\mu = \left(\frac{\partial G}{\partial m}\right)_{P,T}. \qquad (1.3)$$

Indexes in the bottom of brackets specify a constancy of pressure and temperatures. Change of the mass of system can be connected as with chemical processes in system, for example, reduction of quantity of any substance at its dissociation, and to the processes which are not carrying of chemical character, for example, with evaporation.

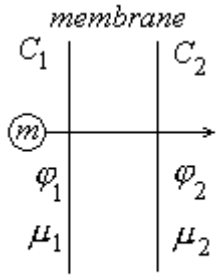

Fig. 1.4.

At transfer 1 *mol* of substances through semipermeable membrane, change of electrochemical potential $\Delta\overline{\mu}$ takes place due to doing of a work various kind: chemical, osmotic, electric.

Let's consider process of a transfer through a cellular membrane of one *mol* ions. We shall find for this case carried out works.

1. Chemical work, is carried out owing to change of substance character (synthesis, decomposition, oxidation, hydration, etc.) at transition from a condition 1 with chemical potential μ_1 on one side of a membrane in a condition 2 with chemical potential μ_2 on other side of a membrane is equal:

$$\Delta A_{chem} = \mu_2 - \mu_1. \qquad (1.4)$$

2. Osmotic work, is carried out at increase in concentration of transferable substance from C_1 up to C_2. It can be found from the following reasons. At transfer of substance through semipermeable membrane there is a heterogeneous system. Concentration of particles in the heterogeneous system containing 1 *mol* of particles, submit to Boltzmann distribution $C = C_0 e^{-\frac{\Delta W_\mu}{RT}}$, where ΔW_μ is the potential energy of one *mol* particles with concentration *C* in some field, C_0 - concentration of particles at absence of a field, $R = 8.31\ \frac{J}{mol \cdot K}$ - a universal gas constant, *T* - absolute temperature of system. Using Boltzmann distribution for concentration C_1 and C_2 and excluding C_0, we shall find osmotic work on creation of heterogeneous system with the given concentrations:

$$\Delta A_o = RT \ln \frac{C_2}{C_1}, \qquad (1.5)$$

where $C_2 > C_1$.

3. Electric work, is carried out at transfer through a membrane of the charged particles (ions) and occurrence on a membrane of a potential difference $\varphi_1 - \varphi_2$ (or increments of potential $\varphi_2 - \varphi_1$). This work we shall find from determination of a potential difference:

$$\Delta A_e = zF(\varphi_2 - \varphi_1), \qquad (1.6)$$

where *z* is the valence of ions, $F = 96500\ \frac{C}{mol}$ - Faraday constant numerically equal to a charge of one *mol* of one-valent ions, zF - a charge of one *mol* transferable ions through a membrane.

Hence, change of electrochemical potential at transfer 1 *mol* substances through a cellular membrane equally:

$$\Delta\overline{\mu} = \Delta A_{chem} + \Delta A_o + \Delta A_e = (\mu_2 - \mu_1) + RT \ln \frac{C_2}{C_1} + zF(\varphi_2 - \varphi_1). \quad (1.7)$$

Three addends in the formula (1.7) for change electrochemical potentials are the basic. But if the cell is in a constant magnetic field, it is necessary for calculation to add $\Delta\overline{\mu}$ which are corresponding as the fourth addend.

1.3. Mechanism of transmembranes potential occurrence. Nernst potential

Let's consider some model membrane, which permeable only for one kind of ions, for example, potassium ion K^+. Let on both sides of a membrane there is potassium chloride KCl in various concentration, fig. 1.5. We assumed that chlorine ions Cl^- through a membrane will not penetrate.

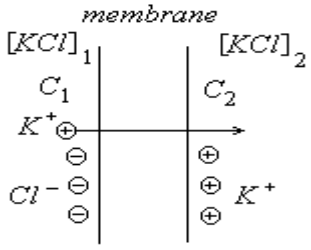

Fig. 1.5.

Let's considering that $[KCl]_1 > [KCl]_2$ as potassium chloride dissociates completely the potassium ions K^+ which concentration on the side 1 (model of the external side of a cellular membrane) more, start diffuse on the side 2 (model of the internal side of a cellular membrane). The side 2 is charged positively, that interferes with the further transition of the potassium ions K^+ on this side. Dynamic balance is established because the arising electric field counterbalances motive force of a concentration gradient on a membrane.

Electric forces also attract to a membrane on the side 1 the chlorine ions Cl^-. On a membrane arise a potential difference.

Let's find size of this potential difference.

We believe that there is no receipt of Gibbs free energy in considered system, fig. 1.5, i.e. $\Delta\overline{\mu} = 0$. Besides character of substance, i.e. transferable through a membrane ions K^+ does not vary, hence, $\Delta A_{chem} = 0$. Thus, the formula (1.7) for change of electrochemical potential looks like:

$$\Delta\overline{\mu} = \Delta A_o + \Delta A_e = 0$$

or

$$\Delta W_e = -\Delta A_e = +\Delta A_o. \quad (1.8)$$

From the formula (1.8) follows, that the increase in electric energy at membrane ΔW_e occurs due to osmotic work ΔA_o.

Substituting in (1.8) expressions for electric (1.6) and osmotic (1.5) works, we find:

$$\Delta\varphi = \varphi_2 - \varphi_1 = -\frac{\Delta A_o}{zF} = \frac{RT}{zF} \ln \frac{C_1}{C_2}, \quad (1.9)$$

where C_1 and C_2 there are concentration of ions K^+ after achievement of balance.

The received formula for a potential difference (increments of potential is more accuracy) on a membrane refers the Nernst formula.

The examined model, fig. 1.5, differs from a biomembrane, for example, a nervous cell (neuron) the following:

1. Though a membrane of neuron there is completely permeable for potassium ions K^+, it a less but permeable for chlorine ions Cl^-.

2. At model, fig. 1.5, concentration of potassium ions K^+ on the side 2 where go its ions, always less, than on the side 1 where from they go (the side 1 is model of the external side of a cell). Really, there is a situation opposite. Inside a cell concentration of ions K^+ is more, than outside.

3. At model the side 2 of a membrane is charged positively concerning a side 1, fig. 1.5. On a real cell a situation is return. On an internal surface of a membrane of a cell (neuron) in a condition of its rest there is potential negative concerning an external surface of a membrane.

4. Through a real cellular membrane, as against model, continuously there is an active flux of sodium ions Na^+ from a cell outside, opposite to a flux of ion K^+. It creates there conditions that inside a cell the concentration of potassium ions is higher, than outside and inside a cell there is a negative potential.

However, despite of these distinctions because a membrane basically permeable for potassium ions, the formula Nernst can be used for calculation of transmembrane potential on a biomembrane:

$$\Delta\varphi = \varphi_i - \varphi_e = \frac{RT}{zF} \ln \frac{[K^+]_e}{[K^+]_i}. \qquad (1.10)$$

In the formula (1.10) index 1 is replaced on *e* - the external side of a membrane, and an index 2 on *i* - the internal side of a cell membrane.

From a deduction of the formula (1.10) follows that chlorine ions do not define potential on a membrane. The potential on a membrane is defined by positive ions for which a membrane is permeable therefore potential as speak has basically potassium character.

In the nervous cells of the warm-blooded the ratio $\frac{[K^+]_e}{[K^+]_i} \approx \frac{1}{28}$. Assuming a body temperature of the man $T = 310\ K$ and valence of potassium ions $z = 1$, we have $\Delta\varphi = -90\ mV$ (actually, on a membrane of neuron $\Delta\varphi = -80\ mV$).

The external surface of a cell can be assumed earthed (the man usually stands on the ground) and consequently its potential is approximately equal zero at a state of cell rest.

The potential on a membrane is always counted from its external surface which potential is assume zero.

The sign a minus means, that potential on the internal side of a cell membrane is negative concerning external side.

Thus, if the cell membrane is permeable only for ions K^+ the potential $\Delta\varphi = -90\ mV$ would be established. If the membrane is permeable only for ions Na^+ (the similar situation is observed during excitation of a cell, see Chapter 2) the sodium potential would be established:

$$\Delta\varphi = \varphi_i - \varphi_e = \frac{RT}{zF} \ln \frac{[Na^+]_e}{[Na^+]_i}. \qquad (1.11)$$

Accepting for nervous cells of warm-blooded the ratio $\frac{[Na^+]_e}{[Na^+]_i} \approx 9.7$, we have $\Delta\varphi = +60\ mV$ (actually, on a membrane of neuron at excitation $\Delta\varphi = +40\ mV$).

Through the cell membranes, for example, neurons the fluxes of ions K^+, Na^+ and Cl^- are observed basically. For chlorine size of Nernst potential $\Delta\varphi = \frac{RT}{zF}\ln\frac{[Cl^-]_i}{[Cl^-]_e} \approx -70\ mV$ at $\frac{[Cl^-]_i}{[Cl^-]_e} \approx \frac{9}{125}$. This size is close to total equilibrium potential on a membrane or to resting potential (at calculation of chlorine potential under Nernst formula the return ratio of concentration used since chlorine is a negative ion).

The resting potential is real transmembrane potential of a cell which is in a condition of rest, i.e. in not excited condition.

For neuron of the man the resting potential is $\Delta\varphi = -80\ mV$. The potential on a membrane is defined not by ion Cl^- which it is practically free diffuse through phospholipid matrix in both sides of a membrane, and ion K^+. Concentration of chlorine ions on both sides of a membrane is in an equilibrium condition (the membrane of neuron is practically indifferent to chlorine ions). Chlorine pumps which could create nonequilibrium distribution of concentration in neuron membranes and muscular cells membrane of the man are not found. Potassium ions aspire diffusing through the some ($\sim 1\%$) open in norm potassium ionic channels from a cell. A neuron membrane it is good permeable for potassium. Cations, as against anions, cannot diffusing through phospholipid matrix of a membrane since the external surface phospholipids matrixes is charged positively, fig. 1.1.

Sodium cation Na^+ can penetrate through a membrane inside of neuron only through open sodium channels. In a resting condition of neuron it is not enough such channels and their existence in an open condition is connected to infringements in work «gate of systems», see paragraph 2.2.1.1. Therefore the membrane нейрона is practically impenetrable for sodium.

Maintenance of the constant ratio $\frac{[Na^+]_e}{[Na^+]_i}$ the same and for potassium ion (K^+) on a membrane is guaranteed special enzyme in a cell membrane - sodium-potassium pump (Na^+/K^+-ATPase), functioning due to hydrolysis of ATP molecules.

1.4. Transmembranes transport of substances

1.4.1. Flux through the cellular membrane of not charged particles

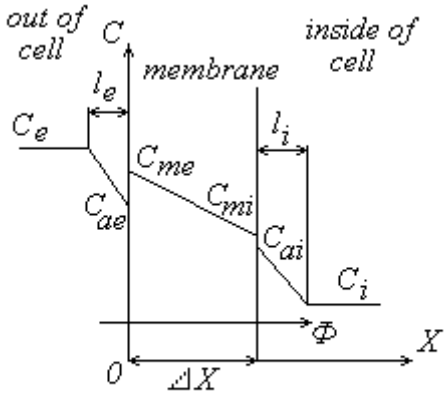

Fig. 1.6.

Let's consider not charged particles motion through a membrane due to simple diffusion through phospholipid matrix, fig. 1.2. In such a way through biomembranes small neutral molecules of oxygen O_2, carbonic gas CO_2 move, for example, etc.

The particle at diffusion goes not only a membrane, but also less mobile nearmembrane layers.

On fig. 1.6 the following designations are used: C_e and C_i - molar concentration of diffusing particles outside and inside of a cell, C_{ae} and C_{ai} - concentration of particles outside and inside of a cell in nearmembrane medium at a surface of a membrane, C_{me} and C_{mi} - concentration of particles outside and inside of a cell into a membrane at its surface.

Jump of concentration on borders of a membrane with the intercellular environment and cytoplasm are resulted by difference affinity (difference of forces of intermolecular interaction) diffusing particles and out of membrane environments, and also particles and molecules of a membrane. Due to it on a membrane there can be an adsorption of particles.

At the external and internal sides of a membrane are nearmembrane layers that saturated with peripheral proteins. Mobility of a liquid in these layers is reduced. Concentration of particles into the nearmembrane layers inside of a cell decreases from size C_{ai} up to size C_i, and outside of a cell from size C_e up to size C_{ae}. Thickness external and internal nearmembrane layers are designated l_e and l_i.

Diffusion of particles inside a membrane submits to the Fick law of diffusion:

$$\Phi = -D^* \frac{dC}{dX}, \qquad (1.12)$$

where $\Phi = \frac{\Delta N}{S\Delta t}$ there is density of particles flux, ΔN - quantity of the particles crossing an area S, perpendicular to a direction of transfer in time Δt, D^* - molar factor of diffusion in $\left[\frac{m^2}{mol \cdot s}\right]$, $\frac{dC}{dX}$ is a gradient of molar concentration in a direction of coordinate *X*.

If to assume, that change of concentration in a membrane occurs linearly the Fick's law can be written down as:

$$\Phi = -D^* \frac{C_{mi} - C_{me}}{\Delta X} = D^* \frac{C_{me} - C_{mi}}{\Delta X}. \qquad (1.13)$$

In cell biophysics the ratio of substance concentration in a membrane at its border to concentration of substance in nearmembrane environments at borders with a membrane refers to the factor of distribution of substance:

$$K = \frac{C_{me}}{C_{ae}} = \frac{C_{mi}}{C_{ai}}. \qquad (1.14)$$

Equality of concentration ratio in (1.14) on both sides of a membrane is one of forms of the Henry law for adsorption, (*K* is a Henry constant for adsorption). For system lipid-water Henry constant is $K \approx 10$.

Using factor of substance distribution the Fick's law can be written down in the following kind:

$$\Phi = \frac{D^* K}{\Delta X}\left(C_{ae} - C_{ai}\right) = P_m\left(C_{ae} - C_{ai}\right), \qquad (1.15)$$

where it is designated $P_m = \frac{D^* K}{\Delta X}$ - factor of membrane permeability for a particle.

The value return to factor of permeability refers to resistance to a flux of substance:

$$R_m = \frac{1}{P_m} = \frac{\Delta X}{D^* K}. \qquad (1.16)$$

External and internal nearmembrane layers as a membrane have resistance to a substance flux R_e and R_i:

$$R_e = \frac{l_e}{D_e^*}; \qquad R_i = \frac{l_i}{D_i^*}, \qquad (1.17)$$

Where D_e^* and D_i^* there are molar diffusion factors of particles in external and internal nearmembrane mediums of a cell. The factor of distribution $K = 1$ since there is no jump of concentration between nearmembrane layers and the basic part out of membrane environments.

Hence, the general resistance of a substance flux for a membrane and nearmembrane layers will be equal:

$$R_g = R_e + R_m + R_i. \qquad (1.18)$$

To the general resistance there corresponds the general factor of membrane complex permeability:

$$P_g = \frac{1}{R_g}. \qquad (1.19)$$

Hence, Fick's law (1.12) for a membrane with the account of the nearmembrane layers can be written down as:

$$\Phi = P_{\text{g}}\left(C_e - C_i\right) = \frac{\left(C_e - C_i\right)}{R_{\text{g}}}. \qquad (1.20)$$

In norm circulation of an intercellular liquid and cell cytoplasm is observed which results in reduction of nearmembrane layers thickness l_e and l_i. It lowers the general resistance to a substance flux R_{g} due to reduction of resistance R_e and R_i. At some pathological, especially inflammatory processes circulation can be slowed down, that results in increase R_{g}, reduction of the general factor of membrane complex permeability P_g and, accordingly, to decrease in flux density of particles Φ through a membrane. It results in decrease in a metabolism of cells. Application of ultrasound (ultrasonic micromassage of tissues) which accelerates motion of cytoplasm and an intercellular liquid is in that case good.

1.4.2. Flux through the membrane of the charged particles. Electrodiffusivity Nernst-Planck equation

Through cell membranes and intercellular organelles due to diffusion move both neutral molecules and ions. Thus through membrane phospholipid matrix of nervous and muscular cells negative chlorine ions Cl^-, for example, move.

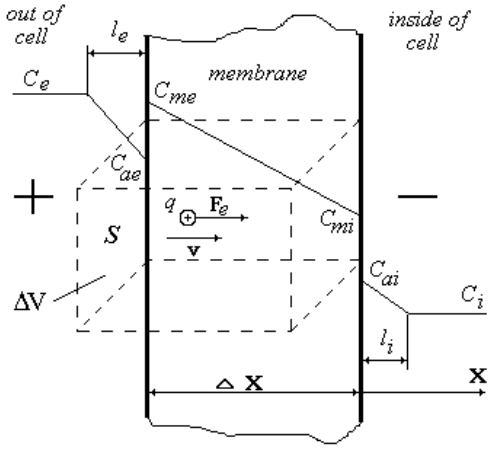

Fig. 1.7.

On process of ions diffusion due to a gradient of concentration in membrane there is influence with electric processes due to a potential difference on a membrane. Therefore process of ions transfer through a membrane refers to as electrodiffusion.

In spite of the fact that cations are not transferred through membrane phospholipid matrix due to passive diffusion it is conveniently to investigate transport of a positive ion. Charge signs of transferable ions we shall take into account later. We shall consider passive (without expenses of energy ATP) motion through a membrane of positive ions with a charge *q*, fig. 1.7.

The density of a charged particles flux through membrane Φ is the sum of two components: density of a flux due to a gradient of concentration Φ_o and due to a gradient of electric potential Φ_e:

$$\Phi = \Phi_o + \Phi_e . \qquad (1.21)$$

The density of a flux due to a gradient of concentration submits to Fick's law (1.12).

Influence nearmembrane layers on density of the charged particles flux through a membrane we shall take into account later.

On the charged particle in a membrane on which there is a potential difference act electric force $F_e = qE$, where *E* is an electric field strength in the membrane.

Let *n* there is numerical concentration of ions in a membrane (number of ions in unit of volume ΔV of a membrane), hence the general number of particles in volume ΔV equally $\Delta N = n\Delta V = nS\Delta X$.

Density of particles flux due to electric force looks like:

$$\Phi_e = \frac{\Delta N}{S\Delta t} = \frac{nS\Delta X}{S\Delta t} = n\mathrm{v}, \qquad (1.22)$$

where *b* there is so-called of an ion mobility.

Taking into account connection of electric field strength and a gradient of potential $E = -\frac{d\varphi}{dX}$, according to (1.22), we receive:

$$\Phi_e = n\mathrm{v} = -qnb\frac{d\varphi}{dX}. \qquad (1.24)$$

Using connection of numerical and molar concentration $n = CN_A$ where $N_A = 6.022 \cdot 10^{23}\ mol^{-1}$ is Avogadro's Number, we find:

$$\Phi_e = -qN_A bC\frac{d\varphi}{dX}. \qquad (1.25)$$

The value qN_A is a charge of one mol of ions transferable through semipermeable membrane. Taking into account determination of Faraday constant *F* (a charge of one mol monovalent ions), we have $qN_A = zF$, where *z* is valence of moving through a membrane ions.

Hence, the density of a particles flux through a membrane due to a gradient of potential can be written down as:

$$\Phi_e = -zFbC\frac{d\varphi}{dX}. \qquad (1.26)$$

The general density of an ions flux through a membrane on which there is a gradient of concentration and a gradient of potential, in view of Fick's law (1.12) it is possible to write down as the equation:

$$\Phi = \Phi_o + \Phi_e = -D^*\frac{dC}{dX} - zFbC\frac{d\varphi}{dX}. \qquad (1.27)$$

This equation refers to electrodiffusivity Nernst-Planck equation. It shows that if on a membrane there is a gradient of concentration and gradient of potential the general density of the charged particles flux is proportional to both gradients.

1.4.2.1. The solution of the Nernst-Planck equation

The solution of the Nernst-Planck equation (1.27) we shall find under condition of a constancy of density of a particles flux through a membrane, i.e. $\Phi = const$.

Let's assume that through a membrane one ions kind transfer. As the potential into the membrane depends linearly (in membrane there are no ferromagnetic particles) $\frac{d\varphi}{dX} = \frac{\Delta\varphi}{\Delta X}$, where $\Delta\varphi$ is a potential (an increment of potential) on a membrane, ΔX - membrane thickness.

We use dimensionless potential:

$$\psi = \frac{zFb\Delta\varphi}{D^*}. \qquad (1.28)$$

Substituting (1.28) in the Nernst-Planck equation (1.27), we shall find:

$$\Phi = -D^* \frac{dC}{dX} - D^* \frac{C\psi}{\Delta X}. \qquad (1.29)$$

Let's introduce a new variable:

$$t = \frac{\Phi}{D^*} + \frac{C\psi}{\Delta X}. \qquad (1.30)$$

Substituting (1.30) in (1.29), we find:

$$t = -\frac{dC}{dX}. \qquad (1.31)$$

Separating variables in the differential equation (1.31), and finding integrals from the left and right parts of equality, we have:

$$\int_0^{\Delta X} dX = -\int_{C_{me}}^{C_{mi}} \frac{dC}{t}, \qquad (1.32)$$

where C_{me} and C_{mi} there are concentration of particles outside and inside of a cell into a membrane at its surface. The origin of coordinates *X* is accepted on external side of a membrane, fig. 1.7.

Interrelation of differentials dt and dC we shall find, using the formula (1.30). Thus it is taken into account, that the density of a particles flux through a membrane is constant $\Phi = const$, i.e. process established (from time not dependent).

$$dt = \frac{\psi}{\Delta X} dC. \qquad (1.33)$$

Besides we shall make replacement of integration limits in (1.32) under the formulas following from (1.30):

$$t_i = \frac{\Phi}{D^*} + \frac{C_{mi}\psi}{\Delta X}; \qquad t_e = \frac{\Phi}{D^*} + \frac{C_{me}\psi}{\Delta X}. \qquad (1.34)$$

Introducing factor of substance distribution $C_{me} = KC_{ae}; \qquad C_{mi} = KC_{ai}$, and also taking into account factor of permeability $P_g = \frac{D^* K}{\Delta X}$, we shall receive:

$$t_i = \frac{1}{D^*}\left(\Phi + P_g \psi C_i\right); \qquad t_e = \frac{1}{D^*}\left(\Phi + P_g \psi C_e\right). \qquad (1.35)$$

As the factor of permeability is taken the general with the account nearmembrane layers in formulas (1.35) values of transferable particles concentration far from surfaces of a membrane are used.

Integrating (1.32), with the account (1.33) and (1.35), we shall find:

$$\Delta X = -\frac{\Delta X}{\psi}\int_{t_e}^{t_i}\frac{dt}{t} = -\frac{\Delta X}{\psi}\ln\frac{t_i}{t_e}. \qquad (1.36)$$

Further (1.36), we find:

$$t_i = t_e e^{-\psi}. \qquad (1.37)$$

Substituting formulas (1.35) in (1.37) and, finding from this equation density of a particles flux Φ, we receive:

$$\Phi = -P_g \psi \frac{C_i - C_e e^{-\psi}}{1 - e^{-\psi}}. \qquad (1.38)$$

The formula (1.38) determines quantitative interrelation between density of one kind ions flux through a membrane, permeability of a membrane for these ions, their concentration on both sides of a membrane and membrane potential.

If dimensionless potential $\psi = 0$ the formula (1.38) transformed in Fick's law for not charged particles (1.20) if to use:

$$\lim \frac{\psi}{1 - e^{-\psi}} = 1 \qquad \text{at} \qquad \psi \to 0.$$

1.5. Transport of substances through a membrane

Many processes in a cell are connected to transport of substances through biomembranes: synthesis ATP, maintenance of ionic composition constancy in a cell, process of a nervous impulse distribution, etc. We shall write the following sections, approximately following [2, 3, 10].

Distinguish passive and active transport.

1.5.1. Passive transport

Passive transport is not connected to expenses of energy and carried out aside smaller electrochemical potential.

Usually distinguish 4 kinds of passive transport (or carry) particles through a biomembrane.

1. Passive diffusion (electrodiffusion). Passive diffusion, fig. 1.8, occurs through phospholipid matrix under action of gradients of concentration and potential on a membrane. Passive diffusion of not charged particles submits to Fick's law (1.20), and the charged particles (electrodiffusion) to the solution of the Nernst-Planck equation (1.38). The most widespread particles moving through a membrane due to passive diffusion it is oxygen, carbonic gas, chlorine ions, etc.

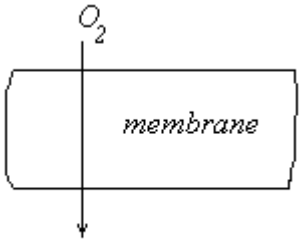

Fig. 1.8.

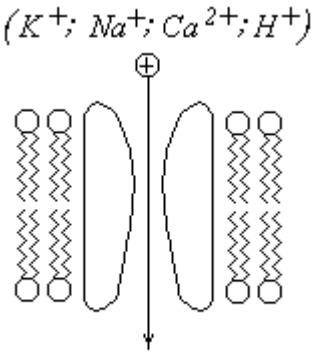

Fig. 1.9.

2. The transfer of ions through channels of biomembranes. This kind of carry is characteristic for excitable (nervous and muscular) cells. There are exist sodium, potassium, calcium, [78] and proton cations channels, fig. 1.9. In some biomembranes (for example, erythrocytes, helminthic myocytes, etc.) are anions Cl^- channels.

Channels are integrated membrane proteins which one of the largest and complex albuminous molecules of an organism. For example, the molecular mass of sodium channel is approximately 300000. Channels consist from several (more often than four) nuclear blocks – subunits, connected among themselves.

Channels are usually intended for creation concerning short-term, intensive fluxes of the ions certain kinds through a membrane if on a membrane there is a gradient of their concentration.

Therefore to each kind of the channel there should correspond to the ionic pump creating this gradient. The passing power open of sodium channel is $\sim 10^7 \frac{ions}{s}$, and potassium channel is $\sim 10^6 \frac{ions}{s}$.

Channels can be in the open or closed conditions. Therefore in them usually is present mobile molecular gating mechanism.

Channels are voltage-gated ion channels, i.e. opening or closed depending on the certain potential difference on a membrane, ligand-gated ion channels, i.e. opening at addition of some particles. For example, acetylcholine molecules, noradrenaline molecules open ligand-gates channels of postsynaptic membranes of many nervous and muscular cells. Mechanosensitive ion channel are opening under the influence of stretch or pressure upon a membrane of a cell. For example, channels in receptor cells of an internal ear. Exist and non regulating (constantly open) ionic channels.

Sodium, potassium, and calcium channels are intended only for transfer of ions through a membrane. Proton channels are intended also for synthesis of ATP molecules.

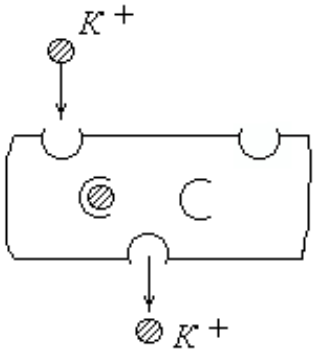

Fig. 1.10.

The ionic channels blockers there are exist. For example, antihypertensive drugs the antagonists of calcium (verapamil, nifedipine, etc.) temporarily block calcium ionic channels, reducing a muscular tone of vessels. Local anesthetics (novocaine, lidocaine, etc.) temporarily block sodium ionic channels, reducing painful sensitivity. It is irreversible block sodium ionic channels such paralytic poisons as tetrodotoxin produced fish Spheroidus rubrides or saxitoxin, produced by the some plankton. On the contrary, poison of a spider karakurt contains latrotoxin which represents not closed calcium channel. It prevent to reduction of muscles. The strong blocking effect on calcium ionic channels exerts tetraethylammonium. There are also activators (openers, mimetics) ionic channels, for example, the medical preparation minoxidil activates potassium channels. Medicinal substances - blockers of ion transfer through ligand-gated channels of postsynaptic membrane (M- and H-cholineblockers, $\alpha-$ and $\beta-$ blockers, etc.) which temporarily block synaptic transfer of excitation impulse are widely applied.

3. Transfer of ions by a mobile translator. The ions transfer by a mobile translator, as well as formation of time channels in a biomembrane of microbes and bacteria, see further, is one of mechanisms of antibiotic-ionophores action (so-called polyenes).

Ionofores there are the substances facilitating of ions transfer through a membrane (nonactin, valinomycin, gramicidin, etc).

Thus barrier function of a membrane is broken that conducts to destruction of microorganisms.

Mobile translators of potassium ions are antibiotics nonactin, valinomycin. The valinomycin molecule, fig. 1.10, a cavity having inside, places in it potassium ion on one side of a membrane and transfers this ion to other side of a membrane.

At presence of valinomycin the ratio of permeability factors for ions K^+ and Na^+ is equal $\frac{P_K}{P_{Na}} = 10^4$. In norm this ratio is equal 25.

There are tranlator for *D*-glucose, lactoses, aminoacids, nucleotides, etc.

4. Relay-race transfer. Relay-race transfer is carried out with the help of two or several translators of a transferable particle through a membrane, fig. 1.11. Thus the particle is consistently transferred in a membrane from one translator to another. As an example of relay-race transfer is motion through a membrane of sodium ions Na^+ with the help of an antibiotic gramicidin.

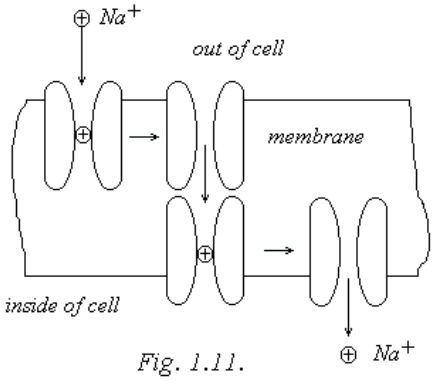

Fig. 1.11.

Gramicidin which create in a membrane half-channel, places in it the sodium ion on out side of a membrane. Diffusive along a membrane, the gramicidin molecule meets other gramicidin molecule a membrane taking place on the internal side and gives it a sodium ion. Then the sodium ion is thrown out inside of a cell.

As gramicidin actually increases permeability of a membrane for ions of Na^+, i.e. breaks normal functioning a cell it is used, for example, as contraceptive ointment blocking functioning of spermatozoon and ovum.

Other example of relay-race transfer carry is a transfer of electrons on a respiratory chain through an internal mitochondrial membrane. Translators are albuminous complexes consistently accepting the electrons, protein-cytochromes and other molecules which are taking place in a membrane.

One of the main features of passive transport is its selectivity. There is ion transfer through channel which aperture radius is approximately equal to ion radius (with a fraction of hydrate cover). Ion Na^+ for K^+ channel will not pass, since is too great for potassium channel aperture. Also ion Na^+ is too great for a valinomycin cavity, therefore the valinomycin molecule does not transfer sodium. There are translators for *D*-glucose, but there are no translators for *L*-glucose. In case of simple diffusion selectivity is defined by affinity of a transferable particle to hydrophilic phospholipids head. For example, by anions can be transferred through phospholipids matrix but it is not possible by cations.

1.5.2. Active transport

Active transport through a membrane occurs at an expense of chemical energy – of free Gibbs energy Гиббса, paragraph 1.2.

There is a primary and secondary active transport.

Primary active transport takes place at work of transport ATPases.

ATPase it is a special enzyme (protein) which is carrying out ions transfer due to hydrolysis ATP aside of the greater electrochemical potential.

Secondary active transport is the connected transport when transfer of one ions to a direction of electrochemical potential increase is caused by transfer of other ions to a direction of electrochemical potential reduction. The work of sodium-calcium exchanger [79] in membranes of muscular cells it is an example of secondary active transport, paragraph 4.1.2.

Usually examine 3 kinds of primary active transport.

1. The sodium-potassium pump (Na^+/K^+ - ATPase).

The sodium-potassium pump works in all cells of an organism, supporting necessary gradients of concentration of ions Na^+ and K^+. It is large protein with molecular mass 170000.

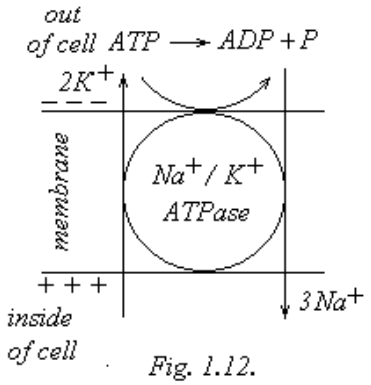

Fig. 1.12.

During evolution has developed so, that for creation of necessary electrochemical potential, the ions Na^+ are expelled from a cell and ions K^+ are pumped up in a cell. The matter is that during evolution, in process of complication of a cell functioning, in it the increasing quantity of various substances necessary for it. Concentration of these substances as a whole became higher above, than in an environment. There is cell due to of osmotic pressure difference turned out under threat of excessive penetration of water into it and break. To get rid of this danger a cell pump out in an environment ions Na^+ which turned out are most suitable for this purpose since their plenty and is possible to lower osmotic pressure considerably. Passing in a cell ions K^+ compensate excessive increase in potential at a membrane. The matter is that an electric field strength in a membrane of a cell is very great $E = -\frac{\Delta\varphi}{\Delta X} = 10^7 \frac{V}{m}$. It conducts to that the membrane is on a limit of electric breakdown, despite of it insulating properties. For comparison we shall notice, that if electric field strength in air attain $E = 3 \cdot 10^6 \frac{V}{m}$ between the electrodes there is a spark discharge. The sodium-potassium pump is activated basically by increase in concentration of ions Na^+ inside a cell.

The scheme of sodium-potassium pump works or Na^+/K^+ - ATPase is shown on fig. 1.12. At hydrolysis of one ATP molecule there is a transfer of 2 ions K^+ inside of a cell that is accompanied by emission of 3 ions Na^+ from a cell. Thus from a cell 1 positive charge is carried away. Hence, the sodium-potassium pump is electrogenic, i.e. it participates in creation of resting potential on a membrane, increasing it approximately on 25%. Though it and not the basic mechanism of creation of resting potential (the basic mechanism is connected with semipermeable membranes), but it is the basic mechanism of maintenance of concentration gradients of Na^+ and K^+ on a membrane.

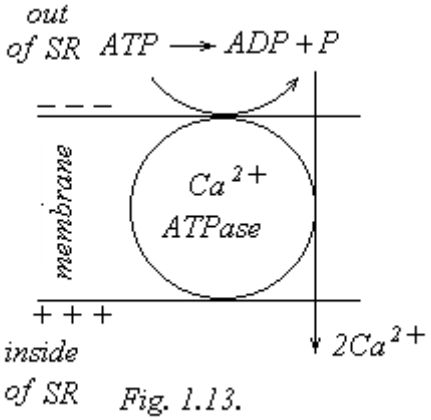

Fig. 1.13.

There are the medicinal substances cardiac glycoside used at heart failure (insufficiency) - digoxinum, strophanthinum, corglyconum, etc., which inhibited Na^+/K^+ - ATPase. These substances have toxic properties. The mechanism of action of these preparations will be considered in paragraph 4.1.2.

2. The calcium pump (Ca^{2+} - ATPase).

The calcium pump or Ca^{2+} - ATPase, fig. 1.13, basically functions in membranes of muscular cells and in membranes of sarcoplasmic reticulum *SR* (special vesicles of muscular fibres - keepers of ions Ca^{2+} where Ca^{2+} - ATPase occupies a third of all membrane surface and there is $\sim 80\%$ of total quantity of integrated proteins). It is enzyme with molecular mass 115000.

The calcium pump is activated by decrease in a gradient of concentration of ions Ca^{2+} on a membrane. It transfers 2 ions Ca^{2+} at hydrolysis of one molecule ATP, therefore it participates in creation transmembranes potential i.e. calcium pump is electrogenic.

We shall note also, that inside of sarcoplasmic reticulum the potential has a sign plus, and outside a minus. Such distribution of potential to membrane *SR* does not result in occurrence of a potential difference between outside surface of *SR* membrane and the internal side of a cell membrane since both these surfaces of membranes are charged negatively. Therefore between these membranes there are no the unnecessary electric currents flowing inside of a cell.

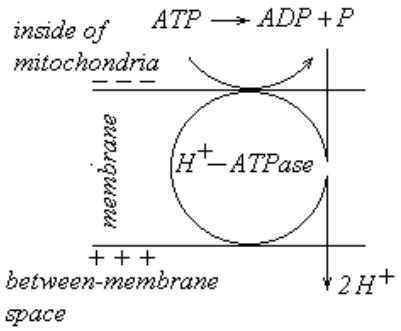

Fig. 1.14.

3. Proton pomp (H^+ - ATPase).

Transfer of protons occurs in internal membranes of mitochondrias and others organells eukaryotic (having a nucleus) cells, chloroplasts (organells of the plant cells participating in photosynthesis), bacterias.

The important property of a proton pomp is it electrogenic. In the mitochondrias the proton pomp, fig. 1.14, at hydrolysis of one molecule ATP transfers 2 hydrogen ions H^+ (formed into so-called biochemical Krebs cycle) inside of mitochondria through an internal membrane of mitochondria in between-membrane space.

It creates a supercritical electrochemical potential gradient of protons on an internal membrane which is necessary for ATP synthesis. The proton pomp pumps up a level of electrochemical potential up to critical to what the name of this enzyme is connected. Thus arises both electric, and concentration components of electrochemical potential on a membrane. Therefore electrogenic H^+ - ATPase is its major property.

1.5.3. Bioenergetics of organism

The bioenergetics is the part of biophysics studying processes of energy transformation in biological structures. The bioenergetics is directly connected to processes of the charged particles transfer through a membrane.

The bioenergetics defines the most part of processes in an organism. Evolution of living organisms was carried out in a direction of reduction of energy intensity of processes since usually carried out in conditions of deficiency of food.

Biopolymers of food: hundreds proteins, fats, polysaccharides in organism break up to monomers: some tens amino acids, fat acids, glycerin, monosaccharides (glucose, etc.). Monomers further turn in carbonic acids, which participate in a tricarboxylic acid cycle (Krebs cycle [4]) with products CO_2 and mitochondrias hydrogen ions H^+. Krebs cycle functions in matrix of mitochondrias, see below. Ions of Hydrogen ions H^+ are necessary for synthesis of ATP molecules.

As the main supplier of free Gibbs energy in organs and tissues of organism is ATP (adenosine triphosphate acid) molecule. Therefore processes of synthesis of ATP molecules are one of the most important bioenergetic processes in an organism.

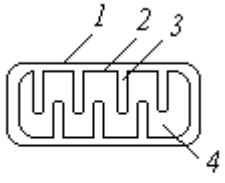

Fig. 1.15.

There are two ways of ATP synthesis.

The first way is glycolysis. Glycolysis it is a series from 10 enzymatic reactions in which at oxidation of a glucose molecule $C_6H_{12}O_6$ 2 ATP molecules are formed. Glycolysis is not basic source of ATP, but its importance

grows in anaerobic conditions, i.e. at lack or absence of oxygen. For example, glycolysis it is intensified at physical exercises when respiration cannot provide sufficient inflow of oxygen to muscles.

As the basic way of ATP synthesis is oxidative phosphorylation. We shall consider this way of ATP synthesis on a basis of chemiosmotic theory open by the English scientist Mitchell, for what he in 1978 has received the Nobel Prize.

According to this theory ATP synthesis takes place on internal membranes of mitochondrias, fig. 1.15.

Mitochondrias is organelles of cells which moving in its cytoplasm, approach to a cell sites in which there is a big necessity of energy. The sizes of mitochondria is $0.5-2\ \mu m$. The quantity of mitochondrias in a cell is many thousand. For example, there are liver cells the mitochondrias make 22% of all cell volume. They are surrounded with a double membrane: external 1 and internal 2. The internal membrane forms numerous crimps or cristae 3 which increase a surface of this membrane. The medium surrounded with an internal membrane, refers to matrix 4.

It is assumed, that mitochondrias operate in a cell as a result of symbiosis. As mitochondrias in the beginning evolution separately from cells of organism as aerobic bacteria, on their membrane there was a standard distribution membrane potential - inside a minus, outside plus (zero). At incorporation the mitochondrias into a cell there should be the strong electric currents directed from a mitochondrias membrane to the internal side of a cell membrane charged negatively the hydrogen ions H^+ carrying away from external side of mitochondrias charged positively. It did not allow mitochondria incorporated into the a cell to synthesize ATP, therefore there was a necessity for one more external membrane 1 which is isolator for an ionic current and does not allow the ions H^+ of between membrane space to leave from mitochondria.

Let's note, that others cells organelles surrounded with a membrane, it is primary evolution together with a cell, for example, sarcoplasmic reticulum (see paragraph 1.5.2) have the opposite distribution of potential in comparison with a membrane of a cell - inside plus, outside a minus, fig. 1.13, therefore there is not need for the second membrane.

There are 2 schemes of ATP synthesis distinguished from each other in mitochondrias on a basis of the chemiosmotic theory.

The main principle of the first scheme has been offered by Mitchell. According to this scheme in the internal membrane of mitochondria exists ATP synthase which is the enzyme having molecular mass approximately 500000 and it is made of two parts: proton channel F_0 and complex F_1 [5], fig. 1.16.

Under this scheme the hydrogen ions H^+ which it is products in Krebs cycle are transferred through an internal mitochondrial membrane with the help of the proton pomp, fig. 1.14, into between membrane space and in part remain in a free condition, and in part incorporate with ascorbate to complex AH_2. This complex is oxidized first translator of electrons through membrane - protein cytochrome *C* on the external side of a membrane according to reaction:

$$AH_2 \rightarrow A + 2H^+ + 2e^-. \qquad (1.39)$$

Two hydrogen ions passes in an environment (in between membrane space), and 2 electrons are transferred to a chain of electrons translators (so-called a respiratory chain) inside of mitochondria.

On an internal membrane of mitochondria there is a difference of electrochemical potential, see (1.7), due to hydrogen ions:

$$\Delta\overline{\mu} = RT \ln \frac{\left[H^+\right]_e}{\left[H^+\right]_i} + zF\Delta\varphi, \qquad (1.40)$$

where the index *e* means external side (outside) of mitochondrial internal membrane, and *i* - its inside, $z = 1$ it is valence of hydrogen ions. Change of chemical potential of hydrogen, obviously, does not occur.

Both terms in the sum, describing osmotic and electric energies are approximately equal among themselves. The electric potentials difference on an internal membrane of mitochondria (outside plus, inside a minus) has enough great size $\Delta\varphi \approx -150\ mV$.

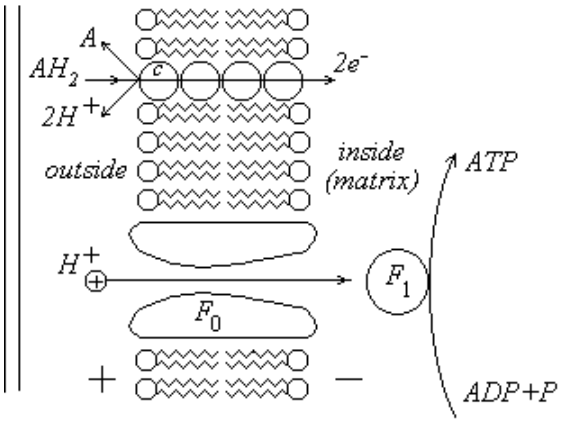

Fig. 1.16.

The proton channel F_0 acts as a proton gun. The proton is accelerated in the channel due to electrochemical potential $\Delta\overline{\mu}$ up to kinetic energy $\frac{mV^2}{2}$ and shock excite inorganic phosphate *P* (orthophosphoric acid H_3PO_4). Phosphate *P* is preliminary installed by second part of ATP synthase F_1 in the necessary position for excitation.

Then ADP (adenosine diphosphatic acid it is result of hydrolysis ATP, see (1.2)) bonds the excited phosphate and turns to ATP:

$$ADP + P + 2H^+ \rightarrow ATP + H_2O. \qquad (1.41)$$

Thus there is a transition of electrochemical potential in energy of macroerg's bonds of ATP molecule:

$$\Delta\overline{\mu} \rightarrow \frac{mV^2}{2} \rightarrow \tilde{P} \rightarrow \sim(ATP), \qquad (1.42)$$

where $\tilde{P}$ there is energy of excitation of phosphate, $\sim(ATP)$ - energy of macroerg's bonds of ATP. The equation (1.42) is the key equation of transformation of energy at ATP synthesis.

Two electrons $2e^-$ belonging to hydrogen atoms (1.39) are transferred to a respiratory chain of oxidation-reduction enzymes inside of mitochondria, fig. 1.16.

The part of protons past through channel F_0 but for the various reasons (the insufficient energy, insufficient excitation of phosphate, etc.) not participating in reaction of ATP molecule synthesis should be utilized with the purpose of prevention decrease in a level of electrochemical potential $\Delta\overline{\mu}$ on a membrane. It occurs in reaction of cellular respiration to participation of the electrons received from a respiratory chain and oxygen transferred owing to simple diffusion into mitochondria:

$$4H^+ + 4e^- + O_2 \rightarrow 2H_2O. \qquad (1.43)$$

Modification of Mitchell scheme has been offered to Finnish scientists Wikstrom. He has assumed that two electrons are not transferred to a membrane and the respiratory circuit is located along a membrane, fig. 1.17.

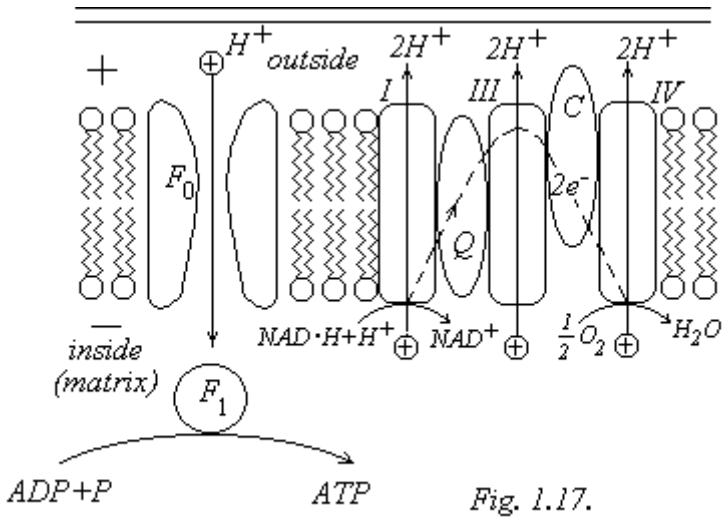

Fig. 1.17.

Under this scheme (submitted is simplified) the system of electrons transport includes three large albuminous complex-channels (I, III, IV), ubiquinone *Q* and cytochrome *C*. Ubiquinone *Q* there is the elementary electrons translator - a small molecule not connected to albumin. Cytochrome C there is albuminous molecule in which at electrons transfer the iron ion in oxidation-reduction reactions accepts conditions Fe^{2+} and Fe^{3+} ($Fe^{3+} + e^- \leftrightarrow Fe^{2+}$).

The intermitochondrial molecule nicotinamide adenine dinucleotide dehydrogenase $NAD \cdot H$ participates in the electrons transfer it is one of the most universal hydrogen translators. Electrons are transferred to a respiratory chain acting to first carrier FAD with the help of molecule $NAD \cdot H$ which giving electrons and hydrogen turns in NAD^+ (nicotinamide adenine dinucleotide):

$$NAD \cdot H + H^+ + FAD \rightarrow NAD^+ + FAD \cdot 2\left(H^+ + e^-\right), \quad (1.44)$$

where FAD there is flavin adenine dinucleotide - the first acceptor of hydrogen and electrons. Then into mitochondrial matrix there is a reducing of $NAD \cdot H$ molecule.

During of electrons transfer complex-channels I, III, IV transfer of hydrogen ions from matrix to between membrane space is carried out. Finally, as well as in Mitchell scheme the electrons incorporate to molecular oxygen and protons H^+ forming water.

Apparently in organism there are both schemes of electrons transfer on a respiratory mitochondrial chain.

Advantage of the second scheme, fig. 1.17, in comparison with the first, fig. 1.16, is higher efficiency. In the second scheme the energy which is turning out at formation of water H_2O (1.43) for transfer of hydrogen ions H^+ by the complex-channels IV from matrix to between membrane space is used. In the first scheme the reaction of water formation directly is not connected to ATP synthesis and energy of this reaction passing in heat is lost. Therefore efficiency of the first scheme approximately is twice less than the second.

If somehow to break connection between cellular respiration and ATP formation in a complex $\left(F_0 - F_1\right)$ i.e. to separate these processes, for example, increasing permeability of a membrane for ions H^+ the ATP synthesis will not occur and all energy of respiration will pass to heat. In role of disconnectors is acted, for example, ionofores dinitrophenol, TTFB, some medicinal hormonal preparations or membrane defect.

We shall note a site of cytochrome *C* in an internal mitochondrial membrane which can be an acceptor of electrons, fig. 1.17. It is put forward in between membrane space can even leave in between membrane space in area of peripheral proteins and diffuse along external side of a membrane capturing of electrons.

The man during evolution has lost ability to synthesize an ascorbic acid which carries out various functions in an organism, for example, participates in synthesis of collagen fibers. It also can, according to the first scheme of cellular respiration, fig. 1.16, to play a role of the electrons donor in a respiratory chain. At other warm-blooded, basically, ability of synthesis of an ascorbic acid exists. Hence, at them cellular respiration can

go at once under two schemes, fig. 1.16 and fig. 1.17. From this point of view clearly why at the beginning of some diseases it is useful to accept so-called «shock dozes» ascorbic acid - the major vitamin. In addition more ancient (atavistic) mechanism of cellular respiration under the first scheme, fig. 1.16 is included. The level of bioenergy processes, i.e. intensity of ATP synthesis in an organism sharply grows, that favorably affects the general resistibility of an organism.

It is possible to make the assumption, that loss by the man of synthesis ability of an ascorbic acid it is connected to development of thinking and due to it increase of efficiency of ATP hydrolysis energy use. The excessive energetics of organism its excessive mobility (hyperactivity) began to prevent correct decision-making due to thought processes. For example, ants moving groups rather big subjects use ATP energy with very low efficiency since the most part of individuals push a subject aside, return to a direction of its movement.

Daily need of the adult man for an ascorbic acid $50-100\ mg$. The «shock doze» can rise till $2\ g$. However excess use of an ascorbic acid results in excessive ATP synthesis in an organism that can intensify excessively power-intensive processes in particular reduction of smooth muscles of vessels. This process can lead to undesirable growth of arterial pressure.

The frequency of ATP molecules synthesis of one ATP-synthase makes approximately $200-300\ molecule/s$. For one day at the man it is mass formed ATP approximately equal to half of the man mass.

It is necessary to pay attention and to other aspect of bioenergy processes in particular in a woman organism. The optimum behavior of pregnant mother is extremely important for a normal birth and development of the child. First of all it is necessity of earlier by time of a child birth of smoking refusal. The matter is that the basic electrons translator on a respiratory mitochondrial chain in scheme Wikstrom, fig. 1.17, is $NAD\cdot H$. At the smoking woman the normal synthesis of this substance in part is replaced by the components passing from the outside, contained in a sigarette smoke. This, obviously concerns and to embryo of the pregnant woman.

The condition of the child who has born from smoking mother since he naturally does not smoke is actually defined by lack of $NAD\cdot H$ synthesis into his organism that results in decrease in intensity of bioenergy processes, first of all ATP synthesis. The insufficient bioenergy level of a child organism slows down his development. One of recommendations on prevention of such position is increase of consumption by the child of an ascorbic acid. Ascorbate being an electrons translator on a respiratory mitochondrial chain in Mitchell's scheme, fig. 1.17, will involve an atavistic chain of cellular respiration which in norm at the man does not operate. Therefore additional consumption of an ascorbic acid by the child can compensate in part lowered ATP synthesis of newborn.

1.5.4. Resting potential. Methods of calculation

The potential of rest is a potential difference (more accuracy an increment of potential) on a membrane counted from its external surface if the excitable cell is in a condition of rest, i.e. in not excited condition.

The potential of a cell external surface is accepted equal to zero.

The reason of difference of the resting potential on a membrane from Nernst potential is permeability of a membrane not only for ions K^+ but also for other ions first of all Na^+ and Cl^-. In a condition of rest through a membrane of a cell continuously there are counter fluxes of these ions, fig. 1.18. Some part of potassium ionic channels ($\sim 1\%$) is always open owing to membrane permeability for ions K^+. Ions Na^+ basically go through sodium channels with destroyed gating system, the ions Cl^- diffuse through membrane phospholipids matrix.

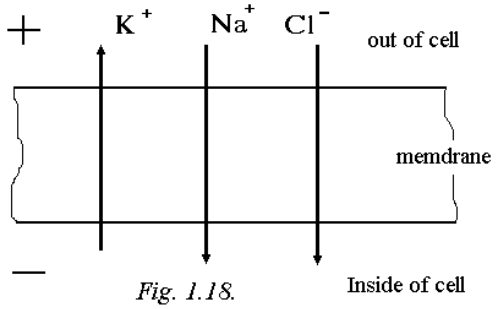

Fig. 1.18.

There are some calculating procedures of resting potential.

1.5.4.1. Goldman – Hodgkin - Katz stationary potential

Goldman – Hodgkin - Katz formula was historically the first formula for calculation of resting potential on membrane. We shall consider substantiation and deduction of this formula [6].

The total density of a flux of positively charged particles through membrane is equal:

$$\Phi = \Phi_{Na} + \Phi_K - \Phi_{Cl}. \qquad (1.45)$$

The sign minus takes into account that the density of chlorine ions flux there are carries a negative charge. Generally, for any number of ions kinds we have:

$$\Phi = \sum_i \Phi_i . \qquad (1.46)$$

We use the formula of the solution of Nernst – Planck equation (1.38) for *i* ion with a positive charge as:

$$\Phi_i = -P_i \psi \frac{C_{ii} - C_{ei} e^{-\psi}}{1 - e^{-\psi}}. \qquad (1.47)$$

For negative ions it is necessary to replace $-\psi$ instead of $-\psi$. In a stationary state of a cell (in a condition of rest), carry of a charge through a membrane is absent therefore $\Phi = \sum_i \Phi_i = 0$ though separate ions fluxes Φ_i can be not equal to zero. Hence, taking into account the formula (1.47) for *i* ion we shall find:

$$\sum_i P_i \left[C_{ii} - C_{ei} e^{-\psi} \right] = 0. \qquad (1.48)$$

From last formula we shall receive value of dimensionless potential:

$$\psi = \ln \frac{\Sigma P_i C_{ei}}{\Sigma P_i C_{ii}}. \qquad (1.49)$$

Taking into account dimensionless potential (1.28) we shall find value of potential on a membrane:

$$\Delta\varphi = \frac{D^*}{zFb} \ln \frac{\Sigma P_i C_{ei}}{\Sigma P_i C_{ii}}. \qquad (1.50)$$

If to apply the received formula to a modeling membrane, fig. 1.5 (at modelling membrane permeability $P_{Cl} = 0$ concentration $[Na^+] = 0$) it should transform in the formula for Nernst potential (1.10). Hence, we have expression $\frac{D^*}{b} = RT$ which refers to Einstein's formulas. Believing through a membrane basically fluxes ions K^+, Na^+ and Cl^- (valence of these ions $z = 1$) we shall receive:

$$\Delta\varphi = \frac{RT}{F} \ln \frac{P_K [K^+]_e + P_{Na} [Na^+]_e + P_{Cl} [Cl^-]_i}{P_K [K^+]_i + P_{Na} [Na^+]_i + P_{Cl} [Cl^-]_e}. \qquad (1.51)$$

In the received formula the ratio of concentration on a membrane for Cl^- ions back to ratio for K^+ and Na^+ ions that is equivalent to change of a charge sign.

The received expression for resting potential on a membrane refers to the Goldman – Hodgkin - Katz formula.

If factors of permeability for ions are used correct (for a membrane of squid giant axon on it carried out basic researches Hodgkin [7] $P_K : P_{Na} : P_{Cl} = 1 : 0.04 : 0.45$) under the Goldman – Hodgkin - Katz formula it is possible to calculate resting potentials for all cellular membranes.

For a membrane of squid giant axon the size of resting potential calculated under the formula (1.51) $\Delta\varphi = -60\ mV$ that meets to experimental results.

The formula (1.51) transform in the formula for Nernst potential (1.10) if all factors of permeability except for potassium are equal to zero i.e. if a membrane permeability only for one kind of ions (for K^+).

The analysis of the formula (1.51) allows to understand also why the potential on a membrane is determined by ions for which it most permeability. In numerator and in a denominator of the formula the main terms there are have the maximal factors of permeability with other conditions being equal.

1.5.4.2. Other ways of resting potential calculation on the membrane

In the formula (1.51) for calculation of resting potential the factor of ions Cl^- permeability has diffuse character. If during excitation of a cell any ionic channels open the channel components of permeability factors start to play the basic role. Channel components of permeability factors it is usual many times more than diffuse factors. For K^+ ions the membrane permeability in a condition of rest has basically channel character since the part of potassium channels is always open.

As it was already specified the potential on a neuron membrane and muscular cells membranes of the man is not determined by Cl^- ions. Concentration of chlorine ions on both sides of a membrane is in equilibrium condition. Chloric pumps which could create nonequilibrium distribution of concentration in neurons membranes and muscular cells membranes of the man are not found. The question on existence in membranes of nervous cells of the man the chloric ionic channels has debatable character (its are, for example, in glandular cells in which membranes Cl^- ions actively participate in electric processes of excitation, and also in cells membranes of non vertebrates). Ions of chlorine diffuse out of neuron and back with identical speeds therefore there are compensate each other fluxes of chlorine ions. Concentration of ions of chlorine there are inside and outside of a cell slave under the existing potential.

Therefore, strictly speaking, chlorine should not is into the formula for the resting potential of neuron.

However, at fast infringement of existing balance the chlorine can short-time there are take part in formation size of membrane potential size.

Thomas [28] had been offered the formula for a resting potential which does not include parameters of chlorine ions:

$$\Delta\varphi = \frac{RT}{F}\ln\frac{\chi P_K\left[K^+\right]_e + P_{Na}\left[Na^+\right]_e}{\chi P_K\left[K^+\right]_i + P_{Na}\left[Na^+\right]_i}. \qquad (1.52)$$

where $\chi = \frac{3}{2}$ there is stoichiometric factor which is taking into account electrogenic of the sodium - potassium pump. The potential on a membrane increases in comparison with the size determined by differences of membrane permeability factors for ions. It occurs because at emission out of a cell by the sodium – potassium pump of 3 Na^+ ions into it enters only 2 K^+ ions. On an internal surface of a membrane there is increase approximately for 25 % the negative potential.

One more way of calculation of the resting potential on a membrane is possible [8] if equilibrium Nernst potentials for ions Na^+ and K^+ are known. In this case the resting potential can be estimated proceeding from the following preconditions.

A condition of rest the general current through a membrane is equal zero since carry of a charge through a membrane is absent $I_K + I_{Na} = 0$. With some approximation it is possible to count that the current through a membrane is depend to potential on a membrane under the Ohm law:

$$I_i = g_i\left(\Delta\varphi - \Delta\varphi_i\right), \qquad (1.53)$$

where g_i there is conductivity of an examined site of a membrane for *i* a kind of ions, $\Delta\varphi$ - the resting potential, $\Delta\varphi_i$ - equilibrium Nernst potential for *i* a kind of ions. The formula (1.53) shows, that the current

through a membrane due to any ion can flow only in case of a difference of membrane potential from equilibrium Nernst potential.

Hence:

$$g_K(\Delta\varphi - \Delta\varphi_K) + g_{Na}(\Delta\varphi - \Delta\varphi_{Na}) = 0. \qquad (1.54)$$

Designating the ratio of membrane conductivities for ions $k = \frac{g_K}{g_{Na}}$ we shall find resting potential as:

$$\Delta\varphi = \frac{\Delta\varphi_{Na} + k\Delta\varphi_K}{k+1}. \qquad (1.55)$$

Taking into account that the ratio of membrane conductivities of a cell for potassium and sodium in a condition of rest approximately equally to the ratio of permeability factors for these ions $k = \frac{g_K}{g_{Na}} = \frac{P_K}{P_{Na}}$ we shall find resting potential of a nervous cell of warm-blooded (for the man) $\Delta\varphi = -82.8\ mV$. At calculation it is accepted that in a condition of rest of a cell: $k \approx 20$, rated Nernst potentials on a membrane of neuron $\Delta\varphi_K = -90\ mV$ and $\Delta\varphi_{Na} = +60\ mV$, see paragraph 1.3.

The formula (1.55) transform to the formula for Nernst potential if permeability of a membrane for ions Na^+ is equal to zero $P_{Na} = 0$.

Further in paragraph 2.2.2.3 we shall prove one more way of calculation of resting potential on a membrane under the formula (2.56):

$$\Delta\varphi = \frac{\sum_i \Delta\varphi_i \omega_i^2 \beta_i}{\Sigma \omega_i^2 \beta_i}, \qquad (1.56)$$

where $\Delta\varphi_i$ there is as before equilibrium Nernst potential for *i* a kind of ions, ω_i - the constants, the dimensional cyclic frequency which depend on capacity and inductance of an excitable membrane ($\omega_{Na} \approx 6000\ s^{-1}$; $\omega_K \approx 3000\ s^{-1}$), β_i - some weight factor which will be determined later in the formula (2.45).

The formula (1.56) transform to the formula for Nernst potential if weight factors $\beta_K = 1$ and $\beta_{Na} = 0$.

Chapter 2. Action Potential

At excitation of a cell on its membrane due to change of permeability of a membrane for ions and occurrence of ionic currents through a membrane there is a change of signs on potential. On the internal side of a membrane there is potential to become positive concerning external side. This process refers to depolarization of membranes or occurrence of action potential. Returning of membrane potential after it depolarization to an initial level (resting potential) refers to repolarization of membranes.

The action potential arises on excitable cells: nervous and muscular (also endocrine cells).

Existence of vivid organism in many aspects is defined by processes of carry of the information in its nervous system. Biophysical bases of occurrence and movement of a separate nervous impulse or action potential represent the big interest both from the point of view biological, and for applied medicine, pharmacology, physiotherapy, anesthesiology, etc.

2.1. Biophysics of the nervous impulse

Nervous cell or neuron, figure 2.1a, is an excitable cell in which condition of rest on the internal side of a membrane there is a negative resting potential concerning external side.

The main purpose of neuron there is perception, carry, processing and the further transfer definitely coded as electric impulses (action potentials) information in an organism.

Neuron always consist of a cell body named “soma” (1) in which there is a nucleus and others organelles, usually short branches named “dendrites” (2) (from Greek dendron - a tree), and a long branch called “axon” (3) or a nervous filament. Nervous excitation covers all surface of a cell and is propagated on axon.

Depending on number of branches neurons are unipolar (one branch - axon), bipolar (is axon and single dendrite) and multipolar (axon and more than two dendrites). At the some sensory neurons there are branch soon after diverge from a cell body 5, figure 2.1b, can bifurcate on two branches. One branch carries excitation from receptors to a cell body another branch from a cell body to spinal cord or a brain. These neurons refer to pseudounipolar. On figure 2.1a it is shown the multipolar neuron.

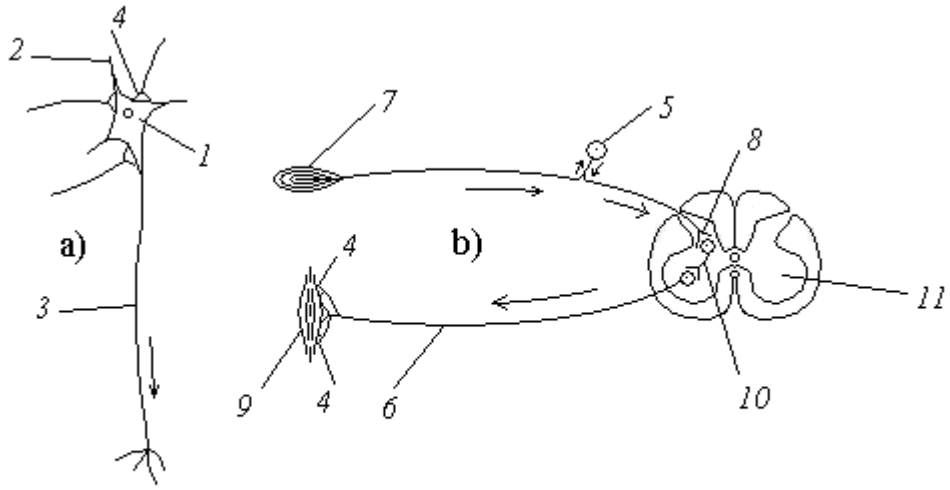

Fig. 2.1.

Axons are communications for efferent signals from a body of nervous cells (soma) to membranes of cells of innervate bodies and tissues or to another neurons.

As against axon on dendrites the signals to a cell body are transferred.

Efferent refer to the nervous (electric) impulses moving from a body of a cell, Afferent - to a body of a cell refer to.

Communication between neurons or neurons and innerving cells is carried out through special contacts - synapses 4 which play a role of biological diodes, i.e. they pass an electric signal only in one direction. The length of the man axon reaches 1 *m*. Neurons are usually incorporated into reflex arches - a way of propagation of action potential, figure 2.1b. The elementary reflex arch will consist of two neurons - sensory 5 and motor 6 (so-called two-neural or monosynaptic reflex arch). The signal from a receptor 7 is transferred to sensory (afferent) neuron 5, and then through synaptic communication 8 is direct on motor (efferent) neuron 6 and further on innerving body, for example, a muscle 9. However transfer of a signal is more often passes on three-neural or polyneural (polysynaptic) reflex arches. Between sensory and motor neurons is present one or the

several inserted neurons 10 included in a spinal cord 11. The information from inserted neurons can be transferred on conducting ways of a spinal cord to a vertical direction in conformable areas of a brain and there to be analyzed. There is also a return stream of the information.

Axons or nervous filaments are non myelinizative and myelinizative.

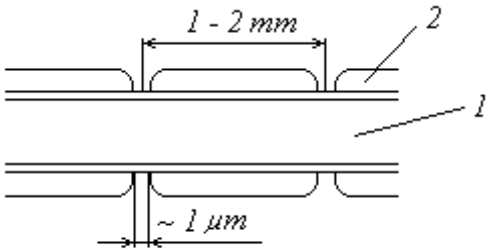

Fig. 2.2.

The non myelinizative nervous filament it is the cylinder in diameter from 0.5 up to $25\ \mu m$ (squid giant axon it reaches by diameter up to $600\ \mu m$) which surface is formed by a cellular membrane. Inside is axoplasma.

The myelinizative nervous filament 1, figure 2.2, is covered with a fatty case (Schwann cells) 2 or myelin envelopment. The myelin envelopment through approximately equal intervals $\sim 1-2\ mm$ interrupt creating open sites of axon membrane in the length $\sim 1\ \mu m$. These open sites there are refers to nodes of Ranvier.

Nervous filaments are incorporated in original electric cables - nervous trunks or nerves.

2.1.1. Action potential of neuron

In a condition of rest the neuron has inside negative resting potential *RP* approximately $-80\ mV$ concerning of a membrane external surface, i.e. there is neuron in the polarized condition, figure 2.3. If to lower potential up to $-50\ mV$ (potential of depolarization *PDep* or a critical level of depolarization) then will take place spontaneous depolarization of membranes. The potential on an internal surface of a membrane changes a sign and reaches approximately $+40\ mV$ - action potential *AP*. Then the membrane potential again spontaneously changes the sign and to become equal approximately $-100\ mV$ - potential of hyperpolarization *PG*. Finally, the potential on a membrane is established at a level of resting potential $RP = -80\ mV$. Change of potential conditionally on figure 2.3 is shown by arrows on the right side. If the membrane potential does not reach size *PDep* the occurrence of *AP* do not occur there is also membrane potential at once comes back to *RP* (small arrows on axes of potential).

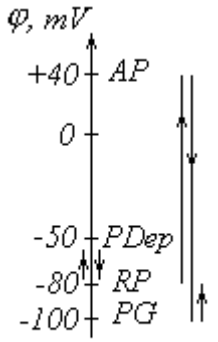

Fig. 2.3.

In a condition of a cell rest as a result of active ionic transport concentration of ions potassium K^+ into axoplasma is supported approximately in 30 times more than outside of neuron and concentration of ions of sodium Na^+ approximately in 10 times is less than outside of neuron.

Initially voltage-gated sodium and potassium ionic channels in a neuron membrane basically are closed. Openly only it is a little potassium ionic channels ($\sim 1\%$) which create at a neuron membrane the potassium channel conductivity in a condition of cell rest.

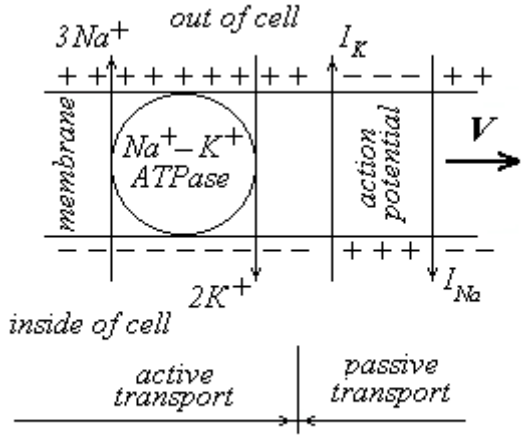

Fig. 2.4.

Voltage-gated ionic channels there are the large albuminous molecules inserted into a plasmatic membrane which open and closed at the certain value of potential on a membrane.

If to lower the membrane potential to value *PDep* and to support this potential to constants with the help of the special device (a method of potential fixing or voltage-clamp for the first time applied by the English scientist K.S. Cole in 1949) in the beginning open sodium ionic channels. Ions Na^+ on gradients of concentration and potential direct inside of a cell (sodium current I_{Na}) charging an internal membrane surface a positive charge up to value *AP*, figure 2.4. If in

rest the ratio of membranes permeability factors for ions was equal $P_{Na} : P_K = 0.04 : 1$ after opening sodium channels this ratio becomes equal $P_{Na} : P_K = 20 : 1$.

Approximate size of action potential can be estimated under the formula (1.11). Thus the action potential has the sodium character.

Then through $1-2\,ms$ the sodium channels are closed. The increasing number of voltage-gate potassium channels gradually opens. Ions K^+ on a gradient of concentration leave a cell (potassium current I_K) back out the negative potential on an internal surface of a membrane. Then basically are closed and potassium channels.

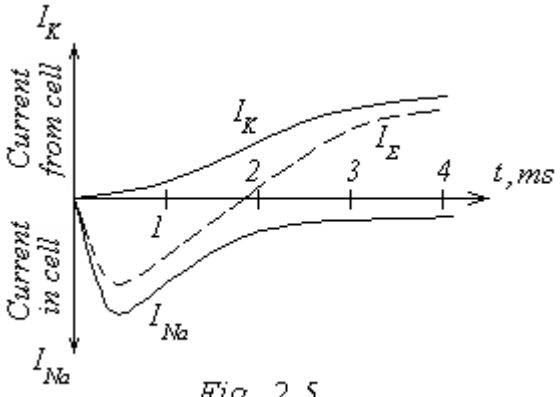

Fig. 2.5.

Dependences of sodium current I_{Na} and potassium current I_K on time, and also a total current I_Σ through membrane received with help a method of potential fixing, are shown on figure 2.5.

Really in the organism these dependences have some other character, figure 2.18, since the potential on a membrane is not fixed.

Processes of ions carry at occurrence *AP* are carried out on corresponding gradients of concentration and potential for these ions and are passive transport. The action potential of neuron is formed due to two types of ions Na^+ and K^+ it is so-called two-ionic system of formation of action potential.

After generation of *AP* or a nervous impulse (frequently as a nervous impulse understand cumulative potential of fibres group of all nerve) a site of a membrane during $5-10\,ms$ is in refractory period i.e. cannot be excited again. At this time the sodium-potassium pump (Na^+/K^+ - ATPase) which is activated by increase of ions Na^+ concentration inside of a cell due to energy of ATP hydrolysis restores initial levels of concentration Na^+ and K^+ on both sides of a nervous fibre membrane resulting a membrane in the initial condition polarized up to a necessary level, figure 2.4.

The *AP* moves with speed ***V*** aside to refractory site opposite since the refractory site is not excitable.

There are the medicinal substances temporarily blocking of sodium ionic channels, for example, anesthetics - lidocaine, novocaine, cocaine, etc. They reduce local sensitivity and reduce a pain.

2.2. Mathematical modeling of action potential

There are various ways of the mathematical description of action potential. Till now the mathematical description of a moving nervous impulse is carried out with the help of Hodgkin – Huxley model more often therefore we shall initially consider this model [9].

2.2.1. Hodgkin – Huxley model

Till now the mathematical description of a moving nervous impulse is carried out with the help of Hodgkin – Huxley model more often.

Let's consider how lines of electric field strength $\boldsymbol{E}$ in the nervous fibre are distributed at occurrence *AP* and its movement along coordinate *X*, figure 2.6.

At depolarization of active site of a nervous fibre membrane there are the electric currents flowing along lines of electric field strength $\boldsymbol{E}$. The currents flowing through a membrane have value I_m. They are directed from plus to a minus of potential i.e. on an active site from inside of a fibre to outside of a fibre. Outside of an active site these currents are directed on the contrary. The longitudinal currents flowing on axoplasma having value I_a are directed from an active site to both sides of a fibre. Outside of a fibre longitudinal currents are directed aside an active site.

On figure 2.6 only the vectors of current density $\boldsymbol{j}_m$ flowing through a membrane and the current density $\boldsymbol{j}_a$ flowing aside opposite refractory a site are shown.

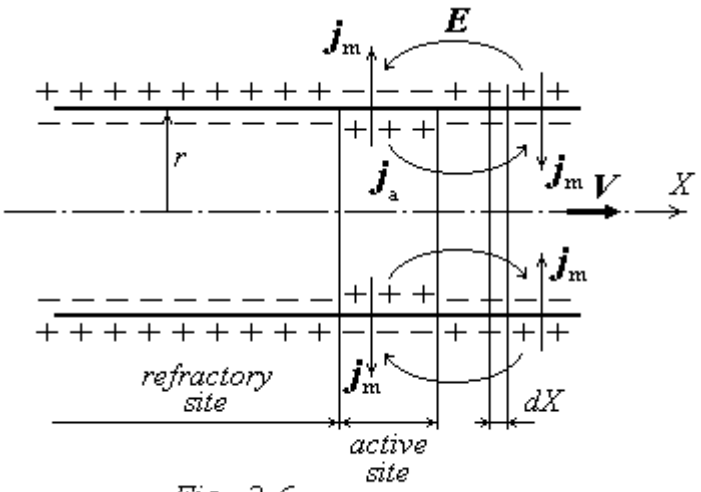

Fig. 2.6.

The movement of ions provided with longitudinal currents reduces potential both on refractory site, and on opposite refractory site. But as the refractory some time is not excitable the membrane of a fibre from the opposite side of an active site is excite. In this direction also there is a movement speed ***V*** of an active site or *AP*. The size of potential of depolarization *PDep* i.e. excitation of this site membrane is determined by opening voltage-gate sodium ionic channels in a membrane. This opening is caused by excess of approaching to a membrane of positive ions charge above taken out from a cell positive ions charge Na^+ due to work Na^+/ K^+ - ATPase used on restoration of initial gradients on a membrane.

As the membrane has capacity the current through a membrane is equal to the sum of a capacitor bias current I_b, and ionic currents I_i:

$$I_m = I_b + \sum_i I_i .$$

The membrane of a nervous cell axon from the electric point of view represents the cylindrical condenser. Therefore, taking into account connection of a bias current with speed of potential change φ on a membrane, we have:

$$I_m = C\frac{\partial \varphi}{\partial t} + \sum_i I_i , \qquad (2.1)$$

where *C* there is capacity of a membrane site, *t* - time.

Under the Ohm law for *i* a kind of ions we shall write down:

$$I_i = g_i^*(\varphi - \varphi_i), \qquad (2.2)$$

where g_i^* there is conductivity of the membrane site of for an examined kind of ions, φ_i - equilibrium Nernst potential for *i* a kind of ions. The current through a membrane is determined by a deviation of potential on a membrane from equilibrium Nernst potential at which the current through a membrane does not flow i.e. at $\varphi = \varphi_i$ a current there is $I_i = 0$.

Taking into account (2.2) the equation (2.1) will be transformed to a kind:

$$I_m = C\frac{\partial\varphi}{\partial t} + \sum_i g_i^*(\varphi - \varphi_i). \qquad (2.3)$$

The received equation (2.3) refers to the equation of currents balance.

If *S* is the area of a membrane site having capacity *C* then divided both parts of the equation of currents balance on area *S*, we shall find:

$$j_m = C_m\frac{\partial\varphi}{\partial t} + \sum_i g_i(\varphi - \varphi_i), \qquad (2.4)$$

where it is designated $j_m = \frac{I_m}{S}$ - membrane current density, $C_m = \frac{C}{S}$ - capacity of unit of a membrane surface (for non myelinizative membrane of squid giant axon $C_m \approx 1\frac{\mu F}{cm^2}$ [10]), $g_i = \frac{g_i^*}{S}$ - conductivity of the membrane area units for *i* a kind of ions.

Let's consider connection between membrane current density and longitudinal currents. The longitudinal current density $j_a = \frac{I_a}{S_a}$ (I_a is a longitudinal current, S_a - the area of cross-section of a nervous fibre) is connected to electric field strength inside nervous fibre *E* under the Ohm law in the differential form:

$$j_a = \gamma_a E = -\gamma_a\frac{\partial\varphi}{\partial X}, \qquad (2.5)$$

where γ_a there is specific conductivity of axoplasm; also connection between electric field strength and a component of a gradient of potential along a strength line $E = -\frac{\partial\varphi}{\partial X}$ is used.

Let's find differential of a longitudinal current density:

$$dj_a = \gamma_a dE = -\gamma_a\frac{\partial^2\varphi}{\partial X^2}dX. \qquad (2.6)$$

Multiplied the received equality on the area of cross-section of a nervous fibre $S_a = \pi r^2$ we shall find change of a longitudinal current:

$$dI_a = S_a dj_a = -\gamma_a\pi r^2\frac{\partial^2\varphi}{\partial X^2}dX. \qquad (2.7)$$

Let's consider a site of a nervous fibre in length dX, figure 2.6. Change of the membrane current through the area dS of a nervous fibre site in the length dX which equal $dS = 2\pi r dX$ we shall find under the formula:

$$dI_m = j_m dS = j_m 2\pi r dX. \qquad (2.8)$$

The increase of the membrane current dI_m causes to reduction of a longitudinal current $-dI_a$. The various direction of currents change is reflected by the sign minus. Hence:

$$dI_m = -dI_a. \qquad (2.9)$$

Substituting in this equality the formulas for changes of currents (2.7) and (2.8) we shall find expression for membrane current density:

$$j_m = \frac{\gamma_a r}{2}\frac{\partial^2\varphi}{\partial X^2}. \qquad (2.10)$$

Substituting the found value of membrane current density (2.10) in the equation (2.4) we receive:

$$\frac{\gamma_a r}{2}\frac{\partial^2\varphi}{\partial X^2} = C_m\frac{\partial\varphi}{\partial t} + \sum_i g_i(\varphi - \varphi_i). \qquad (2.11)$$

The equation (2.11) belongs to group so-called named «the telegraphic equations» [2]. If to use the wave equation:

$$\frac{\partial^2\varphi}{\partial X^2}=\frac{1}{V^2}\frac{\partial^2\varphi}{\partial t^2} \qquad (2.12)$$

for potential on a membrane correct for a wave of potential (action potential) any form $\varphi=\varphi\left[\omega\left(t-\frac{X}{V}\right)\right]$ where ω is a cyclic frequency of a wave, *V* - its speed we shall receive:

$$\frac{\gamma_a r}{2V^2}\frac{\partial^2\varphi}{\partial t^2}=C_m\frac{\partial\varphi}{\partial t}+\sum_i g_i\left(\varphi-\varphi_i\right). \qquad (2.13)$$

The equation (2.13) allows calculate the change of potential φ for a membrane depending on time *t* in any cross-section of a nervous fibre.

2.2.1.1. The theory of functioning of ionic channels "gate"

According to Hodgkin – Huxley model the following scheme of functioning of ionic channels is accepted.

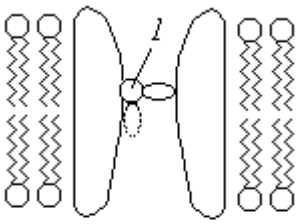

Fig. 2.7.

Ionic channels, figure 2.7, are have "gate" 1 (are shown conditionally) which can be open or closed depending on size and a sign on potential on a membrane. Are experimentally registered "gated" currents which are defined by movement of the ions which are taking place in structure of "gate". "Gated" currents in ~ 1000 times are less than ionic currents through channels. During transition of the channel in the open or closed condition are carried out conformable changes of a molecular complex of the ionic channel. The speedy conformable changes occur in the sodium ionic channel. Time of its transition from the closed state in open state is $\sim 1\,ms$.

The potassium channel for opening should be preliminary activated and only then it can be open. We shall designate probability of the potassium channel activation *n*.

It is experimentally established that the probability of opening of the potassium channel is equal n^4.

In a condition of rest some part of potassium channels is always open. Therefore a membrane in rest is penetrable for ions K^+.

Let's consider functioning of the sodium channel. Evolutionary it should be closed more reliably since it is necessary to support strictly difference of ions Na^+ concentration on a membrane, Reduction of this difference due to increase in concentration of sodium inside a cell initiates work Na^+/K^+ - ATPase and results in additional energy consumption.

Therefore conformable changes of a molecular complex of the sodium ionic channel at decrease in potential on a membrane more complex than potassium the channel. The sodium channel initially is in inactive state. It is necessary for resulting at first in non inactive state from which it can be activated. And only then the sodium channel will open. The probability of transition in non inactive state is equal *h*. The probability of activation of the sodium channel is equal *m*.

It is experimentally established that the probability of opening of the sodium channel is equal m^3h.

On figure 2.8 the block-diagram of sequence of opening i.e. conformable transitions of sodium and potassium channels is shown, and also probabilities of channels transitions from one condition in another are specified.

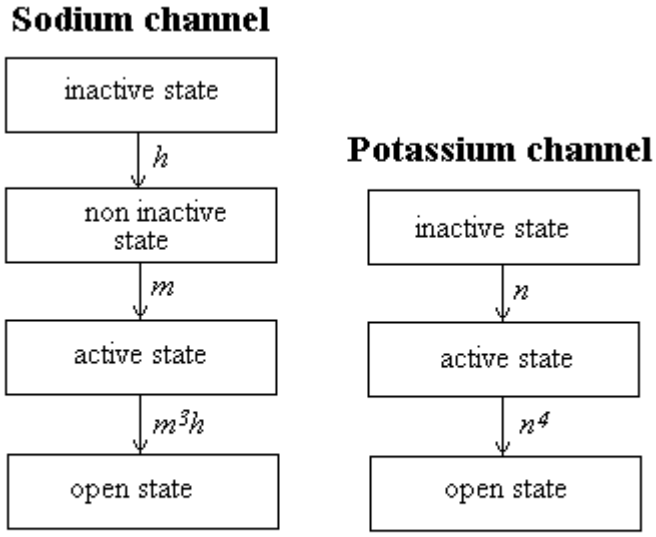

Fig. 2.8.

All probabilities in Hodgkin – Huxley model are functions of time. These functions can be found from the kinetic equations:

$$\frac{dn}{dt} = \alpha_n(1-n) - \beta_n n, \qquad (2.14)$$

$$\frac{dh}{dt} = \alpha_h(1-h) - \beta_h h, \qquad (2.15)$$

$$\frac{dm}{dt} = \alpha_m(1-m) - \beta_m m. \qquad (2.16)$$

Factors α_n, α_h, α_m, β_n, β_h, β_m apparently do not depend on time. Hodgkin and Huxley have suggested calculate them under experimentally selected formulas:

$$\alpha_n = \frac{0.01(V+55)}{1-e^{-\frac{V+55}{10}}}, \qquad \beta_n = 0.055e^{-\frac{V}{80}}, \qquad (2.17)$$

$$\alpha_h = 0.0027e^{-\frac{V}{20}}, \qquad \beta_h = \frac{1}{1+e^{-\frac{V+35}{10}}}, \qquad (2.18)$$

$$\alpha_m = \frac{0.1(V+40)}{1-e^{-\frac{V+40}{10}}}, \qquad \beta_m = 0.108e^{-\frac{V}{18}}. \qquad (2.19)$$

Let's note the main distinction of functioning of ionic channels for sodium and for potassium.

The ionic channel for sodium after its opening has certain «life time» in an open condition. On figure 2.5 it is shown, that at this time through the channel flows the sodium current I_{Na}. "Life time" makes it approximately $1-2\,ms$ and is determined by a structure and functioning of molecular transformations of the "gated" mechanism. Then the channel is closed irrespective of potential on a membrane. "Life time" of the sodium channel in an open condition determine the duration of action potential.

The potassium channel has no strictly certain "life time". The current through the potassium channel I_K after its opening is reduced in process of reduction of membrane potential under the Ohm law (2.2) $I_K = g_K^*(\varphi - \varphi_K)$ and stops after achievement of Nernst potential for potassium $\varphi = \varphi_K$. Then the potassium channel is closed during the refractory period of a nervous fibre. Average time of closing of the

potassium channels on an active site of a nervous fibre, figure 2.6, determines the duration of the refractory period.

Hodgkin and Huxley have assumed that specific conductivity of a membrane for potassium is equal:

$$g_K = \bar{g}_K n^4. \qquad (2.20)$$

Specific conductivity of a membrane for sodium is equal:

$$g_{Na} = \bar{g}_{Na} m^3 h, \qquad (2.21)$$

where $\bar{g}_K$ and $\bar{g}_{Na}$ there are the maximal specific conductivity of a membrane for potassium and sodium at completely open "gates" of ionic channels.

Taking into account formulas for specific conductivities of membrane (2.20) and (2.21) the equation (2.13) it is possible to write down as:

$$\frac{\gamma_a r}{2V^2}\frac{d^2\varphi}{dt^2} = C_m \frac{d\varphi}{dt} + \bar{g}_K n^4(\varphi - \varphi_K) + \bar{g}_{Na} m^3 h(\varphi - \varphi_{Na}) + g_Y(\varphi - \varphi_Y), \qquad (2.22)$$

where g_Y there is specific conductivity of a membrane for other ions which move through a membrane due to simple diffusion so-called specific conductivity for a current of outflow. The current of outflow is determined by movement basically of chlorine ions Cl^-, and also in a small degree and other ions except for ions Na^+ and K^+.

The received equation (2.22) refers to Hodgkin - Huxley equation.

Hodgkin - Huxley equation well describes propagation of action potential (nervous impulse) on a nervous fibre and change of potential on neuromembrane depending on time in any point of a nervous fibre.

2.2.1.2. The solution graph of Hodgkin – Huxley equation. Deformities of Hodgkin – Huxley model

Equation of Hodgkin – Huxley has been solved by them in 1952 numerically manually (the computer yet was not) and then since 1959 this equation repeatedly was solved on the computer. The results of the solution which are shown on figure 2.9 coincide with the results received experimentally. The membrane potential φ (or *AP*) on an internal surface of nervous fibre membrane is function of two variables: longitudinal coordinate *X* and time *t* i.e. $\varphi = \varphi(X, t)$. If to fix coordinate *X* the graph of potential dependence φ from time looks like, shown on figure 2.9.

Such dependence of potential change on a membrane on time takes place consistently in each point of non myelinizative nervous fibre. For a myelinizative nervous fibre this dependence of potential on time is observed only in nodes of Ranvier, figure 2.2, on open sites of a plasmatic membrane. The action potential *AP* as though jumps from nodes on nodes. It increases speed of a nervous pulse. However there is a restriction in distance between nodes of Ranvier, and hence in speed of a nervous impulse. The distance between nodes of Ranvier should be such that an electric field of one node was capable to excite a membrane in the next node. Otherwise the action potential cannot be propagated on a nervous fibre.

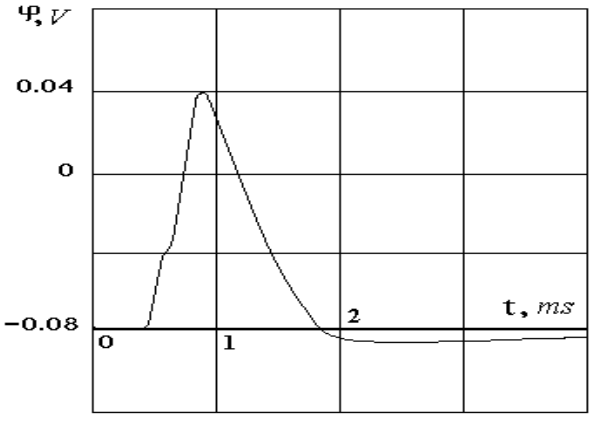

Fig. 2.9.

The nervous fibre works by a principle «all-or-none». I.e. the action potential or arises or does not arise. There are no big and small action potentials. All impulses propagating on nervous fibres have identical amplitudes. Depending on diameter of a nervous fibre the speed of a nervous impulse changes only. The more diameter of a nervous fibre there is more speed of a nervous impulse. Speeds of nervous impulses in an organism of the man are in the range $0.5-120\ m/s$.

The Hodgkin – Huxley model has a number of essential deformities and contradictions.

First that all formulas of the model are selected proceeding from results of experiments in a method of voltage-clamp. Really the potential on a membrane is not fixed therefore, for example, formulas for factors (2.17) - (2.19) depend on time. Whether these formulas will look like (2.17) - (2.19) at change of potential on a membrane? On this question of the answer is not present. Frequently resulted analytical solutions of the equations (2.14) - (2.16) [6] for unstable potential on a membrane obviously are unacceptable. All aforesaid including empirical character of laws for probabilities conformable transformations of ionic channels in (2.20) and (2.21) does not allow to consider this theory as self-coordinated.

Second complex empirical dependences of factors α_n, α_h, α_m, β_n, β_h, β_m on potential specify that in Hodgkin – Huxley model some basic physical phenomenon is not taken into account.

Thirdly deformity of the Hodgkin – Huxley model of nervous impulse propagation will be that at opening voltage-gate ionic channels the ions through them move on a spiral. It creates rather strong magnetic field of ionic channels which needs to be taken into account using inductance of a membrane. However in the equation (2.13) inductance is absent.

2.2.2. Inductance-capacitor model

In a basis of Hodgkin – Huxley model there is a linear differential equation (2.13) from which strictly speaking it is impossible to receive the solution as a stable solitary wave. For overcoming this contradiction in Hodgkin – Huxley model very complex phenomenological dependence between conductance of ionic channels and potential in the same points of a nervous fibre is used. Historically used dependence is based on that with the help of "potential fixing» method smooth change of ionic currents was revealed. Such change of currents has been explained by consequence of similar change of ionic channels conductivity. Authors of this model specified limitation of its mathematical party [7].

This limitation is connected to the following general-physical reasons. According of Hodgkin – Huxley model the membrane of a nervous fibre has only capacitor properties but at occurrence of electromagnetic wave there is a continuous transition of energy from electric in the magnetic form and back. On the data [11] on distance $1.3\,mm$ from a surface of a nerve the magnetic field of the nervous impulse propagating on a sciatic nerve of a frog reaches $120\ pT$. But big enough inductance of system is necessary for keeping a magnetic field without strong dispersion of energy as radiation.

Cole and Baker [12] specified existence of the big inductance of neuromembrane. This inductance exists only during time while the membrane is in the excited condition. In a condition of rest inductance has no biotissue and its relative magnetic permeability $\mu \approx 1$ [13].

2.2.2.1. Inductive properties of the neuron membrane

Let's consider inductive properties of neuron excitable membrane.

The great number of ionic channels in parallel located in a membrane should have rather big inductance. Therefore smooth change of ionic currents at excitation of neuromembrane is in many respects display of the electromagnetic induction law action. Taking into account capacity of a membrane it is possible to assimilate the ionic channel to an open oscillatory contour. As electric analogue of a nervous fibre membrane it is possible to use the film medium in which these contours freely float, fig. 2.10.

The ionic channels cooperate with each other in process depolarization of neuromembrane with the help of electric and magnetic fields. The lines of a magnetic field strength which calculation it will be given below also are shown on fig. 2.10.

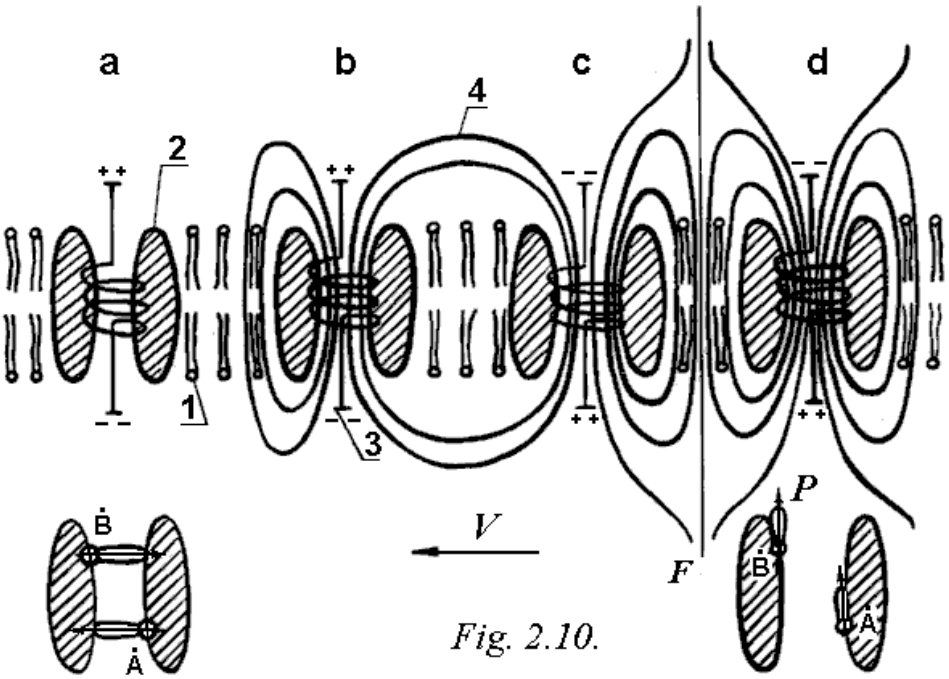

Fig. 2.10.

In not excited area of neuromembrane the ionic currents through channels are absent since they are closed, and the magnetic field does not arise (fig. 2.10, the channel "a"). In depolarize area the magnetic field of one channel pushes away the next channel (channels "c" and "d"). On the border of depolarization the magnetic field of one channel "c" can influence another "b" due to different directions of a potential difference on the ends of ionic channels - contours. Thus the magnetic field of the channel "c" opens the channel "b".

In a basis of opening of the channel "b" there is "gate system" connected with transitions of electrons or paramagnetic groups - radicals $\dot{A}$ and $\dot{B}$ having magnetic moment ***P*** from singlet state (opposite directed) in triplet state (equally directed). As shown in [14] a constant of speed of such transition α is magneto-dependent:

$$\alpha \sim \frac{1}{\tau} \sim (g_A - g_B)\mu_B H\,, \qquad (2.23)$$

where τ there is a constant of reaction time, g_A and g_B - Lande g-factors for radicals $\dot{A}$ and $\dot{B}$, $\mu_B = 9.27 \cdot 10^{-24}\ \frac{J}{T}$ - Bohr magneton, H –magnetic field strength. At opening ionic channels there should be an even number (minimum two) equally directed magnetic moments. The minimum possible size of the total magnetic moment for two equally directed vectors ***P*** is $\sum_{i=1}^{2} P_i = 2\mu_B$. If to accept internal diameter of the ionic channel $d = 0.8\,nm$ [15], and his height $H = 8\,nm$ the internal volume of channel equal $V = \frac{\pi d^2 H}{4} = 4.02\ nm^3$. As a rule in estimated calculations we shall not do distinctions between geometrical characteristics of channels for various types of ions. Hence magnetization of such system is:

$$J = \frac{\sum P}{V} = 4.61 \cdot 10^3\ \frac{J}{T\,m^3}\,. \qquad (2.24)$$

To this size of magnetization there corresponds an induction of a magnetic field $B_P = \mu_0 J = 5.8\, mT$ where $\mu_0 = 4\pi \cdot 10^{-7}\ \frac{N}{A^2}$ there is a magnetic constant. The received estimation of a magnetic field induction into the ionic channel due to open "gate system" is minimally possible.

Usually such order of constant magnetic field induction is applied in the magneto-therapeutic procedures.

After passage of action potential the magnetic field of the current arising due to a hyperpolarizing potential difference closes ionic channels. Owing to a known time delay of work of various types channels their opening in not excited part of a membrane is carried out due to a magnetic field of sodium channels, and closing (after passage of action potential) - due to a magnetic field of potassium channels.

Thus due to own magnetic field neuromembrane the excitation of one channel results in excitation next being propagated further with speed ***V*** (fig. 2.10).

According to Cole and Baker [12] the inductance of unit of the membrane area of squid giant axon $L_m = 0.1\frac{H}{cm^2} = 10^3\ \frac{H}{m^2}$. In Ranvier nodes of myelinizative nervous fibres of warm-blooded the ionic channels density in 20 times more [15] i.e. $L_m = 2 \cdot 10^4\ \frac{H}{m^2}$.

This inductance can be created only due to spiral (solenoidal) movement of ions in the ionic channel. Such assumption is especially correctly (data on a chemical compound and structure of ionic channels a little) because modern representations about channels structure assume that channels are formed by the integrated proteins having structure of a α-spiral [16]. Besides we shall note, that the sizes of Na^+ ions ($0.19\, nm$) and K^+ ($0.266\, nm$) [10] much less than internal diameter of the ionic channel $d = 0.8\, nm$.

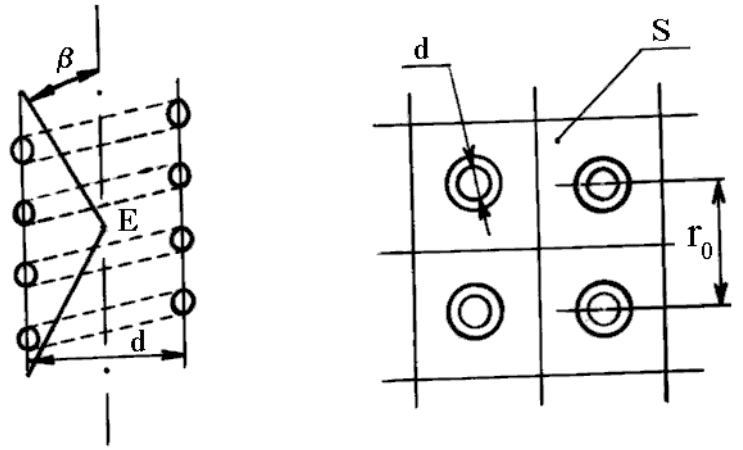

Fig. 2.11.

Let's find a magnetic field inside the ionic channel (fig. 2.11a), arising due to spiral movement of ions. If to assimilate the channel to the solenoid at propagation of action potential there will be inside it a field with an induction [17]:

$$B_E = \frac{\mu\mu_0}{2} \cdot \frac{I\, n}{h_1} 2\cos\beta\,, \qquad (2.25)$$

where h_1 there is a fraction of a way through the channel which the ion passes on a spiral, *I* - a current through the channel, *n* - number of a solenoid turns.

For calculation of B_E it is necessary to know size of a current through the channel during propagation of action potential. From a condition that the density of a current in an excitable membrane of squid giant axon reaches $j = 1\frac{mA}{cm^2} = 10\ \frac{A}{m^2}$ [10], and in Ranvier nodes of myelinizative nervous fibre accordingly

$j = 200\,\frac{A}{m^2}$ if to know the area of membrane *S* falling one channel there is possible to find a current through channel $I = jS$, fig. 2.11b. For a finding of this area we use data that at an excitable membrane of myelinizative nervous fibre on $1\,\mu m^2$ fall $N = 10^4$ ionic channels in Ranvier nodes [15].

On one micron of a membrane it is stacked $N_0 = \sqrt{N} = 100$ channels, and distance between them is $r_0 = \frac{1}{N_0} = 0.01\,\mu m$. Hence the area falling one channel is $S = r_0^2 = 10^{-16}\ m^2$, and a current through channel $I = 2 \cdot 10^{-14}\ A$.

It is necessary to know also number of solenoid turns *n*, i.e. quantity of coils which the ion are done at movement in the channel moving on spirals.

It is known that connection of inductance with characteristics of the solenoid looks like:

$$L = \mu\mu_0 \frac{n^2}{h_1} S. \qquad (2.26)$$

Taking into account thickness of biomembrane $H \approx 8\,nm$, we shall accept a fraction of a way through the channel which the ion passes on a spiral, $h_1 = 0.6H = 5\,nm$. Hence, number of coils which ion are done in the channel $n = \sqrt{\frac{L_m h_1}{\mu\mu_0}} = 8.9$ where $L_m = \frac{L}{S} = 2 \cdot 10^4\ \frac{H}{m^2}$. It is possible to find a step of spiral Δh on which the ion goes $\Delta h = \frac{h_1}{n} = 0.56\,nm$. It is very close to a step of α-spiral - $0.54\,nm$ [16] that specifies validity of the resulted estimations. Therefore at the further analysis we shall assume that the ion goes in the channel on a spiral with step $\delta = 0.54\,nm$.

Value $\tan\beta = \frac{d}{h_1} = 0.16$ i.e. angle $\beta = 9^o 6^/$, fig. 2.11a. Substituting the received value in the formula (2.25) we shall find $B_E = 4.4 \cdot 10^{-11}\ T$. The received value of a magnetic field induction in the channel due to spiral movement of ions is much less than what arises for a couse "gate systems" of channel $B_P = 5.8\,mT$.

Let's calculate now a magnetic field arising near to a membrane of a nervous fibre during its excitation. For this purpose we shall find distribution of a magnetic field induction along line *F* - *F* (fig. 2.10). Each ionic channel has the magnetic moment P_K arising as a result of summation of the magnetic moments of "gate system" and spiral movement of ions in the channel. In any point of M on line *F* - *F*, fig. 2.10, it is possible to find a magnetic field induction under formula $B_M = B_1 - B_2$ (fig. 2.12).

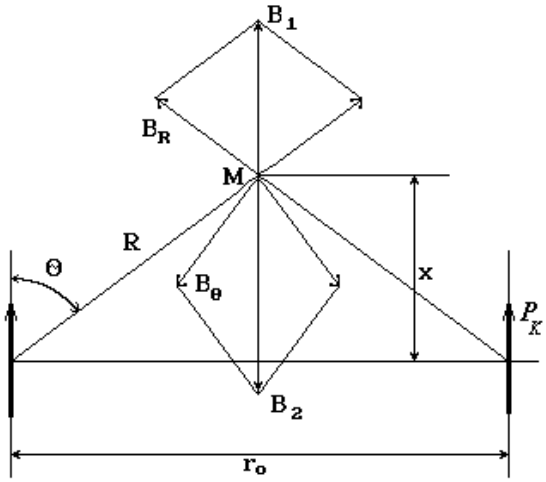

Fig. 2.12.

Values of radial B_R and tangential B_Θ components of a field induction of the magnetic moment are under formulas [17]:

$$B_R = \frac{2\mu\mu_0 P_K \cos\Theta}{4\pi R^3},\ B_\Theta = \frac{\mu\mu_0 P_K \sin\Theta}{4\pi R^3}, \qquad (2.27)$$

where Θ there is a angle between a vector of the magnetic moment and the radius-vector in examined point M, and *R* is the module of a radius-vector (fig. 2.12).

After simple transformations we shall find:

$$B_M = \frac{4\mu\mu_0 P_K}{\pi r_o^3}\cdot\sin^3\Theta(2\cos^2\Theta - \sin^2\Theta). \qquad (2.28)$$

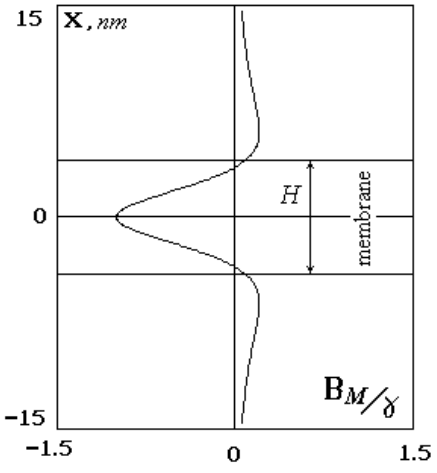

Fig. 2.13.

The graph of function (2.28) recounted to coordinate *X* under formula $X = \frac{r_0}{2\tan\Theta}$ is shown on fig. 2.13. On the figure the value $\gamma = \frac{4\mu\mu_0 P_K}{\pi r_0^3}$.

Investigating function (2.28) on an extreme we shall find that for $X = \pm \frac{r_0}{2\sqrt{2/3}} = 6{,}12\,nm$ i.e. on distances of $2.12\,nm$ from surfaces of a membrane on its both sides there are areas of high magnetic field inductions. In these areas all particles having the magnetic moment will be move.

Value of the magnetic field induction a in points of maxima on both sides of a membrane can be calculated under the formula:

$$(B_M)_{\max 2} = \frac{32}{25}\left(\frac{2}{5}\right)^{1/2} \frac{4\mu\mu_0 P_K}{\pi r_0^3}. \qquad (2.29)$$

Substituting numerical values in the formula (2.29) we shall receive $(B_M)_{\max 2} = 0.006\,mT$. In the central part of a membrane between channels from the formula (2.28) under condition $\Theta = \frac{\pi}{2}$ we shall find $(B_M)_{\max 2} = 0.03\,mT$. Both these sizes there is less than induction of a field inside the channel arising due to it "gate system" $B_P = 5.8\,mT$.

Thus the maximal magnetic field in a membrane at propagation on it of action potential is arises inside ionic channels. Thus value of the magnetic field induction inside the ionic channel is comparable with the sizes used in a magnetotherapy [18, 19].

Hence the medical action of a constant magnetic field on an organism apparently is connected to its influence on "gate system" of ionic channels, and with reduction of intensity of passive ionic transport. As the greatest intensity of ionic currents through a membrane is observed with neurons it is possible to assume the center of influence of a constant magnetic field on an organism there is the nervous system. Thus influence of a magnetic field basically reduces (inactivate) intensity neuroregulative processes.

It is interest on the basis of the offered model of a nervous impulse carry consider interaction of coherent laser radiation with an excitable biological tissue.

Coherent laser radiation will influence propagation of action potential if an open oscillatory contour - the ionic channel - will resonate on frequency of the laser electromagnetic waves.

Cyclic frequency of a resonance can be found under the formula:

$$\omega = \frac{1}{\sqrt{LC}}, \qquad (2.30)$$

where ω there is cyclic frequency of electromagnetic waves, *C* - capacity of one channel which can be found from a condition that the membrane of myelinizative nervous fibre has specific capacity $C_m = 0.05\,\frac{\mu F}{cm^2} = 5\cdot 10^{-4}\,\frac{F}{m^2}$ [15]. Taking into account the area of the membrane falling one channel we shall receive $C = C_m S = 5\cdot 10^{-20}\ F$. Hence according to (2.30) resonant frequency is $\omega = 3\cdot 10^{15}\ s^{-1}$, where it is accepted that inductance of one channel is $L = L_m S = 2\cdot 10^{-12}\ H$.

Meaning that $\omega = \frac{2\pi V_C}{\lambda}$ where V_C there is speed of light, λ - length of a wave of laser radiation we shall find what length of a wave will be the most effective. The following here is necessary the remark. Phase speed of electromagnetic waves V_C in the environment where the wave cooperates with the resonating vibrator more than phase speed of light in vacuum - so-called an abnormal dispersion. However to take into account this phenomenon in estimated calculation there is no necessity as far from a resonance phase speed of

light is less than in vacuum. Accepting $V_C = 3 \cdot 10^8 \frac{m}{s}$ we shall find

$$\lambda = \frac{2\pi V_C}{\omega} = 630 \cdot 10^{-9} m = 630\, nm$$

The received value of length of a wave coincides with length of a wave of red light radiated the helium - neon laser. But this type of the laser as shows experience most frequently and is effectively applied in laser therapy. Additional excitation of ionic channels - oscillatory contours in membranes of biological tissue by coherent laser radiation apparently explains the therapeutic action of this radiation expressing in accelerated healing of various surface ulcer formations.

From the carried out biophysical analysis it is possible do a conclusion that radiation of the helium - neon laser as against action of a constant magnetic field has basically activate character on membrane processes in an organism.

2.2.2.2. Ionic channels as quantum-mechanical systems

Voltage-gated ionic channels are one of key albuminous structures in biological membranes. Ionic channels in a membrane are intended for fast creation of the big ionic fluxes due to passive transport. In particular through open sodium and potassium ionic channels in neuromembrane 10^7 and 10^6 ions in second are transferred [10] Elucidation of character of ions movement in the channel assumes knowledge of structure of all orders of an albuminous molecule (or molecules) structure which the ionic channel will consist. However data on a structure of ionic channels now are limited. Most full now the channel formed by gramicidin A - hydrophobic peptide formed of 15 alternating L- and D-amino acids [1], fig. 2.14, is characterized.

This channel can be used as some model of channels in a biomembrane. Sodium ionic channel of neuromembrane is protein with molecular mass in a range $250 - 300\ kDa$ [20]. The cavity of the channel is filled with molecules of water. Potassium ionic channel worse of sodium ionic channel is investigated.

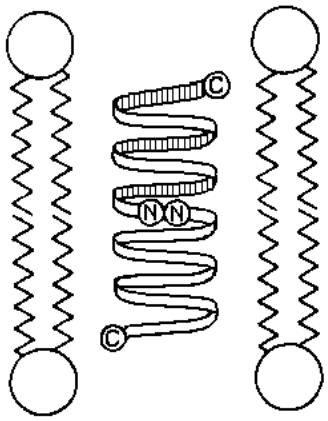

Fig. 2.14.

In this paragraph it is carried out the quantum-mechanical the analysis of ions movement in the channel and some features of ionic channels structure are found out on the basis of known experimental data about biomembrane and ionic channels characteristics.

Among the major experimental results concerning to ionic channels it is possible to note: registration of ionic currents through separate ionic channels, establishment α-spiral structure membrane proteins and detection of significant inductance of neuromembrane during it excitation.

According to Cole and Baker [12, 15] the inductance of unit of a membrane area of squid giant axon $L_m = 0.1 \frac{H}{cm^2} = 10^3 \frac{H}{m^2}$. $L_m = 0.1 \frac{H}{cm^2} = 10^3 \frac{H}{m^2}$. In Ranvier nodes of myelinizative nervous fibres of warm-blooded the ionic channels density approximately in 20 times more [15] i.e. $L_m = 2 \cdot 10^4 \frac{H}{m^2}$.

Such big inductance can be created only due to spiral (solenoidal) movement of ions in the ionic channel. The spiral structure of the channel formed by two molecules of gramicidin A, fig. 2.14, non covalent compounded N-ends in the middle of membrane phospholipids bilayer is established, for example. Gramicidin channel is cation-selective. It is impenetrable for ions of chlorine. Permeability of the channel for monovalent cations there are changes in the following order: $Cs^+ > Rb^+ > K^+ > Na^+ > Li^+$. Inside the channel is filled with water. Ions pass through the channel one by one since its diameter of the channel is $0.4 - 0.5\, nm$. An ion entering into the channel in part dehydrated. Moving of cation is accompanied by carry 5 - 7 molecules of water [1].

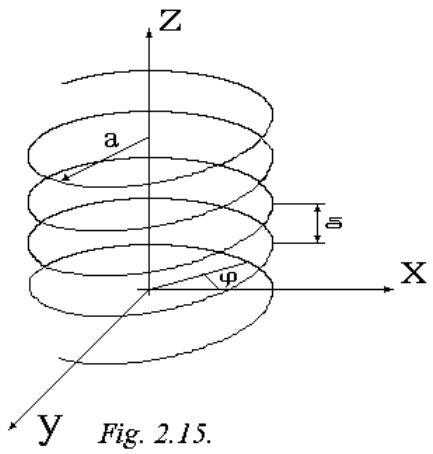

Fig. 2.15.

Let's discuss also a question whether the organization of a spiral trajectory of cation movement is possible at their interactions with the water which is taking place inside of sodium and potassium channels of neuromembrane. Receipt of an ion in the channel is accompanied by partial replacement of its hydrate water cover on the polar groups covering a cavity of the channel and including atoms of oxygen. The sizes of ions dehydrated radiuses of sodium and potassium is $0.095\,nm$ and $0.133\,nm$ [21] in comparison with the sizes of corresponding channels pores $0.31\times 0.51\,nm^2$ (elliptic pore) and $0.33\times 0.33\,nm^2$ [1] allows to organize spiral movement of ions. It is possible that the model of the ionic channel offered Hille [22, 23] is closest to true. According to this model the ion (in particular sodium) in the channel has an environment from three molecules of water which placed: in lateral, in front, and behind of a moving ion. These molecules of water especially lateral are strictly coordinated by the sizes of the ionic channel and form hydrogen bonds with three atoms of oxygen in the channel. Apparently spiral movement of an ion is accompanied by spiral movement of a lateral water molecule so the ion and a molecule of water vary positions. From this point of view in model Hille organically there is a spiral movement of an ion.

Let's present a trajectory of ion movement into the ionic channel as a spiral with step $\alpha = 0.54\,nm$, fig. 2.15.

Analyzing movement of an ion in the ionic channel we shall find the wave function ψ describing an ion in the channel.

For its finding it is necessary to solve Schrodinger equation for an ion moving in the channel. But essentially uncertain size in this equation for the given task is change of ion potential energy at its movement in channel $U(Z)$ where *Z* is coordinate across a membrane.

The assumption of ion spiral movement in the channel is actually equivalent to knowledge of potential energy $U(Z)$.

Schrodinger equation for stationary states of wave function we shall write down as:

$$\Delta\psi + \frac{2m}{\hbar^2}(E - U_0)\psi = 0, \qquad (2.14)$$

where $\Delta\psi$ there is Laplacian of wave function, *m* - mass of ion, $\hbar = 1.054\cdot 10^{-34}\ Js$ - Planck's resulted constant, $E - U_0 = T$ - a difference between full energy of ion in the channel and its potential energy (not dependent on time) which is equal to kinetic energy at excess by energy of ion of potential barrier level $E > U_0$, fig. 2.16. Only this case is the interest since the mass of ion is too great for occurrence of tunnel effect.

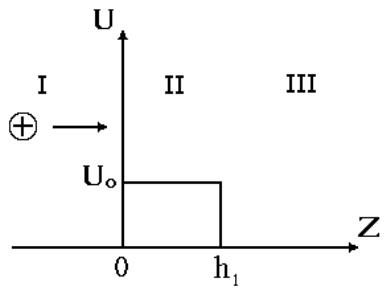

Fig. 2.16.

In connection with that movement of ion has spiral character we shall translate in the equation (2.14) to spiral coordinates under formulas:

$$X = a\cos\varphi; \qquad Y = a\sin\varphi; \qquad Z = \nu\varphi, \qquad (2.15)$$

where *X* and *Y* there are coordinates in section perpendicular axes of the channel, *Z* - coordinate along an axis of the channel, *a* - radius of spiral movement of ion in the channel, φ - an angle of ion rotation around of the channel axis, $\nu = \frac{\delta}{2\pi}$ - a constant equal to a step of ion spiral movement δ divided on 2π.

The equation (2.14) in spiral coordinates will be written down as:

$$4\frac{\partial^2\psi}{\partial\varsigma^2}\left(\frac{4}{a^2\sin^2\varsigma}+\frac{1}{\nu^2}\right)-\frac{16\mathrm{ctg}\varsigma}{a^2\sin^2\varsigma}\frac{\partial\psi}{\partial\varsigma}+\frac{2mT}{\hbar^2}\psi=0, \qquad (2.16)$$

where it is accepted $\varsigma=2\varphi$.

To find the exact solution of this equation it is not possible therefore we shall consider special cases. We shall assume that the radius of the ionic channel is great in comparison with step of spiral movement of ion i.e. $a>>\nu$. In this case wave function has no restrictions on the amplitude.

Translate according to (2.15) to coordinate $Z=\frac{\nu\varsigma}{2}$ there we receive:

$$\frac{\partial^2\psi}{\partial Z^2}+k^2\psi=0, \qquad (2.17)$$

where is $k^2=\frac{2mT}{\hbar^2}$.

In this variant the task of ion passage above a potential barrier has the standard solution [24]. The result of the solution consists that the potential barrier is completely transparent if on its length the integer of half waves of wave function is pack up. On the basis of it we shall estimate the quantum-minimal size of a current through the channel. The current through the ionic channel is determined by a ratio $I=qn_iVS$ where $q=1.6\cdot10^{-19}\ C$ there is a charge of an ion, n_i - numerical concentration of ions in the channel, *V* – velocity of ion, $S=0.158\ nm^2$ - the area of section of a pore for the sodium the channel [1]. Taking into account $n_i=\frac{m_i}{Sh_1}$ where $m_i=1$ there is number of ions in the channel [1, 10] we receive $I=\frac{qV}{h_1}$ where $h_1=8\ nm$ - length of a spiral site of the channel. On length of a spiral of the channel the integer n_k de Broglie half waves should be pack up i.e. $2\pi an=n_k\frac{\lambda}{2}$ where *n* - number of turns which are made an ion in the channel. Substituting $\lambda=\frac{2\pi\hbar}{mV}$ we receive $mVan=n_k\frac{\hbar}{2}$ where $\hbar$ - Planck's resulted constant, and *m* - mass of ion.

Hence velocity of ion is equal $V=\frac{n_k\hbar}{2man}=\frac{n_k\hbar\delta}{2mah_1}$. Substituting the received value of velocity in the formula for a current through the channel we find:

$$I=\frac{n_kq\hbar\delta}{2mah_1^2}. \qquad (2.18)$$

The minimal current will be for $n_k=1$. The radius of ion movement into the channel can be estimated under the formula $a=\sqrt{\frac{S}{\pi}}-r_i$ where *S* there is the area of the channel pore, r_i - radius of ion. The radius of ion movement of sodium is $a_{Na}=0.149\ nm$, and ions of potassium is $a_K=0.032\ nm$.

At calculation under this formula we shall receive minimal potassium current $I_K=0.88\cdot10^{-12}\ A$, and minimal sodium current $I_{Na}=0.32\cdot10^{-12}\ A$. For calculation it is accepted $m_K=64.7\cdot10^{-27}\ kg$, and $m_{Na}=38.2\cdot10^{-27}\ kg$.

Thus the measured current through single channel $I_m \approx 10^{-12}\ A$ [20] is in area of minimally possible quantum sizes. Hence its smooth change essentially cannot be as is observed in experiment.

Let's consider the second case believing the radius of the channel is small enough so $a << \nu$. In this case the second addend in brackets (2.16) can be neglected and Schrodinger equation will become:

$$\frac{\partial^2 \psi}{\partial \varsigma^2} - \mathrm{ctg}\varsigma \frac{\partial \psi}{\partial \varsigma} + k_1^2 \sin^2 \varsigma \cdot \psi = 0, \qquad (2.19)$$

where is $k_1^2 = \frac{mTa^2}{8\hbar^2}$.

Let's consider movement of ion above a potential barrier of the ionic channel in the extent h_1, fig. 2.16. The ion goes along axis *Z*. We shall solve this task similarly [25].

Let's consider area I (outerside of a cell). Wave function we shall write down as a flat wave and a wave with amplitude A_1 is a straight forward, and with amplitude B_1 is reflected from a potential barrier:

$$\psi = A_1 \exp(ikZ) + B_1 \exp(-ikZ), \qquad (2.20)$$

where *k* there is the wave number in area I is approximately equal to wave number in the equation (2.17).

The area II. In this area wave function as the solution of the equation (2.19) it is possible to present as [26]:

$$\psi = A_2 \exp\left[ik_1 \cos\left(\frac{2Z}{\nu}\right)\right] + B_2 \exp\left[-ik_1 \cos\left(\frac{2Z}{\nu}\right)\right], \qquad (2.21)$$

where there is $\varsigma = 2\varphi = \frac{2Z}{\nu}$. The value is $k_1 = \frac{a}{h}\left[\frac{m(E-U_0)}{8}\right]^{1/2}$.

The area III (inside a cell). In this area there is no reflected wave therefore wave function has a simple kind:

$$\psi = A_3 \exp(ikZ). \qquad (2.22)$$

Believing conditions of ion movement before and after membrane approximately identical in (2.22) wave number *k* it is accepted same as well as in (2.20).

On the border of areas I - II at $Z = 0$ a condition should satisfy:

$$\psi(0+) = \psi(0-), \qquad (2.23)$$

$$\psi'(0+) = \psi'(0-). \qquad (2.24)$$

From the condition (2.23) follows:

$$A_1 + B_1 = A_2 \exp(ik_1) + B_2 \exp(-ik_1). \qquad (2.25)$$

As the derivative of wave function in the field of II is equal:

$$\psi'(Z) = i\frac{2k_1}{\nu} \sin\left(\frac{2Z}{\nu}\right)\left\{B_2 \exp\left[-ik_1 \cos\left(\frac{2Z}{\nu}\right)\right] - A_2 \exp\left[ik_1 \cos\left(\frac{2Z}{\nu}\right)\right]\right\}, \qquad (2.26)$$

that $\psi'(0+) = 0$.

Derivative of wave function in area I is equal:

$$\psi'(Z) = ik[A_1 \exp(ikZ) - B_1 \exp(-ikZ)] \qquad (2.27)$$

Hence $\psi'(0-) = ik(A_1 - B_1)$. Thus from a formula (2.24) we shall receive:

$$A_1 = B_1. \qquad (2.28)$$

Let's consider border of areas II - III. On this border a condition should satisfy:

$$\psi(h_1+) = \psi(h_1-), \qquad (2.29)$$

$$\psi'(h_1+) = \psi'(h_1-). \qquad (2.30)$$

The condition (2.29) results in the equation:

$$A_3 \exp(ikh_1) = A_2 \exp\left[ik_1 \cos\left(\frac{2h_1}{\nu}\right)\right] + B_2 \exp\left[-ik_1 \cos\left(\frac{2h_1}{\nu}\right)\right]. \quad (2.31)$$

The condition (2.30) results in the equation:

$$\frac{2k_1}{\nu} \sin\left(\frac{2Z}{\nu}\right)\left\{B_2 \exp\left[-ik_1 \cos\left(\frac{2h_1}{\nu}\right)\right] - A_2 \exp\left[ik_1 \cos\left(\frac{2h_1}{\nu}\right)\right]\right\} = \quad (2.32)$$

$$= A_3 k \exp(ikh_1)$$

We normalize wave function ψ for what we shall accept in (2.20) $A_1 = 1$. Then from (2.28) follows $B_1 = 1$. Hence the equation (2.25) looks like:

$$A_2 \exp(ik_1) + B_2 \exp(-ik_1) = 2. \quad (2.33)$$

We use designations:

$$\alpha = \frac{\exp\left[ik_1 \cos\left(2h_1/\nu\right)\right]}{\exp(ikH)}; \qquad \beta = \frac{\exp\left[-ik_1 \cos\left(2h_1/\nu\right)\right]}{\exp(ikH)}; \quad (2.34)$$

$$\gamma = \frac{k\nu}{2k_1 \sin\left(2h_1/\nu\right)}.$$

The equations (2.31) and (2.32) will be transformed to a kind:

$$A_3 = \alpha A_2 + \beta B_2, \quad (2.35)$$

$$\gamma A_3 = \beta B_2 - \alpha A_2. \quad (2.36)$$

Solving the system of the equations (2.33), (2.35), (2.36) it is received:

$$A_3 = \frac{2\exp(-ikh_1)}{\cos W + i\gamma \sin W}, \quad (2.37)$$

where is $W = -2k_1 \sin^2\left(\frac{h_1}{\nu}\right)$.

Let's find passage factor *D* of the charged particles above a potential barrier i.e. factor of penetration of ions through a membrane. Taking into account that the square of the wave function module $|\psi|^2$ is a probability of particle detection in the given point we find probability of its detection after a membrane in the field III i.e. factor of passage [25]:

$$D = |A_3|^2. \quad (2.38)$$

Carrying out transformations (2.37) we have:

$$A_3 = \frac{2(\cos kh_1 - i \sin kh_1)(\cos W - i\gamma \sin W)}{\cos^2 W + \gamma^2 \sin^2 W}. \quad (2.39)$$

Hence the passage factor is equal:

$$D = \frac{4}{\cos^2 W + \gamma^2 \sin^2 W}, \quad (2.40)$$

where there is coefficient $\gamma^2 = -\frac{(k\nu)^2}{4W(2k_1 + W)}$.

In liquids the ion during thermal movement the most part of time so-called relaxation time oscillate around of balance position jumping on the next place in process of free space (hole) occurrence [17]. The maximal speed of ions movement during fluctuation $V_{\max}$ can be estimated on the basis of approximate to

equality $\frac{mV_{\max}^2}{2} \approx kT$ where in this case $k = 1.38 \cdot 10^{-23} \frac{J}{K}$ is Boltzmann constant, $T = 310\ K$ - temperature of an organism. Hence $V_{\max} = \sqrt{\frac{2kT}{m}} \approx 473 \frac{m}{s}$. Thus the ion oscillates with the speed approximately equal to the most probable speed of thermal movement of a gas molecule. As at a remove of an ion it is needed the work function the jump of an ion on the next place it is carried out with smaller speed $V = \theta V_{\max}$ where θ there is some factor (less than unit) work function of an ion is taking into account. We shall assume that speed of ion jump outside of and inside the channel is approximately identical. This speed determines length of ion probability wave. If the received value of wave length has the order corresponding to distance between nucleus in solid and liquid substances ($\sim 3 \cdot 10^{-10}\ m$ [17]) it specifies an opportunity of interferences effects at interaction of a moving ion with the particles covering an interior of the ionic channel [24]. The given condition is carried out for size $\theta \geq 0.05$. In this case the wave length of probability, for example, ion Na^+ is $\lambda = \frac{2\pi\hbar}{mV} \approx 7{,}33 \cdot 10^{-10}\ m$, for ion K^+ almost is twice less.

Outside of a potential barrier (membrane) is $k^2 = \frac{2mT}{h^2}$. Size of kinetic energy at jump of ion Na^+ (for $\theta = 0.05$ and hence speeds of jump $V = 23.7 \frac{m}{s}$) is $T = \frac{mV^2}{2} \approx 1.07 \cdot 10^{-23}\ J$. Thus $k_2 = 7.36 \cdot 10^{19}\ m^{-2}$. Taking into account that $\nu = \frac{\delta}{2\pi} \approx 8.6 \cdot 10^{-11}\ m$ where δ there is a step of α - spiral equal $0.54\ nm$ we receive $k\nu = 0.074$.

Let's estimate the size $k_1 = \frac{a}{\hbar}\left[\frac{m(E - U_0)}{8}\right]^{1/2}$ for ions of sodium. Size of kinetic energy of ion at jump inside channel $T_1 = E - U_0 = \frac{mV^2}{2}$ hence, $k_1 = \frac{a}{\hbar}\frac{mV}{4}$. Radius of ion movement of sodium $a = 0.149\ nm$. Hence $k_1 = 0.32$ and factor in (2.40) is $\gamma^2 = -\frac{0{,}137}{W(0{,}64 + W)}$.

The curve of dependence (2.40) $D(W)$ represents rather complex curve. For the accepted values h_1, ν, k_1 the size is $W = -2k_1 \sin^2\left(\frac{h_1}{\nu}\right) \approx -0{,}64$. On fig. 2.17 calculation of dependence of size *D* from *W* in a narrow range $-0.7 < W < -0.3$ is shown.

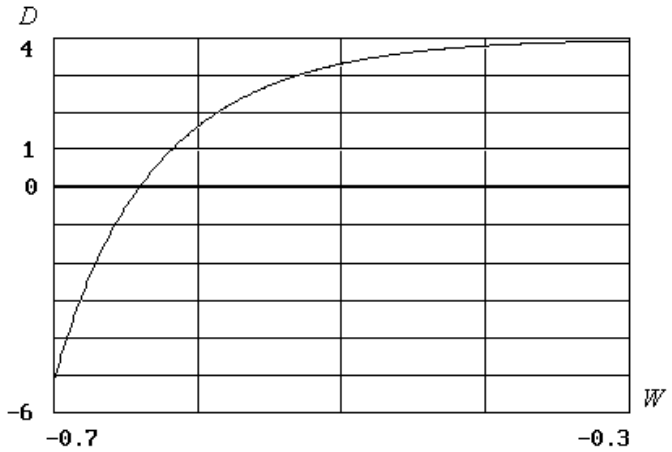

Fig. 2.17.

Really the factor of passage should be less units and more zero. Thus according to (2.40) the inequality should be observed:

$$\frac{4}{\cos^2 W + \gamma^2 \sin^2 W} \le 1. \qquad (2.41)$$

Hence:

$$\sin^2 W \ge \frac{3}{\gamma^2 - 1}. \qquad (2.42)$$

In an examined range of values the condition equivalent (2.42) $W^2 \ge \frac{3}{\gamma^2 - 1}$ is obviously realized. In connection with $W = -2k_1 \sin^2\left(\frac{h_1}{\nu}\right)$ the range of values *W* is in area $-2k_1$. Hence the ratio $\gamma^2 >> 1$ is correct and $W^2 \ge \frac{3}{\gamma^2}$. Taking into account definition $\gamma^2 = -\frac{(k\nu)^2}{4W(2k_1 + W)}$ in (2.40) we find $-W \ge \frac{24k_1}{12 + (k\nu)^2}$. Using definition $W = -2k_1 \sin^2\left(\frac{h_1}{\nu}\right)$ we receive $\sin^2\left(\frac{h_1}{\nu}\right) \ge \frac{12}{12 + (k\nu)^2}$ or $\sin\left(\frac{h_1}{\nu}\right) \ge 1 - \frac{(k\nu)^2}{24}$.

Taking into account a little sizes $\frac{(k\nu)^2}{24}$ in comparison with unit we receive a condition $\frac{h_1}{\nu} = \pi\left(\frac{1}{2} + 2m\right)$ where *m* is an integer. Hence that the channel was transparent for an ion the condition should be observed:

$$\frac{h_1}{\delta} = \frac{1}{4} + m, \qquad (2.43)$$

i.e. on length of a spiral site of the ionic channel the whole and a quarter number of steps of ion spiral movement should be pack up. To this requirement taking into account known spatial scale of the channel can to satisfy the following parameters, for example: if number of turns of ion spiral movement in the channel proceeding from the data on inductance of neuromembrane $n = 9$, paragraph 2.2.2.1, length of a spiral site of

the channel is $h_1 = 5.13\,nm$. Quantization of length of a spiral site of the channel well correlates with step-by-step (step $0.153 + 0.132 + 0.147\,nm$) change of length polypeptide chain of proteins [27].

2.2.2.3. Propagation of action potential on nervous fibre

Let's consider on the basis of inductance-capacitor model of neuromembrane the nervous impulse propagation.

The nervous fibre it is the active "vivid" medium investigated not finally. Therefore to find the differential equation describing propagation of an electromagnetic wave on this medium it is possible only with the certain degree of approximation. In this case the concept of a deduction of the equation is conditional enough. The basic requirements to the process of equation deduction in such situation it is possible assume: first not the contradiction to the basic equations of electrodynamics and other physical laws, second sufficient evidence of conclusions during a deduction, thirdly conformity of the basic positions used at the deduction to experimentally proved positions of Hodgkin – Huxley theory, see paragraph 2.2.1, with the account its lacks marked earlier, and fourthly the main thing - conformity of results of the solution of the received equation to experimental data.

Distribution of strength lines of electric field ***E*** in a nervous fibre at occurrence of action potential and its movement along coordinate *X* is shown on fig. 2.6.

Let's consider density of the ionic current j_i through the separate ionic channel - open oscillatory contour, fig. 2.10. For an ionic channel - contour it is possible to write down the equation of a current oscillations and a voltage as:

$$-L_i S_i \frac{\partial j_i}{\partial t} = j_i S_i R_i + (\varphi - \varphi_0), \qquad (2.44)$$

where L_i there is inductance individual *i* channel, R_i - its active resistance, S_i - the area of the membrane site falling one channel, φ_0 - resting potential. At record it is taken into account that capacitor bias current is taken already into account in the equation of current balance (2.4) according to Hodgkin – Huxley model which we further use.

Using the Ohm law (2.2) for *i* ionic channel as $j_i = g_i(\varphi - \varphi_i)$ where φ_i there is the Nernst potential for the examined kind of ions, and substituting this formula in (2.44) for a membrane conductivity we shall receive a ratio:

$$g_i = -\frac{(\varphi - \varphi_0)\beta_i}{L_i S_i \partial\varphi / \partial t} - (\varphi - \varphi_i)\frac{\partial g_i}{\partial t}\beta_i / (\partial\varphi / \partial t) \qquad (2.45)$$

where $\beta_i = -\dfrac{1}{1 + (R_i / L_i)(\varphi - \varphi_i)/(\partial\varphi / \partial t)}$.

Substituting (2.45) in (2.4) taking into account $C_i = C_m S_i$ there is capacity of the membrane site falling one channel, and designating $\omega_i^2 = \dfrac{1}{L_i C_i}$ we shall receive:

$$\frac{j_m}{C_m}\frac{\partial\varphi}{\partial t} = \left(\frac{\partial\varphi}{\partial t}\right)^2 - (\varphi - \varphi_0)\Sigma(\varphi - \varphi_1)\omega_i^2\beta_i - \\ -\frac{1}{C_m}\Sigma\frac{\partial g_i}{\partial t}(\varphi - \varphi_i)^2\beta_i \qquad (2.46)$$

According to the Ohm law for a longitudinal current in a nervous fibre, fig. 2.6, we shall write down:

$$I_a = \gamma_a \frac{S_a}{\Delta X}(\varphi - \varphi_0), \qquad (2.47)$$

where ΔX there is length of a fibre site, S_a - the area of its cross-section. Under the law of an electromagnetic induction with the account (2.47) for EMF of an electromagnetic induction ε we have:

$$\varepsilon = -(\varphi - \varphi_0) = -L\frac{\partial I_a}{\partial t} = -\gamma_a S_a L_1 \frac{\partial \varphi}{\partial t}. \qquad (2.48)$$

where $L_1 = \frac{L}{\Delta X}$ there is inductance of unit of fibre length. Then proceeding from (2.6) and (2.48) we receive:

$$dj_a = -\frac{\varphi - \varphi_0}{S_a L_1 \partial\varphi / \partial t}\left(\frac{\partial^2 \varphi}{\partial X^2}\right)dX. \qquad (2.49)$$

In this analysis in formulas (2.6) and (2.47) size γ_a is not a constant specific conductivity of axoplasma, and there is some specific impedance size describing also longitudinal reactive properties of a nervous fibre.

Hence the longitudinal current is equal:

$$dI_a = S_a dj_a = -\frac{\varphi - \varphi_0}{L_1 \partial\varphi / \partial t}\left(\frac{\partial^2 \varphi}{\partial X^2}\right)dX. \qquad (2.50)$$

Using (2.9) with the account (2.8) $dI_m = j_m 2\pi r dX$ we shall find:

$$j_m = \frac{\varphi - \varphi_0}{2\pi r L_1 \partial\varphi / \partial t}\frac{\partial^2 \varphi}{\partial X^2}. \qquad (2.51)$$

Substituting value of a current density through a membrane (2.51) in the equation (2.46) we shall find:

$$V^2(\varphi - \varphi_0)\frac{\partial^2 \varphi}{\partial X^2} = \left(\frac{\partial \varphi}{\partial t}\right)^2 - (\varphi - \varphi_0)\sum(\varphi - \varphi_i)\omega_i^2 \beta_i - \sum\frac{(\varphi - \varphi_i)^2}{C_m}\frac{\partial g_i}{\partial t}\beta_i. \qquad (2.52)$$

At the deduction (2.52) it was accepted that capacity of unit of a nervous fibre length is $C_1 = 2\pi r C_m$. Value $V = \frac{1}{\sqrt{C_1 L_1}}$ it is speed of a nervous impulse.

Let's consider in more detail process of neuromembrane hyperpolarization. At attained by the potential φ to resting potential φ_0 in the equation (2.52) last addend play an essential role. From (2.2) follows that during this moment there is $g_i = \frac{j_i}{\varphi - \varphi_i}$. Near to equilibrium resting potential φ_0 speed of change of membrane currents is equal to zero since in the beginning of hyperpolarization the total current depends not on potential difference on membrane but only from concentration ions gradients on a membrane that results to $j_{i0} = const$ [2] hence:

$$\frac{\partial g_i}{\partial t} = -\frac{j_{i0}}{(\varphi-\varphi_i)^2}\frac{\partial \varphi}{\partial t}. \qquad (2.53)$$

Substituting (2.53) in (2.52) we receive:

$$V^2(\varphi-\varphi_0)\frac{\partial^2\varphi}{\partial X^2} = \frac{\partial\varphi}{\partial t}\left(\frac{\partial\varphi}{\partial t}+A\right)-(\varphi-\varphi_0)\sum(\varphi-\varphi_i)\omega_i^2\beta_i\,, \qquad (2.54)$$

where $A = \frac{\sum j_{i0}\beta_i}{C_m}$ there is the value determining an inclination of the potential graph in the beginning of hyperpolarization i.e. at $\varphi = \varphi_0$. According to experiments [29] there is $A = 110\,\frac{V}{s}$.

For finding-out of possible solutions of the equation (2.54) we shall transform it to a kind:

$$V^2(\varphi-\varphi_0)\frac{\partial^2\varphi}{\partial X^2} = \frac{\partial\varphi}{\partial t}\left(\frac{\partial\varphi}{\partial t}+A\right)-(\varphi-\varphi_0)^2\omega_0^2. \qquad (2.55)$$

In (2.55) it is accepted $\sum\omega_i^2\beta_i = \omega_0^2 = const$, and also:

$$\varphi_0 = \frac{\sum\varphi_i\omega_i^2\beta_i}{\Sigma\omega_i^2\beta_i}. \qquad (2.56)$$

The formula (2.56) is correct if to assume according to experiment that resistance of a membrane in rest for ions K^+ is close to zero, and for Na^+ - to infinity (i.e. $\beta_K \approx 1$, and $\beta_{Na} \approx 0$), and also to take into account that the resting potential is close to Nernst potential for ions K^+ [2].

Let's assume that process of hyperpolarization is absent i.e. $A = 0$. Then the solution of the equation (2.55) the received Fourier method of variables dividing as well as "the telegraphic equation" underlying Hodgkin – Huxley model the damping wave is:

$$\varphi = \varphi_0 + \varphi_{\max}\exp(-\alpha V t)\cdot\sin(\delta X+\Theta), \qquad (2.57)$$

where α there is value return constant length of a nervous fibre, $\delta = \sqrt{k^2-\alpha^2}$, $k = \frac{\omega_0}{V}$ - wave number, Θ - an initial phase, $\varphi_{\max}$ - initial value of potential amplitude.

However in a nervous fibre basically other class of solutions is realized - not dumping solutions as solitary Gauss waves:

$$\varphi = \varphi_0 + \varphi_{\max}\exp\left[-\frac{\{k(X-X_0)-\omega_0(t-t_0)\}^2}{2}\right], \qquad (2.58)$$

where X_0, and t_0 there are the constants describing origin of coordinates axes *X* and *t*. We shall note that the solution of the equation (2.55) is also the return solitary wave:

$$\varphi = \varphi_0 + \varphi_{\max}\exp\left[-\frac{\{k(X-X_0)+\omega_0(t-t_0)\}^2}{2}\right], \qquad (2.59)$$

arising, for example, at artificial depolarization of the center of long axon.

Let's estimate currents through neuromembrane during propagation on it of action potential in a conditional point $X = X_0$. We shall assume that the component of potential for *i* channel looks like the similar (2.58):

$$\varphi_i = \varphi_{0i} + \varphi_{\max i} \exp\left[-\frac{\omega_i^2 (t - t_{0i})^2}{2} \right]. \qquad (2.60)$$

where t_{0i} there is the time of achievement of the potential maximal value for the given type of ions. The formula (2.60) is correct if one kind of ions is transferred to a membrane (in experiment) only.

In the formula (2.60) are made some redesignation. φ_{0i} it is Nernst potential for the given kind of ions.

Let's base on the equation (2.45) at absence of hyperpolarization i.e. without taking into account the second addend in the right part:

$$g_i = -\frac{(\varphi_i - \varphi_{0i})\beta_i}{L_i S_i \partial\varphi_i / \partial t}. \qquad (2.61)$$

Let's multiply numerator and a denominator (2.61) on C_1 - capacity of the membrane falling one ionic channel. Taking into account $C_m = \frac{C_1}{S_1}$ and also $\omega_i^2 = \frac{1}{L_1 C_1}$ we shall find:

$$j_i = g_i (\varphi_i - \varphi_{0i}) = -\frac{(\varphi_i - \varphi_{0i})^2 \beta_i \omega_i^2 C_m}{\partial\varphi_i / \partial t}. \qquad (2.62)$$

Function (2.60) satisfies to the equation:

$$\frac{\partial\varphi_i}{\partial t} = -(\varphi_i - \varphi_{0i})\omega_i^2 (t - t_{i0}). \qquad (2.63)$$

Therefore the formula (2.62) will be transformed to a kind:

$$j_i = \frac{(\varphi_i - \varphi_{0i})\beta_i C_m}{(t - t_{i0})}. \qquad (2.64)$$

Using the formula (2.60) we shall find density of a current for *i* kind of ions as:

$$j_i = C_m \cdot \beta_i \varphi_{\max i} \cdot \left| \frac{\exp\{-[\omega_i (t - t_{0i})]^2 / 2}{t - t_{0i}} \right|. \qquad (2.65)$$

The sign on the module is connected by that in the equation (2.55) at $A = 0$ the time enters in the second degree, and in the formula (2.65) (consequence of the solution of this equation) in the first degree.

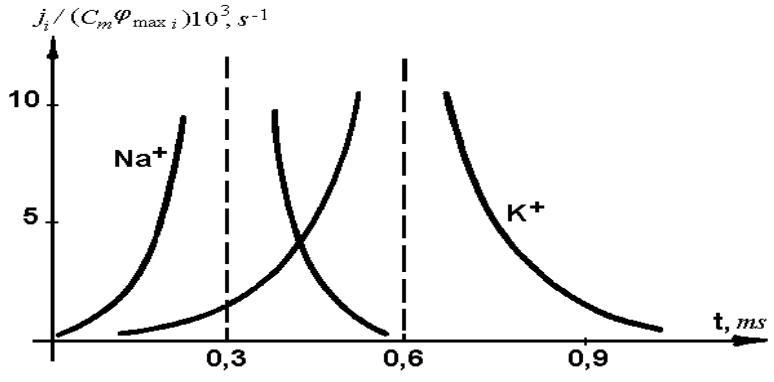

Fig. 2.18.

On fig. 2.18 graphs of density of the sodium and potassium components of ionic current calculated under the formula (2.65) at $\omega_{Na} \approx 6000\ s^{-1};\quad \omega_K \approx 3000\ s^{-1}$ are shown. Values of frequencies ω_{Na} and ω_K are calculated under the formula $\omega_i = \frac{2\pi}{T_i}$ ($T_{Na} = 1\,ms, T_K = 2.1\,ms$) [29] proceeding from continuance of change of ionic currents in processes of action potential propagation. The aspiration of ionic currents density to infinity is caused by neglect viscous resistance to ions movement i.e. $R_i = 0$, and accordingly $\beta_i = 1$ at excitation of a membrane. The similar effect always takes place at calculations, for example, resonant curves at the compelled oscillations.

Let's calculate on the basis of offered model epy size of a nervous fibre inductance. If experimentally received speed of a nervous impulse for squid axon $V = 20\frac{m}{s}$, and capacity of unit of fibre length $C_1 = 0.157\ \frac{\mu F}{cm}$ [10, 29] from the formula $V = \frac{1}{\sqrt{C_1 L_1}}$ we find inductance of unit of nervous fibre length $L_1 = 0.039\ \frac{H}{cm}$ that corresponds for axon in diameter $d \approx 1\,mm$ [16] the inductance $L_m = \frac{L_1}{\pi d} = 0.12\ \frac{H}{cm^2}$ falling on unit of the membrane area. This value is practically equal received by Cole and Baker [20] $L_m = 0.1\frac{H}{cm^2}$.

Let's calculate also length of solitary wave λ of an electric impulse. From determination of wave number $k = \frac{2\pi}{\lambda} = \frac{\omega}{V}$ we have $\lambda = \frac{2\pi V}{\omega}$. The length of a wave is determined by the minimal size of frequency ω_i. Using $\omega_K \approx 3000\ s^{-1}$ we have $\lambda = 4.2\,cm$ that corresponds, for example, to the data [20].

For a finding of time dependence of potential on a membrane it is used the wave equation:

$$V^2 \frac{\partial^2 \varphi}{\partial X^2} = \frac{\partial^2 \varphi}{\partial t^2}. \qquad (2.66)$$

Then the equation (2.55) will be written down as:

$$(\varphi - \varphi_0)\frac{\partial^2 \varphi}{\partial t^2} = \frac{\partial \varphi}{\partial t}\left(\frac{\partial \varphi}{\partial t} + A\right) - (\varphi - \varphi_0)^2 \omega_0^2. \qquad (2.67)$$

As against Hodgkin – Huxley equation (2.22) the equation (2.67) does not include speed of a nervous impulse that is natural because dependence of potential on a membrane from time in section of a nervous fibre is not connected to speed of movement of action potential on a fibre. The equation (2.67) can be integrated once. Having designated $Z = \varphi - \varphi_0$ and using identity $\left(\frac{Z'}{Z}\right)' = \frac{\left[Z''Z - (Z')^2\right]}{Z^2}$, we shall find:

$$\frac{dZ}{dt} - (B - \omega_0^2 t)Z + A = 0, \qquad (2.68)$$

where *B* there is a constant of integration. The similar equation arises by consideration of Hermite functions of the second kind [30]. The solution of the equation (2.68) looks like:

$$Z = \exp\left[-\frac{\left(B-\omega_0^2 t\right)^2}{2\omega_0^2}\right]\left\{C_2 - A\int_0^t \exp\frac{\left(B-\omega_0^2 t\right)^2}{2\omega_0^2}\,dt\right\}, \qquad (2.69)$$

where C_2 there is a constant of integration. Using a condition $Z=0$ $\left(\varphi=\varphi_0\right)$ at $t=t_0$ it is the point started of hyperpolarization (fig. 2.19) we shall find:

$$C_2 = A\int_0^{t0} \exp\frac{\left(B-\omega_0^2 t\right)^2}{2\omega_0^2}\,dt\,. \qquad (2.70)$$

Thus the final solution of the equation (2.68) looks like:

$$Z = A\frac{\int_0^{t0}\exp[\,(B-\omega_0^2 t)^2/\left(2\omega_0^2\right)]dt}{\int_t \exp[(\,B-\omega_0^2 t)^2/\left(2\omega_0^2\right)]}\,. \qquad (2.71)$$

The result of calculation of potential on a membrane according to (2.71) is shown on fig. 2.19.

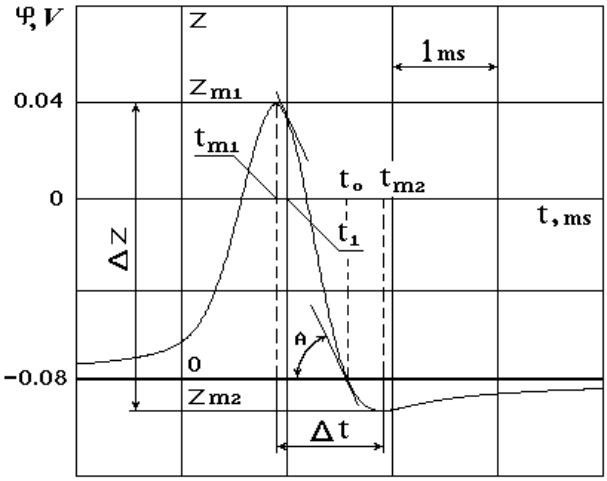

Fig. 2.19.

The constant *B* has been found proceeding from experimental data about time t_{m1} of achievement of the maximal potential (action potential):

$$B = \omega_0^2 t_{m1} + \frac{A}{Z_{m1}}, \qquad (2.72)$$

where $Z_{m1} = \varphi_{\max} - \varphi_0$. In calculations accepted $\varphi_{\max} = 0.04V$.

Proceeding from experimental dependence of potential on time it is possible to find the size ω_0^2 which is included in the equations (2.67) and (2.68). Really the curve, fig. 2.19, has an inclination *A* twice: first time according to the equation (2.68) for $t_1 = \frac{B}{\omega_0^2}$, and the second for $t=t_0$ $\left(Z=0\right)$. Substituting in the formula for t_1 the size of a constant *B* found serially through Z_{m1} and Z_{m2} where Z_{m2} there is the

maximum of hyperpolarization achievable at the moment of time t_{m2}, (fig. 2.19), we shall find time intervals from t_1 up to both extremes. Then after simple transformations we shall receive:

$$\omega_0^2 = \frac{A}{|Z_{m2}|Z_{m1}} \frac{\Delta Z}{\Delta t}, \qquad (2.73)$$

where $\Delta Z = Z_{m1} - Z_{m2}$ and $\Delta t = t_{m2} - t_{m1}$. Substituting parameters of an experimental curve [29] in the formula (2.73) we shall find size $\omega_0^2 \approx 8{,}8 \cdot 10^6 \ s^{-2}$ which was used in calculations.

The equations (2.54) and (2.55) except for the solution as a solitary wave (fig. 2.19) have the solution of resting potential $\varphi = \varphi_0$. Jump of potential is necessary for transition from this type of the solution to the solution (2.58). It explains necessity application to a membrane of depolarize potential for reception of action potential.

The major advantage of the submitted inductance-capacitor model of neuromembrane in comparison with Hodgkin – Huxley model is absence in it of absolutely inexplicable experimental functions (2.17) - (2.19).

The inductance-capacitor model of neuromembrane operates only with constants that is specifies its self-coordination.

2.2.2.4. Energy of action potential

At occurrence in any place of neuromembrane (the active polarized medium) the action potential there is a realization of polarization energy of the membrane reserved at work $Na^+ - K^+ - ATPase$. Process of energy realization is transferred together action potential.

Let's consider a task of calculation on the basis of inductance-capacitor model of neuromembrane the sizes of released energy at carry of one action potential on a nervous fibre.

To take advantage of a usual technique of calculation of a solitary wave energy we shall accept that the membrane 1 is non-polarized, fig. 2.20, and on its internal surface is propagated the electric wave 2 corresponding under the form to action potential.

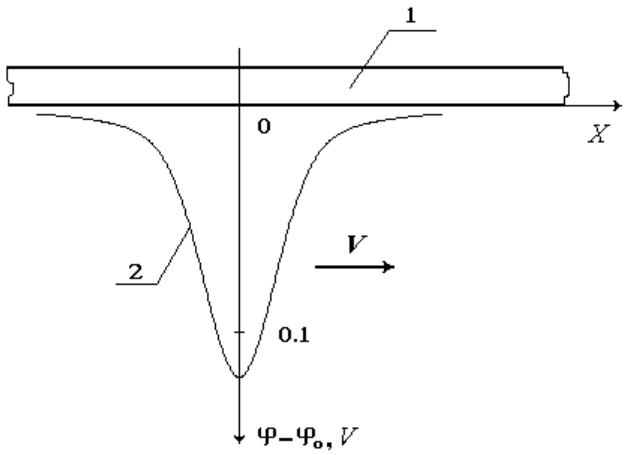

Fig. 2.20.

For simplification of calculations we shall accept that process of hyperpolarization is absent, i.e. $A = 0$. In this case energy of a solitary wave will be equal to the sum energies of the electric and magnetic fields formed by this wave [31]. This energy also will be equal to the energy released in action potential.

As energy of electric field is equal to energy of a magnetic field [25] in wave we shall calculate only energy of electric field, and result we shall double.

For a finding of electric field energy of a solitary wave we shall pass in (2.55) to spatial coordinates replacing $\frac{\partial^2 \varphi}{\partial X^2}$ on Laplacian $\Delta\varphi$. Meaning the form of a nervous fibre we shall pass to cylindrical

coordinates. In this case according to (2.55) propagation of action potential is described by the following nonlinear equation:

$$V^2(\varphi-\varphi_0)\left[\frac{1}{r}\frac{\partial}{\partial r}\left(r\frac{\partial\varphi}{\partial r}\right)+\frac{\partial^2\varphi}{\partial X^2}\right]=\frac{\partial\varphi}{\partial t}\left(\frac{\partial\varphi}{\partial t}+A\right)-(\varphi-\varphi_0)^2\omega_0^2, \quad (2.74)$$

where *r* there is radial coordinate.

For the solving of this equation at $A=0$ we shall search as:

$$Z=\varphi-\varphi_0=F(r)\Phi(X,t). \quad (2.75)$$

The equation (2.74) expend a two equations: the linear equation:

$$\frac{1}{r}\frac{\partial}{\partial r}\left(r\frac{\partial F}{\partial r}\right)-\Theta^2F=0, \quad (2.76)$$

where Θ there is a constant, and the nonlinear equation:

$$\Phi\frac{\partial^2\Phi}{\partial X^2}+k^2\Phi^2=\frac{1}{V^2}\left(\frac{\partial\Phi}{\partial t}\right)^2, \quad (2.77)$$

where $k^2=\left(\frac{\omega_0}{V}\right)^2+\Theta^2$ is a square of wave number.

Let's find the solution of the linear equation (2.76) inside a fibre under a boundary condition: on internal surface of membrane at $r=R$ the potential satisfies to the nonlinear equation (2.77).

Inside a fibre the solution can be written down as cylindrical function of 1-st type $I_0(\Theta r)$, and outside of a fibre as cylindrical function of 2-nd type $K_0(\Theta r)$ [32] where $\Theta=\frac{1}{R}$ and *R* there is a radius of a nervous fibre. Outside of a fibre the solution of the equation (2.76) does not represent interest since change of potential on an external surface of a nervous fibre approximately on two order is less than on internal of fibre. Hence energy of external field does not bring the appreciable contribution to the general energy of a solitary wave.

The nonlinear equation (2.77) has some kinds of solutions from which in a nervous fibre the solution as a running solitary wave is most frequently realized:

$$\Phi=\Phi_{\max}\exp\left[-\frac{\{k(X-X_0)-\omega(t-t_0)\}^2}{2}\right], \quad (2.78)$$

where $\omega=Vk$ there is cyclic frequency of a wave, X_0 and t_0 - coordinate and time at the achievement of a potential maximum.

The solution of the equation (2.74) at $A=0$ inside and outside of a fibre can be written down as:

$$\varphi=\varphi_0+\varphi_{i.e\max}\frac{I(K)_0(\Theta r)}{I(K)_0(\Theta R)}\exp\{-[k(X-X_0)-\omega(t-t_0)]^2/2\}. \quad (2.79)$$

The index *i* designates inside of a fibre, and *e* – outside of a fibre. The designation of cylindrical function in brackets is concerns to propagation of potential outside of a fibre.

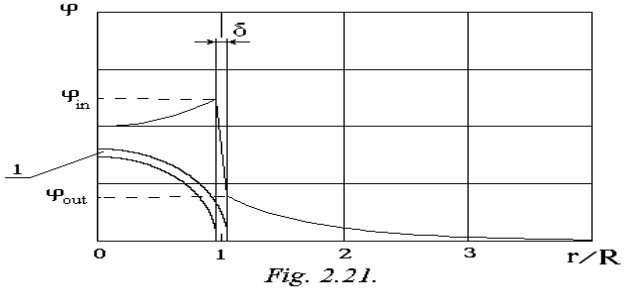

Fig. 2.21.

On fig. 2.21 distribution of potential in cross-section of a nervous fibre 1 for the fixed size *X* and the moment of time *t* is shown.

For a finding of electric energy of a solitary wave – action potential - we shall use the formula [31]:

$$U_E = \frac{1}{2}\varepsilon_a \int_V |\nabla\varphi|^2 dV , \qquad (2.80)$$

where ε_a there is absolute dielectric permeability of substance in which the solitary wave is propagated. As we believe that on аксону only one action potential is propagated the integration is carried out on all volume of nervous fibre *V*.

Taking into account that change of potential has axial symmetry the square of the module of a potential gradient can be written down as:

$$|\nabla\varphi|^2 = \left(\frac{\partial\varphi}{\partial r}\right)^2 + \left(\frac{\partial\varphi}{\partial X}\right)^2 . \qquad (2.81)$$

First we shall find energy of electric field inside a fibre due to action potential propagating on a membrane,.

Full energy of solitary wave *U* as it was marked above should be twice more than calculated under the formula (2.80), hence:

$$U = \varepsilon_a \int_0^R \int_0^{2\pi} \int_{-\infty}^{+\infty} \left[\left(\frac{\partial\varphi}{\partial r}\right)^2 + \left(\frac{\partial\varphi}{\partial X}\right)^2\right] r dr d\psi dX . \qquad (2.82)$$

Integrating on an angle ψ we receive:

$$U = 2\pi\varepsilon_a \left[\int_0^{R+\infty}\int_{-\infty}\left(\frac{\partial\varphi}{\partial r}\right)^2 r dr dX + \int_0^{R+\infty}\int_{-\infty}\left(\frac{\partial\varphi}{\partial X}\right)^2 r dr dX\right]. \qquad (2.83)$$

For a finding of the first integral in the sum (2.83) we shall use the formula (2.79). For integration it is possible to choose any moment of time therefore for simplification of a task we shall accept $t = t_0$. Besides the origin of coordinates we shall take in a point $X = X_0$. In this case there is $X_0 = 0$. Hence:

$$\int_0^{R+\infty}\int_{-\infty}\left(\frac{\partial\varphi}{\partial r}\right)^2 r dr dX = \frac{\varphi_{\max}^2}{k[I_0(\Theta R)]^2}\int_0^1 [I_1(\xi)]^2 \xi d\xi \int_{-\infty}^{+\infty} \exp(-\chi^2) d\chi = \frac{\varphi_{\max}^2\sqrt{\pi}}{k} 0.04 . \qquad (2.84)$$

In (2.84) it is taken into account $\frac{dI_0(\xi)}{d\xi} = I_1(\xi)$, the value $\Theta = \frac{1}{R}$, cylindrical function $I_0(1) = 1.27$ [32], and last integral it is equal $\sqrt{\pi}$ [33].

Let's consider the second addend in the formula (2.83):

$$\int_0^{R+\infty}\int_{-\infty}\left(\frac{\partial\varphi}{\partial X}\right)^2 r dr dX = \frac{k\varphi_{\max}^2}{[I_0(\Theta R)]^2}\int_0^1 [I_0(\xi)]^2 \xi d\xi \int_{-\infty}^{+\infty} \chi^2 \exp(-\chi^2) d\chi = 0.2\varphi_{\max}^2 k R^2\sqrt{\pi} \qquad (2.85)$$

Integrals of formulas (2.85) and (2.84) which include the cylindrical functions of the zero $I_0(X)$ and first order $I_1(X)$ are equal accordingly 0.64 and 0.07.

Let's find now energy of an electric field inside a membrane of a nervous fibre.

Assuming the electric field strength *E* inside a membrane of a nervous fibre approximately homogeneous its energy we shall calculate under the formula:

$$U_{mE} = \frac{1}{2}\varepsilon_{am}\int_V E^2 dV\,, \qquad (2.86)$$

where ε_{am} there is dielectric permeability of a membrane substance.

Taking into account that element of a membrane volume $dV = 2\pi R\delta dX$ where δ is thickness of a membrane, and also energy of electromagnetic field twice more calculated under the formula (2.86) we have formula for energy of electromagnetic field:

$$U_m = \varepsilon_{am}\int_{-\infty}^{+\infty} E^2 2\pi R\delta dX\,. \qquad (2.87)$$

Considering the transmembrane potential changing linearly, and using longitudinal distribution of potential according to (2.79) under condition $r = R$, $t = t_0$ and $X_0 = 0$ is received:

$$E = \frac{\varphi_{\max}}{\delta}\exp[-(kX)^2/2]. \qquad (2.88)$$

Substituting (2.88) in (2.87) we receive:

$$U_m = 2\pi\sqrt{\pi}\varepsilon_{am}\frac{\varphi_{\max}^2}{k\delta}R. \qquad (2.89)$$

For the finding of full energy of action potential we shall substitute (2.84) and (2.85) in (2.83), and result we shall summarize with (2.89). We neglect energy of a field outside of a fibre. In result we shall receive:

$$U = 2\pi\sqrt{\pi}\varepsilon_0\frac{\varphi_{\max}^2}{k}\{[0.04 + 0.2(kR)^2]\varepsilon + (R/\delta)\varepsilon_m\}, \qquad (2.90)$$

where $\varepsilon_0 = 8.85\cdot 10^{-12}\ \frac{F}{m}$ there are electric constant, $\varepsilon = 77$ - relative dielectric permeability of cytoplasm, $\varepsilon_m = 5$ - relative dielectric permeability of a membrane substance [13]. Accepting length of a solitary wave $\lambda = 0.042\ m$ (see paragraph 2.2.2.3) that gives wave number $k = \frac{2\pi}{\lambda} = 150\ m^{-1}$ the maximum transmembrane potential $\varphi_{\max} = 0.12\ V$, radius of a nervous fibre (for squid giant axon) $R = 0.0005\ m$, and thickness of a membrane $\delta = 8\cdot 10^{-9}\ m$ we shall receive energy of a solitary wave $U = 3\cdot 10^{-9}\ J$.

Hence at passage on a nervous fibre of one action potential the energy $3\,nJ$ is released.

From (2.90) it is possible to do the conclusion that only 0.025% all energy of action potential are in electromagnetic field inside a fibre (outside of a fibre on two order is less). The basic energy is concentrated inside a membrane. It specifies that at distribution of action potential practically there are no losses of energy on radiation in an environment.

Let's estimate what quantity of monovalent ions is transferred through a membrane at occurrence in the given place of action potential. For this purpose we use the formula:

$$N \approx \frac{2U}{\varphi_{av}e}, \qquad (2.91)$$

where φ_{av} there is average value of action potential on coordinate *X*, *e* - the elementary charge equal to a charge of a monovalent ion transferable through a membrane. The factor 2 takes into account that at first into the cell goes the certain number of ions Na^+, and then almost same number of ions K^+ leaves, and the potential on a membrane comes back to resting potential.

Average size of potential can be calculated under the formula:

$$\varphi_{av} = \frac{2}{\lambda}\int_0^{\lambda/2} \varphi_{\max} \exp[-(kX)^2/2]dX \approx \frac{\varphi_{\max}}{\sqrt{2\pi}} = 0.048\,V\,, \qquad (2.92)$$

where it is taken into account that $k\lambda = 2\pi$.

Using $e = 1.6\cdot 10^{-19}\ C$ according to (2.91) it is received $N = 7.8\cdot 10^{11}$ ions that makes $1.3\ pmol$. This size is correlate with resulted in [8] that specifies validity of the carried out calculation of energy of action potential.

2.2.2.5. The physical and mathematical nature of action potential

The acrtion potential is a solitary wave. But this wave is not soliton since at counter interaction of two such waves they are mutually destroyed [77]. Hence stabile character of action potential is not connected to balance of the nonlinear effects resulting in increase of a fronts steepness of a solitary wave and a dispersion of this wave in some medium. Such balance is the reason of solitons stability [48].

Thus there should be other mechanism of stability of a solitary wave of action potential.

This mechanism is connected with the general-physicals principles following from spontaneous infringement of system symmetry [78].

During propagation of action potential on a nervous fibre membrane in primary electrical symmetric system of the polarized membrane, fig. 2.22a, there is arise local infringement of symmetry, fig. 2.22b. In the state of fig. 2.22b is absent symmetry of rotation to the any axis directed perpendicularly to a membrane.

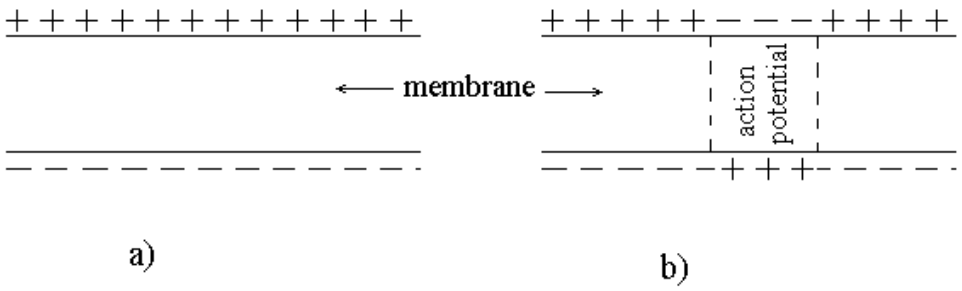

Fig. 2.22.

For the mathematical analysis of local infringement of symmetry we shall find the Lagrangian of the equations for action potential (2.67).

Let's pass to dimensionless potential on a membrane under the formula $Z = \frac{\varphi - \varphi_0}{\varphi_0}$. The equation (2.67) will be transformed to a kind:

$$Z\frac{\partial^2 Z}{\partial t^2} = \frac{\partial Z}{\partial t}\left(\frac{\partial Z}{\partial t} + A^*\right) - Z^2\omega_0^2\,. \qquad (2.93)$$

where dimensionless size $A^* = \frac{A}{\varphi_0}$.

It is possible to find by direct substitution in (2.95) that Lagrangian of the equation (2.93) looks like:

$$L = \frac{1}{2}\left(\frac{\partial Z}{\partial t}\right)^2 - \omega_0^2\frac{Z^2}{2} - \frac{\partial Z}{\partial t}\left(\frac{\partial Z}{\partial t} + A^* + A^*\ln\frac{\partial Z}{\partial t}\right)\ln Z\,. \qquad (2.94)$$

Lagrangian of fields $L = T - V$ is a difference between kinetic $T = \frac{1}{2}\left(\frac{\partial Z}{\partial t}\right)^2$ and potential *V* parts of energy density of this field.

The formula (2.94) satisfies to Lagrange equation [78]:

$$\frac{d}{dt}\left(\frac{\partial L}{\partial \dot{q}}\right)-\frac{\partial L}{\partial q}=0, \qquad (2.95)$$

where the following designations are accepted: the generalized coordinate $q=Z$ the generalized velocity $\dot{q}=\frac{\partial Z}{\partial t}$. In transformations of a potential part of Lagrangian equality $\frac{d}{dt}\left(\frac{\partial L}{\partial \dot{q}}\right)=\dot{q}\frac{\partial}{\partial Z}\left(\frac{\partial L}{\partial \dot{q}}\right)$ is used.

The Lagrangian (2.94) it is possible to decompose in two addends:

$$L=L_0+L_{\text{int}}, \qquad (2.96)$$

where the first addend $L_0=\frac{1}{2}\left(\frac{\partial Z}{\partial t}\right)^2-\omega_0^2\frac{Z^2}{2}$ is the Lagrangian of a free electric field, and the second addend $L_{\text{int}}=-\frac{\partial Z}{\partial t}\left(\frac{\partial Z}{\partial t}+A^*+A^*\ln\frac{\partial Z}{\partial t}\right)\ln Z$ - the Lagrangian of interactions of electric field and a membrane [79].

The potential part of the free field Lagrangian looks like as $V=\omega_0^2\frac{Z^2}{2}$. Parabolic function $V(Z)$ is symmetric and has one minimum equal $V_{\min}=0$ in the point $Z=0$.

Not disturbing symmetry of the potential part of the free field Lagrangian we shall write down it as [79]:

$$V=-\omega_0^2\frac{Z^2}{2}+\frac{h^2}{4}Z^4, \qquad (2.97)$$

where *h* there is the constant small parameter.

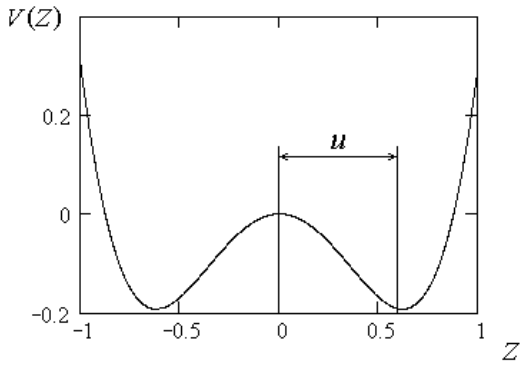

Fig. 2.23.

New function $V(Z)$, fig. 2.23 (scale conditional), according to (2.97) has two equal minimums $V_{\min}(Z_0)=-\frac{\omega_0^4}{4h^2}$ for $Z_0=\pm\frac{\omega_0}{h}$.

Let's move the origin of coordinates of function (2.97) in a point of the right minimum, fig. 2.23. In this case old coordinate *Z* can be written down as:

$$Z=Z_0+u, \qquad (2.98)$$

where Z_0 there is new horizontal coordinate of a point concerning the right minimum.

Having substituted (2.98) in (2.97), we shall find:

$$V = -\omega_0^2 \frac{Z_0^2}{2} - \omega_0^2 Z_0 u - \omega_0^2 \frac{u^2}{2} + \\ + \frac{h^2}{4}\left(Z_0^4 + 6Z_0^2 u^2 + u^4 + 4Z_0^3 u + 4Z_0 u^3\right) , \quad (2.99)$$

Taking into account $Z_0 = \frac{\omega_0}{h}$ we find:

$$V = -\frac{\omega_0^4}{4h^2} + \omega_0^2 u^2 + \frac{h^2}{4} u^4 + h\omega_0 u^3 = \\ = V_{\min} + \omega_0^2 u^2 + h\omega_0 u^3 + \frac{h^2}{4} u^4 , \quad (2.100)$$

where it is used $V_{\min} = -\frac{\omega_0^4}{4h^2}$.

For transition to the previous value of potential function $V = \omega_0^2 \frac{Z^2}{2}$ we aim $h \to 0$ also we shall replace a sign in (2.100). In result for $Z = 0$ we shall receive:

$$V_{\min} = V + \omega_0^2 u^2 = \omega_0^2 \frac{Z^2}{2} + \omega_0^2 u^2 = \omega_0^2 u^2 . \quad (2.101)$$

Thus local infringement of electric field symmetry on a membrane from fig. 2.22a up to fig. 2.22b, is consequence of occurrence of some solitary wave with frequency $\omega_v = \omega_0 \sqrt{2}$.

The deduction stated above shows that by the formal physical and mathematical nature occurrence of a solitary wave of action potential is similar to occurrence of Higgs boson in the quantum theory of a field [79]. But it is only formal similarity. For example, scalar Higgs boson has mass, and it is difficult for action potential to attribute any physically proved mass.

It is possible to assume that "boson's" nature of action potential defines the stability of this solitary wave as well as the soliton's nature of pulse waves defines stability of pulse waves [61, 80].

Besides Higgs boson it is the microcosm particle which does not submit to Pauli principle of interdiction. The essence of Pauli principle will be that some microcosm particles cooperating with each other, for example, fermions cannot have the same energy (identical quantum numbers). Inherently Pauli's principle is a carry of a principle of impermeability to energy area. Bosons of microcosm do not submit Pauli's to principle, i.e. they can have identical energy in the same point of space. At transition in area of a macrocosm the principle of the impermeability is restored therefore two "bosons" of the macrocosm (action potentials) cannot be in the same place of space. Otherwise they will mutually be destroyed.

Chapter 3. Mechanics of muscular contraction

Muscles are intended for creation of an active mechanical tension in various parts of organism. There are three kinds of muscles: cross-striated skeletal muscles, cross-striated cardiac muscles (myocardium) and smooth muscles of internal organs, blood vessels, gastrointestinal tract, skin, etc. The big contribution to studying active properties of a muscular tissue was brought by the English scientist, Nobel prize laureate A. Hill who has empirically established the basic equation in mechanics of muscular contraction. In 1954 the English scientists A. Huxley and H. Huxley have formulated sliding filament model. A. Huxley for the first time tried to construct the quantitative biophysical theory of muscular reduction based on this model. Russian biophysicist V.I. Desherevsky has improved A. Huxley theory having received the good conformity with A. Hill's empirical equation.

3.1. Muscular cell

The muscular cell having usually lengthened form is intended for creation of force at active reduction of it longitudinal size.

The work made by cells of muscular tissue (myocytes) is made due to the energy received as a result of hydrolysis of adenosine triphosphate (ATP) molecules.

Excitable muscular cell it is electrical controlled system.

Muscles ensure the functioning of skeleton, lungs, hearts, vessels, etc., and also are generators of heat.

Let's consider more in detail structure and biomechanical processes in skeletal muscles. Their name - cross-striated - is connected by that under a microscope in the muscular fibre alternating dark and light strips are observed.

Muscular fibres of skeletal muscles in different muscles have length $5-50\,mm$, and diameter $10-100\,\mu m$. They are result of fusion of set of cells and contain accordingly set of nucleus. Such structure refers to symplast when borders between cells are absent. It is caused by that there is no necessity innervation each separate cell. As against skeletal striated muscles the myocardium and smooth muscles basically will consist of separate cells. Frequently there is a muscular fibre of a skeletal muscle refer to multinuclear muscular cell [81].

Let's consider in more detail a structure of a muscular fibre of cross-striated muscles [34]. Inside the fibre except for usual organelle such as nucleus, mitochondrias, etc., is contractive apparatus of the cell or the cellular force mechanism. It will consist from 1000 - 2000 parallel myofibrils (threads) in diameter $d=1-2\,\mu m$, sarcoplasmic reticulums (SR) – bubbles contains calcium ions, and T - systems which is tubules in diameter $\sim 0.05\,\mu m$ run across the fibre.

The electronic microphoto of a muscular fibre fragment is represented on fig. 3.1 where there are well visible separate myofibrils and SR.

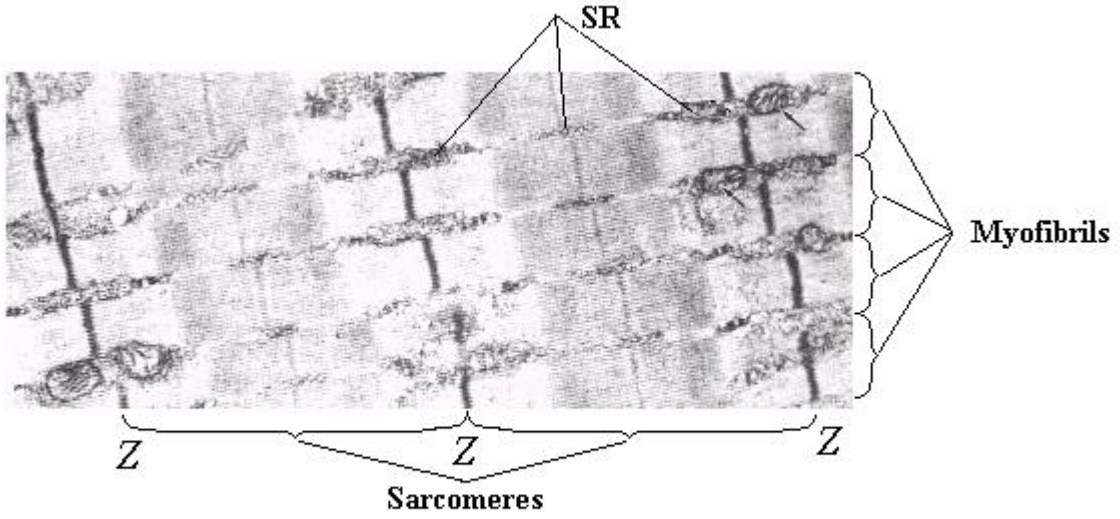

Fig. 3.1.

Myofibril will consist of set of consecutively connected structural elements – sarcomeres which also can be seen on fig. 3.1. Sarcomeres are separated from each other by thin dark lines so-called Z-bands. Sarcomere is elementary contractive unit of the cellular force mechanism in the muscular fibre and will consist from actin (thin) and myosin (thick) threads.

On fig. 3.2 the electronic microphoto of sarcomere of rested muscle is shown. On microphoto it is visible, that actin 1 and myosin 2 threads are located in parallel each other. Due to this their mutual moving occurs strictly in one direction that allows create the big mechanical tension σ (pulling effort) in cells of muscles.

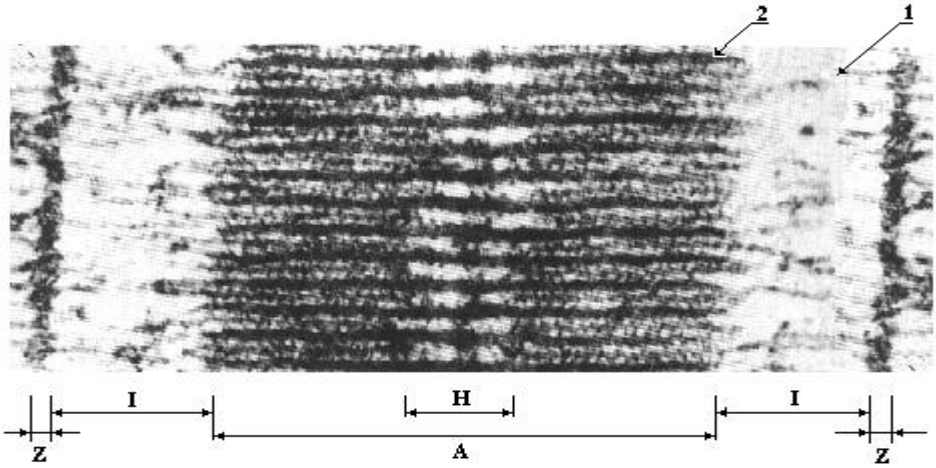

Fig. 3.2.

In everyone sarcomere between Z-bands it is possible to allocate central rather dark zone A, and two light zones I adjoining to Z-bands. In the middle of zone A of the weakened muscle there is light more strip H - area where threads myosin are not overlap by actin threads.

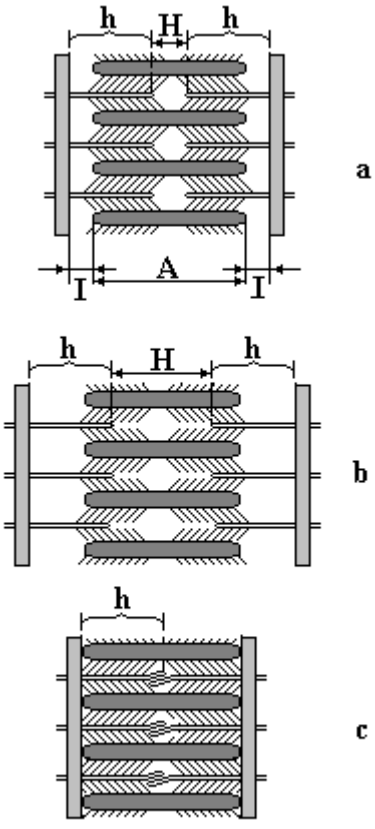

Fig. 3.3.

Schematically the sarcomere structure is shown on fig. 3.3. In myofibril the Z-bands use as borders between sarcomeres. Thin actin threads on the one side are fixed in Z-bands. Thick myosin threads are located between actin threads and connected to them by myosin bridges - projecting fragments of myosin threads. On fig. 3.3a the scheme of sarcomere in the resting condition is shown, on fig. 3.3b at the presence of a muscle stretching, and on fig. 3.3c at presence strong contraction of muscle. Strip H in the latter case disappears owing to overlapping in the middle of the A-zone actin threads attached to opposite Z-bands of sarcomere.

In cross-section of sarcomere, fig. 3.4, actin and myosin threads are form hexagonal system in which everyone myosin thread 2 with the help myosin bridges is connected to six actin threads, and everyone actin thread 1 cooperates with three myosin threads.

Thus sarcomere it is the orderliness system of thick and thin threads are located hexagonally in cross-section between two Z-bands immersed in sarcoplasma.

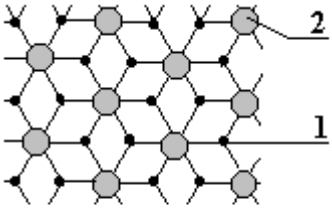

Fig. 3.4.

Let's consider a structure of actin and myosin threads.

Actin (thin) thread in diameter $\sim 8\,nm$ and length $\sim 1\,\mu m$ (fig. 3.5a) there is represents a tape of protein actin globular monomers 1 twisted in a spiral like two twisted parallel threads of a beads. In a groove of this spiral it is located two-threads superspiral of tropomyosin 2. Actin thread has places of connection of myosin bridges it is the active centers 4 located along the thread with interval in length $40\,nm$, fig. 3.5b. At absence of calcium ions the active centers are closed by molecules of tropomyosin.

The important role in the act of linkage of myosin bridges with the active centers of actin threads is played protein troponin 3. Troponin molecules are connected with actin 1 and tropomyosin 2 near to the active center 4. Attaching four Ca^{2+} ions (fig. 3.5b) the troponin molecule 3 influences on tropomyosin 2. It shifts a tropomyosin threads opening the active center 4 for connection of the myosin bridge (the head of myosin) which in the given figure is not shown.

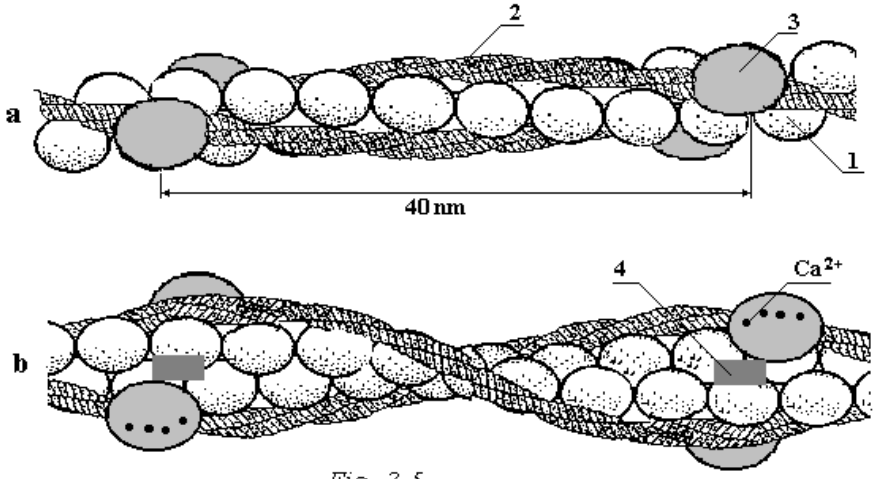

Fig. 3.5.

The myosin molecule will consist of the head and neck. Thick myosin thread is in diameter $\sim 12\,nm$ and length $1.5\,\mu m$ formed as a result of aggregation of myosin molecules due to electric intermolecular forces of interaction between their necks. The fragment of aggregation is represented on fig. 3.6a. The scheme of the aggregated myosin molecules to the myosin (thick) thread is represented on fig. 3.6b.

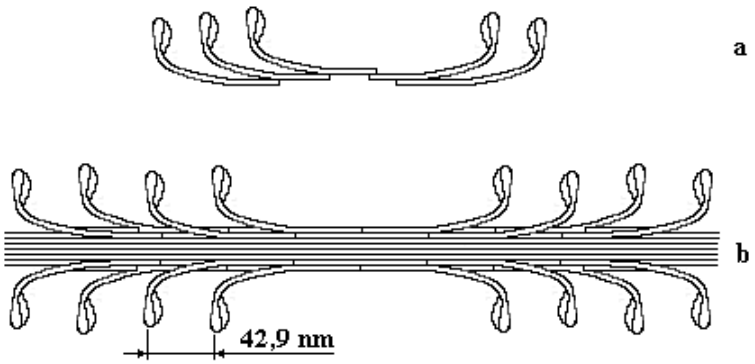

Fig. 3.6.

Projecting the head of myosin molecules are myosin bridges. The heads are located in pairs opposite each other on myosin thread by interval $14.3\,nm$. Transition from one pair to next is accompanied with the turn on 120^0 than the hexagonal structure of arrangement of actin and myosin threads is determined. On fig. 3.6b the longitudinal section of myosin threads is schematically represented. On it the bridges located in a plane of figure that is with an interval $14.3 \times 3 = 42.9\,nm$ are visible (the pairs revolved on 120^0 and 240^0 are not visible).

In a basis of the biochemical processes resulting in muscular contraction i.e. mechano-chemical phenomena lays the activity of myosin heads spontaneously joining to the active centers of actin with formation of actin-myosin complex.

On the other hand the adenosine triphosphate (ATP) molecule contacting with the myosin head (despite of the big breaking strength of actin-myosin complex) provides the fast dissociation of actin-myosin complex (disconnection of bridges).

Also due to energy of ATP hydrolysis in released of myosin head occur conforming transformations and the bridge thus turn aside a Z-band under the angle 90^0 to the actin thread getting potential energy, fig. 3.7a. In such form it is ready will join the next active center on actin thread and to make work on mutual movement of myosin threads between actin threads.

For maintenance of mechano-chemical process at presence interaction of actin and myosin threads presence as enough ATP and enough Ca^{2+} ions is necessary. In a rested muscle there is concentration about $\sim 10^{-7}\ \frac{mol}{l}$ of free Ca^{2+} ions in sarcoplasma. Myofibrils start to be contracted when concentration of free ions Ca^{2+} in sarcoplasma becomes equal $0.4-1.5\cdot 10^{-6}\ \frac{mol}{l}$, and maximal contraction is observed at increase of concentration up to $5\cdot 10^{-6}\ \frac{mol}{l}$.

The role of Ca^{2+} ions consists in initiation of opening of the active center 4 on actin threads, fig. 3.5b. Therefore to opened active centers of a thin actin thread can join the heads of myosin bridges located near.

After that the heads of myosin due to internal elastic forces passively turns around of the hinging site of the neck moving myosin thread is closer to Z-band.

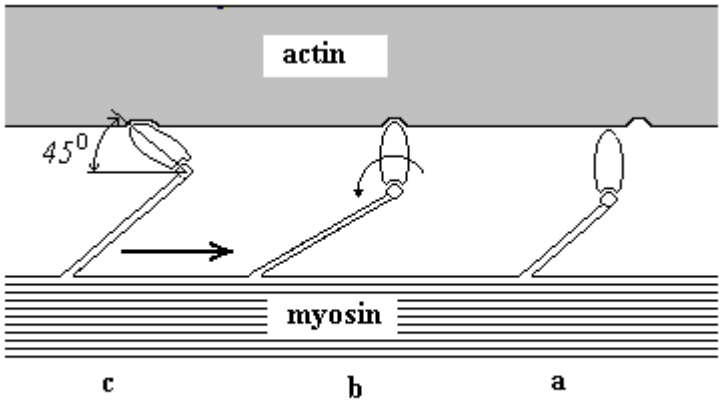

Fig. 3.7.

On fig. 3.7 the scheme of a cycle of work of the myosin bridge is shown. In the position fig. 3.7a is shown the bridge before connection to the active center of actin. In the position fig. 3.7b the bridge has joined the active center actin and began force turn. It is passively elastic being turning it pull myosin thread. In the position fig. 3.7c the bridge has stopped to pull and brakes mutual slide of threads. Then the bridge due to ATP hydrolysis was disconnected, actively turned aside Z-band, has got potential energy and is ready to join the active center of actin (position on fig. 3.7a).

Everyone myosin bridge can be considered as the step-by-step engine making for a duty cycle moving on $5-10\ nm$. Asynchronous work of bridges provides uniform retraction actin threads between myosin threads.

The scheme of electromechanical conjugation in sarcomere is represented in fig. 3.8. For contraction of a skeletal muscle the Ca^{2+} ions come to myofibrils 2 from sarcoplasmic reticulum 1 which is used as calcium depot in a muscular fibre. Concentration of Ca^{2+} ions in SR attain $10^{-2}\ \frac{mol}{l}$ i.e. on membranes SR there

is the very big gradient of Ca^{2+} ions concentration but in rest the membrane SR are completely impenetrable for these ions. The basic role in electromechanical conjugation is played the sites of SR adjoining to Z-bands. Alongside are tubules of T-systems 3 - cylindrical deepenings in the external membrane of myocyte 4 as little sack located across the fibre near to Z-band. SR surround everyone myofibril.

After of synaptic transfers of excitation on myocyte, see paragraph 4.1.1, on its external membrane 4 the action potential (electric wave) 5 (fig. 3.8) is propagated with the velocity $3-5\frac{m}{s}$. Its amplitude is $\sim 100-130\ mV$, and duration in each point of membrane $\sim 3\ ms$. Depolarize membrane of T-tubules the action potential quickly reaches the membrane of SR terminal sites 1 where opened voltage-gated calcium channels 6. Already through $20\ ms$ it results to volleying emission of Ca^{2+} ions (calcium volley). Ions of calcium Ca^{2+} come in area of actin-myosin contact in myofibril and contraction of myocyte begins.

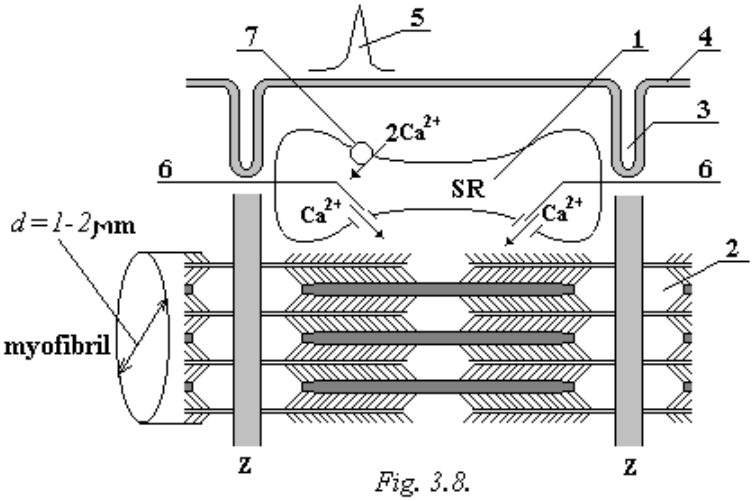

Fig. 3.8.

The relaxation of muscular fibres is connected to activation of calcium pump work (Ca^{2+} - ATPase), see paragraph 1.5.2 and fig. 1.13, returning Ca^{2+} ions back into SR. When concentration of Ca^{2+} ions in sarcoplasma is reduced up to $10^{-7}\frac{mol}{l}$ there are begins active with use of energy ATP disconnection of myosin bridges.

Thus electromechanical conjugation in muscles are begins occurrence of action potential on the external myocyte membrane and conclude the muscle contraction. It includes the following phases:

1) Propagation of action potential on an external membrane of a muscular fibre and its transfer through T-system to the sarcoplasmic reticulum;

2) Opening voltage – gated calcium channels of SR that results to volleying emission of Ca^{2+} ions in sarcoplasma. It is the condition of opening of the actin active centers $\rightarrow$ close of myosin bridges $\rightarrow$ shortening of sarcomere;

3) Activation of calcium pump (Ca^{2+} - ATPase) in membranes of SR pumping Ca^{2+} ions from sarcoplasma to back in SR.

The stretching of sarcomere occurs not independently, and due to work of other muscles (so-called extensors) or due to forces elasticity (heart), due to gravitational forces (extremities), due to forces of the surface tension (diaphragm), etc.

At death of organism coming of ATP to actin-myosin complex stops the myosin bridges fixed on the place remaining attached to actin under equilibrium angle approximately 45^0 for myosin molecule, fig. 3.7c. There is arises cadaveric stiffness. After a stretching of a muscle external effort (force break actin-myosin complex) repeatedly cadaveric stiffness does not arise.

3.2. Hill's equation

For the analysis of muscular contraction mechanisms we shall consider two modes of a muscle contraction: isometric and isotonic.

The main difference of a muscle isometric contraction is the constancy of its length. The conditional scheme of experiment for finding of the force at muscle isometric contraction is shown on fig. 3.9.

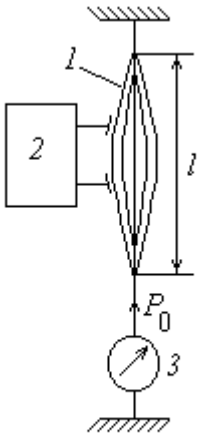

Fig. 3.9.

The muscle is fixed so that its length during experiment was kept by a constant $l = const$.

The fixed muscle 1 influences electric impulses of electroimpulsator 2. The sensor of force 3 registers size of force given the muscle at its contraction. The maximal value of force at presence isometric contraction we shall designate P_0.

Isotonic contraction is carried out at action on the muscle of constant stretching force. For maintenance of the force constant there is certain weight *P* to the muscle suspended, fig. 3.10. At submission of electric impulses on a muscle 1 from electroimpulsator 2 it is reduced lifting the weight 3. Change of length and velocity of the muscle reduction is registered by the device 4.

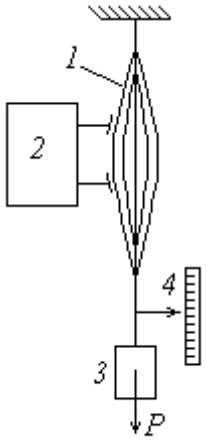

Fig. 3.10.

English physiologist A. Hill in 1938 has experimentally received dependence of reduction velocity of a frog sartorius muscle from weight *P*, fig. 3.11 [35]. Velocity of the muscle reduction at increase in weight *P* decreases. At attainment of weight $P > P_0$ the muscle cannot counteract force of the stretching and starts to be stretched.

The force P_0 is the maximal force given by a muscle at isometric contraction since at this weight the velocity of the muscle reduction $V = \frac{dl}{dt} = 0$ i.e. its length is constant $l = const$.

Usually the muscle is contracted in the general mode which is not isometric or isotonic.

A. Hill has selected the equation describing the curve of muscle isotonic contraction so-called the Hill's equation:

$$(P + a)V = b(P_0 - P), \qquad (3.1)$$

where *a* and *b* there are Hill's constants, *V* - velocity of the muscle reduction.

The Hill's equation is the basic equation of mechanics of active muscular contraction. From (3.1) follows that velocity of muscle reduction depending on the stretching force corresponds to the hyperbolic law and is equal:

$$V = \frac{b(P_0 - P)}{P + a}. \qquad (3.2)$$

The maximal velocity of muscular reduction as follows from the curve on fig. 3.11 will be for $P = 0$ since at reduction of force *P* the numerator (3.2) grows, and the denominator decreases. Take into account the value of constant $a \approx 0{,}25P_0$, see (3.25), this velocity is equal $V_{\max} = \frac{bP_0}{a} \approx 4b$.

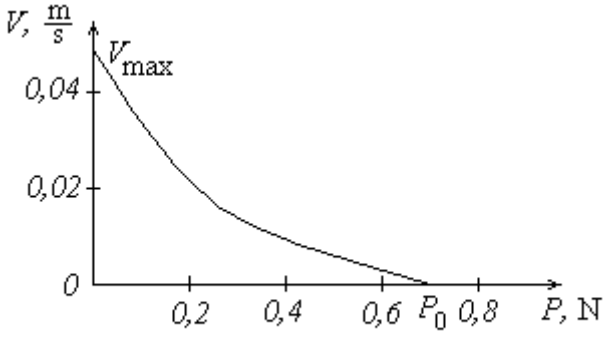

Fig. 3.11.

3.2.1. Capacity of the muscle

At contraction of a muscle there is liberated heat. Hill has experimentally shown that liberated heat at muscle contraction it is proportional only to size of muscle reduction Δl and does not depend on weight i.e. $\Delta Q = a\Delta l$, where *a* there is Hill's constant.

Thermal capacity of a muscle (heat production) is equal to quantity of heat in unit of time liberated by a muscle at contraction:

$$N_Q = \frac{\Delta Q}{\Delta t} = a\frac{\Delta l}{\Delta t} = aV . \qquad (3.3)$$

Mechanical capacity of a muscle is equal to the force given by a muscle multiplied in the velocity of its reduction $N = PV$. Therefore general capacity of a muscle is equal:

$$N_\Sigma = N + N_Q = (P + a)V . \qquad (3.4)$$

Thus in the left part of the equation (3.1) there is general capacity of a muscle.

Using the formula for the velocity of muscle reduction (3.2) we shall find dependence of mechanical capacity of a muscle on loading:

$$N = PV = P\frac{b(P_0 - P)}{P + a}. \qquad (3.5)$$

We research the formula (3.5) on extremum. For this purpose we shall find value of force at which capacity of the muscle is maximal. The condition of extremum is $\frac{dN}{dP} = 0$. From this condition take into account the value of a constant $a \approx 0{,}25P_0$, see (3.25), we find:

$$P_{\text{opt}} = \sqrt{a(P_0 + a)} - a \approx 0.31P_0 , \qquad (3.6)$$

where P_{opt} there is so-called optimum force at which the muscle give the maximal capacity.

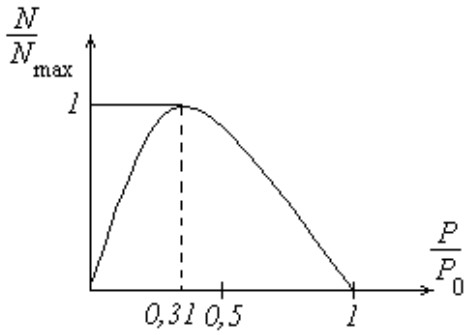

Fig. 3.12.

The graph of dependence of relative muscle contraction capacity (concerning the maximal capacity $N_{\max}$) from relative force of contraction (concerning force at isometric contraction P_0) is shown on fig. 3.12.

From fig. 3.12 is the follows recommendation on elevating of weights. From the point of view of optimum use of a muscle capacity it is necessary the maximal weight which man can elevate to divide approximately into three equal parts and to elevate these parts separately.

It is possible to find efficiency of a muscle as the ratio of mechanical capacity to the general capacity:

$$\eta = \frac{N}{N_\Sigma} = \frac{P}{P + a}100\% . \qquad (3.7)$$

Efficiency of a muscle depends on size of loading and at optimum force P_{opt} is approximately 55%.

3.3. Biomechanics of muscular contraction. V.I. Desherevsky theory

The theory of muscular contraction especially for cross-striated muscles now it is well developed and confirmed experimentally. On fig. 3.13 the scheme of work of actin-myosin force mechanism is shown. In figure M it is a loading mass, and *P* - the external force applied to a muscular fibre.

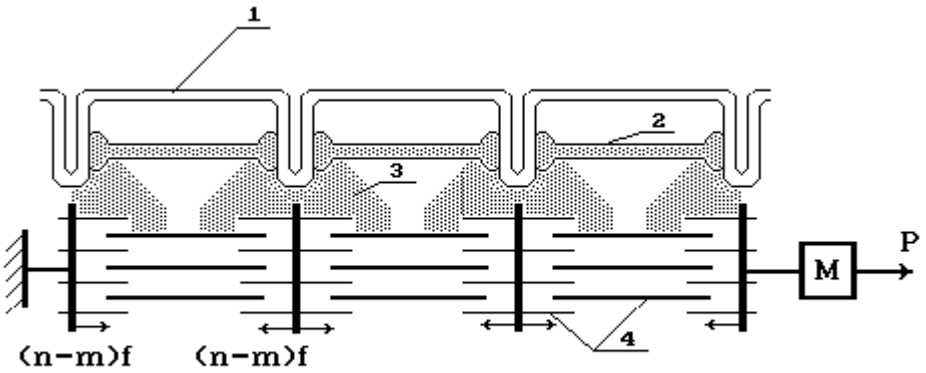

Fig. 3.13.

For the beginning works of actin-myosin cellular force mechanism very fast increase of concentration of Ca^{2+} ions approximately in 10 ones is necessary, and increase local in the field of contact of actin with myosin. Extracellular Ca^{2+} ions basically cannot participate in this process since for diffusion of these ions from the external membrane of a muscular fibre (cell) 1, fig. 3.13, to actin-myosin force mechanism 4 needs big time.

Therefore the calcium passing from extracellular space collects in sarcoplasmic reticulums 2 due to work of special enzyme - calcium pump (Ca^{2+} - ATPase), see paragraph 1.5.2 and fig. 1.13.

At depolarization of a cell external membrane through cakcium ionic channels of the sarcoplasmic reticulums the Ca^{2+} ions 3 it is quickly shoot out in area of actin-myosin force mechanism - so-called "calcium volley".

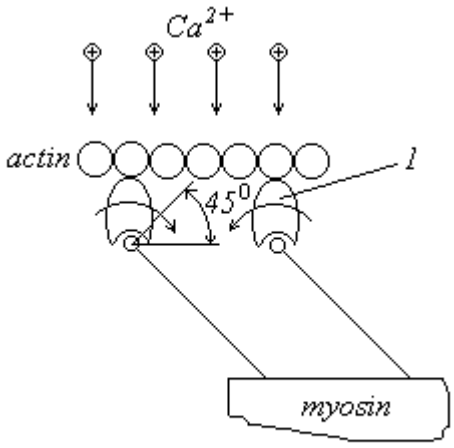

Fig. 3.14.

After the ending of the muscle contraction process approximately 80% of Ca^{2+} ions come to back in sarcoplasmic reticulums by ionic pumps - Ca^{2+} - ATPase. Approximately 20% are thrown out for limits of cell by Ca^{2+} - ATPase and Na^{+} - Ca^{2+} exchanger, see paragraph 4.1.2.

At the presence of Ca^{2+} ions there is connection of myosin bridges 1, fig. 3.14, with actin and then them passive-elastic force turn to occurrence of effort. This bridges state refers to as a pulling state.

Then bridges not at once are disconnected from actin and brake mutual sliding of actin and myosin threads. Such bridges state refers to braking, fig. 3.7c.

After that bridges with use of hydrolysis energy of ATP molecule are disconnected from actin and pass in a free state actively turned back under the angle 90^0 to actin threads, fig. 3.7a.

The new cycle begins connected of bridges and actin and their transition in pulling state, fig. 3.7b.

Though this theory of muscular contraction is most full realized in cross-striated muscular fibres, and in smooth muscular fabrics the principle of muscles contraction is similar. However histologic researches specify that sarcoplasmic reticulum in smooth muscles is less developed.

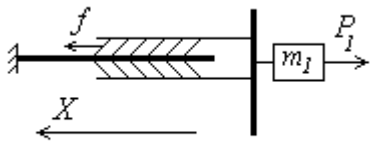

Fig. 3.15.

Let's consider interaction actin and myosin on the basis of Desherevsky theory [36]. A calculating element of muscular contraction in this theory is one myosin thread in half-sarcomere, fig. 3.15.

Let's offer that in the given position of one myosin thread in half-sarcomere numbers of a bridges in states – free, pulling and braking accordingly it is equal: γ , *n, m*. Density of bridges about $10^{17}\ \frac{bridges}{m^2}$ of the muscle section.

The second Newton law for one myosin thread in half-sarcomere, fig. 3.15, looks like:

$$m_1 a = m_1 \frac{dV_1}{dt} = (n-m) f - P_1, \qquad (3.8)$$

where m_1 there is conditional fraction of M mass falling one myosin thread in half-sarcomere, *f* - the force created by one bridge ($\sim 3 \cdot 10^{-12} N$), P_1 - a fraction of the external loading *P* falling one myosin thread in half-sarcomere, *a* - acceleration, V_1 - velocity of half-sarcomere contraction, *t* - time, $(n-m)$ - the difference between numbers of pulling and braking bridges, $(n-m)f$ - the pulling force of one myosin thread in half-sarcomere.

Let's use concept of a constant of process velocity. The constant of process velocity k_i is a value inversely proportional of the process time t_i.

$$k_i = \frac{1}{t_i}. \qquad (3.9)$$

Hence the value $\frac{n_i}{t_i} = k_i n_i$ it is numbers of bridges in unit of time passing from one state in another.

Let's accept the following constants of transitions velocities, fig. 3.16.

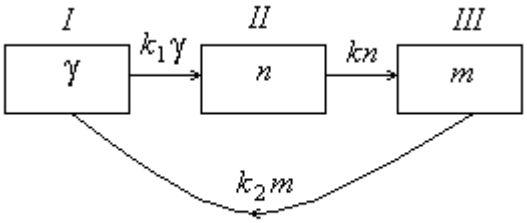

Fig. 3.16.

From the free state *I* in pulling state *II* (connected of bridges, creation actin-myosin complex) there is the constant of process velocity k_1, from the pulling state *II* in braking state *III* (mutual sliding of threads) - *k*, from braking state *III* in the free state *I* (disconnection of bridges, disintegration actin-myosin complex) - k_2.

It is experimentally established that the ratio $\frac{k_2}{k_1} = \frac{t_1}{t_2} \approx 3$. Time of actin-myosin complex creation take into account of opening the active center 4 on actin thread with the help of calcium ions, fig. 3.5, is t_1 approximately three ones is more than time of its disintegration t_2.

Believing that connection actin and myosin is chemical reaction of the first order we shall write down the kinetic equation for velocity of bridges numbers change in the pulling state:

$$\frac{dn}{dt} = k_1 \gamma - kn. \qquad (3.10)$$

Similarly it is possible to receive and the equation for reaction of disintegration of actin-myosin complex i.e. for speed of bridges numbers change in the braking state:

$$\frac{dm}{dt} = kn - k_2 m. \qquad (3.11)$$

Let's consider the stationary or established state. In this condition the muscle is reduced uniformly $V_1 = const$. The number of bridges taking place in each state does not change $n = const$, $m = const$, and $\gamma = const$. Transition of bridges from any state in the following is compensated by transition of bridges from the previous state.

Hence derivatives on time in the equations (3.8), (3.10), (3.11) are equal to zero. By time of joining and separation of bridges in comparison with time of muscle contraction it is neglected. We receive three algebraic equations:

$$(n-m) f - P_1 = 0, \qquad (3.12)$$

$$k_1 \gamma - kn = 0, \qquad (3.13)$$

$$kn - k_2 m = 0. \qquad (3.14)$$

Size γ it is number of bridges in a free condition can be expressed through *n* and *m* using total of bridges in one myosin thread in half-sarcomere $\theta = const$:

$$\gamma = \theta - n - m. \qquad (3.15)$$

Let's solve system from 4 equations (3.12) - (3.15).

Having substituted the equation (3.15) in (3.13) we shall receive:

$$k_1(\theta - n - m) - kn = 0. \qquad (3.16)$$

Let's find from the equation (3.14) $n = m\frac{k_2}{k}$ and having substituted this expression in the equation (3.16) we shall receive:

$$m = \frac{k_1 k \theta}{(k_1 + k_2)k + k_1 k_2}, \qquad (3.17)$$

$$n = \frac{k_1 k_2 \theta}{(k_1 + k_2)k + k_1 k_2}. \qquad (3.18)$$

Substituting the found values *n* and *m* in the equation (3.12) we shall find:

$$\left(P_1 + \frac{k_1 \theta f}{k_1 + k_2}\right)k = \frac{k_1 k_2}{k_1 + k_2}(\theta f - P_1). \qquad (3.19)$$

Transition of bridges from a pulling state in braking state occurs during creation of force effect by them. The constant of velocity of this process *k* it is value inversely proportional of the process time τ.

$$k = \frac{1}{\tau} = \frac{V_1}{\delta}, \qquad (3.20)$$

where V_1 there is the relative sliding velocity of actin and myosin threads, $\delta = V_1 \tau$ - value of threads sliding at unitary of joining and separation of bridges ($\sim 10\, nm$).

Hence substituting (3.20) in (3.19) we shall find:

$$\left(P_1 + \frac{k_1 \theta f}{k_1 + k_2}\right)\frac{V_1}{\delta} = \frac{k_1 k_2}{k_1 + k_2}(\theta f - P_1). \qquad (3.21)$$

Having multiplied the received equation in number sequence located half-sarcomere $2N$ (*N* it is sarcomeres number) on length of a muscle and in number parallel myosin threads N_0 in a muscle (on fig. 3.13 it is conditionally shown $N=3$ и $N_0=3$) we shall receive:

$$2NN_0\left(P_1+\frac{k_1\theta f}{k_1+k_2}\right)\frac{V_1}{\delta}=2NN_0\frac{k_1k_2}{k_1+k_2}\left(\theta f-P_1\right). \quad (3.22)$$

Let's bring N_0 inside of brackets:

$$\left(P_1N_0+\frac{fN_0k_1\theta}{k_1+k_2}\right)\frac{2NV_1}{\delta}=\frac{2Nk_1k_2}{k_1+k_2}\left(\theta fN_0-P_1N_0\right). \quad (3.23)$$

Taking into account that velocity of muscle reduction at a consecutive located sarcomeres $V=2NV_1$ and the force created by parallel located myosin threads of the muscle $P=P_1N_0$ we shall receive the Hill's equation (3.1):

$$\left(P+a\right)V=b\left(P_0-P\right). \quad (3.24)$$

From the deduction follows that the value $P_0=N_0\theta f$ is the force created by a muscle at isometric contraction. In this case all θ myosin bridges are joined with actin threads and create pulling effort. Separated bridges do not occur.

The muscle creates the maximal effort at isometric contaction since in this case sliding of threads be relative each other does not occur, and all myosin bridges are connected with actin threads and create effort. At sliding threads the part of bridges is disconnected from actin threads for a new joining.

Constants *a* and *b* in the Hill's equation with the account $\frac{k_2}{k_1}=\frac{t_1}{t_2}\approx 3$ are equal:

$$a=\frac{N_0\theta fk_1}{k_1+k_2}=\frac{P_0k_1}{k_1+k_2}=\frac{P_0}{1+k_2/k_1}\approx 0{,}25P_0, \quad (3.25)$$

$$b=2N\delta\frac{k_1k_2}{k_1+k_2}=\frac{lk_1k_2}{k_1+k_2}, \quad (3.26)$$

where $l=2N\delta$ there is reduction of all muscle at one joining and separation of bridges.

From the deduction (3.24) the physical sense of the Hill's equation follows. It is actually 2-nd Newton law for a muscle.

From consideration of work the actin-myosin cellular force mechanism it is visible that actively be stretched a muscle cannot. The force turn of a myosin bridge can occur only in one side.

In smooth muscles processes are similar but are less ordered.

There is a group of medicinal substances - antagonists of calcium (verapamil, nifedipine, etc.) which temporarily block calcium ionic channels of sarcoplasmic reticulum. These channels the excessive quantity can be synthesized in an organism. Time blockade of a fraction of calcium ionic channels reduces intensity of "calcium volley" and reduces force of smooth muscles contraction of blood vessels. Antagonists of calcium it is the antihypertensive group of medicinal substances reducing a vascular tone first of all arterioles due to that their hydraulic resistance decrease and as consequence arterial pressure is reduced.

Chapter 4. Surface biopotentials. Electrocardiography

Functioning of tissues and organs is connected to their electric activity. Electrical excitation of an organs tissue usually it is a necessary condition and cause further mechanical, physical or chemical functional activity. Thus in an organism the electric field is created.

The major diagnostic method based on registration of electric field arising at work of heart is electrocardiography (ECG). Thus registration on a surface of a body of the biopotentials arising at work of heart is carried out. The man at registration of the electrocardiogram should be in the condition of rest for exception of the biopotentials arising at work of other muscles.

At ECG two electrodes 3 and 4, fig. 4.1, the bodies enclosed to different sites allow to register a potential difference between terminals 5. These potentials refer to surface biopotentials.

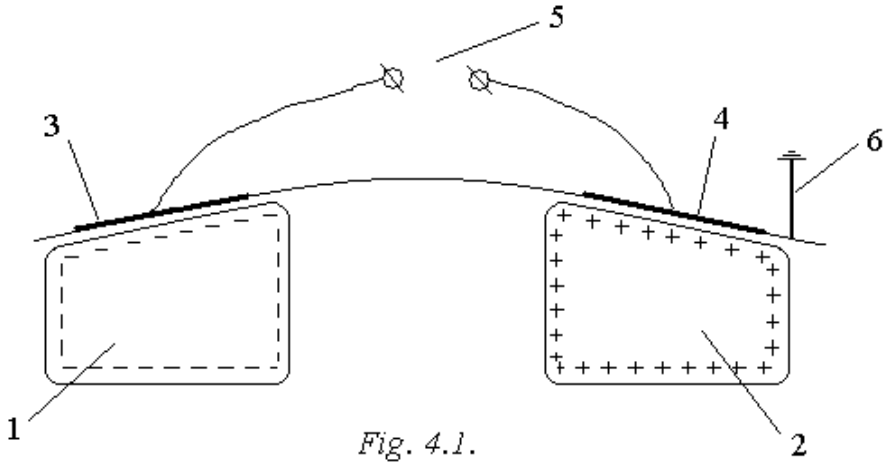

Fig. 4.1.

The term "biopotentials" describe two interconnected but nevertheless various electrobiophysical phenomena.

First phenomenon it is occurrence of a potential difference between internal and external surfaces of a cell membrane. This transmembrane potential is rather significant size which can be calculated on the methods described in paragraph 1.5.4. For example, in a resting condition of a muscular cell between surfaces of a membrane there is a potential difference (more accuracy it is a potential increment) approximately $-90\,mV$. In the electrodiagnostics this potential difference does not measure usually.

Second phenomenon it is occurrence of a potential difference between external surfaces of membranes of various cells or groups of cells 1 and 2, fig. 4.1. In a rest condition of muscular cells the potential on a cell external surface can be believed equal to zero. Thus on an internal surface of a cell membranes there is a significant negative potential (conditional cell 1).

It is connected by that the external surface of a cell actually earthed 6 (it is connected to the ground), fig. 4.1, since the man usually stands on the ground, is in the air environment, constantly touches various subjects, washes, etc. Therefore any charge which has arisen on the external surface of cell membranes practically at once flows away in environment. Hence in the resting condition of cell groups 1 and 2 there is no potential difference between external surfaces of various cell groups (between terminals 5).

Absolutely other situation can be observed during excitation of cell group, for example, 2 on fig. 4.1. At the moment of occurrence of positive potential on an internal surface of a cell membrane there is a short-term negative potential on its external surface. It is connected by that all charge from the external surface of membrane has not time instantly flow in environment. Appearing on the external surface of membrane the negative potential is very small (for example, for ECG it makes up to $-5\,mV$). This potential quickly disappears due to grounding of the cell external surface and consequently peak character has. If to measure the potential difference with the help of electrodes 3 and 4 between external surfaces of two cell groups one of which 1 is in the resting condition (the surface potential is equal to zero), and another 2 during excitation there is possible to register a small peak potential difference (at the moment of change transmembrane potential on cell group 2). This potential difference is investigated in a diagnostic method - ECG.

Let's note that the surface peak potential on the excited cell group 2 quickly disappears also the potential difference between terminals 5 quickly to become equal to zero in spite of the fact that this potential is measured between surfaces of not excited 1 and excited 2 cell groups. Thus the surface potential is connected to the non-stationary moments of excitation process of a tissue.

There are considered two problems of ECG.

The direct problem is a finding of the biophysical mechanism of the electrocardiogram occurrence on the basis of the known data on work of heart and ECG modelling.

Inverse (or diagnostic) a problem is a finding of the condition and principles of heart work dependence on character of its electrocardiogram, and also modelling of the electric heart generator on the basis of the electrocardiogram. The inverse problem of the electrocardiogram usually has no single-valued solution. The same electrocardiogram the hearts of people having various physiological including pathophysiological features can give. From this point of view speak about a level existing unspecific of ECG.

4.1. Biopotentials of muscular cells

Biopotentials of the organs consisting in basic from the muscular cells are investigated in diagnostic methods of ECG and electromyography. Electromyography is a registration on a body surface of the biopotentials arising at work of muscles and nervous trunks innervate these muscles. A peak range it is up to $50\ mV$.

The surface biopotentials measured between sites of a body surface are connected with membrane potentials. Therefore we shall consider all over again membrane potentials of muscular cells.

In the resting condition of the muscular cell on its membrane due to various permeability of membrane for various ions and active transport of the charged particles through a membrane there is the potential difference. This potential difference refers to as resting potential (RP) of a muscular cell. In the cell resting condition on the internal side of a membrane the potential is negative in relation to its external side. The outside of a cell membrane actually earthed therefore its potential is close to zero.

The resting potential of the cell refer to potential difference on its membrane in the resting condition of the cell counted from the membrane external surface which potential is accepted equal to zero.

It is conditionally considered that in the resting condition on the membrane internal side the potential negative, and on the external side - positive. The muscular cell membrane is in the polarized condition.

At cell excitation on its membrane due to change of the membrane permeability for ions and occurrence of ionic currents through the membrane there is a change of potential signs i.e. on the membrane internal side the potential to become positive concerning outside. This process refers to depolarization of membranes. Returning of membrane potential after it depolarization to the initial level (resting potential) refers to repolarization of membranes.

The potential on a cell membrane during its excitation refer to action potential (AP).

Contraction of a muscular cell probably only after on its membrane the action potential was propagated. The action potential of a muscular cell is the starting mechanism for its contraction.

Muscular fibre innervate the nervous fibre approached to it, fig. 4.3a. The nervous fibre terminal 1 refers to synapse (Greek connection). The place of contact refers to as synaptic connection.

The action potential on a muscular cell can arise intactly i.e. for the account depolarization of cell membranes in area synaptic connections or for the account depolarization of membranes from an external source of the voltage.

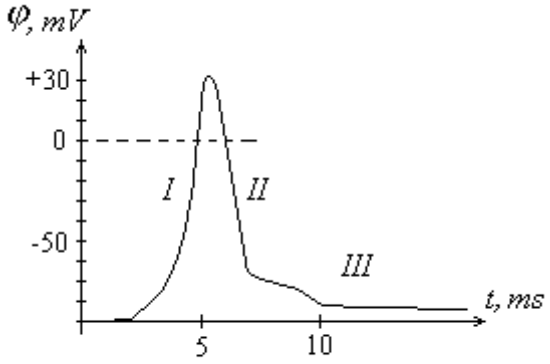

Fig. 4.2.

The action potential is transferred from one muscular fibre to another. For fibres of cross-striated muscles typically structure of the tissue as symplast. It is characterized by absence of borders between cells and a plenty of nucleus in the general cytoplasm. It reduces number of the nervous fibres necessary for innervation of a muscle. In the myocardium which will consist of separate cells between them there are intercellular gap junctions - nexus which promote transfer of excitation from one cell to other cell.

On fig. 4.2 dependence of potential on a membrane of a cross-striated (skeletal) muscle fibre during excitation from time is shown. This

dependence frequently name action potential. In figure it is possible to allocate three areas: *I* – the phase depolarization, *II* - the phase repolarization, *III* - the phase trace depolarization. In a skeletal muscular fibre the potential after achievement of the maximal size (action potential AP) $+30-+40\,mV$ and fast falling up to $\sim -70\,mV$ then slowly falls coming nearer to resting potential (RP) $\sim -90\,mV$. This phenomenon refers to trace depolarization.

4.1.1. Synaptic connection

Let's consider in more detail functioning of a synaptic transfers of excitation impulse on membrane of a skeletal muscular fibre, fig. 4.3a.

Into the synapse 1 there are babbles - liposomes or synaptic vesicles 3 in diameter $\sim 50\,nm$ filled mediator (in particular acetylcholine). At achievement by the action potential of the terminal of a nervous fibre the action potential passes on presynaptic membrane 4. Synaptic vesicles 3, fig. 4.3b, approach to presynaptic membrane 4 and due to their integration in the membrane (exocytose) there is the emission of mediators in synaptic cleft 6 width $\sim 25-50\,nm$.

The reason of exocytose completely till now is not clear. Apparently it is carried out due to movement in the non-uniform magnetic field to excited presynaptic membrane vesicles filled acetylcholine molecules having the magnetic moment. Calculation of the magnetic field induction B at the membrane has been carried out in paragraph 2.2.2.1, fig. 2.13.

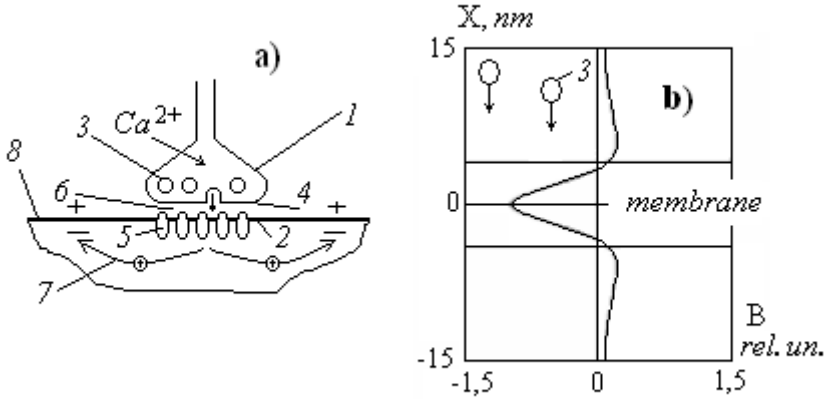

Fig. 4.3.

Vesicles filled acetylcholine 3 there are aspire in area of local increase of the magnetic field B which arises at both surfaces of presynaptic membranes at passage on it of the action potential, fig. 4.3b. Thus it is established that inside of synapse during this moment through opened voltage-gate channels appear Ca^{2+} ions which on the one hand promote integration of vesicles with presynaptic membrane and to emission mediator in the synaptic cleft. On the other hand Ca^{2+} ions raise osmotic (concentration) pressure into synapse that promotes movement vesicles filled mediator to the presynaptic membrane.

Locating are in the synaptic cleft the molecules of mediator contact with ligand-gated ionic channels 5 which are in the postsynaptic membrane of the muscular fibres 2. Time of synaptic cleft crossing by the acetylcholine molecule no more $0.1\,ms$. Ligand-gates ionic channels 5 are not selective i.e. through them can is transferred various ions: Na^+, K^+, Ca^{2+}. For short time $\sim 1\,ms$ during which channels 5 are open through each of them transferred some tens thousand ions of Na^+ and K^+. In result the potential difference on the postsynaptic membrane 2 significantly decreases due to decrease in negative potential on its endocellular side.

There is a potential difference and the electric field strength between sites of extrasynaptic membranes 8 of muscular fibres and it the postsynaptic membrane 2. Movement of positive ions along strength lines of electric field 7 aside of extrasynaptic membrane of the muscular fibre results to decrease in negative potential on

extrasynaptic membrane 8 below the depolarization potential (PDep) i.e. to excitation of the muscular fibre and propagation on its membrane of action potential (AP).

In the synaptic terminals of the central nervous system, at innervation of vessels smooth muscles, etc. the mediator is other substance - noradrenaline.

Medicinal substances there are time blockers of acetylcholine ligand-gates channels of postsynaptic membranes (M- and H-cholineblockers) are widely applied. Temporarily block of ions transfer through ligand-gate channels of postsynaptic membranes which are activated noradrenaline $\alpha-$ and $\beta-$ blockers, for example, doxazosin, atenolol (it is applied as antihypertensive preparations), etc.

Distinctive feature given synaptic connections is that it can transfer the electric signal (excitation) only in one side, for example, from a nervous fibre to the muscular cell. From this point of view the synaptic connection plays role of the biological diode.

There are exist electric synapses in which activation voltage-gates ionic channels of postsynaptic membranes is carried out electrotonic due to electric field of presynaptic membranes. Electric synapses are usually used for maintenance of less important functions of an organism. They are distributed at invertebrates, fishes. As against chemical synapse the electric synapse have no one-way conductivity.

Synaptic connections arise and are liquidated during all human life. Synapses can be formed between axon of one nervous cell and dendrite another, between axon one cell and a body (soma) other cell, between axon or dendrite one nervous cell and the body another not the nervous cell (muscular cell, photoreceptor in the visual analyzer, hair cell in the acoustic analyzer, etc.).

Neurons of a brain there are form set synaptic contacts. On the surface neuron there can be some thousand synaptic connections. The average density of the synaptic neuron brain connections of the man determines his intellectual opportunities. At early stages of the organism development when basically are formed synaptic connections of the brain neurons the number of dendrites on neurons is much more than at later age. In the first months after a birth of the man the velocity of synaptic connections formation reaches 40000 in second. At this time the man absorbs very large quantity of the information about world around. At insufficient quantity of the absorbed information or its quality the intelligence of the child develops slowly. Crying of the child frequently testifies to “information hunger” when many dendrites remain without synapses are involved back in the neuron body that apparently causes in the child unpleasant sensations. The decrease quantity of dendrites reduces intellectual opportunities of the child. With the purpose of the given process minimization in order to prevent the slowed down development of the child in the first months of his life it is necessary to create to the child maximum big stream of the different quality information: visual, acoustical, tactile, etc. With this purpose it is recommended to not lull the child by rocking, constantly to change color scale surrounding him, to speak with the child, to create an intelligent acoustic background (music, speech of radio, TV, etc.). Naturally it demands significant physical and psychological efforts from mother. The aspiration of mother in afterbirth period to be realized in professional sphere faster is unproductive from the point of view of successful development of her child.

4.1.2. Biopotentials of cardiomyocytes

Cardiac muscle - myocardium has series of essential differences from a skeletal muscle. First of all the myocardium is functions as syncytium. Cells of the myocardium (cardiomyocytes) though are separated from each other but there are in such close interrelation that excitation of one cell is transferred on next due to gap junctions - nexus. In gap junctions the contact special membrane ionic channels – connexons is carried out through which ions can freely diffuse from the cell in the cell. It is connected by that connexons of two next contacting cells form the uniform channel taking place through the gap. This channel can be bent not preventing with contraction of myocardium. In heart are available separate atrial and ventricular syncytiums. Besides action potential of the myocardium cell is considerably longer than at neuron or skeletal muscle. It is connected by that is necessary to keep the muscle in the contracted condition long time at the unitary impulse of excitation.

The scheme of ions movement through the membrane of the myocardium cell (fibre) is shown on fig. 4.4.

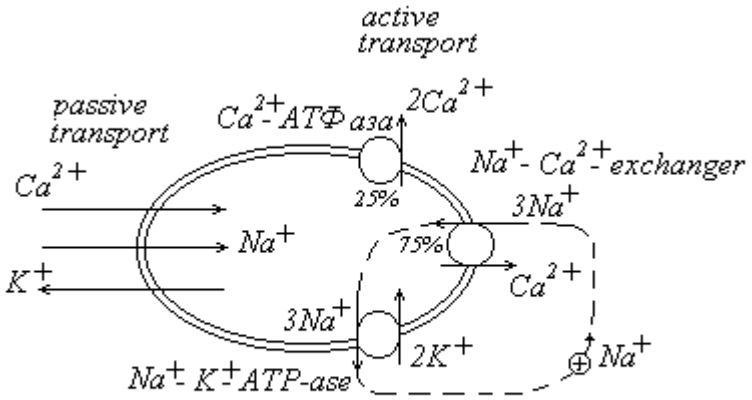

Fig. 4.4.

The action potential on the membrane of cardiomyocyte is formed due to passive transport through a membrane of three kinds of ions Na^+, K^+ and Ca^{2+} - so-called three-ionic system of action potential formation.

Myocardium cells are typical myocardial fibres (TMF) and atypical myocardial fibres (ATMF).

Let's consider occurrence of action potential on typical myocardial fibres (TMF) which 99% all mass of myocardium will consist. TMF carries out contractile function of the myocardium.

In the resting condition the resting potential (RP) on the internal side of a cell membrane (concerning external side) $-90\,mV$, factors of the membrane permeability for potassium and for sodium has ratio as $P_K : P_{Na} = 20:1$. All voltage-gates ionic channels are closed except for potassium channels which the fraction is always open. The relation of the ions concentration are playing the basic role in formation of the action potential outside and inside cell following:

$$\frac{[K^+]_o}{[K^+]_i} = 0.028; \qquad \frac{[Na^+]_o}{[Na^+]_i} = 9.7; \qquad \frac{[Ca^{2+}]_o}{[Ca^{2+}]_i} = 20000\,.$$

The essential role in formation of the action potential is played the Ca^{2+} ions. Inside a cell in cytoplasm in the resting condition the ions of calcium should be very little in order to prevent occurrence of chaotic operation of the actin-myosin force mechanism of a muscular fibre.

For decrease in concentration of Ca^{2+} ions in a cell in there are cardiomyocytes membranes constantly works electrogenic $Na^+ - Ca^{2+}$-exchanger. In the processes of evolution it has arisen with the purpose to use powerful system of $Na^+ - K^+$-ATPase for removal of Ca^{2+} ions from a cell. Energetically the activity $Na^+ - Ca^{2+}$-exchanger is provided with the electrochemical potential $\Delta\bar{\mu} = RT \ln \frac{[Na^+]_o}{[Na^+]_i} + zF\Delta\varphi$ arising due to the concentration difference of sodium Na^+ ions on the membrane (i.e. actually for account of the $Na^+ - K^+$-ATPase). Ions of Na^+ there are move on the gradient of concentration and potential to cell inside, and ions Ca^{2+} against these gradients outside. $Na^+ - Ca^{2+}$-exchanger throws out from a cell one Ca^{2+} ion in exchange for input of 3 Na^+ in a cell i.e. it reduces negative potential on the internal side of membrane. The increase in concentration of Na^+ ions inside a cell makes active work of the $Na^+ - K^+$-ATPase directed on removal of sodium from a cell. Energy of ATP hydrolysis is not necessary directly for work of $Na^+ - Ca^{2+}$-exchanger it is works for account $Na^+ - K^+$-ATPase. Work $Na^+ - Ca^{2+}$-exchanger it is the example of secondary active

transport. Teamwork $Na^+ - K^+$-ATPase and $Na^+ - Ca^{2+}$-exchanger create circulation of Na^+ ions which on fig. 4.4 is shown by the dotted line. Motive forces of this circulation it is $Na^+ - K^+$-ATPase.

Upon termination of contraction process of the muscle approximately 80% of Ca^{2+} ions pump down in sarcoplasmic reticulums by ionic pumps Ca^{2+}-ATPase. Approximately 20% of Ca^{2+} ions leave for limits of cell by help $Na^+ - Ca^{2+}$-exchanger and $Na^+ - K^+$-ATPase. On $Na^+ - Ca^{2+}$-exchanger are fall fraction 75% of all Ca^{2+} ions removed of a cell. The remaining there are 25% of ions take out by the membranous Ca^{2+}-ATPase.

With the help of medicinal substances - cardiac glycoside (digoxinum, strophanthinum, corglyconum, etc.) there is inhibited functioning of $Na^+ - K^+$-ATPase. It results in decrease in the concentration difference of sodium ions on a membrane due to break of circulation of Na^+ ions and as consequence to delay of the $Na^+ - Ca^{2+}$-exchange work intensity. Concentration of endocellular Ca^{2+} grows. There is increases contractive activity of a myocardium that is used at cardiac insufficiency. The considered mechanism of cardiac glycoside action shows that their prescription needs to be carried out with the big care.

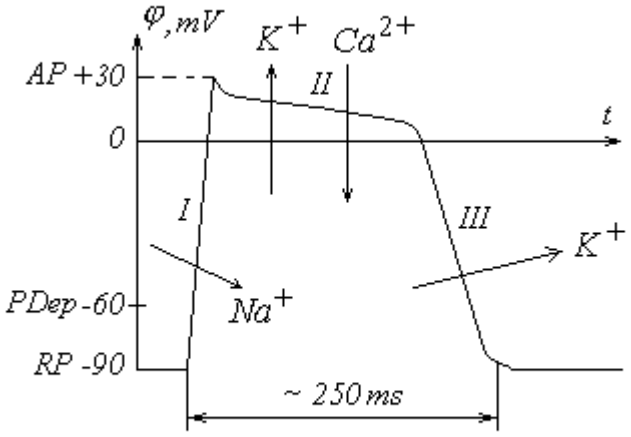

Fig. 4.5.

At excitation of cardiomyocyte (TMF) due to decrease in potential on the membrane from size *RP* equal $-90\,mV$ up to size of potential of depolarization (*PDep* – potential of depolarization after which achievement begins spontaneous depolarization of the cell membranes) equal $-60\,mV$ it is accepted to consider three phases of potential change onits membrane, fig. 4.5. These phases are carried out due to passive transport of ions.

I - the phase of depolarization. The relation permeabilities for ions potassium and sodium becomes $P_K : P_{Na} = 1:20$. Ions of sodium Na^+ through opened sodium ionic channels enter into the cell. The internal surface of a membrane is charged for $1-2\,ms$ up to $+30\,mV$. Then sodium channels are closed. Passive ions fluxes through channels of the cardiomyocyte membrane are conditionally shown on fig. 4.5.

II – the phase of slow repolarization (plateau). Ions of potassium K^+ through opened potassium ionic channels leave the cell. But sharp reduction of positive potential inside the cell due to carrying out of the positive charge by K^+ ions is compensated entering through opened in a membrane of cardiomyocyte calcium channels by ions of calcium Ca^{2+}. Time of process is approximately $\sim 200\,ms$. Then calcium channels are closed. During the phase *II* small falling potential is observed.

III - the phase fast repolarization. The proceeding output of potassium K^+ ions through open potassium channels reduces potential on the internal side of the cardiomyocyte membrane up to the initial level of resting potential $-90\,mV$. Time of process is $\sim 50\,mV$. Then basically are closed and potassium channels.

Further ionic pumps and $Na^+ - Ca^{2+}$-exchanger due to active transport restore initial concentration of ions Na^+, K^+ and Ca^{2+}.

Let's consider change of potential on the membrane of atypical myocardial fibres (ATMF). From ATMF will consist sinoatrial and atrioventricular nodes, the His bundle and branches of His bundle, Purkinje fibers i.e. it is conducting system of the heart.

At ATMF of sinoatrial node (driver of the rhythm – cardiac pacemaker) consisting of approximately 5000 fibres which is located in the right atrium in the mouth superior vena cava is not of resting potential. For these cells spontaneous continuous electric parametrical oscillations with period *T*, fig. 4.6, are characteristic.

These oscillations begin a slow current of ions Na^+ inside of the cell so-called spontaneous slow diastolic depolarization (SDD) which duration actually regulates the period of cardiac contractions *T*. Thus ions Na^+ move inside of the cell through open calcium channels. These channels permeable both for Na^+ and for Ca^{2+} therefore some researchers believe that in basis SDD the current of ions Ca^{2+} is mainly for which on a membrane of cardiomyocytes there is a big concentration gradient.

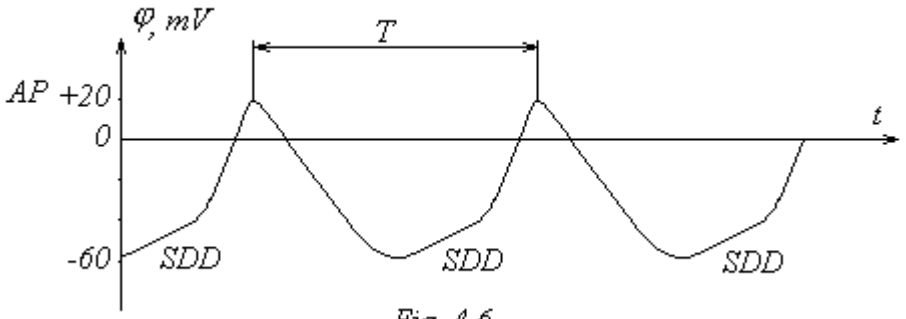

Fig. 4.6.

Then owing to opening of sodium channels the velocity of potential change increases reaching action potential (AP) then slower recession of potential begins. Further process spontaneously repeats.

If sinoatrial node on what or to the reasons ceases to work the spontaneous electric oscillations after the while begin in atrioventricular node. Heart continues to be contracted but with smaller frequency.

4.2. Propagation of excitation on myocardium

Before the beginning of contraction of heart approximately for $0.02 - 0.04\,s$ there is the excitation of the myocardium cells i.e. them depolarization. This depolarization initiates cardiac contraction. The rhythm of heart contraction is set by spontaneous parametrical oscillations membranous potential of cells in sinoatrial node (the basic driver of the heart rhythm) 2, fig. 4.7, which is in the right atrium in the mouth superior vena cava 1.

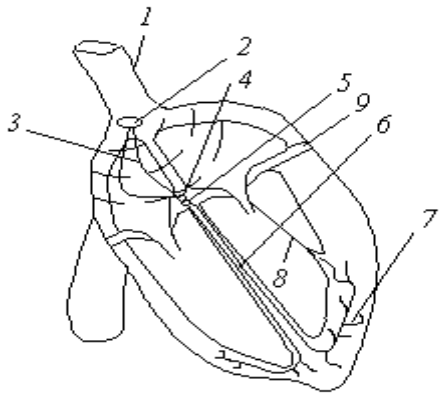

Fig. 4.7.

Further excitation is propagated on the myocardium in the following sequence: sinoatrial node 2 $\rightarrow$ internodal tracts 3 and the myocardium of atrium $\rightarrow$ atrioventricular node 4 $\rightarrow$ His bundle 5 $\rightarrow$ the right and left branches of His bundle 6 $\rightarrow$ Purkinje fibers 7 $\rightarrow$ myocardium of ventricles.

Transition of excitation it is direct from the atrium to the ventricles it is impossible since they are separated from each other by the unexcitable fibrous tissue 9. On the myocardium of ventricles the excitation goes from the

apex of heart to its base. In walls of ventricles excitation goes from within to outside.

Velocity of propagation of the depolarization wave on internodal tracts is $\sim 1\frac{m}{s}$, on atrium $\sim 0.3\frac{m}{s}$, on atrioventricular node $\sim 0.02-0.05\frac{m}{s}$, on branches of His bundle $\sim 2-3\frac{m}{s}$, on Purkinje fibers $\sim 4-5\frac{m}{s}$, on the myocardium of ventricles $\sim 0.4\frac{m}{s}$.

Small velocity of propagation of excitation on atrioventricular node is necessary for creation so-called atrioventricular delays $\sim 0.1\,s$. Due to this delay blood has time to flow from atrium at their contraction in still relaxed ventricles.

Big in comparison with the basic myocardium the velocity of propagation of excitation on branches of His bundle and Purkinje fibers is necessary that before the beginning of contraction of the main mass of myocardium of ventricles need to pull the tendinous chordas 8 due to contraction of papillary muscles. These chordas are connected with cusps of the atrioventricular valves of heart (mitral and tricuspid). Otherwise during the overflowing of blood from atrium in ventricles there will be high-frequency self-oscillations (flutter) of valves cusps [61]. During contraction of ventricles the tension of the tendinous chordas 8 is necessary since without such tension thin cusps of valves will not oppose to pressure in ventricles and there will be return flow of blood from ventricles into atrium.

Though frequency of cardiac contractions is determined by frequency of spontaneous oscillations of sinoatrial node it can be regulated also by the central nervous system with the help of nervous ways of vegetative nervous system.

4.3. Biophysical bases of electrocardiography

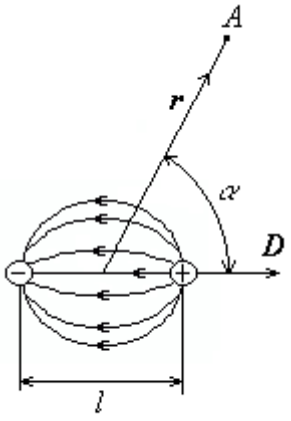

Fig. 4.8.

Biophysical bases of electrocardiography were laid by Dutch scientist W. Einthoven for what in 1924 he has received the Nobel Prize.

W. Einthoven's basic achievement will be that he has opened vector essence of cardiac electrogenesis. It has allowed to understand principles of the electrocardiogram occurrence i.e. time dependence of registered biopotentials of heart, and also to explain features of its form.

W. Einthoven's theory assimilates heart to an equivalent currents dipole in the homogeneous conducting environment, fig. 4.8.

The current dipole it is the poles of the current source placed in conducting environment.

The positive pole of the current source refers to as source, and negative - the sink. The current outside of the current dipole flows along lines of force from a source to the sink.

Dipole moment of current dipole it is product of the general current *I* flow from the source to the sink on distance between them ***l***:

$$\boldsymbol{D} = \boldsymbol{Il}. \qquad (4.1)$$

Dipole moment of current dipole it is vector value. The direction of vector ***D*** is from the sink to the source.

It is simple to find that potential of the electric field of the current dipole in any point *A* on distance *r* from the dipole, fig. 4.8, it is possible to calculate under the formula:

$$\varphi_A = \frac{\rho D \cos\alpha}{4\pi r^2}, \qquad (4.2)$$

where ρ there is specific resistance of environment in which it is placed the current dipole, α - the angle between the direction of the dipole moment ***D*** and radius a vector ***r*** to the researched point *A*.

During excitation of the myocardium on it the wave of depolarization 1, fig. 4.9, propagates. The front of the depolarize wave on external surface of the myocardium divides potentials of a different sign in the conducting environment: not excited part of the myocardium charged positively (or is more exact with zero potential since the surface of heart actually it is earthed) and the excited part charged negatively with negative potential concerning not excited part of the myocardium (at this time inside a cells is the changing positive potential). In more detail the nature of the charge on external surface of the myocardium is analysed in the beginning of chapter 4, fig. 4.1. Therefore the front of the depolarize wave can be presented as elementary current dipoles 2. The dipole moment of each of current dipoles has the size and direction $\boldsymbol{D}_i$.

Summarizing vectorially the dipole moments of elementary current dipoles we receive the dipole moment of the equivalent dipole of heart. In medicine the equivalent dipole moment it is accepted refer to as integrated electric vector of heart (IEVH).

$$\boldsymbol{D} = \sum_i \boldsymbol{D}_i \,. \qquad (4.3)$$

The model which electric activity of the myocardium is replaced with action of one the equivalent current dipole refers to as the dipole equivalent electric generator of heart.

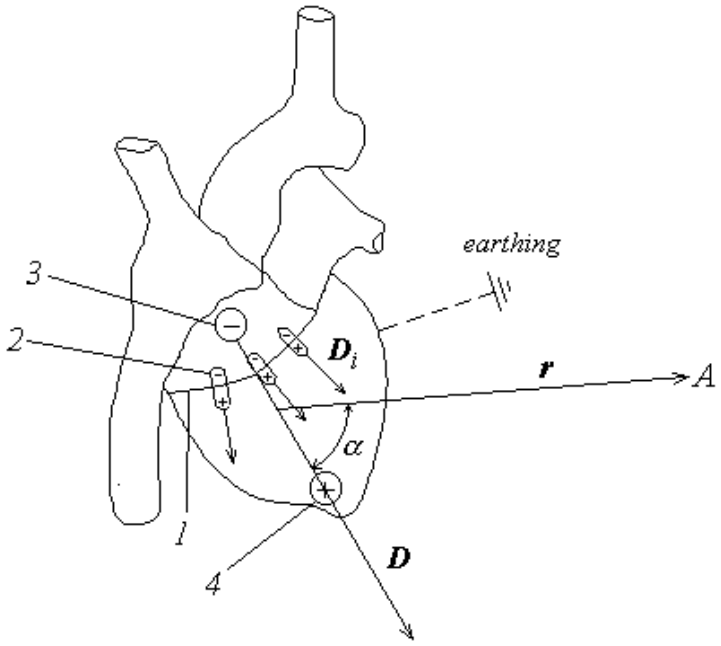

Fig. 4.9.

The equivalent dipole can be presented as set equivalent the sink 3 and the source 4. In process cardiac cycle IEVH changes the size and direction.

The potential of the electric field generated by the myocardium falls in inverse proportion to square of distance from the equivalent current dipole $\varphi_{dip} \sim \frac{1}{r^2}$.

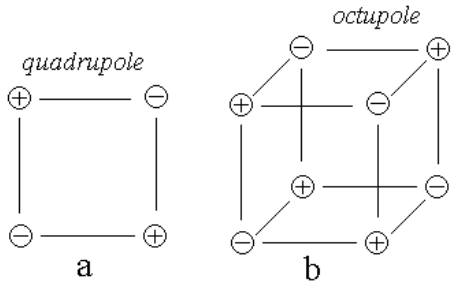

Fig. 4.10.

At small distance from heart the potential dependence on distance more complex. In this case dipole approximation of the equivalent electric generator of heart is not absolutely correct and necessary to take into account quadrupole, fig. 4.10a, and octupole, fig. 4.10b, the components of potential.

Generally the system of charges of the different sign

refers to multipole. For quadrupole $\varphi_q \sim \frac{1}{r^3}$, and for octupole $\varphi_{oc} \sim \frac{1}{r^4}$.

Thus near to the heart it is necessary to examine the multipole equivalent electric generator of heart which potential with precision of octupole addend changes under the law:

$$\varphi = \varphi_{dip} + \varphi_q + \varphi_{oc}. \qquad (4.4)$$

For practical purposes diagnostics of cardiac diseases it is possible to be limited to dipole approximation.

4.3.1. Theory of Einthoven

W. Einthoven's theory assimilates heart from the electric point of view to the single equivalent current dipole in the homogeneous conducting environment.

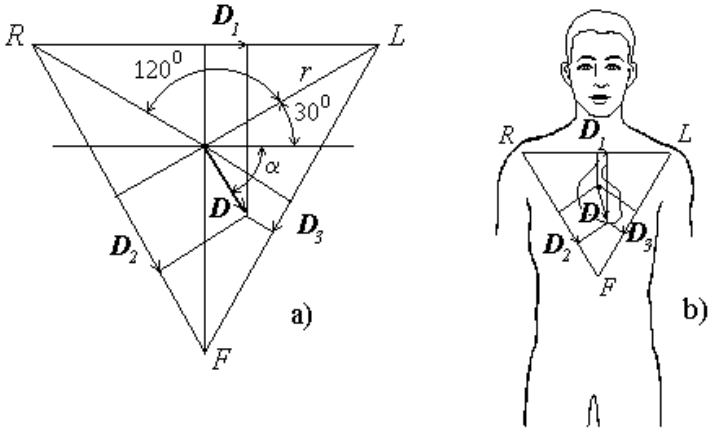

Fig. 4.11.

Einthoven has suggested to measure potential differences between nodes of the equilateral triangle, fig. 4.11a, on the surface of a body (triangle of Einthoven). The center of this triangle coincides with a projection of the application point IEVH to the chest which place in atrioventricular node, fig. 4.11b. The nodes of the triangle designate letters *R* (right), *L* (left), *F* (foot). During the cardiac cycle the IEVH changes the size and direction. The end of the vector writes the complex space curve.

Model of Einthoven has contradictions:

1. Organism not the homogeneous conducting medium.
2. The curve wrote by the end of IEVH is space, and triangle of Einthoven is flat.
3. The single current dipole cannot be good model of electric activity of heart.

Despite of these assumptions the theory of Einthoven till now is the basic biophysical model used in electrocardiography at the analysis of electrocardiograms.

Let's find the potential difference between points *L* and *R*. The potential in point *L* created by the current dipole with dipole moment ***D*** is equal:

$$\varphi_L = \frac{\rho D \cos(\alpha + 30^\circ)}{4\pi r^2}. \qquad (4.5)$$

The potential in point *R*, is equal:

$$\varphi_R = \frac{\rho D \cos(\alpha + 150^\circ)}{4\pi r^2}. \qquad (4.6)$$

The potential difference between points *L* and *R* is equal:

$$\varphi_L - \varphi_R = \frac{\rho D[\cos(\alpha + 30^0) - \cos(\alpha + 150^0)]}{4\pi r^2} = \frac{\rho D\sqrt{3}\cos\alpha}{4\pi r^2}. \quad (4.7)$$

The module of the projection of the dipole moment vector ***D*** on the direction *LR* we shall designate D_1, fig. 4.11. Taking into account, that $D_1 = D\cos\alpha$ it is possible to write down $\varphi_L - \varphi_R \sim D_1$. Hence it is possible to make the important conclusion.

The potential difference between two nodes of Einthoven triangle is proportional to projection of IEVH to the line connecting these two nodes. This potential difference is function of time since it changed in process cardiac cycle. Potential differences between nodes of Einthoven triangle refer to as the main (standard) leads.

I it is main lead *LR*. The voltage in this lead is $U_1 = \varphi_L - \varphi_R \sim D_1$.

II it is main lead *FR*. The voltage in this lead is $U_2 = \varphi_F - \varphi_R \sim D_2$.

III it is main lead *FL*. The voltage in this lead is $U_3 = \varphi_F - \varphi_L \sim D_3$.

Sum the resulted formulas it is possible to receive that $U_2 = U_1 + U_3$. The received equality refers to as formula of Einthoven. Formula of Einthoven allows monitor technical correctness of the electrocardiogram registration. Usually the monitoring is carried out on the maximal (peak) values of voltage in the main lead.

Direction of IEVH at its maximal size in process depolarization of ventricles refers to as the electric axis of heart. The electric axis of heart is close to its anatomic axis. Therefore having constructed on the basis of the received electrocardiograms in three main leads with the help of triangle of Einthoven the direction of the electric axis of heart it is possible to receive representation about position of heart in the thorax.

4.3.1.1. The linear electrocardiogram

The linear electrocardiogram or simply the electrocardiogram (ECG) is a graph of change in time (for the cycle of work of heart) instant values of the potential difference in corresponding lead.
The electrocardiogram reflects cumulative electric depolarization and repolarization all cells of the myocardium. On fig. 4.12 the model electrocardiogram in *II* the main lead is shown.

The maximal amplitude size of potential difference $\Delta\varphi$ of the electrocardiogram (wave *R*) makes in norm $1-2\,mV$, fig. 4.12. Change of potential on the cardiomyocyte membrane in process of depolarization $\sim 110\,mV$ i.e. on two order it is higher. This difference as already it was specified earlier is connected by that the electrocardiogram fixes total change of cardiomyocyte potentials on the external surface of cells. The basic change of potential in process of depolarization occurs on the internal side of the cell membrane. The external side of membrane actually earthed. The potential on it changes little and quickly disappears. Therefore the electrocardiogram is only small reflection those powerful electric processes which occur in myocardium cells.

The linear electrocardiogram schematically shown on fig. 4.12 in norm will consist from the *P* wave, complex *QRS* and the *T* wave. These electric impulses are separated by sites of zero potential. The *P* wave arises in time $\sim 0.02\,s$ till the beginning of the atrium contraction it reflects the depolarization atrium and initiates their contraction. Complex *QRS* reflects the depolarization of ventricle. Thus it is assumed that *Q* wave reflects depolarization of interventricular septum, *R* – depolarization of the main mass of the ventricular imyocardium, *S* – depolarization of heart base of ventricles.

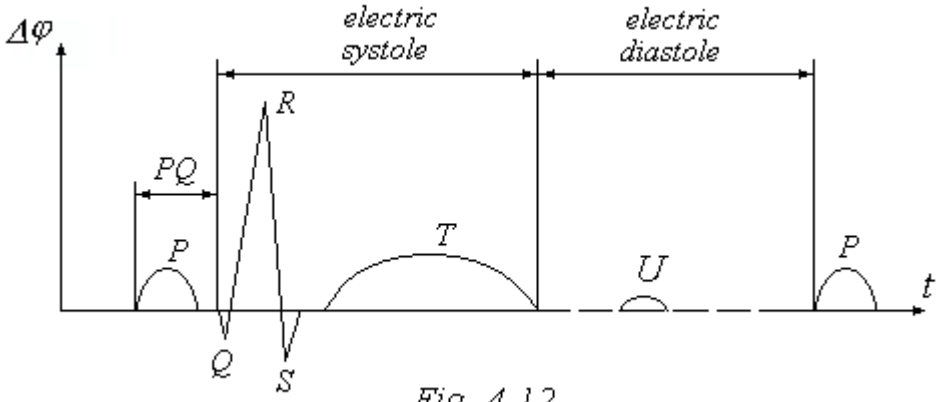

Fig. 4.12.

The *T* wave it is registered during time of ventricular repolarization.

Change of sign on potential *Q* and *S* waves arises due to rotation IEVH ***D*** in process of cardiac cycle.

Sometimes the after *T* wave on the electrocardiogram it is possible to observe small *U* wave.

The interval from the beginning *Q* wave up to the end *T* wave refers to as electric systole and from the end *T* wave till the beginning *P* wave of the following cardiac cycle - electric diastole.

Arising on interval *PQ* isoline appears when the atriums completely depolarize and excitation is propagated on conducting system of heart - atrioventricular node, His bundle, the right and left branches of His bundle, Purkinje fibers. Duration of interval *PQ* makes $\sim 0.12 - 0.2\ s$. Into this interval include the atrioventricular delay which is necessary for overflowing of the blood from contracted atriums in still relaxed ventricles.

Isoline between complex *QRS* and *T* wave arises when all myocardium ventricle depolarize.

Thus it is necessary to mean that potential difference which on the electrocardiogram is reflected by waves it is registered only in dynamics i.e. in process of the myocardium depolarization or repolarization.

Between these two processes arise time stationary conditions when positive ions of electrolit surrounding the myocardium quickly compensate small negative potential on the external cell surface of myocardium completely excited. Therefore the potential difference between the external cells sides of the excited and not excited parts of myocardium disappears very quickly. It explained the presence isolines on the electrocardiogram. The potential difference between the internal cells sides of the excited and not excited parts of the myocardium thus naturally is kept but this potential difference is not registered on the electrocardiogram.

As the form of the linear electrocardiogram reflects dynamics (velocity) of the membranous potential change it corresponds approximately to the first derivative on time from the membranous potential

$$\Delta\varphi \sim \frac{d\varphi_m}{dt}.$$

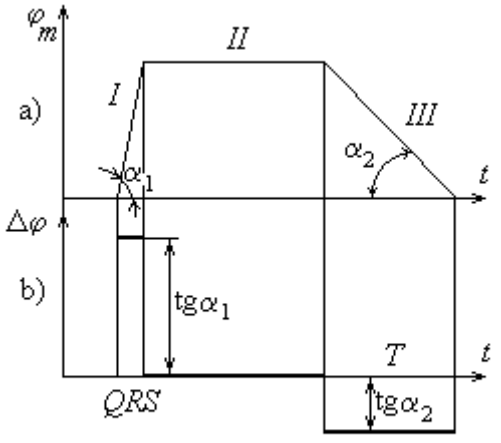

Fig. 4.13.

On fig. 4.13a the simplified graph of potential change on the cardiomyocyte membrane of the ventricle (fig. 4.5) and the first derivative on time from this graph, fig. 4.13b, very roughly modeling the electrocardiogram is shown. We remind that the first derivative reflects a tangent of the inclination angle of tangent to the graph of function $\Delta\varphi \sim \mathrm{tg}\alpha$.

In phase *I* of the fast depolarization of cardiomyocytes membranes of ventricles the complex *QRS* average on all cells on the electrocardiogram is observed. Isoline on the electrocardiogram between complex *QRS* and *T* wave is corresponds to a phase *II* when the potential on a membrane of cells practically does not vary. At this time is $\Delta\varphi \sim \frac{d\varphi_м}{dt} \approx 0$. In phase *III* of the fast repolarization of cardiomyocytes on the modeling electrocardiogram, fig. 4.13b, is observed *T* wave having return polarity concerning the real electrocardiogram, fig. 4.12. It is necessary to note that the full explanation of the form of

electrocardiogram till now is not final.

Are available on extremely measure three questions answers on which have debatable character:

1. Where on the electrocardiogram is the wave reflecting repolarization of atriums?

On the given question there are such explanations. The impulse reflecting repolarization of atriums is latent by considerably more powerful ventricular complex *QRS*. But complex *QRS* in norm is too narrow to hide rather long repolarization of atriums. Repolarization of the myocardium cells the process less determined than them depolarization therefore it is longer. For example, for ventricles the ratio of repolarization duration to them depolarization duration is usual more than 3. Duration of depolarizative *P* wave and *QRS* complex are approximately identical.

The second explanation is connected by that the impulse of repolarization of atriums because of the big duration "is spread" on all electric systole and consequently is not observed.

2. Why *T* wave in norm has the same polarity as *R* wave?

Repolarization of cardiomyocytes, for example, ventricles begins with interventricular septum and comes to the end the base of ventricles. The front of the repolarizative wave passes the same way as front of the depolarizative wave. Though in connection with smaller determinancy of process of cells repolarization front of the repolarizative wave is less orderliness. But as elementary current dipoles at the front of wave of repolarization are directed opposite to the current dipoles of the wave of depolarization the *T* wave should have return polarity be relative of *R* wave.

One of possible explanations of the given contradiction consists that during time of repolarization of the ventricular myocardium the external skew layer of the myocardium which creates additional conditions for active increase in ventricular volume at their filling by the blood actively works. The *T* wave is reflection depolarization of this layer of the myocardium. Some researchers [37] believe that process repolarization propagates on the myocardium in the opposite direction to process depolarization. First of all there is repolarizative the base of ventricles and in the end the interventricular septum. However they lead to not result of the morpho-physiological reasons and direct proofs of it.

In paragraph 4.3.2 shown as it is possible to explain positive *T* wave with the help of inductance-capacitor model of the myocardium excitable tissue.

3. Than occurrence *U* wave explains on ECG?

One explanation will be that *U* wave reflects the trace potentials in a phase of higher excitation of the myocardium after systole. Other speculation: *U* wave it is connected to intensive active current of calcium ions at pumping them in sarcoplasmic reticulum of the myocardium cells after the ending of contractive process.

Under the electrocardiogram in the certain degree there are judge about state of heart and its pathology.

For example, the major diagnostic attribute on the linear electrocardiogram it is displacement from isoline of potential on the site between *S* and *T* waves. Such displacement specifies presence of the myocardium ventricles site excite more slowly i.e. faulted due to failure of the coronary blood circulation. There is potential difference $\Delta\varphi$ between the excited myocardium and exciting more slowly in the pathological center, fig. 4.14a. The given situation arises owing to occurrence of the centers of ischemia, infarction, necrocytosis, etc.

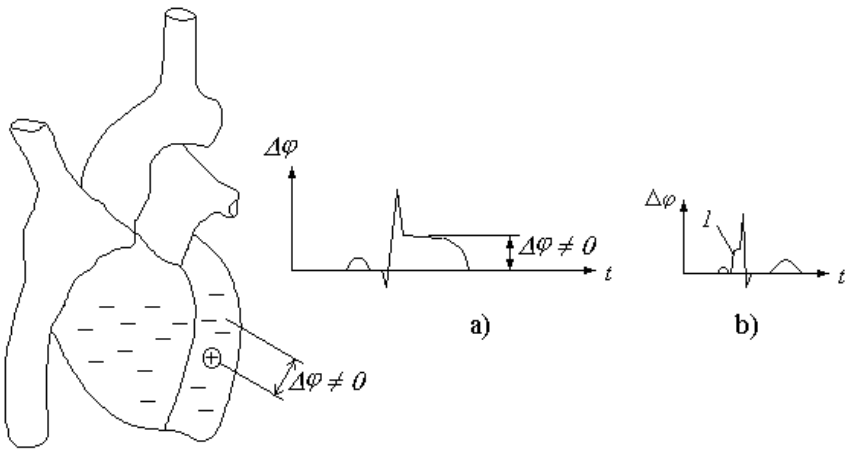

Fig. 4.14.

At fault of the myocardium the delay of depolarozative process and as consequence large width of complex *QRS* is possible.

The hypertrophy of the myocardium, i.e. it is growth with the increase of its mass, for example, at the arterial hypertension lead to increase in amplitude and width зубца *R*.

Presence of additional pathological conducting ways between atriums and ventricles (syndrome of Wolf-Parkinson-White) results in premature excitation of the ventricular myocardium, fig. 4.14b, so-called Δ -wave 1 on the electrocardiogram, etc.

It is necessary to note that the electrocardiogram is formed basically by external layers of myocardium. According to some information in formation of the electrocardiogram the top muscular layer thickness $1-2\,mm$ participates basically. Electrogenesis of internal layers it is shielded by external conducting layers of the myocardium. Therefore the pathology of external layers of myocardium, for example, its ischemia usually is better shown on the electrocardiogram than the same pathology of internal layers which can be not found at all on the electrocardiogram.

4.3.1.2. Vectorelectrocardiography

Vectorelectrocardiogram it is a curve which writes the end IEVH for the cycle of heart work.

Vectorelectrocardiogram (VECG) it is a space curve therefore usually examine its projections on frontal, horizontal and sagittal planes. VECG it is possible to receive from two linear electrocardiograms summing them under the angle or it is mutually perpendicular as reception of Lissajous's figures. In mathematics such curve name hodograph of vector ***D***.

The scheme of formation of VECG projection in one of the planes on the basis of two linear electrocardiograms is shown on fig. 4.15. VECG will consist of three loops *P*, *QRS* and *T*.

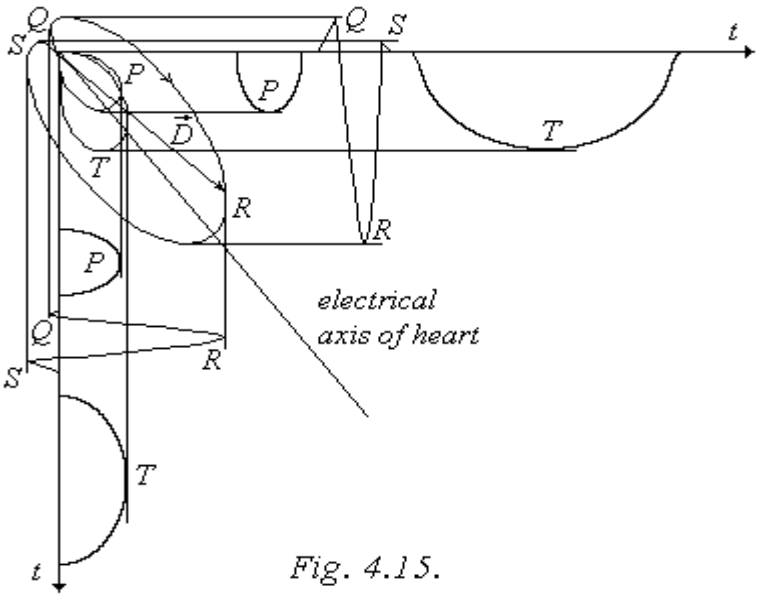

Fig. 4.15.

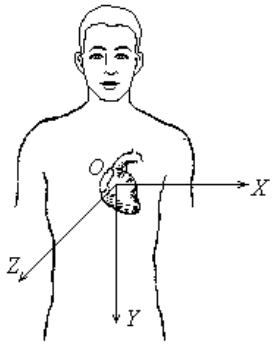

Fig. 4.16.

Registration of loops *P*, *QRS*, *T*, in three mutually perpendicular planes - frontal *F*, horizontal *H*, and sagittal *S* refers to vectorelectrocardiography.

On fig. 4.16 the coordinate axes used in VECG are shown. The axis *X* is directed from the right hand to left, axis *Y* - downwards, axis *Z* - from the back to chest. The beginning of coordinates is placed in atrioventricular node of heart. Planes *XOY* is the frontal, *XOZ* - horizontal, *YOZ* - sagittal.

In norm of the loops *QRS* and *T* of vectorelectrocardiogram in three mutually perpendicular planes look like, fig. 4.17.

The direction of the area development in planes of registration vectorelectrocardiogram depends on area of the maximal mass concentration of the myocardium i.e. numbers of the excitable cells generating biopotentials. Therefore the amplitude of the sum of the vectors dipole

moments of elementary current dipoles directed aside of the left ventricle of heart is more than amplitude of the sum of the vectors directed aside of right ventricle. Owing to what in norm development of the area in process cardiac cycle goes aside of left ventricle of heart.

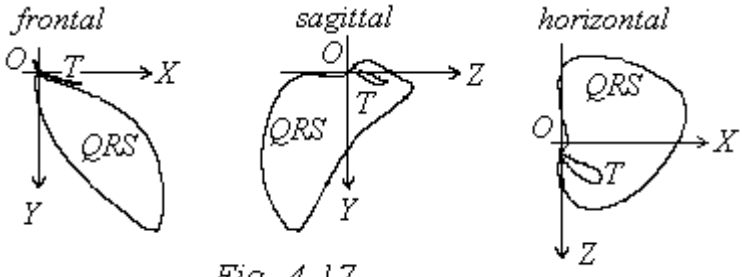

Fig. 4.17.

For VECG so-called orthogonal leads (mutually perpendicular or by it similar, for example, Mac-Fi-Parungao) *OX*, *OY*, *OZ*, fig. 4.16 are usually used. Thus in lead *OX* electrodes are placed as in the first main lead (right wrist – left wrist). In lead *OY* electrodes are placed on the left shin (ankle) and in area of a neck from the back side. In lead *OZ* electrodes are placed on the chest and on back in the projection of heart.

Synthesis VECG including spatial from linear orthogonal electrocardiograms it is carried out with the help of a computer.

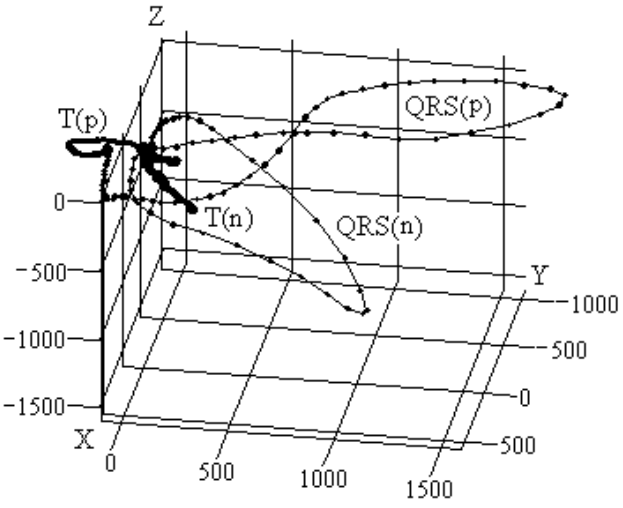

Fig. 4.18.

In connection with that hodograph of vector ***D*** is characterized by the spatial curve the more full information on the condition of cardiac electrogenesis in frameworks of dipole approximation gives spatial VECG. On fig. 4.18 for the example are shown spatial vectorelectrocardiogram. There are designations for the ventricular complex in norm - QRS(n), T(n) and for pathology QRS(p), T(p). On coordinate axes the voltage in μV is designated. It is possible to notice that excitation of the apex of heart actually does not occur. The form and area QRS loop with all presentation specify the hypertrophy left ventricle being consequence of practically full exception of work of all upper part of heart owing to the infarction.

The lack VECG there is not present evident the time intervals. On fig. 4.18 identical time intervals are marked by points on curves. Isoline of the linear electrocardiogram on VECG looks as a point therefore VECG it is used more often when it is necessary to find spatial localization of pathological process in heart. In this case VECG gives more full information than linear electrocardiogram.

Modern electrocardiography assumes simultaneous use of the linear electrocardiogram and VECG for more accurate statement of the diagnosis.

4.3.1.3. Phase electrocardiography

During diagnostics of cardiac diseases the analysis of additional characteristics of vector ***D*** is interest: for example, angular speed of its rotation ω, linear speed of moving of the vector end ***speed***, and also parameter ωD representing product of the angular speed module of a vector on the module of its size during each moment of time.

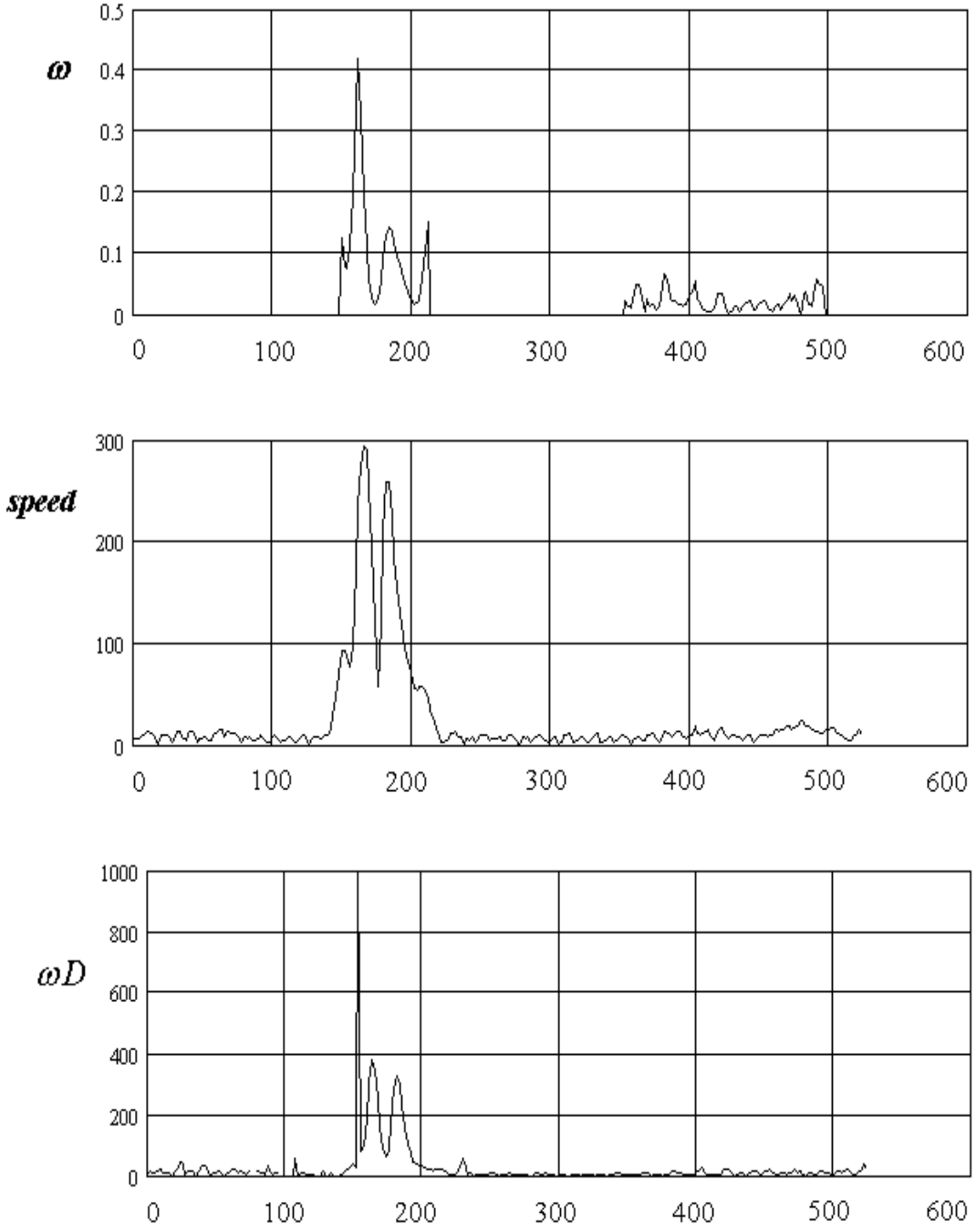

Fig. 4.19.

Each of these characteristics gives the contribution to increase of accuracy of disease diagnostics.

On fig. 4.19 the norm of these parameters is shown. On the axis of abscissas is the time in *ms* on the axis of ordinates relative units is marked.

Distinctive feature of all of three (additional to the linear electrocardiogram) parameters in norm is presence expressed bimodal structures. This bimodal structure of the signal reflects the following feature of the myocardium contraction. At contraction of the ventricular walls and emission from them blood in vascular system weaker interventricular septum can to hold out created pressure only in the isometric mode hence it should be contacted beforehand. Therefore character of signals should reflect in norm at first the contraction of interventricular septum, and then – ventricles walls.

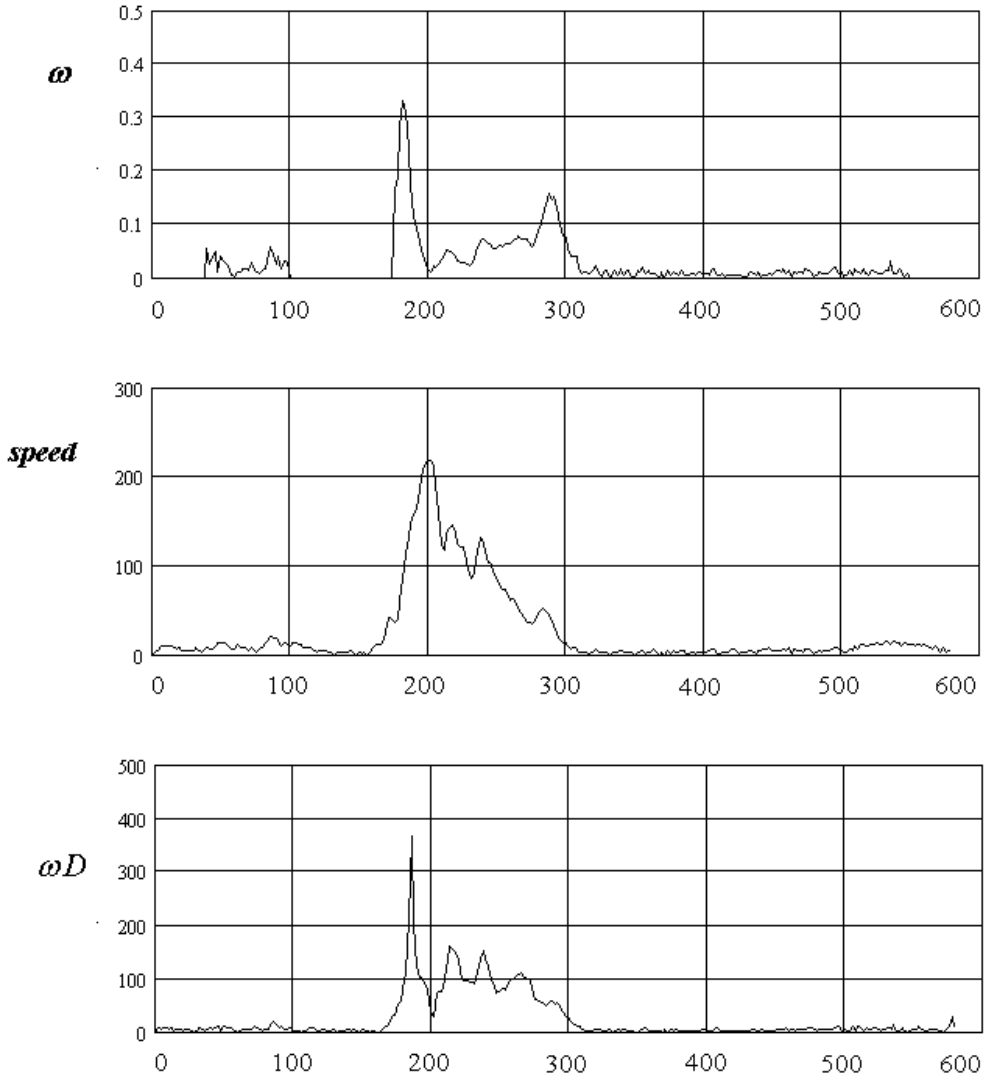

Fig. 4.20.

The sharp initial peak of a curve present on all curves but the most expressed on the curve ωD probably corresponds to fanous transition of excitation from interventricular septum on the myocardium of ventricular walls.

On fig. 4.20 results for the patient who has transferred the heart attack of a myocardium are submitted.

Process of excitation it is especial in the myocardium of left ventricle (the curve ***speed***) develops actually twice more slowly norms. There is practically disappeared characteristic for norm bimodality that is consequence of defeat of the wall of left ventricle.

4.3.2. Electrodynamics of myocardium on the basis of inductance-capacitor model

The analysis of occurrence and formation of the electrocardiogram i.e. the solution of the direct problem of electrocardiography is the important biophysical problem in connection with wide application in practice of this diagnostic method.

The analysis of change of integrated electric vector of heart ***D*** is a basis of the diagnostics method of heart work – electrocardiography (ECG). Usually carry out registration of vector projections on the allocated directions there is measuring corresponding potential differences.

Let's consider electric processes in heart on the basis of inductance-capacitor model.

The electrogenesis of atriums and ventricles are two different problems though its and the interconnected electrodynamic problems. For atriums it is necessary to carry out the separate analysis of the equivalent electric

generator. As example we shall consider the work of dipole equivalent electric generator of heart (DEEGH) for ventricles of hearts. We shall assume that heart has active resistance *R*, inductance *L* (in the excited condition), and capacity *C*.

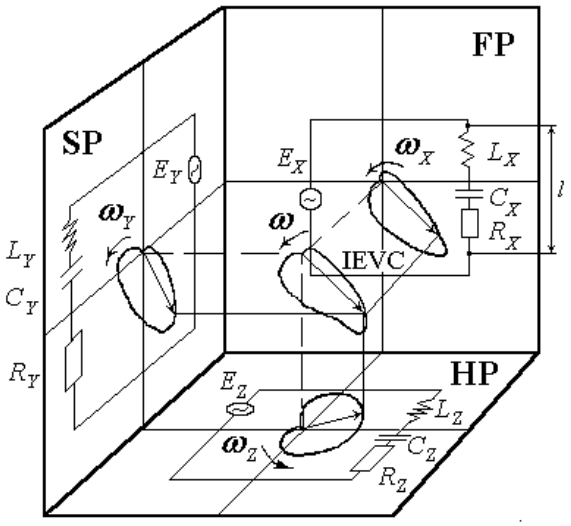

Fig. 4.21.

Let's present model of DEEGH as three mutually perpendicular oscillatory contours located in the frontal FP, horizontal HP and sagittal SP planes, fig. 4.21. Electromotive force (E.M.F.) *E* in all contours it is assumed identical. For ventricles the direct driver of the rhythm is atrioventricular node.

Let's consider work of one of three mutually perpendicular oscillatory contours. For convenience of calculations the indexes concerning to the concrete contour it is not designated in formulas.

Equation of Kirchhoff for instant values of voltage in a contour looks like:

$$U_R + U_L + U_C = E, \qquad (4.8)$$

where in the left part there is the sum of voltage on corresponding resistance. Using the known expressions connecting voltage and a current *i* we shall receive:

$$iR + \frac{d(Li)}{dt} + \int \frac{idt}{C} = E. \qquad (4.9)$$

Active resistance of a myocardium is determined first of all by resistance of cytoplasm and intercellular liquid therefore it can be assumed to constants during cardiac cycle. Inductance of the excitable membrane as it was already marked exists only during excitation and is connected to spiral movement of ions in ionic channels. Therefore it is difficult to assume that evolutionary the mechanism of active regulation of inductance could be generated. We shall assume the inductance of heart also constant size.

As in process cardiac cycle there is a change of capacity *C* connected with cyclic frequency of rotation IEVH the electric oscillations in contour of DEEGH have parametrical character [38].

We differentiate (4.9) on time *t* having divided the equation on *L* and having designated $\omega_0^2 = \frac{1}{\sqrt{LC}}$

- own frequency of the current oscillations in contour of DEEGH we shall find:

$$\frac{d^2 i}{dt^2} + \frac{R}{L}\frac{di}{dt} + \omega_0^2 i = \frac{1}{L}\frac{dE}{dt}. \qquad (4.10)$$

The equation (4.10) describes parametrical oscillations of nonlinear oscillator as own frequency of heart oscillations can vary due to change of capacity *C*.

Let's find the solution of this equation by its multiplication to any function $f(t)$:

$$f(t)\frac{d^2 i}{dt^2} + f(t)\frac{R}{L}\frac{di}{dt} + \omega_0^2 f(t) i = \frac{1}{L}\frac{dE}{dt} f(t). \qquad (4.11)$$

Let's subordinate function $f(t)$ to the condition [30]:

$$f(t)\frac{d^2i}{dt^2} + f(t)\frac{R}{L}\frac{di}{dt} = \frac{d}{dt}\left(\frac{di}{dt}f(t)\right), \qquad (4.12)$$

from which follows that:

$$f(t) = \exp\left(\int \frac{R}{L}dt\right). \qquad (4.13)$$

The equation (4.11) after multiplication on $f(t)$ becomes:

$$f(t)\frac{d}{dt}\left(\frac{di}{dt}f(t)\right) + \left(\omega_0 f(t)\right)^2 i = \frac{1}{L}\frac{dE}{dt}f(t)^2. \qquad (4.14)$$

Let's use the new variable under the formula:

$$d\Theta = \frac{dt}{f(t)}. \qquad (4.15)$$

Proceeding from the equation (4.14) function $f(t)$ has dimension reverse to cyclic frequency. Therefore we shall designate this function $f(t) = \frac{1}{\omega_d}$.

Let's increase the equation (4.14) on distance between the source and the sink in contour of DEEGH. This distance *l* conditional is shown on fig. 4.21 for a contour in the frontal plane. We shall copy the equation (4.14) in new designations:

$$\frac{1}{\omega_d}\frac{d}{dt}\left(\frac{1}{\omega_d}\frac{dD}{dt}\right) + \left(\frac{\omega_0}{\omega_d}\right)^2 D = \frac{l}{\omega_d^2 L}\frac{dE}{dt}, \qquad (4.16)$$

where $D = il$ and function Θ according to (4.15) represents the angle of rotate of vector *D* which rotates with cyclic frequency ω_d.

According to (4.13) time dependence ω_d taking into account that *R* and *L* are constants looks like:

$$\omega_d = \omega_{t0}\exp\left[-\frac{R(t-t_0)}{L}\right], \qquad (4.17)$$

where ω_{t0} there is cyclic frequency of vector *D* rotation at the moment of time t_0.

That the change of angular speed reflects the experimental fact can be judged under the known ratio of repolarization time and depolarization time of ventricles. The ratio of these times i.e. durations of *T* wave and complex *QRS* lays in the range $1.3-2.7$ [39]. It specifies decrease in angular speed of vector *D* rotation *D* in process of cardiac cycle.

According to [15] falling of potential of the driver of the rhythm consisting from the atypical myocardial fibres, hence and $\frac{dE}{dt}$ in interval *Q-T* occurs under the exponential law. Therefore it is possible to assume that in the right part of the equation (4.16) there is a size close to the constant. Designating this size C_1 and also taking into account that $d\Theta = \omega_d dt$ from (4.16) we receive the equation:

$$\frac{d^2D}{d\Theta^2}+\left(\frac{\omega_0}{\omega_d}\right)^2 D=C_1. \qquad (4.18)$$

Besides it is natural to assume that during evolution electric parameters of the myocardium were formed in so that own frequency ω_0 became equal to frequency ω_d of vector ***D*** rotation of dipole moment of DEEGH $\omega=\omega_d=\omega_0$. Then the equation (4.18) becomes:

$$\frac{d^2D}{d\Theta^2}+D=C_1. \qquad (4.19)$$

The solution of this equation is dependence of the module of the vector *D* of dipole moment from the angle of rotation and time which is convenient for writing down as:

$$D=A\sin^2(\Theta+\varphi)/2+B\cos^2(\Theta+\varphi)/2. \qquad (4.20)$$

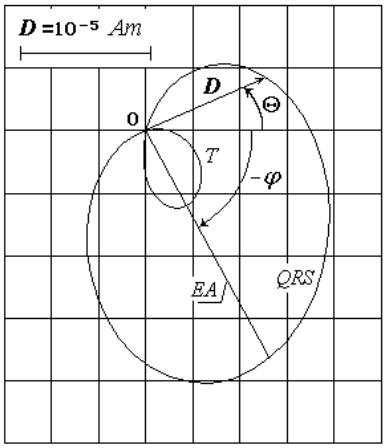

Fig. 4.22.

In the formula (4.20) *A* and *B* are the constants of integration so $C_1=\frac{A+B}{2}$. The angle φ is the inclination angle of the electric heart axis (EA) or axes of vectorelectrocardiogram loops.

On fig. 4.22 it is shown the vectorelectrocardiogram of loops *QRS* and *T* plotted under the formula (4.20). The angle φ is accepted equal $2.3\,rad$ that approximately corresponds to norm.

In fig. 4.22 the origins of the angle Θ and φ also are shown. Positive it is assumed the direction counter-clockwise. Sizes of constants *A* and *B* will be determined further.

Projecting on the chosen line the leads of the loop potential in fig. 4.22 (in this case for the example it is chosen the horizontal direction of projection) it is possible to plot linear electrocardiograms (ECG) under the formula:

$$U=kD\cos\Theta=\left(R\frac{\cos^2(\Theta+\varphi)/2}{\cos\varphi}-T\frac{\sin^2(\Theta+\varphi)/2}{\cos\varphi}\right)\cos\Theta, \qquad (4.21)$$

where *k* there is the constant factor agreeing dimension of potential difference *U* and dipole moment *D*. *R* and *T* is amplitudes waves of EGG. From comparison of formulas (4.20) and (4.21), and also fig. 4.22 the connection of projections of lengths of the loops main axes *QRS* and *T* equal accordingly *B* and *A* on the line of lead with amplitudes of waves of the linear ECG $R=kB\cos\varphi$ and $T=-kA\cos\varphi$ is visible. The fig. 4.22 is plotted for lengths of the loops main axes $B=2.0\cdot10^{-5}\ Am$ [2] and $|A|=\frac{B}{R/T}=0.67\cdot10^{-5}\ Am$. Amplitudes of the ECG waves are accepted $R=1.5\,mV$ and $T=0.5\,mV$.

As $\omega=\frac{d\Theta}{dt}$ dependence of the angle of the vector ***D*** rotation on time taking into account (4.17) it is possible to find under the formula:

$$\Theta=Q_0[1-\exp(-R(t-t_0)/L)]-\varphi, \qquad (4.22)$$

where $Q_0=\frac{\omega_{t0}L}{R}$ there is quality factor of the equivalent contour at the moment of time t_0, φ - the angle under which is directed the main axis of loop *QRS* (electric axis of heart *EA*), fig. 4.22.

The quality factor naturally is not a constant in process of the cardiac cycle. Taking into account (4.17) it is possible to see that during of electric systole it falls under the law:

$$Q = \omega L / R = Q_0 \exp[-R(t - t_0)/L]. \qquad (4.23)$$

Unfortunately it is traditional зубец *Q* and size of quality factor designated by one letter. It is concerns to *R* wave and value of resistance. It is supposed that it will not cause difficulties. On fig. 4.23 graphs of changes of cyclic frequency $\boldsymbol{\omega}$ of the vector ***D*** rotation (curve 1) and quality factor *Q* (curve 2) depending on time are shown. Curves are plotted for $\frac{R}{L} = 9\ s^{-1}$ and $Q_0 = 4.4$ ($\omega_{t0} = \frac{Q_0 R}{L} \approx 40\ \frac{rad}{s}$).

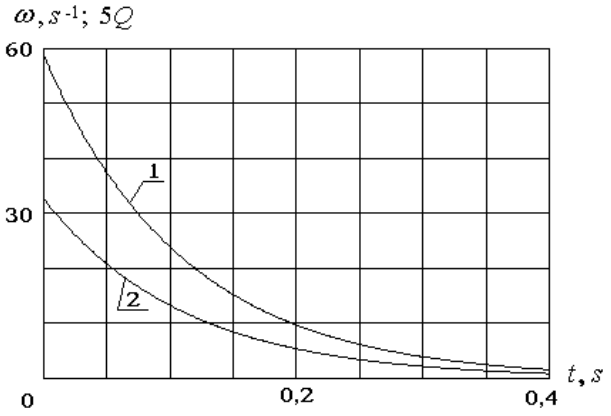

Fig. 4.23.

On fig. 4.24 dependences of dipole moment *D* (curve 1), to linear electrocardiogram *U* (curve 2) and $\cos\Theta$ (curve 3) on time plotted under formulas (4.20), (4.21) and (4.22) are shown. Curves are plotted for the above-mentioned of sizes *R*, *T*, Q_0, $\frac{R}{L}$ at $\varphi = 0$ (i.e. *EA* of heart coincide with the line of lead that is most typical for norm of the second standard lead).

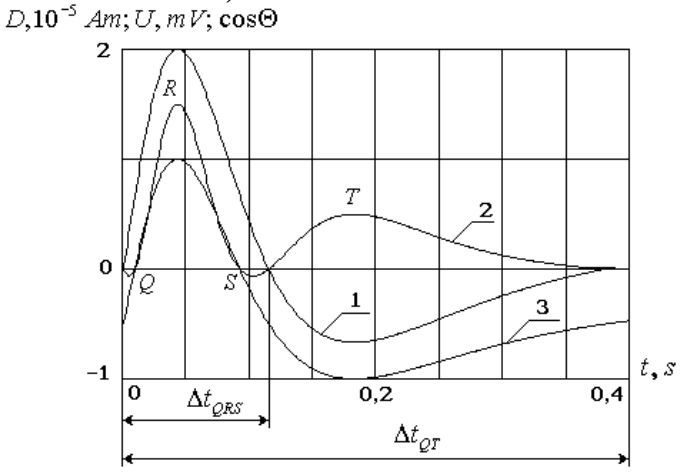

Fig. 4.24.

From graphs it is visible that (since the curve 2 is proportional to product of curves 1 and 3) the positive values waves *R* and *T* are determined by identical signs on sizes *D* and $\cos\Theta$ while negative values of waves *Q* and *S* it is different signs. Parameters for calculation were selected so that the ECG corresponded to norm.

As at $t = t_0$ according to (4.22) is $\Theta = -\varphi$ from (4.21) we have $U = R$ hence t_0 it is time of achievement of the maximum *R* wave.

4.3.2.1. Calculation of zero and maximums of the linear electrocardiogram

According to the formula (4.21) zero of ECG arise or at equality to zero of expression in brackets or at zero of value $\cos\Theta$.

Let's consider in the beginning the second case. If $\cos\Theta = 0$ the angle is $\Theta = \pm\frac{\pi}{2}$. And the sign a minus corresponds to the end *Q* wave on isoline, and a sign plus to the beginning *S* wave on isoline, fig. 4.24. We shall designate:

$$\Theta_{Q2} = -\frac{\pi}{2}; \qquad \Theta_{S1} = -\frac{\pi}{2}. \tag{4.24}$$

Values of these angles do not depend on the angle φ of heart *EA* inclination.

Let now became zero expression in brackets (4.21). In this case we have:

$$\Theta = \pm 2\mathrm{arctg}\sqrt{R/T} + 2n\pi - \varphi, \tag{4.25}$$

where *n* there is integer. The beginning of *Q* wave i.e. the beginning of the electric systole corresponds to the sign minus in the formula (4.25) and to number $n = 0$. The end of *S* wave corresponds to the sign plus in the formula (4.25) and to number $n = 0$. The end of *T* wave i.e. the end of the electric systole corresponds to the sign minus in the formula (4.25) and to number $n = 1$. Using indexes at the angles similar (4.24) we have:

$$\Theta_{Q1} = -2\mathrm{arctg}\sqrt{R/T} - \varphi, \tag{4.26}$$

$$\Theta_{Q2} = 2\mathrm{arctg}\sqrt{R/T} - \varphi, \tag{4.27}$$

$$\Theta_{T2} = -2\mathrm{arctg}\sqrt{R/T} + 2\pi - \varphi. \tag{4.28}$$

It is the interest to find coordinates of maximums waves *R*, *T*, *Q* and *S*. For this purpose it is researched electrocardiogram on the extremum. It is possible to see proceeding from the formula (4.21) that the condition $\frac{dU}{d\Theta} = 0$ gives:

$$\frac{\sin(2\Theta+\varphi)}{\sin\Theta} = -\frac{R-T}{R+T}. \tag{4.29}$$

To find from the formula (4.29) value Θ as general solution it is not possible. But if to put $\varphi = 0$ that is correct for norm of the second standard lead to solve the equation (4.29) it is possible. Thus there is the equation:

$$\sin\Theta\left(2\cos\Theta + \frac{R-T}{R+T}\right) = 0. \tag{4.30}$$

The condition $\sin\Theta = 0$ gives position of the ECG two maximum:

$$\Theta_R = 0; \qquad \Theta_T = \pi. \tag{4.31}$$

Substitution (4.31) in the formula for a linear ECG (4.21) at $\varphi = 0$ shows that these angles really determine values of waves *R* and *T* maximums.

The becoming to zero of the bracket in the formula (4.30) gives position of the waves *Q* and *S* maximums:

$$\Theta_Q = -\arccos\frac{1}{2}\left(-\frac{R-T}{R+T}\right), \tag{4.32}$$

$$\Theta_S = \arccos\frac{1}{2}\left(-\frac{R-T}{R+T}\right). \tag{4.33}$$

Substituting (4.32) and (4.33) in the formula (4.21) for the ECG at $\varphi = 0$ we find value of maximums *Q* and *S*. For $\varphi = 0$ these maximums identical:

$$Q = S = -\frac{1}{8}\frac{(R-T)^2}{R+T}. \qquad (4.34)$$

The sign minus indicates negativity waves *Q* and *S*. At values *R* and *T* used earlier the sizes of waves amplitudes $Q = S = -0.0625\ mV$.

Let's consider position of zero and maximums of the ECG in time coordinate. It is important since the scanning of the standard linear electrocardiogram is carried out in time. Connection between time and angular coordinate can be found proceeding from the formula (4.22):

$$t = t_0 - \frac{L}{R}\ln\left(1-\frac{\Theta+\varphi}{Q_0}\right). \qquad (4.35)$$

Hence taking into account (4.24), (4.26) - (4.28), (4.31) - (4.33) we shall find:

$$t_{Q1} = t_0 - \frac{L}{R}\ln\left(1+\frac{2\mathrm{arctg}\sqrt{R/T}}{Q_0}\right), \qquad (4.36)$$

$$t_Q = t_0 - \frac{L}{R}\ln\left\{1+\frac{\arccos\left[\frac{1}{2}\left(-\frac{R-T}{R+T}\right)\right]}{Q_0}\right\}, \qquad (4.37)$$

$$t_{Q2} = t_0 - \frac{L}{R}\ln\left(1-\frac{-\frac{\pi}{2}+\varphi}{Q_0}\right), \qquad (4.38)$$

$$t_R = t_0, \qquad (4.39)$$

$$t_{S1} = t_0 - \frac{L}{R}\ln\left(1-\frac{\frac{\pi}{2}+\varphi}{Q_0}\right), \qquad (4.40)$$

$$t_S = t_0 - \frac{L}{R}\ln\left\{1-\frac{\arccos\left[\frac{1}{2}\left(-\frac{R-T}{R+T}\right)\right]}{Q_0}\right\}, \qquad (4.41)$$

$$t_{S2} = t_0 - \frac{L}{R}\ln\left(1-\frac{2\mathrm{arctg}\sqrt{R/T}}{Q_0}\right), \qquad (4.42)$$

$$t_T = t_0 - \frac{L}{R}\ln\left(1-\frac{\pi}{Q_0}\right), \qquad (4.43)$$

$$t_{T2} = t_0 - \frac{L}{R}\ln\left(1+\frac{2\mathrm{arctg}\sqrt{R/T}-2\pi}{Q_0}\right), \qquad (4.44)$$

From the analysis of formulas (4.36) - (4.44) it is possible to infer that values of times t_{Q1}, t_{S2}, t_{T2} (formulas (4.36), (4.42), (4.44)) do not depend on angle φ i.e. positions of heart *EA* and have completely general character. Values of times t_Q, t_R, t_S, t_T (formulas (4.37), (4.39), (4.41), (4.43)) are deduced in the

assumption $\varphi = 0$ (approximately for norm of the second standard lead). The rests of the time t_{Q2}, t_{S1} (formulas (4.38), (4.40)) depend on angle φ i.e. position of heart *EA*.

Let's find expressions for intervals of the ECG not dependent on position of heart *EA*. Such intervals two are the duration of complex *QRS* (Δt_{QRS}) and duration of electric systole *QT* (Δt_{QT}). We shall find duration of complex *QRS*:

$$\Delta t_{QRS} = t_{S2} - t_{Q1} = 2\frac{L}{R}\operatorname{arcth}\left(\frac{2\operatorname{arctg}\sqrt{R/T}}{Q_0}\right). \qquad (4.45)$$

In the formula (4.45) the identity $\ln\left(\frac{1+Z}{1-Z}\right) = 2\operatorname{arcth} Z$ is used.

For duration of the electric systole we have:

$$\Delta t_{QT} = t_{T2} - t_{Q1} = \frac{L}{R}\ln\left(\frac{1+\frac{2\operatorname{arctg}\sqrt{R/T}}{Q_0}}{1+\frac{2\operatorname{arctg}\sqrt{R/T}}{Q_0}-\frac{2\pi}{Q_0}}\right). \qquad (4.46)$$

The ratio $\frac{\Delta t_{QT}}{\Delta t_{QRS}}$ does not depend on size $\frac{L}{R}$, and as it was already marked from direction of heart *EA*.

Thus on basis of parameters easily measured on the linear electrocardiogram - ratio of intervals and amplitudes of waves $\frac{R}{T}$ it is possible to find size of electric quality factor of heart Q_0 on the maximum *R* wave.

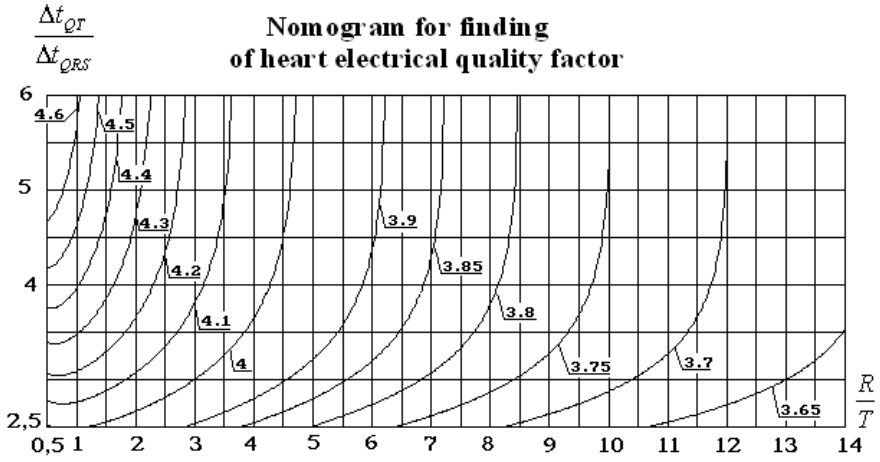

Fig. 4.25.

On fig. 4.25 graphs of dependence $\frac{\Delta t_{QT}}{\Delta t_{QRS}}$ on the ratio of wave amplitudes $\frac{R}{T}$ are submitted at various Q_0 - nomogram for find of the heart electric quality factor at small deviations from norm.

Experience of clinical practice shows that frequently is far-reaching pathological process is not reflected in controllable parameters of the ECG. But the size of quality factor of heart thus varies since the quality

factor is the cumulative parameter dependent on the basic electric characteristics of heart: capacities, inductance and active resistance $Q = \frac{1}{R}\sqrt{\frac{L}{C}}$.

Therefore controlling with the help fig. 4.25 tendency of the head quality factor change during some time and having found out, for example, its reduction is possible to judge development of pathological process even if other controllable parameters of the ECG are within the limits of norm.

For calculation of characteristic times of the ECG with the help of formulas (4.36) - (4.44) it is necessary to estimate the ratio $\frac{L}{R}$.

The end of *Q* wave and the beginning of *S* wave, fig. 4.24, are defined by zero value $\cos\Theta$. Therefore the angle of the vector ***D*** rotation between these points on the ECG is equal π. Hence $\omega_{t0} = \frac{\pi}{\Delta t_R}$ where Δt_R there is time interval between examined points t_{Q2} and t_{S1} measured on the ECG. Taking into account formula $Q_0 = \frac{\omega_{t0} L}{R}$ we find $\frac{L}{R} = \frac{\Delta t_R Q_0}{\pi}$. The size of the quality factor Q_0 can be defined under the nomogram, fig. 4.25, or is more precisely the calculation under the ratio $\frac{\Delta t_{QT}}{\Delta t_{QRS}}$ with the help of formulas (4.45) and (4.46).

In examined points of the ECG it is simple to calculate quality factor of "electric heart". Connection between quality factor and angle Θ in conformity with formulas (4.22) and (4.23) is under the formula:

$$Q = Q_0 - (\Theta + \varphi). \qquad (4.47)$$

Let's find values of limiting angles of the heart electric axis at which waves *Q* and *S* disappear. Equating times of the beginning and the end *Q* wave i.e. formulas (4.36) and (4.38), we find:

$$\varphi_Q = \frac{\pi}{2} - 2\text{arctg}\sqrt{\frac{R}{T}}. \qquad (4.48)$$

Also equating times of the beginning and the end *S* wave i.e. formulas (4.40) and (4.42) it is received:

$$\varphi_Q = -\frac{\pi}{2} + 2\text{arctg}\sqrt{\frac{R}{T}}. \qquad (4.49)$$

Hence that on the ECG were observed waves *Q* and *S* it is necessary, that *EA* of hearts laid in the range $\varphi_Q < \varphi < \varphi_S$. For the accepted amplitudes of waves *R* and *T* the size $\varphi_Q = -0.52\ rad = -30^0$ and $\varphi_S = 0.52\ rad = 30^0$.

Let's make the table of the basic calculated parameters of the linear ECG for the second standard lead ($\varphi = 0$) using above mentioned values of electric parameters of the equivalent contour.

Point	Wave amplitude, *mV*.	Angles, *degree*.	Zero and maximums, *s*.	Angular speed, *rad/s*.	Qua-lity factor	Time intervals, *s*.
Q_1		-120	$t_0 - 0.0432$	59	6.49	$\Delta_{QT} = 0.38$

Q	-0.0625	-104.5	$t_0 - 0.0385$	56.5	6.22	$\Delta_{QRS} = 0.11$
Q_2		-90	$t_0 - 0.0339$	54.3	5.97	$\Delta_{RT} = 0.126$
R	1.5	0	t_0	40	4.4	$\Delta t_R = 0.083$
S_1		$+90$	$t_0 + 0.049$	25.7	2.83	
S	-0.0625	$+104.5$	$t_0 + 0.0595$	23.5	2.58	
S_2		$+120$	$t_0 + 0.0718$	20.9	2.3	
T	0.5	$+180$	$t_0 + 0.126$	11.5	1.26	
T_2		$+240$	$t_0 + 0.336$	1.9	0.21	

4.3.2.2. Spatial modeling of heart electrogenesis

The carried out analysis concerns only to one projection and one lead of the ECG. For other projections the situation is similar.

The much greater interest represents the solution of the problem of spatial modeling DEEGH. Therefore there is a necessity of addition of oscillatory contours or finding of the equivalent oscillatory contour for spatially located under the angles to each other or perpendicularly several oscillatory contours.

Let's consider the addition of three oscillatory contours located in space mutually perpendicularly, fig. 4.21. These oscillatory contours model change of projections of integrated electric vector ***D*** in mutually perpendicular planes.

Let's attribute to the oscillatory contour the vector which is perpendicular planes of the contour, and the length of it changes during one cycle of oscillation proportionally to change of cyclic frequency of the current in contour, and the direction is determined by a rule of the right screw concerning the current in a contour. Thus collinear vectors we do not distinguish. During one oscillation the vector changes the direction on opposite since it is consequence of changes direction of the current in the contour. As a result of addition of three mutually perpendicular oscillatory contours there is the total equivalent oscillatory contour located in space *XYZ*, fig. 4.26. We shall consider the principle of reception of the spatial contour characteristics.

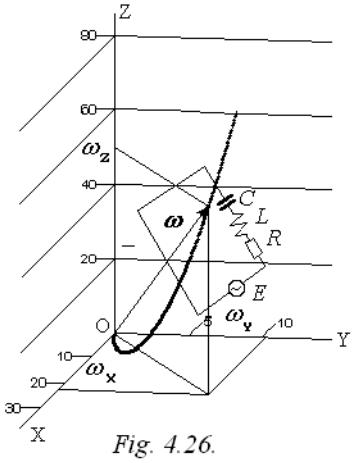

Fig. 4.26.

Let module of the cyclic frequency of the oscillatory contour in plane *YOZ* (i.e. cyclic frequency of oscillations of the current and the voltage in it) is function of time $\omega_X(t)$, in two other planes accordingly $\omega_Y(t)$ and $\omega_Z(t)$, fig. 4.26. Then the total vector of frequency of the equivalent spatial oscillatory contour is equal:

$$\boldsymbol{\omega}(t) = \omega_X(t)\boldsymbol{i} + \omega_Y(t)\boldsymbol{j} + \omega_Z(t)\boldsymbol{k}, \qquad (4.50)$$

where $\boldsymbol{i}, \boldsymbol{j}, \boldsymbol{k}$ there are units of axes *X*, *Y*, *Z*. The total equivalent oscillatory contour at change of cyclic frequencies $\omega_X(t)$, $\omega_Y(t)$, $\omega_Z(t)$ will change the position in space so that the total vector of cyclic frequency in it $\boldsymbol{\omega}(t)$ was perpendicular planes of the equivalent oscillatory contour.

If there are examined three mutually perpendicular contours the module of cyclic frequency of the equivalent contour looks like:

$$\omega(t) = \sqrt{\frac{1}{L_X C_X} + \frac{1}{L_Y C_Y} + \frac{1}{L_Z C_Z}}, \qquad (4.51)$$

where C_X, C_Y, C_Z, L_X, L_Y, L_Z (fig. 4.21) there are capacities and inductance of three examined oscillatory contours. From the formula (4.51) it is possible to infer that capacity and inductance of the equivalent contour is not determined only their product $LC = \frac{1}{\omega^2}$ determined unequivocally. Actually the

capacity and inductance of the equivalent oscillatory contour are completely determined. It follows that total energy as electric so magnetic fields in three contours should be equal corresponding energies in the equivalent contour:

$$\frac{CU_{\max}^2}{2} = \frac{C_X U_{X\max}^2}{2} + \frac{C_Y U_{Y\max}^2}{2} + \frac{C_Z U_{Z\max}^2}{2}, \quad (4.52)$$

$$\frac{LI_{\max}^2}{2} = \frac{L_X I_{X\max}^2}{2} + \frac{L_Y I_{Y\max}^2}{2} + \frac{L_Z I_{Z\max}^2}{2}, \quad (4.53)$$

where $U_{\max}$ and $I_{\max}$ there are the maximal voltage and currents in the equivalent contour and three composing contours.

Besides it is necessary to take into account that:

$$\frac{LI_{\max}^2}{2} = \frac{CU_{\max}^2}{2}, \quad (4.54)$$

$$\frac{L_X I_{X\max}^2}{2} = \frac{C_X U_{X\max}^2}{2}, \quad (4.55)$$

$$\frac{L_Y I_{Y\max}^2}{2} = \frac{C_Y U_{Y\max}^2}{2}, \quad (4.56)$$

$$\frac{L_Z I_{Z\max}^2}{2} = \frac{C_Z U_{Z\max}^2}{2}. \quad (4.57)$$

On fig. 4.26 the result of total vector hodograph of cyclic frequency calculation is shown. Also the equivalent oscillatory contour which plane is perpendicular to the total vector of cyclic frequency $\omega(t)$ is shown.

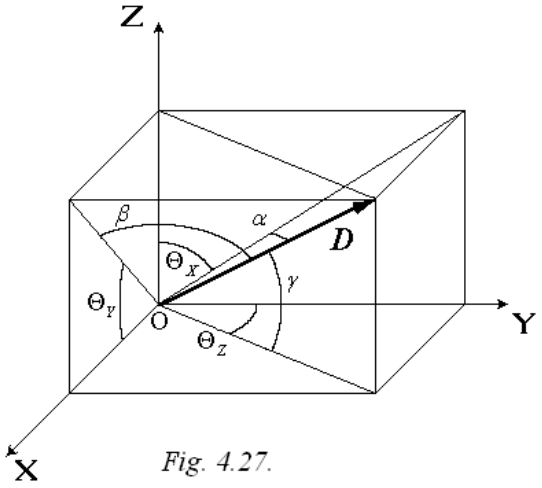

Fig. 4.27.

The cyclic frequency changed under the law (4.17) where for the frontal plane it is accepted $\omega_{t0X} = 29\ s^{-1}$, $\left(\frac{R}{L}\right)_X = 4\ s^{-1}$, for the horizontal plane $\omega_{t0Y} = 10\ s^{-1}$, $\left(\frac{R}{L}\right)_Y = 8\ s^{-1}$, for the sagittal planes $\omega_{t0Z} = 40\ s^{-1}$, $\left(\frac{R}{L}\right)_Z = 12\ s^{-1}$. The time was $t_0 = 0.064\ s$.

Let's receive in calculation spatial loops *QRS* and *T*. For this purpose we shall use angles for vector ***D*** beginning from the origin of coordinates which end writes in space the loop *QRS* and *T* as shown in fig. 4.27. Between these angles there are mathematic expressions:

$$\sin^2\alpha + \sin^2\beta + \sin^2\gamma = 1, \quad (4.58)$$

$$\cos^2\alpha + \cos^2\beta + \cos^2\gamma = 2, \quad (4.59)$$

$$\mathrm{tg}\Theta_X \mathrm{tg}\Theta_Y \mathrm{tg}\Theta_Z = 1, \quad (4.60)$$

$$\sin\alpha = \cos\beta\cos\Theta_Y = \cos\gamma\sin\Theta_Z,$$

$$\sin\beta = \cos\alpha\sin\Theta_X = \cos\gamma\cos\Theta_Z, \quad (4.61)$$

$$\sin\gamma = \cos\beta\sin\Theta_Y = \cos\alpha\cos\Theta_X,$$

$$\cos^2\alpha = \frac{1}{1+\sin^2\Theta_X tg^2\Theta_Z}, \quad (4.62)$$

$$\cos^2\beta = \frac{1}{1+\sin^2\Theta_Y tg^2\Theta_X}, \quad (4.63)$$

$$\cos^2\gamma = \frac{1}{1+\sin^2\Theta_Z tg^2\Theta_Y}. \quad (4.64)$$

Setting laws of the angles change Θ_X, Θ_Y and Θ_Z according to the formula (4.22) we shall plot in the frontal, sagittal and horizontal planes the a projection of spatial loops *QRS* and *T* on corresponding planes. The projections are represent the vectors hodographs $D\cos\alpha$, $D\cos\beta$ and $D\cos\gamma$ in these planes. We shall plot also the total spatial loop.

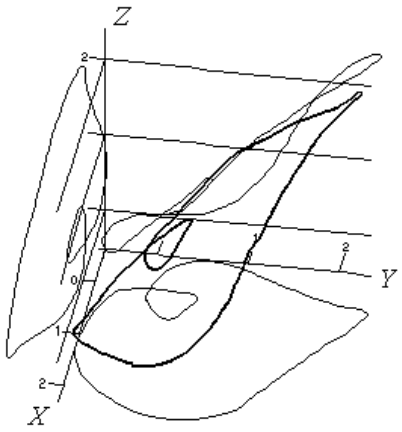

Fig. 4.28.

The result of calculation is shown on fig. 4.28. All calculations in the given section are carried out with the help of program MathCAD. Calculation is carried out for the following electric parameters of a myocardium: the axis *A* of complex *QRS* (*EA* of hearts) is equal $2.7\cdot10^{-5}\ Am$, the axis *B* of *T* loop is equal $-0.7\cdot10^{-5}\ Am$. The time is $t_0 = 0.064\ s$, angular frequency $\omega_{t0} = 29\ s^{-1}$ and $\frac{R}{L} = 6\ s^{-1}$ for three mutually perpendicular directions *OX, OY, OZ*. The angle of inclination of the heart electric axis is $\varphi = 2.3\ rad$.

Electric parameters of heart were selected so that projections of modeling VECG approximately corresponded to projections of one real VECG for complex *QRS* received at medical inspection of the patient.

4.3.2.3. Occurrence of electric reverberators on the excitable surface of myocardium

During work of the cardiac muscle there is a strict sequence of contraction of its separate sites. Such sequence is necessary for creation of conditions of emission by heart of blood shock volume in aorta or pulmonary trunk.

There are the situations connected to pathological processes in cardiovascular system when the sequence of fibres contraction of the myocardium is disturbed and arises dangerous cardiac arrhythmia - fibrillation. Thus separate sites of the cardiac muscle start to be excited and contracted spontaneously. On the electrocardiogram, for example, of ventricles during this moment are observed periodic oscillations [40] close to sine wave.

The analysis of the fibrillation phenomenon has shown that excitation of the myocardium occurs in its separate sites and frequently has the form of spiral autowaves - reverberators [41]. Thus mechanical spiral waves of contraction of the myocardium (mechanical reverberators or flutter) are preceded the electric spiral waves of the myocardium excitation (electric reverberators).

For research of the electric reverberator we use model of the excitable tissue having in the excited condition the inductance. The equation (2.55) deduced for the cylindrical nervous fibre which defines the movement of nervous impulse along coordinate *X* is correct and for propagation of the action potential to flat

and volumetric geometry as it takes place, for example, in the myocardium. It is necessary to choose correctly only kind of Laplacian $\Delta\varphi$ coordinates in the equation:

$$V^2(\varphi-\varphi_0)\Delta\varphi=\frac{\partial\varphi}{\partial t}\left(\frac{\partial\varphi}{\partial t}+A\right)-(\varphi-\varphi_0)^2\omega_0^2\,. \qquad (4.65)$$

Having designated $k=\frac{\omega_0}{V}$ we shall receive:

$$\Delta Z+k^2Z=\frac{1}{V^2Z}\left(\frac{\partial Z}{\partial t}\right)^2. \qquad (4.66)$$

In the equation (4.66) it is designated $Z=\varphi-\varphi_0$ besides for the myocardium cell process of hyperpolarization is absent i.e. $A=0$.

Resting potential φ_0 it is necessary to calculate with take into account of the difference of ions Ca^{2+} concentration on the cardiomyocytes membrane.

Let's assimilate the myocardium of the excitable plane (syncytium) [41] and we shall pass in (4.66) to polar coordinates:

$$\frac{1}{r}\frac{\partial}{\partial r}\left(r\frac{\partial Z}{\partial r}\right)+\frac{1}{r^2}\frac{\partial^2 Z}{\partial\Theta^2}+k^2Z=\frac{1}{V^2Z}\left(\frac{\partial Z}{\partial t}\right)^2, \qquad (4.67)$$

where *r* there is polar radius, and Θ - the polar angle counted counter-clockwise.

Let's find the solution of the equation (4.67) as:

$$Z=Z_0(r)\exp\left[-(\omega t+\Theta)\right], \qquad (4.68)$$

where $Z_0(r)$ there is the function dependent only from radius. Substitution (4.68) in (4.67) gives Euler's equation [26]:

$$r^2\frac{\partial^2 Z_0}{\partial r^2}+r\frac{\partial Z_0}{\partial r}+Z_0=0\,. \qquad (4.69)$$

The solution of the equation (4.69) looks like:

$$Z_0=Z_{0m}\sin\left(\ln\frac{r}{r_0}\right), \qquad (4.70)$$

where Z_{0m} and r_0 there are constants of integration. Thus Z_{0m} is a peak deviation of potential from the resting potential φ_0. Hence the solution of the equation (4.67) can be written down as:

$$Z=Z_{0m}\sin\left(\ln\frac{r}{r_0}\right)\exp[-(\omega t+\Theta)]\,. \qquad (4.71)$$

Let's consider the form of equipotential lines on the excitable surface of the myocardium. We shall assume $Z=const$ and shall designate $B=\frac{Z}{Z_{0m}}$ then from (4.71) we shall find:

$$r=r_0\exp\left\{\arcsin\left[B\exp(\omega t+\Theta)\right]\right\}. \qquad (4.72)$$

The received ratio defines the form of an electric reverberator.

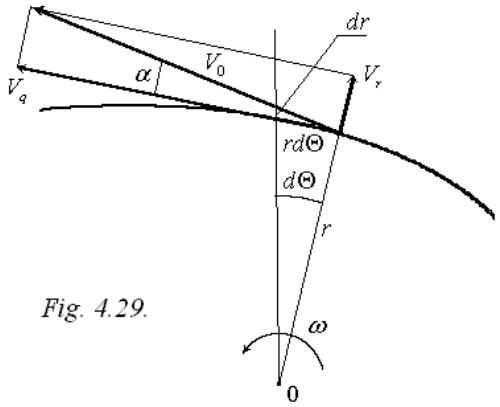

Fig. 4.29.

Let's consider in more detail its some kinematic characteristics, fig. 4.29. Speed of growth of the reverberator can be found under the formula:

$$V_r = \frac{\partial r}{\partial t} = r\omega \mathrm{tg}\left(\ln\frac{r}{r_0}\right). \qquad (4.73)$$

Taking into account that:

$$\mathrm{tg}\,\alpha = \frac{1}{r}\frac{\partial r}{\partial \Theta} = \mathrm{tg}\left(\ln\frac{r}{r_0}\right).$$

Let's find $\alpha = \ln\left(\frac{r}{r_0}\right)$ it is angle between tangential speed V_q of propagation of the spiral autowave front and the total speed V_0. Since V_r it is the radial speed of propagation of the spiral wave then $V_q = \frac{V_r}{tg\,\alpha} = r\omega$. Thus ω it is angular speed of the reverberator rotation. Total speed of propagation of the reverberator front is $V_0 = \frac{r\omega}{\cos\left[\ln\left(r/r_0\right)\right]}$.

The step of the autowave spiral depends on radius under the formula:

$$\lambda = \frac{2\pi V_r}{\omega} = 2\pi r \mathrm{tg}\left(\ln\frac{r}{r_0}\right). \qquad (4.74)$$

At the moment of time $t = t^*$ the form equipotential lines is determined under the law following from (4.72):

$$r = r_0 \exp\left[\arcsin\left(D\exp\Theta\right)\right], \qquad (4.75)$$

where there is $D = B\exp\left(\omega t^*\right)$. For various values *D* the equipotential lines of reverberator calculated under the formula (4.75) are submitted on fig. 4.30 (curve 1 for $D = 0.1$; curve 2 for $D = 0.01$; a curve 3 for $D = 0.001$).

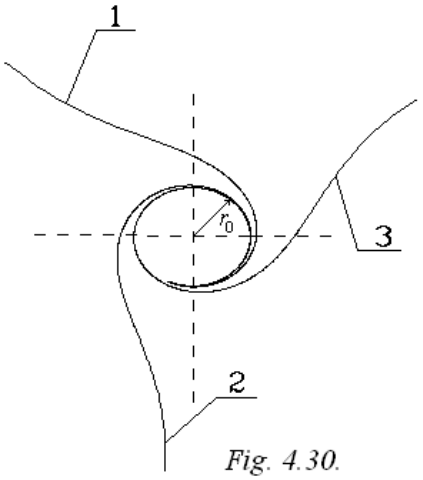

Fig. 4.30.

Apparently from fig. 4.30 the equipotential lines on the one hand are indefinitely reeled up on of the reverberator nucleus in radius r_0 on the other hand depart from the nucleus with increasing step, see (4.74). The reverberator nucleus it is area of the myocardium where there is a spontaneous periodic cells excitation.

The reverberator cannot keep the spiral structure far from the nucleus. When the angle α amounted $\frac{\pi}{2}$ the spiral propagation of the excitation front stops to exist. The minimal step of the spiral autowave $\lambda_{\min}$ is determined by the refractory period of the myocardium cells $\tau_r = 0.3\,s$ [41].

The value is $\lambda_{\min} = V_r \tau_r$. Velocity of propagation of the traveling wave on myocardium we shall accept $V_0 \approx 0.4 \frac{m}{s}$. At the big radiuses when V_0 aspires to V_r the size is $\lambda_{\min} = V_r \tau_r \approx 0.12\,m$. The maximal angular speed of the spiral wave rotation we find from the condition $\lambda > V_r \tau_r$ and the formula (4.74). The size is $\omega < \frac{2\pi}{\tau_r} \approx 21\,s^{-1}$. Angular speed of the reverberator rotation can be less than maximal size as the period of reverberator, as a rule, in $1.5-2$ ones is more than medium refractory [42]. On the other hand in [41] it is marked that in a homogeneous medium the reverberator sends waves with the refractory period. Really the radius of the reverberator on the myocardium is limited to other excited sites and equal $r = 0.5-1\,cm$ hence the maximal tangential speed $V_{q\max} = r\omega \approx 0.21 \frac{m}{s}$ (at $r = 0.01\,m$). As $\cos\alpha = \frac{V_q}{V_0}$, fig. 4.29, the angle amount to about values $\sim 0.56\,rad$. Proceeding from the formula $\alpha = \ln\left(\frac{r}{r_0}\right)$ we find radius of the reverberator nucleus $r_0 = 0.6\,cm$.

Under these conditions the maximal radius size which the spiral autowave on unlimited excitable surface could attain at unitary excitation of the nucleus is $r_{\max} = r_0 \exp\left(-\pi/2\right) = 2.9\,cm$. Radial speed of the reverberator growth is $V_r = r\omega \operatorname{tg}\alpha = 0.13 \frac{m}{s}$ on radius $r = 0.01\,m$. Assuming this speed of average

we find the time of the reverberator life $t = \frac{r_{\max}}{V_r} = 0.22\ s$. Hence at unitary excitation of the nucleus the spiral autowave can rotate on the angle $\Theta = \omega t = 4.6\ rad$. It coincides with the result of numerical experiment shown in [42] where is marked that the reverberator was lost after two revolutions.

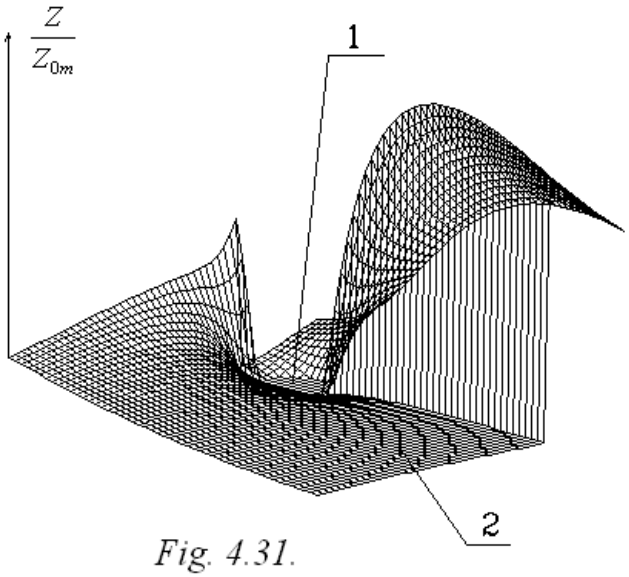

Fig. 4.31.

On fig. 4.31 the graph of propagation of excitation on the myocardium surface plotted on the basis of the equation (4.71) with help of program MathCAD is shown for the fixed moment of time. On the graph the area of the reverberator nucleus 1 where calculation was not carried out, and the spiral equipotential lines 2 departing from the nucleus is well visible. Calculation shows that excitation arises on the opposite ends of the reverberator nucleus and starts to be propagated around of the nucleus as two branches.

The equations of movement of the spiral autowave on the excitable surface of myocardium can be found, for example, in [43].

Chapter 5. Influence on organism by the high-frequency electromagnetic field

Influence on the organism by the high-frequency electromagnetic field results in the series of positive and negative effects. Positive effects are applied in medicine to treatment - high-frequency physiotherapy. Basically it is heating up of tissues of the organism and not thermal influence on physiological processes. At high-frequency physiotherapy the biological tissue usually is not resulted in a condition of excitation.
Influence on the organism tissue a high-frequency electromagnetic field with the surgical purposes is not subject of our analysis.
It is important to know also negative effects of influence by the high-frequency electromagnetic field with the purpose of possible decrease in negative consequences.

5.1. Features of influence of the MW-radiations on the organism tissue with purpose of its heating

Microwave therapy (name conditional) is applied basically to influence on a tissue of organism by electromagnetic waves of the SHF-range (superhigh-frequency range) which frequency is in limits from $3 \cdot 10^8\ Hz$ up to $3 \cdot 10^{10}\ Hz$. Wide application of microwave therapy in medicine basically is connected to thermal influence of fields of the MW - range, i.e. a range of electromagnetic waves which lengths lay in the interval $\lambda = 10\,mm \div 1\,m$.

It is important correctly to estimate biophysical features of influence of electromagnetic radiation of the MW - range on tissues of organism and in particular thermal effect at MW - therapies. However existing methods of biophysical estimation of thermal effect are frequently based on completely various formulas [15, 44, 45].

Let's consider absorption of the MW - radiations of small intensity in tissues of organism. Absorption of electromagnetic radiation in tissues is determined by Bouguer law:

$$\frac{\Delta I}{\Delta X} = -\alpha I\,, \qquad (5.1)$$

where ΔX is the thickness of an absorbing layer, coordinate X is directed in depth of a man body, α - parameter of absorption of electromagnetic waves, I - intensity of electromagnetic radiation into the tissues, I_0 - intensity of electromagnetic radiation falling on the tissue, fig. 5.1.

The quantity of heat q allocated in unit of time in unit of tissue volume (heat production) on coordinate X is equal:

$$q = -\frac{\Delta I}{\Delta X} = \alpha I\,. \qquad (5.2)$$

The sign minus are indicates that reduction of intensity of radiation in the tissue is connected to increase in it heat production q.

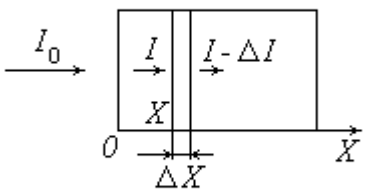

Fig. 5.1.

For finding of the absorption parameter of electromagnetic waves in the organism tissue we shall consider Maxwell equations for the electromagnetic field as [25]:

$$\mathrm{rot}\boldsymbol{H} = \boldsymbol{j} + \varepsilon_a \frac{\partial \boldsymbol{E}}{\partial t}, \quad (5.3)$$

$$\mathrm{rot}\boldsymbol{E} = -\mu_a \frac{\partial \boldsymbol{H}}{\partial t}, \quad (5.4)$$

$$\mathrm{div}\boldsymbol{E} = 0, \quad (5.5)$$

$$\mathrm{div}\,\boldsymbol{H} = 0, \quad (5.6)$$

where $\boldsymbol{H}$ and $\boldsymbol{E}$ is magnetic field strength and electric field strength in tissue, $\boldsymbol{j} = \sigma\boldsymbol{E}$ - density of the macrocurrent in the tissue, σ - specific electrical conductivity of tissue, $\varepsilon_a = \varepsilon_0\varepsilon$ is absolute dielectric penetrance and $\mu_a = \mu_0\mu$ - absolute magnetic permeability of tissue, ε_0 and μ_0 - electrical and magnetic constants, ε - relative dielectric penetrance and μ - relative magnetic permeability of tissue.

We shall be limited to consideration of flat monochromatic waves.

Let's find a rotor from the equation (5.3) with the account (5.6):

$$\mathrm{rotrot}\boldsymbol{H} = \mathrm{graddiv}\,\boldsymbol{H} - \Delta\boldsymbol{H} = -\Delta\boldsymbol{H} = \sigma\mathrm{rot}\boldsymbol{E} + \varepsilon_a \frac{\partial \mathrm{rot}\boldsymbol{E}}{\partial t}. \quad (5.7)$$

Substituting in (5.7) the equation (5.4) we shall find:

$$\Delta\boldsymbol{H} - \varepsilon_a\mu_a \frac{\partial^2 \boldsymbol{H}}{\partial t^2} = \sigma\mu_a \frac{\partial \boldsymbol{H}}{\partial t}. \quad (5.8)$$

Similarly:

$$\Delta\boldsymbol{E} - \varepsilon_a\mu_a \frac{\partial^2 \boldsymbol{E}}{\partial t^2} = \sigma\mu_a \frac{\partial \boldsymbol{E}}{\partial t}. \quad (5.9)$$

Let's search the solutions of the wave equations (5.8) and (5.9) as flat attenuating monochromatic waves propagating on axes *X*:

$$\boldsymbol{H} = \boldsymbol{H}_0 \exp(-qX)\exp i(\omega t - pX), \quad (5.10)$$

$$\boldsymbol{E} = \boldsymbol{E}_0 \exp(-qX)\exp i(\omega t - pX), \quad (5.11)$$

where $\boldsymbol{H}_0$ and $\boldsymbol{E}_0$ there are initial amplitudes of waves, ω - cyclic frequency of waves, *p* - wave number, *q* - parameter of absorption for strengths of electric and magnetic fields.

Substituting (5.10) and (5.11) accordingly in (5.8) and (5.9) and equating the real and imaginary parts of the equations we find:

$$p^2 - q^2 = \varepsilon_a\mu_a\omega^2, \quad (5.12)$$

$$2pq = \sigma\mu_a\omega. \quad (5.13)$$

Solving system of the equations (5.12) and (5.13) we find:

$$p = \omega\sqrt{\frac{\mu_a}{2}\left(\sqrt{\varepsilon_a^2 + \frac{\sigma^2}{\omega^2}} + \varepsilon_a\right)}, \quad (5.14)$$

$$q = \omega\sqrt{\frac{\mu_a}{2}\left(\sqrt{\varepsilon_a^2 + \frac{\sigma^2}{\omega^2}} - \varepsilon_a\right)}. \quad (5.15)$$

The parameter of absorption of medium for electromagnetic radiation is complex function absolute dielectric penetrance ε_a and absolute magnetic permeability μ_a of tissue, its specific electrical conductivity σ (inverse value of specific resistance $\rho = \frac{1}{\sigma}$), and frequencies of electromagnetic radiation ω:

$$\alpha = \omega \sqrt{2\mu_a \left(\sqrt{\varepsilon_a^2 + \frac{\sigma^2}{\omega^2}} - \varepsilon_a \right)}. \qquad (5.16)$$

In connection as $I \sim E^2$ and $I \sim H^2$ the formula (5.16) is translated from the parameter of absorption of strengths electric *E* and magnetic *H* fields *q* to the parameter of absorption of radiation intensity α by the introduction of factor 2 i.e. $\alpha = 2q$.

Tissues of organism represent compositing material consisting from the component, having electro-conducting (blood, muscles) and dielectric (skin, fat, bones) properties.

Let's consider the case when the current of conductivity in tissues it is great in comparison with the current of displacement i.e. $\sigma >> \varepsilon_a \omega$. Thus is $\sqrt{\varepsilon_a^2 + \frac{\sigma^2}{\omega^2}} \approx \frac{\sigma}{\omega}$. Hence:

$$\alpha \approx \sqrt{2\mu_a \sigma \omega}. \qquad (5.17)$$

In tissues of organism there are no ferromagnetic materials therefore it is possible to assume that relative magnetic permeability of the tissue $\mu \approx 1$. Hence absolute magnetic permeability of the tissue μ_a is equal to the magnetic constant $\mu_a = \mu\mu_0 = \mu_0 = 4\pi \cdot 10^{-7} \frac{H}{m}$ and the formula (5.17) becomes:

$$\alpha \approx \sqrt{2\mu_0 \sigma \omega}. \qquad (5.18)$$

The quantity of heat allocated in unit of time in unit of electro-conducting tissue volume on coordinate *X* is equal:

$$q = \alpha I = k_1 \sqrt{2\mu_0 \sigma \omega} I, \qquad (5.19)$$

where $k_1 < 1$ is the factor of proportionality which is taking into account losses of electromagnetic radiation to surrounding space. Usually there is $k_1 \approx 0{,}7$.

Let's find thermal effect in the tissues of organism having dielectric properties. The thermal effect in such tissues depends on the relation of dielectric and electro-conducting properties. For definiteness we shall assume that dielectric properties of the tissue in *n* ones are more expressed than electro-conducting properties:

$$\varepsilon_a \approx n \frac{\sigma}{\omega}. \qquad (5.20)$$

The value $\frac{1}{n} = \operatorname{tg}\delta$ where δ there is angle of dielectric losses [46] describing the ratio of imaginary and real components of relative dielectric penetrance of a tissue.

From the formula (5.16) we shall find the parameter of absorption:

$$\alpha = \omega \sqrt{2\mu_a \varepsilon_a \left(\sqrt{1 + \frac{1}{n^2}} - 1 \right)} = \omega \sqrt{2\mu_a \varepsilon_a \left(\frac{1}{\cos\delta} - 1 \right)}. \qquad (5.21)$$

The quantity of heat allocated in unit of time in unit of the dielectric tissue volume on coordinate *X* is equal:

$$q = \alpha I = k_2 \omega \sqrt{\varepsilon} I, \qquad (5.22)$$

With the account $\mu \approx 1$ the factor is $k_2 \approx k_1 \sqrt{2\mu_0 \varepsilon_0 \left(\frac{1}{\cos\delta} - 1 \right)}$. The factor k_2 takes into account the constants which are included in the formula (5.22) for parameter of absorption such as magnetic

constant μ_0, electric constant $\varepsilon_0 = 8.85 \cdot 10^{-12} \frac{F}{m}$, and also angle of dielectric losses δ of the tissue and loss of electromagnetic radiation energy to surrounding space k_1. Taking into account $c = \frac{1}{\sqrt{\mu_0 \varepsilon_0}}$ - speed of light in vacuum it is possible to write down $k_2 \approx \frac{k_1}{c}\sqrt{2\left(\frac{1}{\cos\delta} - 1\right)} = \frac{2k_1 \sin \delta/2}{c\sqrt{\cos\delta}}$. Inverse dependence of factor k_2 on speed of light in vacuum specifies small absorbing ability of dielectric tissues of organism.

Thus intensity of the MW - radiations in the tissues of organism falls on exponential law (following from (5.1) integrated form of Bouguer law):

$$I = I_0 \mathrm{e}^{-\alpha X}. \qquad (5.23)$$

The parameter of absorption α grows with increase in frequency of radiation ω (5.22) therefore long waves will more deeply penetrate into tissues of organism.

The depth of penetration of the electromagnetic field intensity in the organism tissue can be found under the formula $\lambda = \frac{1}{\alpha}$. On this depth intensity of electromagnetic field there is decreases in $\mathrm{e} \approx 2.718$ ones.

For electro-conductive tissues according to (5.17) we have $\lambda = \frac{1}{\sqrt{2\mu_a \sigma \omega}} = \sqrt{\frac{\rho}{2\mu_a \omega}}$. For the strength of the electric field $E \sim \sqrt{I}$ the depth of penetration is equal $2\lambda = \frac{1}{\sqrt{2\mu_a \sigma \omega}} = \sqrt{\frac{2\rho}{\mu_a \omega}}$.

On fig. 5.2 dependences of relative intensity of radiation calculated on the formula (5.23) on depth *X* of penetration in electro-conducting tissue at CMW - therapy (curve 1) and at DMW - therapy (curve 2) are shown. CMW - therapy is centimeter microwave therapy, DMW - therapy is decimeter microwave therapy. For calculation it is accepted: specific electrical conductivity of tissue $\sigma = 2\frac{S}{m}$ in area CMW - therapies (for skeletal muscle) and $\sigma = 1.2\frac{S}{m}$ in area DMW - therapies [13]. There is cyclic frequency of electromagnetic field influence $\omega = 2\pi \cdot 2375 \cdot 10^6 \frac{rad}{s}$ for CMW - therapy and $\omega = 2\pi \cdot 460 \cdot 10^6 \frac{rad}{s}$ for DMW - therapy. The parameter of absorption calculated under the formula (5.18) for CMW - therapy $\alpha = 274\ m^{-1}$ and for DMW - therapy $\alpha = 93.3\, m^{-1}$.

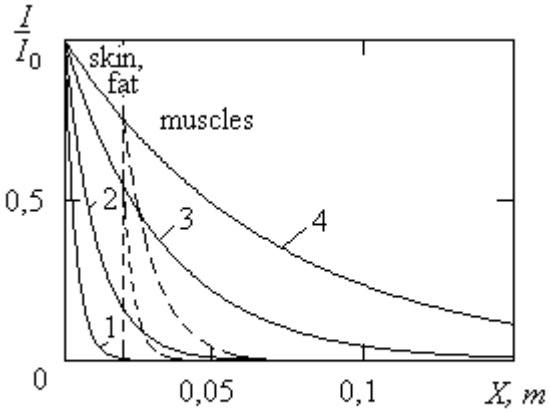

Fig. 5.2.

From fig. 5.2 it is visible that depth of penetration of electromagnetic radiation in electro-conducting tissues of organism is less than $2\,cm$ at CMW - therapy and $\sim 5\,cm$ at DMW - therapy. The ratio of depths of penetration is inverse to the ratio of parameters $\sigma\omega$ at CMW and DMW - therapies: $\sqrt{\frac{(\sigma\omega)_{\text{CMW}}}{(\sigma\omega)_{\text{DMW}}}} = 2.93$.

On fig. 5.2 the graphs of dependence of radiation intensity on depth of penetration into the fatty tissue having expressed dielectric properties also are shown: at CMW - therapy (curve 3) and at DMW - therapy (curve 4). For calculation it is accepted: angle of dielectric losses for a fatty tissue at CMW – therapy $\delta = 15.3^0$ and at DMW – therapy $\delta = 37.7^0$. There is relative dielectric penetrance at CMW – therapy $\varepsilon = 6.5$, at DMW – therapy $\varepsilon = 5.5$ [13]. There is a parameter of absorption for CMB - therapy $\alpha = 31\,m^{-1}$, for DMW - therapy $\alpha = 14.5\,m^{-1}$.

With account factor k_2 the parameter of absorption in formula (5.22) for the dielectric tissue calculated under the formula:

$$\alpha = \frac{2\sin\delta/2}{c\sqrt{\cos\delta}}\omega\sqrt{\varepsilon}\,. \qquad (5.24)$$

Actually the depth of penetration into tissues of organism will vary in the beginning under the law corresponding to curves 3 and 4 since superficial layers (skin, fat) have appreciably dielectric properties where absorption of electromagnetic radiation is less. Then, in the muscular layer there will be sharper absorption of energy of the MW - radiations approximately under the law corresponding to curves 1 and 2. The dotted line shows the law of absorption in skeletal muscle for CMW - and DMW - therapies conditionally transferred in anatomic area of a muscular layer.

General depth of heating due to penetration of the MW - radiation in tissue does not exceed $6-8\,cm$ according to [3]. It is higher than calculative size $4-6\,cm$ (at thickness of skin and fatty layer $\sim 2\,cm$) shown on fig. 5.2 due to thermal conductivity and convective heat exchange as the result of blood circulation.

Numerical calculation of thermal effect *q* under formulas (5.19) and (5.22) is possible at the data about intensity I_0 of MV – radiation falling on tissues of organism. Therefore its size is regulated depending on concrete conditions of physiotherapeutic procedure carrying out.

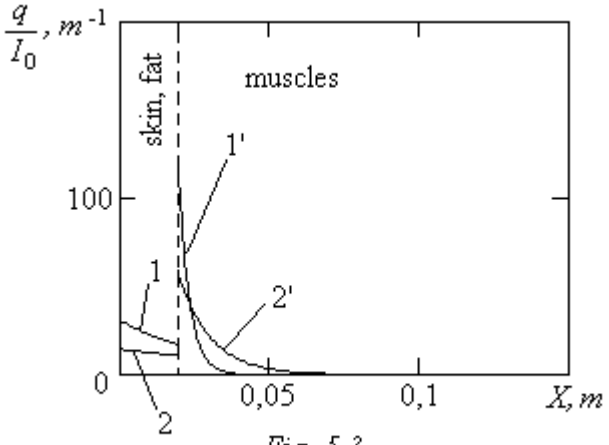

Fig. 5.3.

On fig. 5.3 the result of dependence calculation of the relative thermal effect calculated under the formula following from (5.2) on depth of the organism tissue is shown:

$$\frac{q}{I_0} = -\frac{1}{I_0}\frac{dI}{dX}. \qquad (5.25)$$

Actually sharp vary of heat production on the border fat – muscle is not present since anatomical it is transition occurs smoothly. Calculation shows that the maximum of heat is allocated in the muscular layer directly adjoining to the fatty layer. The skin and fat are heated up much more poorly than muscles. As a whole heating of tissues at CMW - therapy (curves 1-1') is more than at DMW - therapy (curves 2-2') is especial in the field of transition to the muscular layer. But at DMW - therapy are heated up more deeply laying tissues.

As follows from the carried out analysis of the MW – radiations influence on biological tissues, at presence of the authentic data on electric parameters of the tissue practically exact calculation of effects of the MW – radiations thermal action on an organism is possible.

The waveguide-radiator settles down near to the body, fig. 5.4. It represents the metal pipe filled with the dielectric or simply by air inside which there is the conductor stimulating electromagnetic wave.

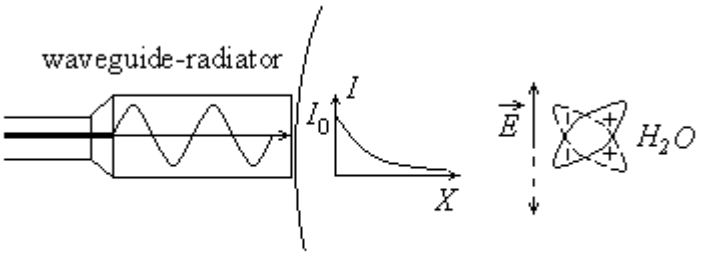

Fig. 5.4.

The electromagnetic wave polarizes molecules of substance first of all waters periodically reorienting them as electric dipoles (orientable polarization). The electromagnetic wave also influences free ions of biological tissues and causes alternating current of conductivity. Thus in substance arise both currents of displacement and currents of conductivity which have on frequencies of MW-therapy about one order. All it is results in heating substance.

Water solutions of the organism absorb energy SHF-fields to the greatest degree and are more heated up. Therefore more heat it is allocated in the liquids filling various volumes and cavities: in muscles, blood, and in osseous and fatty tissues, hypoderm it is less. The dry skin gets heat very poorly.

Allocation of heat in the tissues results in rise in temperature of tissues in the field of influence, to amplification of blood circulation, improvement of metabolism, rise of pain-allaying and anti-inflammatory action.

Indications for MW-therapy it is basically chronic inflammatory diseases of nervous system (neuralgia, neuritis, etc.), pulmonary organs (bronchitis, pneumonia, etc.), urethra, prostate, disease of joints and vertebrarium in a stage of the aggravation (lumbago, artritis bursitis, periarteriits, etc.), pustular diseases of skin.

SHF-radiation is dangerously for an organism. At work with SHF devices the intensity of influence on the personnel should not exceed $I \sim 0.1 \frac{W}{m^2}$. SHF waves it is cause of the neuro-humoral regulation failure, change of functions of the some endocrine glands in particular sexual glands, act on DNA, RNA, disturbing their function.

Contra-indication to use of MW-therapy is ischemic illness of heart, cardiosclerosis, pregnancy (influence on the area of ovary), epilepsia, etc.

Further we shall briefly consider other features of influence of the MW - radiations on an organism in particular its molecular and genetic activity. Now it is possible basically only on the basis of experiments and clinical observation [47].

5.2. Features of not thermal influence of the MW - radiations on biological tissues

Not thermal effects of influence of the MW - radiations are caused that the frequency range of electromagnetic waves both in case DMW - therapies, and in case CMW - therapies lays in out-of-dispersive areas between ranges of $\beta -$ and $\gamma -$ dispersions, see paragraph 5.4.3. Therefore the basic polarizing processes in dielectric fabrics are connected with orientable polarization of water molecules. Besides in large albuminous molecules under action of the MW - radiations mobility of separate structural elements is raised, so-called molecular polarization, see paragraph 5.4.1. There are also currents of conductivity. All these processes also lead to transformation of radiation energy to thermal energy therefore at the molecular level strictly to distinguish the thermal and not thermal effects difficultly.

A series of authors, for example [44, 45], specify on nonlinear in particular square-law dependence of thermal effect on intensity of radiation. The similar kind of dependence is possible only at great intensity of electromagnetic radiation. It is connected by that at approaching to the limit of polarization saturation even the small increase in polarizing effect demands great force influence on the connected charges in a tissues of organism, i.e. the high strength of electric field in electromagnetic wave.

For example, in [48] it is offered at the big intensity of electromagnetic radiation cubic dependence of the polarization vector on the electric field strength. It means square-law dependence of the tissue dielectric susceptibility on electric field strength $\chi \sim E^2$. Taking into account connection of the relative dielectric penetrance and dielectric susceptibility $\varepsilon = 1 + \chi$, and also that for water-filled tissues in the field of the MW – range is $\varepsilon >> 1$ (for water $\varepsilon = 81$) we shall find $\varepsilon \sim \chi \sim E^2 \sim I$. According to (5.22) for the dielectric tissues it is possible to write down $q \sim I^{\frac{3}{2}}$. If to assume correct square-law dependence of thermal effect on intensity the relative dielectric penetrance of the tissue should be proportional to the fourth degree of the electric field strength. In this case is main the fifth member of series of the polarization vector on strength of electric field [49]. About existence of similar materials in the lifeless nature under our data in references is no.

Importance of nonlinear effects of MW-radiations influence on the tissue of an organism will be that they can explain its high genetic danger [47]. The matter is that the MW - radiation has big enough lengths of waves ($\lambda = 0.01 - 1\,m$). Energy of radiation quantums is small and on the basis of general physics positions cannot be connected to intensity of radiation. Therefore action of the MW - radiations on molecules of substance in particular on a gene does not carry quantum character. Even more short-wave radiation, for example, infra-red which energy of quantums considerably higher does not harmful influence on cells DNA.

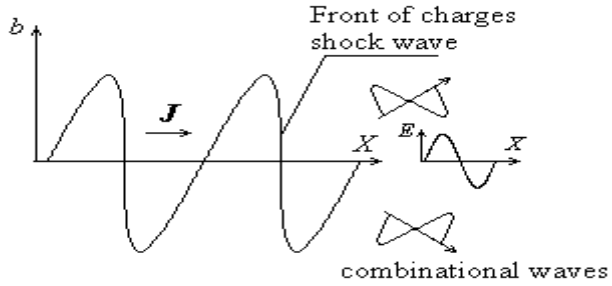

Fig. 5.5.

As some authors assumed the nonlinear distortions of free charges movement waves in substance at influence of the powerful MW - radiations are so great that can lead to overturning of wave front of the energy flux density vector of the charges ***J*** with simultaneous occurrence of ambiguity of the wave profile form [50]. But even if such script also is not realized at the big intensity of radiation there is a thin shock front of the charge movement wave, fig. 5.5, in which, first, occurs strong dissipation of the wave energy, and, second, occurs reflection of the wave from shock front [51]. Thus direct and return waves sum results in greatest very local growth of energy. These local clots of movement energy of the charged particles can be commensurable with energy of chemical bonds of atoms in molecule and consequently to have destroying effect on large molecules.

Addition of waves in the nonlinear medium always results in occurrence of combinational waves [52] which frequencies frequently considerably exceed frequency of initial influence. The given phenomenon results in occurrence of the electromagnetic waves corresponding to combinational frequencies of charges waves. Growth of frequency there is lead to even greater energy dissipation (5.22) electromagnetic radiations. Thus combinational waves form much-data-flow mode of the charged particles [50] with a direction of separate flows of charges movement and electromagnetic waves in the different sides from the place of formation of the shock wave.

In the nonlinear anisotropic medium with numerous borders what is the tissue of an organism the much-orientation of flows of charges movement and combinational electromagnetic waves it is caused by distinction of dispersion and refraction of these waves. Thus at the front shock waves of the charged particles movement the actually areas of the microexplosions destroying molecular bonds are created. Hence, molecular activity of the MW - radiations is connected to the nonlinear effects arising in tissues of an organism.

5.3. Comparative features of influence of the electromagnetic field on organism at inductothermy and UHF - therapy

Current and electromagnetic fields high (HF) $200\,kHz \div 30\,MHz$ and ultrahigh (UHF) ($30 \div 300\,MHz$) frequencies are used in medicine during treatment: for heating, change of a functional condition of tissues, and also at surgical interventions.

Among the most widespread physiotherapeutic procedures of examined frequency ranges it is possible to allocate inductothermy and UHF - therapy.

Let's consider similarity and distinction in mechanisms of action of the electromagnetic field on the tissues of organism in these two procedures.

5.3.1. Inductothermy

Inductothermy it is the method using the high-frequency electromagnetic field for heating of organs and tissues of an organism where the primary factor of influence is the magnetic component of the field.

Change of the magnetic field in any point of space is necessarily accompanied by occurrence of the variable electric field therefore at inductothermy the influence on the tissues is carried out by electromagnetic field. The range of frequencies is in the high-frequency part of β - dispersions spectrum, see paragraph 5.4.3.

At influence of electromagnetic field on electro-conductive tissues of an organism on the share of magnetic field there is fall the basic part of full energy of electromagnetic field [25]. Thus due to the magnetic component of field in tissues there are vortical currents of conductivity - Foucault's currents. Vortical currents are formed in the electro-conductive tissues containing electrolytic solutions. Energy of vortical currents will be transformed to thermal energy. Hence the action of the variable magnetic field can be used for heating of tissues.

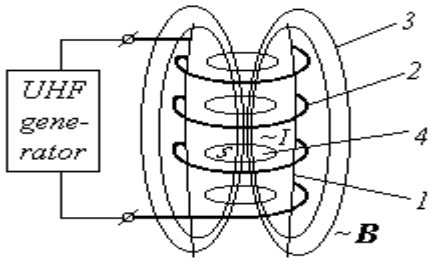

Fig. 5.6.

Usually at inductothermy, fig. 5.6, is applied local influence on body, for example, extremities 1, the variable magnetic field (force lines 3) with use of the coil from a thick electric conductor 2 (inductor). Thus there are closed vortical currents 4. Inductor can made as spiral (solenoid) covering extremity. Such inductor applied to influence on extremities joints.

It is possible the inductor as the flat spiral imposed on the body surface, for example, on the chest or inductor as one long turn used at influence on surface of vertebrarium, etc.

The further analysis of thermal effect occurrence we shall carry out following [53].

The vortical current is equal $I = \frac{\varepsilon}{R}$ where $\varepsilon = -\frac{d\Phi}{dt}$ is electromotive force of electromagnetic inductance which is proportional to speed of the magnetic flux change Φ, and R - resistance of the tissue. Taking into account that at perpendicularity of the vortical current contour limited to area S and vector of the magnetic field $\boldsymbol{B}$ induction the magnetic flux is $\Phi = BS$, we find:

$$I = -S\frac{dB}{R\,dt} = -\frac{SS_1}{\rho l}\frac{dB}{dt} = -\frac{k_1}{\rho}\frac{dB}{dt}, \qquad (5.26)$$

where it is accepted $R = \rho\frac{l}{S_1}$, ρ - specific resistance of the heating tissue, S_1 - the area of section of the tissue through which the vortical current flows (area S_1 is located in the plane fig. 5.6), l - length of the conducting contour. Hence $k_1 = \frac{SS_1}{l}$ - the parameter which is taking into account the sizes of heating organ. Areas S and S_1 are perpendicular each other.

Let the induction of the magnetic field changes under the law $B = B_{\max}\cos\omega t$. Hence, taking into account (5.26) the vortical current is equal:

$$I = \frac{k_1}{\rho}B_{\max}\omega\sin\omega t. \qquad (5.27)$$

The power allocated as heat in the organ:

$$P = I^2R = I^2\rho\frac{l}{S_1} = k_1^2\frac{B_{\max}^2\omega^2}{\rho^2}\sin^2\omega t\,\rho\frac{l}{S_1}. \qquad (5.28)$$

Let's replace variable induction of the magnetic field $B = B_{\max}\sin\omega t$ with effective value B_{eff} equivalent on power. Then the quantity of heat allocated in unit of time in unit of volume of the tissue (heat production) at inuctothermy is equal:

$$q = \frac{P}{V} = k\cdot\frac{\omega^2}{\rho}B_{eff}^2, \qquad (5.29)$$

where P there is average value of heat allocated in unit of time (thermal capacity), V - volume of the heating tissue, $k = \frac{k_1^2 l}{S_1 V}$ - the parameter dependent on the sizes of heating organ. We shall consider in addition that the same factor takes into account also dispersion of electromagnetic field energy in environment.

Hence, the heat quantity allocated in unit of time in unit of volume of the tissue at inductothermy is proportional to a square of the magnetic field induction B_{eff}, a square of frequency of field ω, and in inverse proportion to specific resistance of tissue ρ. Really, to change heat production q it is possible only due to change B_{eff}. Frequencies of work of high-frequency physiotherapy devices are strictly regulated with the purpose of avoidance of the radio interference.

From the analysis of the formula (5.29) follows the quantity of heat allocated at influence of the variable magnetic field, it is more in tissues plentiful blood vessels and having smaller specific resistance (muscular

tissues, lungs, liver, etc.). In such tissues intensify lymphokinesis and blood circulation, processes of thermoregulation become more active. The dry skin, fat, bones are heating poor.

Influence can be carried out through easy clothes, through dry plaster bandage.

In case of flat inductor the maximal heating of tissues on $2-4\ ^0C$ occurs on depth $8-12\ cm$. Superficial layers are heating poor.

From not thermal action of the inductothermy we shall note that high-frequency magnetic field stimulates mainly brake processes in nervous system. Thus there is expansion of blood vessels due to the relaxation of smooth muscles in their walls, the bronchismus, spasm of stomach, spasm of intestine, etc. is reduced.

Indications for inductothermy there are first of all chronic inflammatory diseases of internal organs (especially pneumonia, bronchitis, and also stomachic ulcers and duodenum ulcers, cholecystitis, prostatitis).

Contra-indications there are sharp inflammatory processes, ischemic illness of the heart, expressed hypotension, presence of metal objects in a zone of influence, for example, implanted artificial pacemaker.

5.3.2. UHF - therapy

Ultrahigh-frequency therapy (UHF - therapy) refers to the method using the high-frequency electromagnetic field for heating of the organs and tissues of organism. Thus the primary factor of influence is the electric component of the field. Frequency of a devices UHF - therapy work is some higher area of β - dispersion, see paragraph 5.4.3, i.e. practically is in out-of-dispersive areas.

The area of a body is located between two flat isolated electrodes which do not touch a body, i.e. actually between of the capacitor plates.

In the tissues which are taking place in oscillating electromagnetic field due to an electric component of a field there can be currents of conductivity and currents of displacement depending on their structure.

5.3.2.1. UHF - heating up of electro-conducting tissues

Let's consider allocation of heat at UHF - therapy in the electro-conducting tissue placed in oscillating electric field, fig. 5.7.

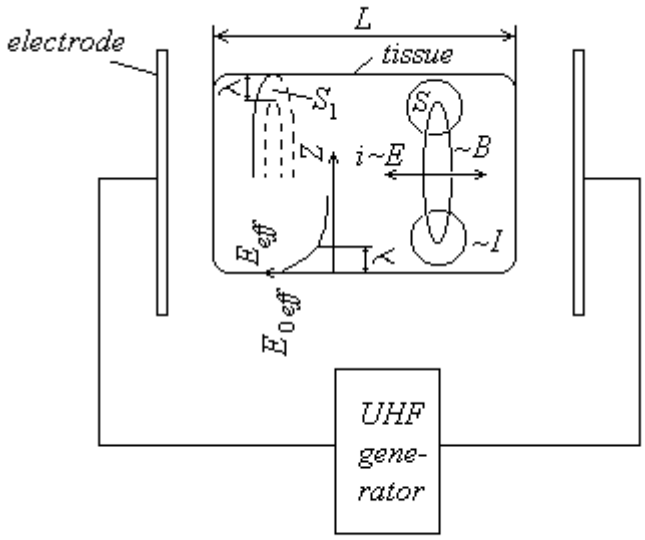

Fig. 5.7.

The oscillating electric field in electro-conducting tissues of organism creates alternating electric current *i*, proportional to strength *E* of this electric field, fig. 5.7. Energy of an ultrahigh-frequency current *i*, basically, according Biot-Savart-Laplace law transform to magnetic field energy with induction *B* [25].

Further, as at inductothermy, due to the law of electromagnetic induction, the oscillating magnetic field *B* causes occurrence of alternating vortical currents *I* which energy transform to thermal energy.

According of the Joule - Lenz law, the quantity of heat allocated in the electro-conducting tissue in unit of volume in unit of time (heat production) is equal:

$$q = k_2 \frac{E_{eff}^2}{\rho}. \qquad (5.30)$$

where ρ is specific resistance of the organism tissues.

In the formula for heat production *q* is oscillating value of electric field strength $E = E_{\max} \sin \omega t$, replaced with effective value E_{eff} equivalent on thermal action. The factor $k_2 < 1$ reflects losses of energy of electromagnetic field on radiation in surrounding space.

Hence, the quantity of heat allocated in unit of time in unit of volume of the conducting tissue at UHF - therapy is proportional to a square of the electric field strength E_{eff} and in inverse proportion to specific resistance of tissue ρ.

Let's note the important feature distinguishing UHF - therapy and inductothermy. Heat production in conducting tissues of an organism at inductothermy depends on frequency (5.29) and at UHF - therapies on frequency does not depend (5.30).

Let's consider the reasons of occurrence of such distinction in more detail.

Electro-conducting tissues of organism show the tendency to shielding of electromagnetic field acting on it. Alternating vortical currents *I* in internal areas of heated up body are directed against an external current *i* and compensate an external current, fig. 5.7. In external areas of heated up body vortical currents *I* and an external current *i* are directed equally, that increases the total current. Therefore the current and an electromagnetic field at UHF - therapy there are decrease in internal areas of body that complicates their heating in this physiotherapeutic procedure.

For a finding of depth of penetration of an electric field in the electro-conducting tissue of organism we shall write down Maxwell equations for such tissue as [25]:

$$\mathrm{rot}\boldsymbol{H} = \boldsymbol{j}, \qquad (5.31)$$

$$\mathrm{rot}\boldsymbol{E} = -\mu_a \frac{\partial \boldsymbol{H}}{\partial t}, \qquad (5.32)$$

$$\mathrm{div}\boldsymbol{E} = 0, \qquad (5.33)$$

$$\mathrm{div}\boldsymbol{H} = 0, \qquad (5.34)$$

where $\boldsymbol{j} = \frac{\boldsymbol{E}}{\rho}$ is density of a current *i*, $\boldsymbol{H} = \boldsymbol{H}(Z)$ and $\boldsymbol{E} = \boldsymbol{E}(Z)$ - magnetic and electric fields strength, *Z* - coordinate directed deep into tissue, fig. 5.7. In the equation (5.31) it is taken into account that occurrence of the magnetic field $\boldsymbol{H}$ occurs due to of alternating density of the current $\boldsymbol{j}$.

Finding a rotor from the equation (5.32) with the account (5.33) we shall receive:

$$\mathrm{rotrot}\boldsymbol{E} = \mathrm{graddiv}\,\boldsymbol{E} - \Delta\boldsymbol{E} = -\Delta\boldsymbol{E} = -\mu_a \frac{\partial \mathrm{rot}\boldsymbol{H}}{\partial t}. \qquad (5.35)$$

Using (5.31) we shall receive:

$$\frac{\partial^2 E}{\partial Z^2} = \mu_a \frac{\partial j}{\partial t} = \frac{\mu_a}{\rho} \frac{\partial E}{\partial t}. \qquad (5.36)$$

The basic gradient of the module of an electric field we believe directed on axis *Z*. The equation (5.36) is parabolic types.

Physically comprehensible solving of the equation (5.36) looks like:

$$E = E_0 \mathrm{e}^{-\frac{Z}{\lambda}} \mathrm{e}^{i\left(\omega t - \frac{Z}{\lambda}\right)}. \qquad \textbf{(5.37)}$$

where $E_0 \mathrm{e}^{i\omega t}$ is oscillating value of electric field strength on a surface of the tissue at $Z = 0$. Last factor in (5.37) reflects oscillatory character of a field. Value λ characterizes depth of penetration of electromagnetic field in the tissue so-called skin-layer. Substituting (5.37) in (5.36) we find that the size of skin-layer λ

depends on frequency of electromagnetic field and specific resistance of the tissue $\lambda = \sqrt{\frac{2\rho}{\mu_a \omega}}$. Than less specific resistance of the tissue and the more frequency of electromagnetic field, the less depth of penetration of electric field into medium and is less depth of heating of electro-conducting tissue.

Let's note that thickness of the skin-layer in accuracy corresponds to depth of penetration of electric field in electro-conducting tissue at influence on it MW - radiations, see analysis of formula (5.23).

According to (5.37) the dependence of effective size of electric field strength E_{eff} on depth of its penetration in electro-conducting tissue under condition of its electric homogeneity has exponential character and looks like:

$$E_{эф} = E_{0эф} \mathrm{e}^{-\frac{Z}{\lambda}}, \qquad (5.38)$$

where E_{0eff} is effective value of electric field strength on the tissue surface at $Z = 0$.

Due to polarization electro-conducting tissues at redistribution in electric field of free ions there is the superficial layer of absorption of electromagnetic field energy thickness λ and in face parts of the heated up volume of the tissue, fig. 5.7. The solution of the task for face zones to similarly above-stated finding of thickness of the skin-layer [54].

Shielding of electromagnetic field is carried out due to suppression of the electric component of a field. Penetration of electromagnetic field into depth electro-conducting tissue occurs on the contrary due to a magnetic component of field. Therefore, in electro-conducting tissue the energy of electromagnetic field is concentrated basically in a magnetic component of a field.

Let's consider in more detail the thermal emission at UHF - therapy in electro-conducting tissues.

We use the formula (5.26) for a vortical current $I = -\frac{SS_1}{\rho l}\frac{dB}{dt}$.

The value S_1 is the area of the tissue section through which the vortical current flows, *l* - length of the electro-conducting contour. The area S_1 through which the vortical current flows is the ring which part is shown on fig. 5.7. Areas *S* also S_1 are perpendicular each other.

The area of a ring is proportional to thickness of the skin-layer $S_1 \sim \lambda$. Area *S* is in a plane fig. 5.7 it also is proportional to thickness of a skin-layer $S \sim \lambda$.

Taking into account oscillatory character of magnetic field induction $B = B_{\max} \cos \omega t$ we shall find:

$$I \sim \frac{\lambda^2}{\rho} \omega B_{\max} \sin \omega t = \frac{\lambda^2}{\rho} \omega B_{eff}, \qquad \mathbf{(5.39)}$$

where oscillatory value of the magnetic field induction is replaced with effective value equivalent on energy.

Under Biot-Savart-Laplace law the magnetic field induction in the tissue is proportional to external current:

$$B \sim i = \frac{E}{\rho} S_1 \sim \frac{E}{\rho} \lambda. \qquad (5.40)$$

Equality (5.40) is correct and for effective values of the magnetic field induction and of electric field strength.

Hence:

$$I \sim \frac{\lambda^2}{\rho} \omega B_{eff} \sim \frac{\lambda^3}{\rho^2} \omega E_{eff}. \qquad (5.41)$$

The quantity of heat allocated in unit of volume in unit of time of the electro-conducting tissue (heat production) with the account (5.41) is equal:

$$q = \frac{I^2 R}{V} = \frac{I^2 \rho l}{V S_1} \sim \frac{I^2 \rho}{\lambda^2} \sim \frac{\lambda^6 \omega^2 E_{eff}^2 \rho}{\rho^4 \lambda^2} \sim \frac{\lambda^4 \omega^2 E_{eff}^2}{\rho^3}. \qquad (5.42)$$

At the deduction (5.42) it is taken into account that volume $V = S_1 L \sim \lambda$, where *L* is length of heated up organ, fig. 5.7.

Using $\lambda = \sqrt{\frac{2\rho}{\mu_a \omega}} \sim \sqrt{\frac{\rho}{\omega}}$ we find:

$$q \sim \frac{\lambda^4 \omega^2 E_{eff}^2}{\rho^3} \sim \frac{E_{eff}^2}{\rho}. \qquad (5.43)$$

From the general physical reasons at absence of losses of electromagnetic field energy in surrounding space follows that the factor before the right part in (5.43) is equal to unit $q = \frac{E_{eff}^2}{\rho}$. If there are losses it is necessary to use the formula (5.30).

The carried out analysis shows that absence of dependence heat production *q* in electro-conducting tissues from frequency of electromagnetic field ω is result to occurrence in such tissues of a skin-layer. Allocation of heat in electro-conducting tissues occurs in the area of the skin-layer which with increase in frequency decreases. Therefore, the increase heat production with increase in frequency is compensated by reduction of volume of the tissue where there is an allocation of heat and dependence heat production from frequency not observed. One of the main distinctions of the inductothermy and UHF - therapies consists in it.

5.3.2.2. UHF - heating up of dielectric tissues

In dielectric tissues under action of electric field there is deformation and orientable polarization of molecules [46]. Rotary oscillations of the polarized molecules or oscillations of ions and ionic groups in the large molecules caused by a variable high-frequency electric field lag behind on the phase oscillations of an electric field. The energy of a field use on overcoming of bonds forces between molecules, ions, ionic groups in molecules, will be transformed to heat.

We use for the description of dielectric properties of substances the approach accepted in the electrical engineer which has suggested Hippel [55]. This approach obviously is not connected to application of Maxwell equations but is effective enough.

Let's model a dielectric tissue the equivalent electric circuit containing in parallel included condenser *C* and resistor *R*, fig. 5.8a, [46]. The biological tissue in a condition of rest has active and capacitor resistance. It is connected by that membranes of cells actually represent condensers. In the excited condition the biological tissue has also inductive properties but to take into account them there is no necessity since high-frequency physiotherapeutic procedures are carried out in the resting condition of the patient and do not cause the depolarization of the excitable fabric. The ratio of active and capacitor properties is determined by a kind of a biotissue.

The current of conductivity (active component of a current) I_R and current of displacement (capacitor component of a current) I_C do not coincide on the phase. The capacitor component of the current outstrips active as shown in the vector diagram on the angle 90^0, fig. 5.8b. It is defined by the following. That there was voltage on capacity the electric current should transfer preliminary on this capacity a charge. The active component of the current and voltage coincide on the phase. It is necessary to note that a current and voltage is scalar values. Their vector representation is conditional.

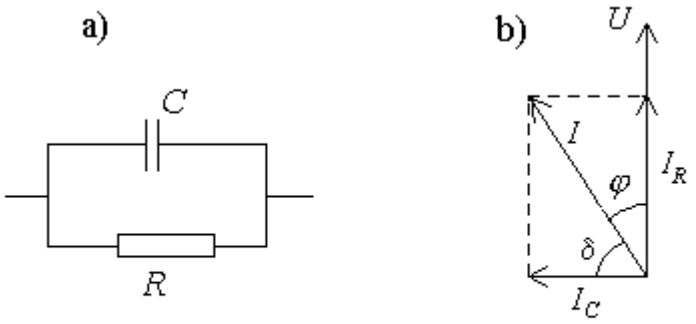

Fig. 5.8.

As the heat in tissues it is allocated only due to an active component of a current I_R the power allocated in a tissue is:

$$P = U_{eff} I_{eff} \cos\varphi = \frac{U}{\sqrt{2}} \frac{I}{\sqrt{2}} \cos\varphi = \frac{UI_R}{2} = \frac{UI_C \mathrm{tg}\delta}{2}, \qquad (5.44)$$

where *I* and *U* is amplitude sizes full of the current and voltage, I_{eff} and U_{eff} - their effective values, φ - the angle (a difference of phases) between the current and voltage $\delta = 90^0 - \varphi$ - the angle of dielectric losses. For example, the size of the angle of dielectric losses for a skeletal muscle of the men in the range of frequencies UHF - therapy is equal $\delta = 26^0$ [13].

The capacitor component of the current is equal:

$$I_C = \frac{U}{X_C} = U\omega C = U\omega\varepsilon\varepsilon_0 \frac{S_2}{L}, \qquad (5.45)$$

where $X_C = \frac{1}{\omega C}$ is a capacitive reactance of the tissue, $C = \varepsilon\varepsilon_0 \frac{S_2}{L}$ - capacity of the condenser formed by electrodes, S_2 and *L* - the area and the linear size of heated up organ, fig. 5.7, so volume of body $V = S_2 L$.

Hence, using effective value of voltage $U_{eff} = \frac{U}{\sqrt{2}}$ we shall find the thermal power allocated in the tissue:

$$P = \frac{U^2 \omega\varepsilon\varepsilon_0 S_2 \mathrm{tg}\delta}{2L} = \frac{U_{eff}^2 \omega\varepsilon\varepsilon_0 S_2 \mathrm{tg}\delta}{L} = \frac{\left(E_{eff} L\right)^2 \omega\varepsilon\varepsilon_0 S_2 \mathrm{tg}\delta}{L} = E_{eff}^2 \omega\varepsilon\varepsilon_0 V \mathrm{tg}\delta. \qquad (5.46)$$

The quantity of heat allocated in unit of volume in unit of time of the dielectric tissue (heat production) is equal:

$$q = \frac{P}{V} = k_2 E_{eff}^2 \omega\varepsilon\varepsilon_0 \mathrm{tg}\delta, \qquad (5.47)$$

where $k_2 < 1$ is the factor reflecting losses of energy on radiation in environment. Thus, the more the angle of dielectric losses δ the more active component of the current and, hence, more energy is allocated as heat in the dielectric tissue. Heat production grows also at increase in frequency of electromagnetic field ω that distinguishes thermal effects in dielectric tissues from those in conducting tissues but to adjust the heat production in tissues due to frequency of the electromagnetic field as already it was specified earlier it is impossible.

The energy absorbed in tissues changes the physical-chemical processes in albuminous structures of a cell, first of all connective and nervous tissues. Allocation of heat in tissues results in expansion of capillaries and arterioles in zone of acting of the field, to amplification of blood circulation, decreasing of arterial pressure,

activization of immune processes, is accompanied by anti-inflammatory, pain-allaying action, affects the central nervous system.

Electromagnetic fields of such frequency which is applied in UHF -therapy cause more effective heating dielectric tissues (bone, fat, periosteum) in comparison with conducting. In it difference of UHF – therapy and inductothermy where conducting tissues better heating. As against inductothermy the maximal thermal effect is observed in more surface areas, up to depth $\sim 8\,cm$. However, occurs heating also deep laying tissues though less great.

Indications to UHF - therapy it is first of all inflammatory (including sharp) diseases of internal organs: lungs, stomach, liver, urinogenital organs. Sharp purulent processes vary localization (abscesses, panaritium, etc.). Diseases of the skeleton, freezing, phantom pains, climacteric and postclimacteric syndromes, etc.

At UHF - therapy not thermal action of an electromagnetic field is important also. Oscillatory molecular processes, molecular and orientable polarization of a biotissues molecules (so-called oscillatory effect at UHF - therapy) result in activization of the osseous tissue that is used, for example, for acceleration of healing after fractures of bones. For amplification of oscillatory effect it is better to use impulse UHF - therapy where impulses duration some micro seconds alternate pauses duration some milliseconds. Thus the thermal effect almost completely disappears.

The same as at inductothermy, and at UHF - therapy it is necessary to watch that in area of influence was not the metal objects, implanted artificial pacemaker.

5.4. Not thermal action of high-frequency electromagnetic field on organism

Due to the processes caused, first of all, by the polarizing phenomena the electromagnetic fields can exert not thermal influence of the man organism.

5.4.1. Classification of dipoles and mechanisms of polarization in biotissue

At influence of an external electric field on a biological fabric there is a displacement relative each other positive and negative charges with occurrence of the additional own electric field directed against the external field, i.e. polarization of the biotissue. Polarizing processes in the biotissue in many aspects are defined by the dipole structure of the biotissue. Distinguish dipoles soft (induced) and rigid.

The soft (induced) dipole which value of the dipole moment increases with increase of the external electric field strength. The soft or induced dipole arises due to space separation of charges under influence of the external electric field.

The rigid dipole which value of the dipole moment does not depend on the external electric field strength. The rigid dipole is determined by structure of molecules or other particles (molecule of water, hydrochloric acid, ethanol, etc.). Such molecules refer to polar.

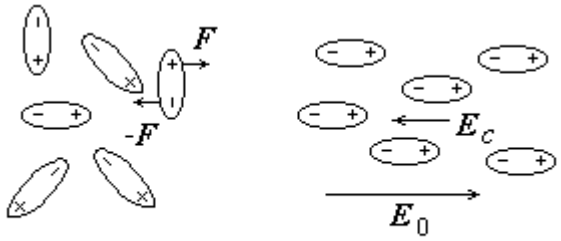

Fig. 5.9.

At polar molecules the centers of negative and positive charges of substance molecules do not coincide. At place of such substance in the external electric field $\boldsymbol{E}_0$ on molecules the moments of forces $\boldsymbol{F}$ start to operate aspiring to rotate molecules along of the electric field force lines, fig. 5.9. This is interfered by thermal movement of molecules. Therefore the external electric field gives molecules only some primary orientation. On fig. 5.9 thermal movement is not taken into account. In substance there is the internal own electric field $\boldsymbol{E}_C$ directed against of the external field $\boldsymbol{E}_0$. Strength of the resulting electric field in the biotissue decreases $E_P = E_0 - E_C$.

Thereof relative dielectric penetrance of the tissue $\varepsilon = \frac{E_0}{E_P} = \frac{E_0}{E_0 - E_C}$ grows.

Occurrence of the dipole molecules certain orientation in the electric field owing to a substance to become an electric dipole refers to the orientable polarization of substance. If the field is switched off the thermal movement destroys the primary orientation of dipole molecules.

As the basic mechanisms of polarization of the biotissue we shall consider:

1. Macrostructural polarization.
2. Molecular polarization.
3. Orientable polarization of molecules of water.
4. Electronic polarization of the atoms.

Polarizing effects of macrostructural polarization are determined by displacement from each other positive and negative ions or groups of ions in an external electric field. The given kind of macrostructural polarization is characteristic for conductors. If in a biotissue there is enough plenty of free carriers of charges – ions the own electric field of polarization $\boldsymbol{E}_C$ attains the big size, and the resulting field in the tissue $E_P = E_0 - E_C$ can decrease considerably.

Therefore relative dielectric penetrance of the tissue can become enough big (for example, at metals where very much free electrons $\varepsilon = \infty$).

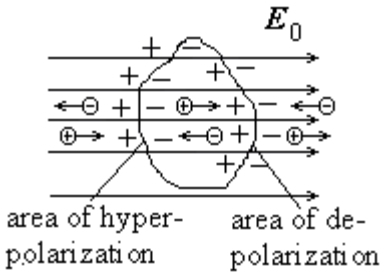

Fig. 5.10.

First of all, macrostructural polarization in living tissues is defined by the biological structure of cells, cellular compartments and organelles. Structures of a cell are the spaces filled with electrolyte and limited to membrane with very low electro-conductivity, fig. 5.10.

At influence on a biotissue of the external electric field $\boldsymbol{E}_0$ there is the movement of ions - positive on the field, negative against the field. The external electric field due to redistribution of ions creates in them induced dipole moment. This dipole moment arises due to accumulation of ions at membranes of cells, cellular compartments or organelles since they are obstacle for ions.

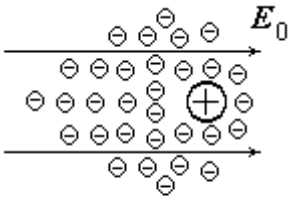

Fig. 5.11.

Inside the cell, fig. 5.10, arises own electric field of polarization $\boldsymbol{E}_C$ and the resulting electric field $E_P = E_0 - E_C$ decreases.

It is possible to attribute to macrostructural polarization and deformation of counterionic atmospheres around of complex ions of polyelectrolyte due to the external electric field since it too the system consisting of the big number of particles, fig. 5.11. At influence of the external electric field $\boldsymbol{E}_0$ the center of the negative charge is displaced concerning the center of the positive charge that leads to the occurrence of own electric field $\boldsymbol{E}_C$ and growth of relative dielectric penetrance of the biotissue.

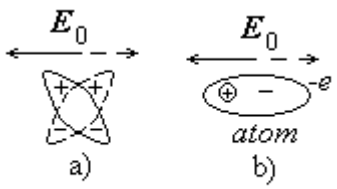

Fig. 5.12.

Molecular kinds of polarization of a biotissue are caused by complex structure biological, first of all albuminous molecules. Molecules of a biotissue will consist of charged particles - ions and ionic complexes. Therefore under action of external electric fields the molecule or their separate parts can have deformation of compression,

stretching, torsion, etc. It results in formation of own electric field of the molecule, i.e. to its polarization.

As already it was specified earlier, see fig. 5.9, under action of an electric field the dipole molecule (rigid dipole) can rotate around of the center of inertia in part compensating the external field. This kind of polarization refers to orientable polarization, fig. 5.12a. Especially important for organism is the orientable polarization of the water dipole molecules since this molecule is usually most distributed in biotissue.

Electronic polarization of atoms, fig. 5.12b, due to displacement in electric field of the centers of a negative charge of electron shell and a positive charge of nucleus usually does not bring the big contribution to the general polarizing effect of the biotissue.

The kinds of polarization considered above excluding orientable polarization are defined by occurrence of induced dipoles.

At switching off the external electric field the induced dipoles in organism disappear, and due to thermal movement of molecules orientable polarization of the water molecules disappears also, i.e. there is a desorientation of rigid dipoles.

5.4.2. Relaxant processes and the dispersion of relative dielectric penetrance of substance

Disappearance of the biotissue polarization at switching off the electric field occurs not instantly. Reduction of polarization is connected with relaxant processes in tissues.

Time of the relaxation is time during which the polarization decreases in $e = 2.718$ ones after switching off the external field owing to the desorientation of rigid dipoles or disappearances of induced dipoles.

Time of a relaxation defines the opportunity and speed of the tissue structures (membranes, molecules, atoms) repolarize in the variable electromagnetic field.

The repolarization as refer to the change of the polarization vector direction of biotissue at change of the electric field direction.

Times of the relaxation for the various tissue components capable to polarizing, and various kinds of polarization vary differ. It is connected by that time of the relaxation depends on the size and a charge of the particles participating in process of repolarization, and from viscosity of environment since dipoles of a biological tissue of the various nature are in the viscous environment.

The degree of polarization and repolarization of tissue structure is defined by the ratio of the relaxation time inherent in it and the period of the variable electric field. Not all dipoles at the given frequency of the electric field have time repolarize.

Minimal time of relaxation at the atoms polarized due to electronic polarization. Very small time of relaxation characterizes orientable polarization of water molecules. Times of relaxation of a biotissue polarized due to molecular polarization of large albuminous molecules and macrostructural polarization it is much more.

Therefore with increase in frequency of the external electric field polarizing mechanisms with big time of relaxations leave process of polarization. Reduction of the period of the electric field oscillations results to that dipoles have not time to be oriented or attain completely the maximal size of induced dipoles. Thus there are decreases the size of own electric field of polarization $\boldsymbol{E}_C$. In this connection reduction of relative dielectric penetrance $\varepsilon = \dfrac{E_0}{E_0 - E_C}$ of a biotissue with growth of frequency of electromagnetic field is observed. At aspiration $\boldsymbol{E}_C \to 0$ the relative dielectric penetrance of a biotissue $\varepsilon \to 1$.

Dependence of relative dielectric penetrance of biotissues on frequency of the electric field refers to as a dispersion of relative dielectric penetrance, and the graph of this dependence of a dispersive curve.

The simplest kind the dispersive curve has for cases when medium is submitted by one sort of dipoles, fig. 5.13. The curve 1 concerns to ice, and a curve 2 to water. Characteristic parameters of curves are:

- size ε_0 it is value to which asymptotically relative dielectric penetrance of substance comes nearer at reduction of the electric field frequency (in the limit at constant of the electric field strength $\boldsymbol{E}_0$). Thus polarization of substance it is maximal (for water $\varepsilon_0 = 81$);

- size ε_∞ it is the minimal relative dielectric penetrance of substance corresponding to the minimal polarization of substance at the maximal frequency of the field in the examined range of frequencies. On fig.

5.13 size $\varepsilon_\infty \approx 3$ is specified for water. Difference ε_∞ from unit in the field of high frequencies is connected by that on the graph the frequency of the electric field is limited to radio-frequency range.

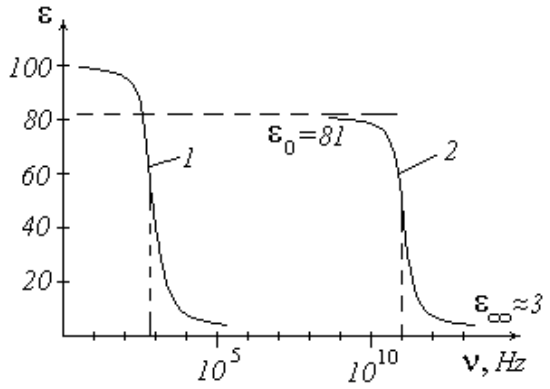

Fig. 5.13.

Areas of sharp falling frequencies of relative dielectric penetrance ε refer to as areas of dispersion.

The area of the relative dielectric penetrance dispersion of ice lays in more low-frequency part of a spectrum than at water. It speaks that in a liquid of substance molecule are less coupled to surrounding molecules than in a solid body. Therefore water to orientatable polarization and repolarization comparative ice is exposed more easily. The area of the dispersion of ice and water basically is in the radio-frequency range. For the water steam where freedom of molecules movement is even more the characteristic dispersion frequency (frequency of the excess of the dispersive curve) is even higher and is equal $2.1 \cdot 10^{13}\ Hz$ - infra-red area of a spectrum.

5.4.3. Dispersion of relative dielectric penetrance of the biological tissue

The relative dielectric penetrance ε non monotonic falls with increase in frequency ν. Non monotonicity of functions $\varepsilon = f(\nu)$ it is defined by the complex composite structure of a biological tissue. At various of the organism tissues the character of function falling $\varepsilon = f(\nu)$ (its dispersion) depending on frequency is various. For example, on fig. 5.14 dependence of relative dielectric penetrance of a skeletal muscle on frequency in radio-frequency range - the dispersive curve of the skeletal muscle [15] is submitted. For convenience of the analysis on the graph on the coordinates axes the decade logarithms of sizes are used.

Relative dielectric penetrance is functionally connected to the impedance of a biotissuec (full electric resistance) proportional dependence.

Such proportionality is defined by that energy of the variable electric current is spent on polarization and repolarization of tissues structures owing to what the impedance of the tissue grows. Therefore further we shall analyze change of these sizes depending on frequency of the electric field in parallel.

In conformity with experimentally found out sites of fast falling of the biotissue relative dielectric penetrance it is accepted to allocate three areas of the electric field influence or three areas of the dispersion. At transition from one area of dispersion to another the character of the basic polarizing processes in biotissue are varies.

1. The area of α-dispersion. It is observed up to frequencies $\sim 1\,kHz$ (the range is $\lg \nu = \lg(1000\ Hz) = 3$).

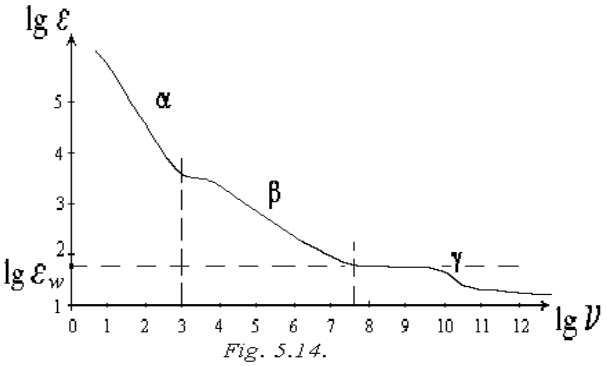

Fig. 5.14.

In connection with the big period of the variable electric field oscillations in this area there are all kinds of polarization and repolarization of tissues: macrostructural polarization, molecular polarization, orientable polarization of water molecules and electronic polarization of atoms. But the basic contribution to size ε is brought with macrostructural polarization of the biotissue.

In a low-frequency site of the spectrum of α -dispersion area the electric current arising under action of the electric field flows practically only on the intercellular liquid since resistance of cells membranes is very great. In a high-frequency site of this of the spectrum area the impedance falls due to decrease in a capacitance $X_C = \frac{1}{2\pi\nu C}$ of the cells membranes. There is a current of displacement current through the membrane as through the condenser.

In living tissues in area of α -dispersion significant excess of size ε is observed in comparison with relative dielectric penetrance of water ε_w - low-frequency increment of the relative dielectric penetrance (for comparison it is used maximal value $\varepsilon_w = 81$ in the radio-frequency range). In this range of frequencies all kinds of polarization and repolarization of the tissue structures are carried out.

In area of α -dispersion falling of relative dielectric penetrance is connected to increase in frequency of the electric field that ions have not time to reach the membranes and the macrostructural polarization connected to accumulation of ions at cells membranes and cellular compartments (fig. 5.10) decreases. Hence initial reduction of relative dielectric penetrance is connected to disappearance of polarization of conductive type.

In high-frequency area of α -dispersion falling of relative dielectric penetrance occurs for the account leaving of polarizing effects determined by deformation counterionic atmospheres polyelectrolytes, fig. 5.11. Leaving of polarizing effects it is connected by that the period of the electromagnetic field oscillations becomes less time of the relaxation of this and so on polarizing phenomenon.

2. Area of the β -dispersion. It is observed up to frequencies $10^{4-5}\ kHz$ (the range is $\lg\nu \approx 3-7.5$).

Polarization and repolarization of biotissues in this area is carried out basically due to molecular polarization, orientable polarization of the water molecules and electronic polarization of atoms.

In low-frequency site of the β -dispersion spectrum the basic contribution to the polarizing phenomena are brought with molecular polarization.

Molecular polarization consists that inside a molecule usually large albuminous under action of the electric field the ions and the ionic groups included in the molecule are displaced. Thus molecules get the dipole moment. It is influences on functional properties of proteins.

At increase in frequency of the electric field the dipole moments of large molecules of biopolymers and their separate dipole segments have not time to be induced and oriented therefore relative dielectric penrtrance is decreases. Thus in basis of the β -dispersion there lays gradual leaving effects of the molecular polarization of particles.

With growth of frequency of the electric field oscillations in areas of the β -dispersion stop to bring the contribution to polarizing effects all over again large albuminous macromolecules, and at the end of the β -dispersion range the smallest. The big width of the β -dispersion frequency range is defined by big interval of

times of the molecular polarization relaxation in connection with the big variety of the albuminous molecules size. This rather smooth transition from area of the α -dispersion to area of the β -dispersion explains.

In a high-frequency part of the β -dispersion spectrum the effects of molecular polarization due to albuminous molecules gradually disappear also relative dielectric penetrance start to be defined basically by the orientable polarization and repolarization of water molecules. But also in this part of the β -dispersion area the relative dielectric penetrance of the biotissue remains more than at water ($\varepsilon_w \approx 81$). Excess $\varepsilon > \varepsilon_w$ determines the top border of the β -dispersion area.

Expenses of energy for polarization and repolarization of molecular structures (albuminous molecules, molecules of water, atoms, etc.) define the impedance of a tissue. Decrease in these expenses results in decrease in the biotissue impedance.

3. Area of the γ -dispersion. It is observed up to frequencies 10^8 kHz (the range is $\lg \nu \approx 9-11$).

Polarization and repolarization biotissues in this area is carried out basically for the account of the orientable polarization of the water molecules and electronic polarization of atoms.

In a low-frequency part of the γ -dispersion spectrum exists rather wide non dispersive area where effects of molecular polarization are not observed any more since their time of the relaxation is more than period of the electric field oscillations but other polarizing phenomena connected basically with water are kept.

In area of the γ -dispersion the reduction of relative dielectric penetrance of a biotissue is caused by gradual reducing of the orientable repolarization of the dipole water molecules, fig. 5.12a.

Energy of an electric current with increase in frequency is ever less lost on reorientation of the water molecules also the impedance of the tissue therefore decreases.

At the further increase in frequency of the electric field as the period of the field oscillations is very small the relaxation connected with the oscillations of separate ions in molecules concerning valent bonds and electronic repolarization of atoms, fig. 5.12b, can be observed only. Only in these processes time of the relaxation remains less period of the electric field oscillations. Therefore relative dielectric penetrance of the tissue is small - high-frequency decrement ε . The remaining polarizing phenomena keep size of relative dielectric penetrance on frequencies are higher 10^{11} Hz on the low level $\varepsilon \approx 3$.

It is possible to note that the remaining polarizing effects (displacement of ions in molecules concerning valent bonds and electronic polarization of atoms at displacement of the electronic shell concerning a nucleus) will lead to the dispersive phenomena in the biotissue in ranges of the electromagnetic field frequencies which are above the top border of radio frequencies (infra-red, visual, ultra-violet light, etc.)

Chapter 6. Influence by the low-frequency impulse electric current on organism

Influence by the low-frequency impulse electric current on organism is used at electrostimulation of an organs and tissues. This influence is carried out with the diagnostic and therapeutic purposes for change of functional condition of cells, organs and tissues.

The basic difference of the electric current application at electrostimulation, for example, from high-frequency physiotherapy will be that at electrostimulation the excitable biotissue is finish up to irritation by external source of the voltage. Therefore the voltage of electrostimulation should exceed potential of depolarization of excitable biotissue *PDep*, fig. 2.3.

At electrostimulation apply impulse and variable currents of a low frequency (LF) or a low-frequency part of the sound frequencies spectrum (SF) the various form, and usually modulated on amplitude.

The electric irritation is carried out with the help of the electrodes enclosed to the body of patient in certain places.

In basis of the electric current action on the organism tissue at electrostimulation lays the change of polarization of cellular membranes at movement of ions in cytoplasm and intercellular space, change of the charge on membranes of cells up to their excitation. Thus on a cell membrane there are areas of hyperpolarization where the potential is increased and depolarization that results the cell in excitation, fig. 5.10.

For the first time electrostimulation of nerves and muscles of a frog has been applied by Italian physiologist L. Galvani from what the electrobiology began to develop.

Researches of irritating action (IA) of the electric current on muscles were carried out by German scientist Dubua-Reymon. He has introduced concept of a threshold current.

The elementary factor of influence on the excitable tissue at electrostimulation is the impulse of electric current *i*, fig. 6.1.

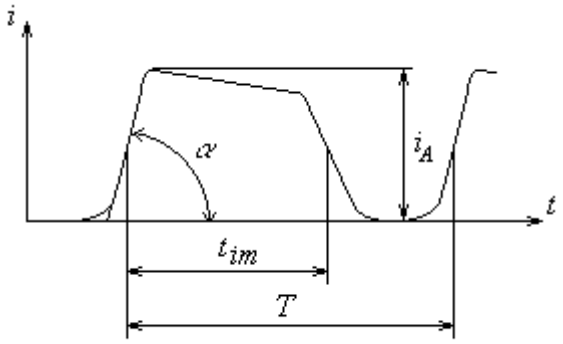

Fig. 6.1.

Irritating action of a single impulse on the muscle depends on lines of the impulse parameters: steepnesse of front - $\tan\alpha$; duration of the impulse - t_{im} , and amplitudes of the impulse - i_A . Essential meaning at electrostimulation has the period of following of impulses *T*.

6.1. Dependence of irritating action of the impulse current on duration of rectangular impulse. Weiss-Lapicque law

The law reflecting dependence of the threshold current i_{th} from duration of the rectangular ($\alpha = 90^0$) electric impulse t_{im} it is the Weiss-Lapicque law one of few electrophysiological laws confirmed with numerous experiments and having biophysical substantiation [56].

Threshold current i_{th} is the minimal force of the current forcing the muscle to be contracted.

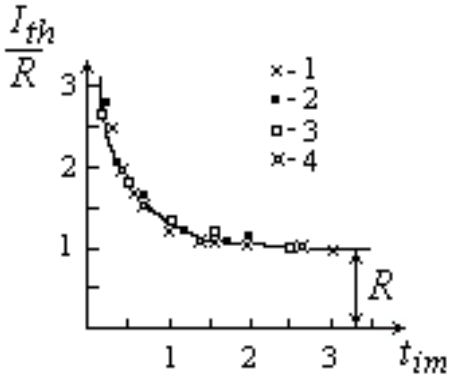

Fig. 6.2.

On fig. 6.2 experimental dependence under the name "force – duration" is shown. On ordinates axis the threshold current in relative units (be relative rheobase *R*) for a wide class of excitable tissue, and on abscissa axis - duration of the impulse is shown.

Time scale various for various objects of research: 1 – the frog gastrochemus muscle, time scale $1\,ms$, 2 – the mollusc muscle, $50\,ms$, 3 - the frog stomach muscle, $2\,s$, 4 – alga spirogyra, $20\,s$.

Weiss-Lapicque law it is possible to write down as the formula:

$$i_{th} = \frac{a}{t_{im}} + R, \qquad (6.1)$$

where t_{im} there is impulse duration, *a* and *R* - constants.

Long impulses or direct current have the greatest irritating effect. Thus value of the threshold current minimally and equally $i_{th} = R$. Size *R* refers to as rheobase.

Duration of the impulse at which the threshold current is equal double rheobase refers to as chronaxy ($t_{im} = t_{chr}$). Hence, the constant is $a = t_{chr}R$. Chronaxy and rheobase use as functional condition parameters of the excitable tissue and are diagnostic parameters in neurology.

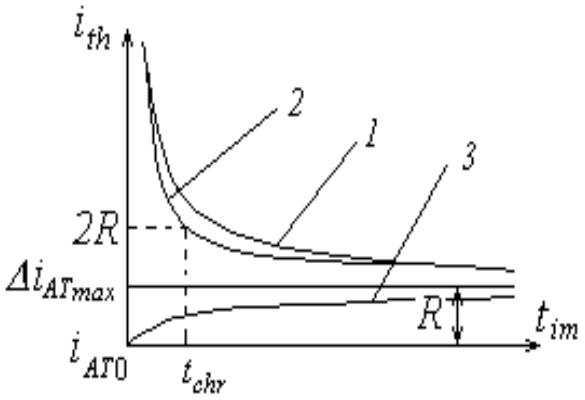

Fig. 6.3.

On fig. 6.3 (curve 1) the dependence of the threshold current i_{th} on the rectangular impulse duration t_{im} plotted under the Weiss-Lapicque law (6.1) is shown.

Let's consider biophysical essence of Weiss-Lapicque law. For excitation of membrane the external electric current i_{ex} should transfer to the membrane certain quantity of positive charge Δq necessary for decrease of membrane potential up to depolarizing potential $PDep = \Delta\varphi_{cr}$, fig. 6.4.

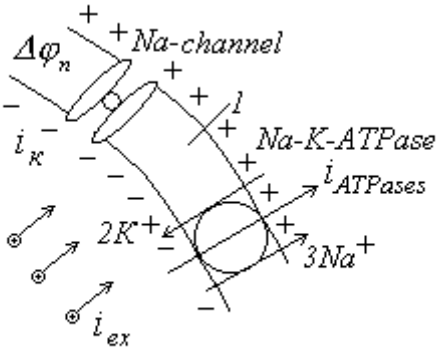

Fig. 6.4.

In a cellular membrane continuously functions the system of active transport it is the sodium - potassium pump or $Na^+ - K^+ - ATPase$ supporting constancy of ions concentration gradients Na^+ and K^+ on the membrane. This system is both concentration and voltage dependent since increase in ions Na^+ concentration in the near membrane layer of cytoplasm increases speed of completion transport *ATPases* by three ions Na^+ and the reduction of potential on membrane lessens carrying out of a positive charge from the cell.

Therefore, the part of the charge transferred to membrane Δq_{AT} will be remove from the cell due to increasing of the active transport first of all $Na^+ - K^+ - ATPase$. Naturally, the active ionic current through a membrane is created and $Ca^{2+} - ATPase$ but its role especial in neurons it is much less $Na^+ - K^+ - ATPase$.

Hence, the total charge which should be delivered to the membrane for decrease in potential on it up to critical level of depolarization *PDep* is possible to present as:

$$\Delta q = \Delta q_{cr} + \Delta q_{AT}, \qquad (6.2)$$

where Δq_{cr} there is the quantity of the charge necessary for decrease of potential on the membrane up to the critical level of depolarization without taking into account increment of the active ionic transport but with account of the current through opened the most sensitive sodium ionic channels. Potassium ionic channels open basically later and they can be not taken into account.

Let's divide this equality into duration of impulse $\Delta t = t_{im}$. Taking into account that $i_{th} = \dfrac{\Delta q}{\Delta t}$ it is the threshold current, and $\Delta i_{AT\max} = \dfrac{\Delta q_{AT}}{t_{im}}$ - the greatest possible increment of the current through membrane due to work *ATPases*, we shall find:

$$i_{tr} = \frac{\Delta q_{cr}}{t_{im}} + \Delta i_{AT\max}. \qquad (6.3)$$

Comparing the received formula with the formula of Weiss-Lapicque law (6.1) we find, that the constant *a* in Weiss-Lapicque law is equal to the quantity of charge Δq_{cr} necessary for decrease of potential on the membrane up to critical level of depolarization $\Delta\varphi_{cr}$, and rheobase $R = \Delta i_{AT\max}$ is equal to the greatest possible increment of the current due to work *ATPases*, i.e. characterizes functional abilities transport *ATPases*.

In connection with that the charge approaching to the membrane results in decrease in potential on the membrane, as a first approximation it is possible to assume that the first composed in the formula (6.3) represents the current of displacement through the membrane $i_{dis} = C\dfrac{d\varphi}{dt}$ where *C* it is capacity of the

researched site cell membranes of the biotissue. Before attainment $\Delta\varphi_{cr}$ it is possible to neglect an ionic current through opened the most sensitive sodium channels.

Therefore quantity of charge Δq_{cr} and consequently also a constant *a* in Weiss-Lapicque law (6.1) it is possible to calculate under the formula:

$$\Delta q_{cr} = a = t_{chr} R = C\left(\Delta\varphi_r - \Delta\varphi_{cr}\right), \qquad (6.4)$$

where $\Delta\varphi_r$ there is resting potential on the membrane, $\Delta\varphi_r - \Delta\varphi_{cr}$ - necessary decrease in potential on the membrane for excitation of tissue.

Taking into account that $\Delta\varphi_r - \Delta\varphi_{cr} = const$ for the given kind of biotissue in the certain condition we infer that the constant *a* in Weiss-Lapicque law characterizes capacitor properties of biomembranes.

The increase in duration of the impulse t_{im} irritating biotissue results in reduction of threshold current i_{th} since for greater time the greater charge is transferred to the membrane. But if the size of the external current does not exceed functionalities of the active transport $i_{ex} < \Delta i_{AT\max}$, fig. 6.3, the potential on the membrane will not decrease to depolarize potential and depolarization of the membranes will not take place. If the *ATPases* do not compensate change of the ions concentration at the membrane due to external and channel currents there results excitation of the cell. In it will be consist the biophysical sense of Weiss-Lapicque law.

The mathematical description of Weiss-Lapicque law (6.1) contains some assumptions. First, the formula (6.1) reflects the hyperbolic law of the threshold current dependence from duration of the impulse. At the hyperbole is observed infinite approach of function - the threshold current i_{th} to horizontal asymptote - rheobase *R*. In reality it is usual through small time (some milliseconds for a skeletal muscle warm-blooded) the threshold current becomes equal to rheobase *R* [56]. More important deviation from the hyperbolic law consists that according to the formula (6.1) chronaxy is $t_{chr} = \frac{a}{R}$. However from the experimental curve follows that at $t_{im} = \frac{a}{R}$ the threshold current is $i_{th} \approx 1.4R$ instead of $i_{th} = 2R$ [10].

Both these of the fact specify that the hyperbole not precisely describes analyzed law. Actually, since the current of ions active transport through the membrane increases gradually the curve “force – duration” goes a little below than designed under the formula 6.1. On fig. 6.3 the given position is reflected by curve 2.

Let's consider in more detail work of active transport at action of the rectangular impulse of electric current on the membrane. Before action of the impulse on the excitable biotissue the certain numbers of molecules *ATPase* works. This numbers of molecules creates the active current through the membrane i_{AT0}, fig. 6.3, corresponding to maintenance of resting potential and compensating the current of outflow. At action of the electric impulse the positive ions including Na^+ go away from cytoplasm to the membrane, fig. 6.4. The increase in concentration of ions Na^+ in the near membrane layer of cytoplasm is the determining factor in activization $Na^+ - K^+ - ATPase$ [15].

If the current impulse is long enough and on size approach to rheobase the greatest possible numbers of molecules *ATPaseы* becomes more active. In this case the current created by the active transport increases on size $\Delta i_{AT\max}$.

As activization of *ATPases* molecules is stochastic process it is possible to assume that for equal time intervals Δt decreases same part $\lambda\Delta t$ of not activated molecules or, that the same, probability for a molecule to transit from not activated in the activated condition for a time unit remains identical and equal λ where λ is the speed constant of the loss of not activated molecules of $Na^+ - K^+ - ATPase$ during increase of the current through membrane. Let on some site of membrane can be in addition activated θ molecules of $Na^+ - K^+ - ATPase$. Constantly working *ATPases* molecules for compensation of the outflow currents through the membrane in our analysis are not taken into account. From θ molecules are during the examined

moment of time for the compensation of the external current *m* molecules it is activated and *n* molecules it is not activated. Hence:

$$\frac{\Delta n}{n} = -\lambda \Delta t, \quad \text{at} \quad \Delta t \to 0 \qquad \frac{dn}{n} = -\lambda dt. \qquad (6.5)$$

Integrating the given formula, we receive:

$$\int_{\theta}^{n} \frac{dn}{n} = -\lambda \int_{0}^{t} dt \to n = \theta \mathrm{e}^{-\lambda t}. \qquad (6.6)$$

At integration it is taken into account that during the initial moment of time at $t = 0$ all $Na^{+} - K^{+} - ATPase$ molecules are not activated (i.e. for simplification of the analysis it is accepted $i_{AT0} = 0$). Taking into account $\theta = n + m$ is possible to find numbers of activated molecules:

$$m = \theta\left(1 - \mathrm{e}^{-\lambda t}\right). \qquad (6.7)$$

The current due to active transport through the examined site of membrane is proportional to numbers of activated $Na^{+} - K^{+} - ATPase$ molecules on this site: $\Delta i_{AT} \sim m, \quad \Delta i_{AT\max} \sim \theta$ where Δi_{AT} it is increase in the current through the membrane due to activization of *ATPases* molecules, $\Delta i_{AT\max}$ - the greatest possible current through the membrane due to active transport. Hence, due to increase of the active transport intensity the dependence of the current change through the membrane on time will be expressed as the formula:

$$\Delta i_{AT} = \Delta i_{AT\max}\left(1 - \mathrm{e}^{-\lambda t}\right). \qquad (6.8)$$

On fig. 6.3 (curve 3) the graph of current change in time is shown due to active transport. Thus, on the graph for origin of coordinates the value of the current Δi_{AT0} through the membrane due to active transport in the cell resting condition is accepted.

Hence, the formula (6.3) describing dependence of the threshold current on duration of the impulse should be transformed to kind:

$$i_{th} = \frac{a}{t_{im}} + \Delta i_{AT\max}\left[1 - \exp\left(-\lambda t_{im}\right)\right]. \qquad (6.9)$$

As rheobase it is equal $R = \Delta i_{AT\max}$ the given formula can be copied as:

$$i_{th} + R\exp\left(-\lambda t_{im}\right) = \frac{a}{t_{im}} + R. \qquad (6.10)$$

Proceeding from the received equality for $i_{th} = 2R$ using $\exp\left(-\lambda t_{chr}\right) \approx 1 - \lambda t_{chr}$ the chronaxy it is possible to calculate from the quadratic:

The solution of this equation is as:

$$t_{chr} = \frac{1}{\lambda}\left[1 \pm \sqrt{1 - \frac{\lambda a}{R}}\right]. \qquad (6.12)$$

Using the approximate formula $\sqrt{1 - x} \approx 1 - \frac{1}{2}x$ we receive $t_{chr} = \frac{a}{2R}$. Last formula is deduced from the condition that the threshold current is equal to two rheobase.

Let's find value of the threshold current if $t_{im} = \frac{a}{R}$. In this case according to (6.10) the threshold current is equal:

$$i_{th} = 2R\left[1 - \frac{1}{2}\exp\left(-\lambda \frac{a}{R}\right)\right] \approx R + \lambda a. \qquad (6.13)$$

Hence, as well as show experiments the threshold current in case of duration of the rectangular impulse $t_{im} = \frac{a}{R}$ less than two rheobase. Therefore to calculate chronaxy under the formula $t_{chr} = \frac{a}{R}$ it is incorrect, since change of the active transport current in process excitation of a biotissue is not taken into account. It is necessary to use the formula (6.13).

If to accept that at $t_{im} = \frac{a}{R}$ the threshold current $i_{th} \approx 1{,}4R$ [10] according to last formula is $0.4R = \lambda a$. Taking into account (6.12), we find $t_{chr} = 0.22\frac{1}{\lambda}$.

Using the data [57] that energy consumption for work of $Na^+ - K^+ - ATPase$ at excitation of a biotissue increase for various cells from 33% up to 70% in comparison with the resting condition it is possible to write down $R = (1.33 \div 1.7) i_{AT0}$. Hence $i_{AT0} = (0.59 \div 0.75)R$.

Though the constant of the loss speed λ of not activated $Na^+ - K^+ - ATPase$ molecules during increase of the current now is unknown but taking into account that after attaining of rheobase practically all molecules should be activated it is possible to conclude that size λ is reverse so-called to useful time $\lambda \approx \frac{1}{\tau}$.

Useful time τ it is time during which current *ATPases* through the membrane (6.8) grows up to $\Delta i_{AT} = \Delta i_{AT\max}\left(1 - \mathrm{e}^{-1}\right) = 0{,}63\Delta i_{AT\max}$. This means that in time τ probability for $Na^+ - K^+ - ATPase$ molecule to transit in the activated condition $\lambda\tau \approx 1$. Chronaxy approximately in 7 ones there is less than size of useful time [58]. Therefore size λ can be estimated from the ratio $\lambda \approx 0.14\frac{1}{t_{chr}}$.

Proceeding from (6.12) it is possible to receive $\lambda a \approx 0.26R$. If for this case to estimate value of the threshold current at $t_{im} = \frac{a}{R}$ that according to (6.13) we shall receive $i_{th} \approx 1.26R$ that differs from the data [10] a little. But also this estimation shows that calculation of chronaxy under the formula $t_{chr} = \frac{a}{R}$, and hence the record of Weiss-Lapicque law as (6.1) is not absolutely correct.

6.2. Biophysical bases of the Dubua-Reymon law

German scientist Dubua-Reymon has found out that excitability of a biotissue increases with increase in speed of the current increase.

On fig. 6.5 it is shown as changes the threshold current from time *t* depending on speed of the current increase through the biotissue [45, 59].

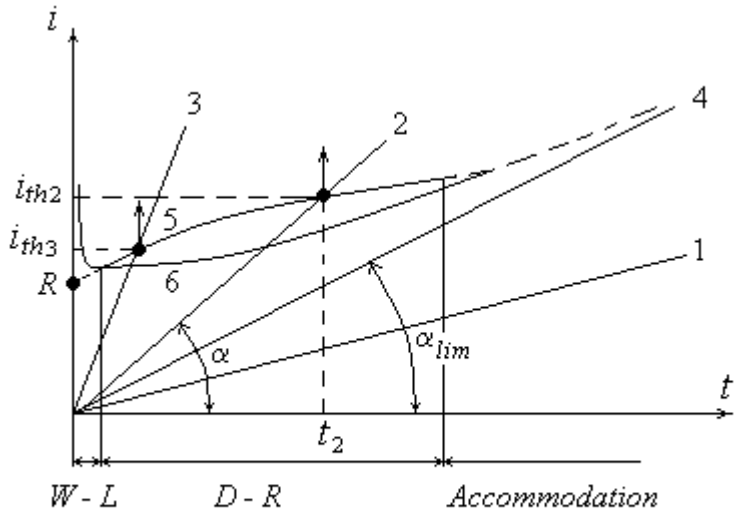

Fig. 6.5.

Points with the arrow reflect size of the threshold current i_{th} and moment of the biotissue excitation. At slow increase of current through a muscle the excitation does not arise (line 1) since the muscle get used to its action. This phenomenon refers to as accommodation. Ability of the muscle to accommodation depends on its functional condition. At a pathological condition of the muscle it changes.

The faster the current (lines 2 and 3) increases the less time interval before excitation and on the contrary, i.e. $i_{th} \sim \frac{1}{\tan\alpha}$. Under excitability of the biotissue (or irritating action of the current) usually mean size reverse to the threshold current [45] $S \sim \frac{1}{i_{th}}$. Hence:

$$S \sim \tan\alpha = \frac{di}{dt}. \qquad (6.14)$$

The formula (6.14) represents essence of the Dubua-Reymon law.

The biophysical explanation of this law will consist in the following.

The total charge which is approached to the membrane for decrease in potential on it up to potential of depolarization *PDep* should be possible to present as (6.2).

The external current in the Dubua-Reymon experiences increased linearly under the law $i = \tan\alpha \cdot t$, fig. 6.5. For an example we examine increase of the current by the line 2. There is time of the current increase, i.e. time of the impulse $t_{im} = t_2$ up to size of the current $i = i_{th2}$. The quantity of the charge transferable this current to the membrane necessary for decrease of potential on membrane up to *PDep* without taking into account amplification of the active ionic transport is equal to the area under line 2, i.e. $\Delta q_{cr} = \frac{1}{2} i t_{im} = \frac{1}{2}\tan\alpha \cdot t_{im}^2$.

Duration of times in the Dubua-Reymon law considered are those that the active current through the membrane has time to become greatest possible and equal rheobase *R*. Therefore size of the charge which is taken out from a cell by the transport *ATPases* in time t_{im} we shall find under the formula $\Delta q_{AT} = R t_{im}$.

Hence, quantity of the charge which should be approached to the membrane by the external current for decrease in potential on it up to *PDep* according to (6.2) equally:

$$\Delta q = \frac{1}{2}\tan\alpha \cdot t_{im}^2 + R t_{im}. \qquad (6.15)$$

As time $t_{im} = \Delta t$ it is the interval before excitation of the cell membrane, i.e. before achievement by the external current of the threshold current $i = i_{th}$ having divided both parts of the previous equality (6.15) on t_{im} and taking into account $i_{th} = \dfrac{\Delta q}{\Delta t}$ we shall find:

$$i_{th} = \frac{1}{2}\tan\alpha \cdot t_{im} + R \,. \qquad (6.16)$$

The received equation is not the equation of a straight line since angle α depends on impulse time t_{im}.

On fig. 6.5 according to the found equation (6.16) the curve 5 connecting points of the cell excitation is shown.

Thus the threshold current at instantaneous increase of the external current is designated *R*. Such external current corresponds to the rectangular impulses and is equal rheobase. Its action on a biotissue has been analysed earlier in paragraph 6.1.

In process of positive ions carry inside cells to the membrane by the external current i_{ex} the potential on membrane starts to fall. The first most sensitive sodium ionic channels start to open, fig. 6.4. The matter is that the sensitivity of the sodium ionic channels to change of potential on the membrane differs from each other. In process of falling potential on a membrane the quantity of the opened channels increases that finally at achievement *PDep* should lead to the cell excitation. But in connection with that the external current increases not instantly, and time of the sodium channel life in the open state is very small $\tau \approx 1\,ms$ simultaneously during decrease in potential on the membrane there is a process of closing (inactivation) already opened ionic channels. At slow enough increase of the current (straight line 4 with the angle of inclination $\alpha_{\lim}$, fig. 6.5) the most of the opened ionic channels have time inactivated, i.e. again to be closed. Therefore excitation of the cell does not arise. The biophysical essence of accommodation of a biotissue consists in it for triangular impulses. The site of the line 5 at accommodation of the tissue is shown by the dotted line.

The equation (6.16) shows that the curve 5 inclination is equal to half of inclination of the straight line 2 ($i = \mathrm{tg}\alpha \cdot t$). Hence:

$$\frac{di_{th}}{dt_{im}} = \frac{1}{2}\frac{i_{th}}{t_{im}} \,. \qquad (6.17)$$

To the given equation function satisfies:

$$i_{th} = k\sqrt{t_{im}} \,, \qquad (6.18)$$

where *k* there is constant.

Taking into account condition: at t_{im} close to 0 the size $i_{th} = R$ the formulas (6.16) and (6.18) can be written down as:

$$\frac{i_{th}}{R} = \frac{k}{R}\sqrt{t_{im}} + 1, \qquad (6.19)$$

Thus, at average speeds of the external current increase at which active current of *ATPases* already to become maximal and equal rheobase *R* but full inactivation of ionic channels has not come yet the dependence of the threshold current on time of the external current increase has parabolic character (curve 5), fig. 6.5. This conclusion coincides with results of experiments [60].

The line 5 frequently refers to as curve of accommodation [60]. The curve of accommodation 5 shown on fig. 6.5 is typical for the norm of nervous-muscular system of the man and warm-blooded animals in case of triangular stimulating impulses. Linear dependence of curve accommodation on time is observed, for example, for peripheral nervous system of amphibians. The convex course of curve accommodation in relation to the axis of time (convexity downwards) is observed at failures of normal functioning of the biotissue and connected to gradual refusal of the tissue from the answer to irritation.

Usually the parabola (curve 5 on fig. 6.5) is replaced the broken curve with the rectilinear sites [60] located under various angles to the axis of time $\dfrac{i_{th}}{R} = \dfrac{t_{im}}{\lambda} + 1$ where λ is a constant of accommodation on

the given site. It is simple to see that value is $\frac{k}{R} = \frac{\sqrt{t_{im}}}{\lambda}$. In the initial part of the curve accommodation for peripheral nervous-muscular system of warm-blooded the size $\lambda = 20 - 60\,ms$, and the constant of accommodation for extensors approximately on 50% is more than for flexors. For example, for the muscle m. brachial. int. of the man top extremity the constant of accommodation is $\lambda = 25.5\,ms$ [60]. Hence, there are for the triangular impulses duration $t_{im} = 100\ ms$ the size is $\frac{k}{R} \approx 0{,}4\,ms^{-1/2}$.

Actually the curve of accommodation cannot attain rheobase *R* at $t = 0$. It is connected by that at small times of the impulse when speed of increase of the current is very great $\tan\alpha \to 90^{o}$ the Weiss-Lapicque law for a rectangular impulse starts to operate. The threshold current there is grows, fig. 6.2.

Hence, on the curve 5, fig. 6.5, in norm it is possible to allocate three areas. For very short impulses some milliseconds area of the Weiss-Lapicque law where the curve 5 has hyperbolic character thus physiological distinction between rectangular and triangular impulses insignificantly. For longer (hundreds milliseconds) triangular impulses there is area of the Dubua-Reymon law where the curve of accommodation 5 in norm has parabolic character convexity upwards. There is area of accommodation where the curve 5 transit in the linear dependence.

The form of curve accommodation depends on two factors: forms of a stimulating impulse and a functional condition of the biotissue.

Frequently for studying accommodative properties of the biotissue use the electric currents increasing exponential with vertical back front, fig. 6.6c. It is connected to the greater simplicity of production of such impulses.

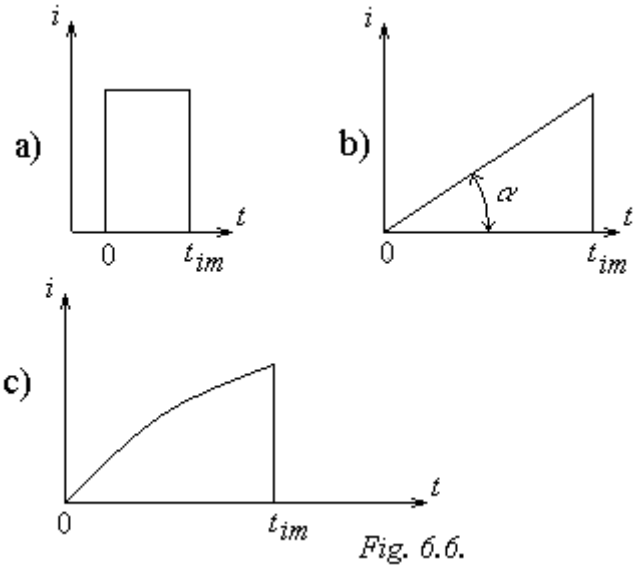

Fig. 6.6.

The electric impulse of the triangular form with vertical back front, fig. 6.6b, transfers from cells inside to the membrane exactly in half of less charge than the rectangular impulse, fig. 6.6a, used in the Weiss-Lapicque law, see paragraph 6.1. The rectangular impulse transfers the greatest possible quantity of the charge to the membrane. For the triangular impulse the curve of accommodation 5 in the area of the Dubua-Reymon law has the parabolic form convexity upwards concerning the axis of time, fig. 6.5. For a rectangular impulse the curve has the hyperbolic form convexity downwards, fig. 6.3. It is natural to assume that for the stimulating impulse exponential forms, fig. 6.6c, which transfers less charge than the rectangular impulse but is more than triangular the form of the curve accommodation will have the intermediate kind.

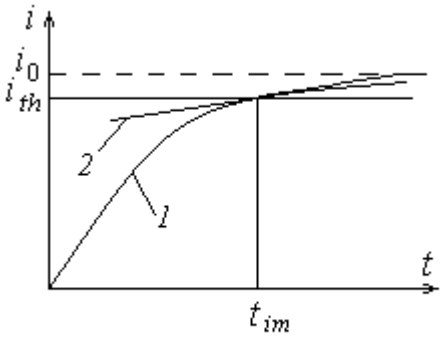

Fig. 6.7.

Let's find the kind of the curve accommodation for the exponential impulse, fig. 6.7, curve 1.

The form of the pulse we shall set as:

$$i = i_0\left(1 - \mathrm{e}^{-\alpha t}\right), \qquad (6.20)$$

where i_0 and α there are parameters of the impulse.

The charge transferred by an external current to the membrane, fig. 6.4, during the impulse t_{im} necessary for its excitation we shall find under the formula (6.2):

$$\Delta q = \int_0^{t_{im}} i\,dt + Rt_{im} = \left(i_0 + R\right)t_{im} + \frac{i_0}{\alpha}\left(\mathrm{e}^{-\alpha t_{im}} - 1\right). \qquad (6.21)$$

Threshold value of the impulse current equally:

$$i_{th} = \frac{\Delta q}{\Delta t} = i_0 + R + \frac{i_0\left(\mathrm{e}^{-\alpha t_{im}} - 1\right)}{\alpha t_{im}}, \qquad (6.22)$$

where as before it is accepted $t_{im} = \Delta t$.

Inclination of the curve accommodation 2, fig. 6.7, to the axis *t* we shall determine as:

$$\frac{di_{th}}{dt_{im}} = -\frac{i_0\left(\mathrm{e}^{-\alpha t_{im}} - 1\right)}{\alpha t_{im}^2} - \frac{i_0\mathrm{e}^{-\alpha t_{im}}}{t_{im}} = \frac{i_{th}}{\alpha t_{im}^2} - \frac{i_0\mathrm{e}^{-\alpha t_{im}}}{t_{im}}. \qquad (6.23)$$

In (6.23) the formula (6.24) following from (6.20) is used:

$$i_{th} = i_0\left(1 - \mathrm{e}^{-\alpha t_{im}}\right). \qquad (6.24)$$

Excluding from system (6.23), (6.24) time of the impulse t_{im} we have:

$$\frac{di_{th}}{dt_{im}} = -\frac{i_n}{t_{im}\ln\left(1 - \frac{i_{th}}{i_0}\right)} - \frac{i_0}{t_{im}}\left(1 - \frac{i_{th}}{i_0}\right). \qquad (6.25)$$

The solution of the differential equation (6.25) is possible only numerically.

If to carry out expansion into series of the function $\ln\left(1 - \frac{i_{th}}{i_0}\right) \approx -\frac{i_{th}}{i_0}$ to the first degree of small parameter there is result of the solution of the equation (6.25) is a straight line $i_{th} = kt_{im}$ where *k* there is a constant. Or with take into account of the active transport is $i_{th} = kt_{im} + R$. The received formula is too rough approximation of the curve accommodation form.

Therefore we shall expanse into series $\ln\left(1 - \frac{i_{th}}{i_0}\right) \approx -\frac{i_{th}}{i_0} - \frac{1}{2}\left(\frac{i_{th}}{i_0}\right)^2$ to the second degree of small parameter.

The further analysis connected to integration (6.25) shows that in at the given approximation in the area of the Dubua-Reymon law the threshold current depends on time of the impulse i_{im} under the law:

$$\frac{i_{th}}{R} = \frac{k}{R} t_{im}^{\frac{3}{2}} + 1. \qquad (6.26)$$

Hence, the curve of accommodation 6 in this area for the exponential impulse and normal condition of a biotissue has convexity downwards concerning the axis of time. Apparently, the form of the curve accommodation in [45] for the triangular impulse similar to curve 6 on fig. 6.5 is defined by application of stimulating impulses with exponential forward front, fig. 6.7c.

The carried out analysis of the electrobiological laws of Dubua-Reymon and Weiss-Lapicque show that they have a strict biophysical substantiation.

Dependence of the threshold current of an excitable tissue on duration of the impulse in norm generally looks like:

$$\frac{i_{th}}{R} = \frac{k}{R} t_{im}^{m} + 1, \qquad (6.27)$$

where the parameter $m = -1$ is correct for rectangular impulses, $m = \frac{1}{2}$ for triangular impulses with linearly increasing forward front and vertical back front, $m = \frac{3}{2}$ for triangular impulses with exponential increasing forward front and vertical back front.

The phenomenon of accommodation of a biotissue to action of the impulse current with increasing forward front is connected with the inactivation of ionic channels for slowly increasing impulse current.

Measuring rheobase and chronaxy for various biotissues, and also finding the straight line 4 of accommodation, fig. 6.5, at increase of the current through the biotissue it is possible to conclude about functional condition transport *ATPases* and ionic channels in membranes of cells.

Besides sizes chronaxy and rheobase give representation about capacitor parameters of cellular membranes, see (6.4), that allows receive the information on quantity cells of full value in the tissue.

Chapter 7. Acoustic analyzer

The acoustic analyzer is intended for the spectral analysis of sound waves and transformation of the received information to the electric (nervous) impulses going to central nervous system (CNS).

Acoustic analyzer anatomical divide on three departments: an external ear, middle ear and inner ear. The block-scheme of transfer of sound wave energy and the acoustical information in the acoustic analyzer is shown on fig. 7.1.

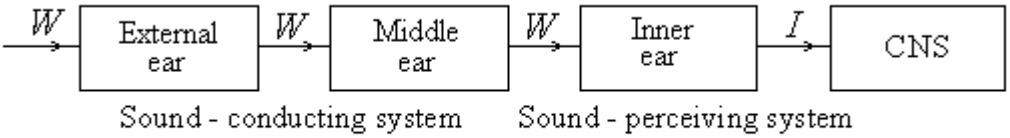

Fig. 7.1.

On block-scheme *W* there is received and transmitted energy, *I* - the information transmitted in CNS as the electric (nervous) impulses propagating on the acoustical nerve.

The acoustic analyzer, fig. 7.2, receives the sound information as a sound wave packet, analyzes, processes it and transfers in CNS.

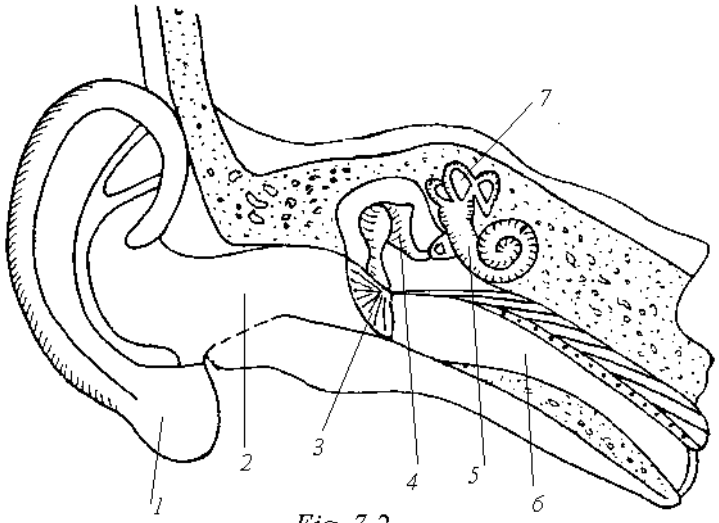

Fig. 7.2.

7.1. External ear

The external ear, fig. 7.2, will consist of an auricle 1 and external auditory canal 2. External auditory canal comes to end by an eardrum 3 which anatomical can be attributed to the middle ear.

The auricle promotes localization of the sound source in sagittal plane.

The auricle has the complex form therefore there sound differently diffract on the auricle depending on source position in sagittal planes. Due to presence of the auricle a man can approximately define where there is sound source behind or above.

In front it is the most important to define the direction on the sound source in the horizontal plane.

In the horizontal plane, fig. 7.3, the man establishes the direction on the sound source due to two phenomena.

First, for approximate localization of the direction on the source the distinction in intensity of the sound falling on eardrums of two ears is used. This distinction is connected by that the head creates obstacle (acoustic shadow) for the sound wave. Therefore audibility of the sound by the ear which is taking place on the source side is better than the opposite ear.

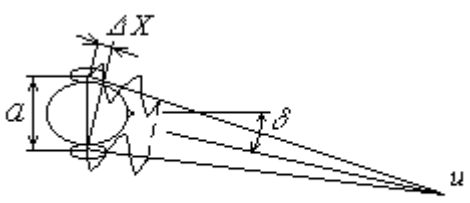

Fig. 7.3.

Second, for exact definition of the direction on the sound source it is used so-called binaural effect. This method is used for exact localization of the sound source (especially at night) which is in front. The binaural effect consists that there is the difference of phases connected to the difference in acoustical paths of waves ΔX propagating from one source *u* to two ears. This difference of phases is analyzed by CNS and defined by the direction on the sound source. Accuracy of the definition of the direction makes approximately $\delta \approx 3^0$. We shall consider due to that this accuracy is attained.

Distance between ears is $a \approx 20\,cm$. In this case the difference in acoustical paths of waves influencing ears $\Delta X = a \sin\delta \approx 1\,cm$. Therefore the sound attains one ear for the while $\Delta t = \frac{\Delta X}{c} \approx 3 \cdot 10^{-5}\ s$ later than another. Hence, the minimal difference of phases of two waves influencing the left and right ear at frequency of the sound, for example, $\nu = 3300\ Hz$ is equal $\Delta\varphi = 2\pi\nu\Delta t \approx 0{,}2\,\pi$, i.e. 36^0. Received rather big difference of phases can be estimated by CNS.

External auditory canal is in diameter $\sim 7\ mm$ plays a role of the resonator. The sound wave passes through external auditory canal and is in part reflected from the eardrum. There is a standing wave. Formation of the standing waves in the sound wave refers to as an acoustic resonance.

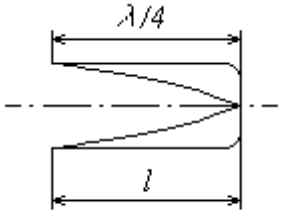

Fig. 7.4.

The acoustic resonance is observed in an air column or in other body which length is multiple quarters of the wave length. At the acoustic resonance there is increase in amplitude of oscillations *A* in two. As there is intensity of a sound $I \sim A^2$ at occurrence of the acoustic resonance the intensity of the sound increases in fore. Hence, external auditory canal can be examined as the spectral amplifier of the sound.

Length of external auditory canal, fig. 7.4, approximately is $l \approx 2.5\,cm$. It corresponds to quarter of the wave length $\frac{\lambda}{4}$. We examine the sound having the greatest wave length (i.e. the minimal frequency) which can create the standing wave in the external auditory canal.

Let's find resonant frequency:

$$\nu_{res} = \frac{c}{\lambda} = \frac{c}{4l} \approx \frac{330}{4 \cdot 0.025} = 3300\ Hz\,.$$

For calculations the speed of sound is accepted $c \approx 330\ \frac{m}{s}$.

Really, the area of sound frequencies corresponding approximately $\nu = 3300\ Hz$ is area of the maximal sensitivity of a human ear. At women resonant frequency is higher than at men reaches up to $\sim 6\ kHz$.

7.2. Middle ear

To the middle ear concerns, fig. 7.2, the eardrum 3, tympanic cavity in volume $\sim 1\,cm^3$ with ear bones 4, auditory (Eustachian) tube 6.

Eustachian tube has length about $4\,cm$ and diameter about $1\,mm$. It carries out communication of the tympanic cavity with atmosphere that air contained in this cavity did not damp oscillations of the eardrum, membranes of oval and round windows. Eustachian tube comes to end in the nasopharynx. Therefore, for example, in order to prevent damage of the eardrum during of a shot (sound impact) the gunners open a mouth for adapting of pressure in the middle ear and atmosphere.

The middle ear works for the following purposes:

1. Amplification of the pressure upon oval window in comparison with pressure upon eardrum (amplifying function).

2. The coordination of acoustic resistances of air in the external auditory canal and liquid mediums of internal ear (coordinating function is the main function of the middle ear).
3. Weakening of oscillations transfer to the internal ear in case of the sound big intensity (protecting function).

7.2.1. The nonlinear characteristic of eardrum

The eardrum has the nonlinear characteristic, i.e. its mechanical properties do not submit to the Hooke's law. The principle of the oscillations superposition on it is carried out approximately. Displacement *S* of eardrum depends on pressure of air *P* upon it under the law:

$$S = \alpha P + \beta P^2 + \gamma P^3,$$

where α, β and γ there are constants.

The nonlinear characteristic of the eardrum results in occurrence so-called combinational tones of Helmholtz at perception of sound. For example, at submission on the ear of two sound tones having frequencies $\nu_1 = 440\ Hz$ and $\nu_2 = 523\ Hz$ the tone by frequency $\nu_3 = 2\nu_1 - \nu_2 = 357\ Hz$ is heard.

There is a method of diagnostics of the eardrum condition based on comparison of amplitudes of the combinational tones of Helmholtz with norm. Thus on the eardrum simultaneously submitted sound frequencies ν_1 and ν_2 the certain amplitudes (in various frequency ranges of the sound spectrum perceived by the man). The registered amplitude of frequency ν_3 of the combinational tone characterizes condition of the eardrum.

7.2.2. Amplifying function of middle ear

Oscillations into the middle ear are transferred from the eardrum through three ear bones: malleus, incus and stapes. Stapes transfers oscillations to the membrane of oval window separating the air medium of the middle ear from the liquid medium of the internal ear.

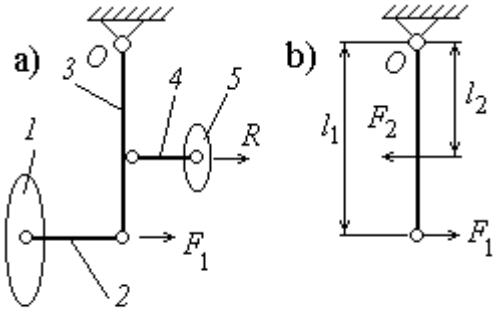

Fig. 7.5.

The mechanical lever equivalent of the middle ear looks as follows, fig. 7.5a. Are shown: the eardrum 1, the lever it is the equivalent of malleus 2, the lever it is the equivalent of the incus 3, the lever it is the equivalent of the stapes 4, the oval window 5. Support *O* at ear bones are not. It is so-called in mechanics an instant support or the instant center of rotation of the lever mechanism. At the other position of levers the support *O* is in the other place.

Let's find the ratio of a force F_1 which the eardrum operates on system of ear bones to force $R = -F_2$ which the system ear bones operates on the oval window, where F_2 is the reaction of oval window. We shall allocate incus 3 with the forces operated on it, fig. 7.5b.

According to the equation of a statics the sum of the moments of all forces around of a point *O* is equal to zero $\sum_{i=1}^{n} \boldsymbol{M}_i = 0$. Hence:

$$F_1 l_1 - F_2 l_2 = 0 \qquad \rightarrow \qquad \frac{F_1}{F_2} = \frac{P_1 S_1}{P_2 S_2} = \frac{l_2}{l_1}, \qquad (7.1)$$

where P_1 there is the force falling on unit of the area S_1 of the eardrum (approximately equal at small displacement to pressure of air upon the eardrum in external auditory canal), and P_2 - the force falling on unit of the area S_2 of the oval window (approximately equal at small displacement to the pressure created by the membrane of oval window on the liquid medium of the internal ear). Pressure of air in the tympanic cavity due to open Eustachian tube is equality atmospheric.

Using (7.1) we shall find the ratio P_2 to P_1:

$$\frac{P_2}{P_1} = \frac{S_1 l_1}{S_2 l_2} \approx 20 \cdot 1{,}3 = 26 . \qquad (7.2)$$

At calculation it is taken into account $\frac{S_1}{S_2} \approx 20$ and $\frac{l_1}{l_2} \approx 1.3$.

Thus, the pressure upon liquid mediums of the internal ear due to lever system ear bonds amplifies approximately in 26 ones in comparison with pressure of air in sound wave on the eardrum.

7.2.3. Coordinating function of middle ear

Function of the coordination of acoustic resistance of air in external auditory canal and liquid mediums of the internal ear at perception of a sound is the main function of the middle ear.

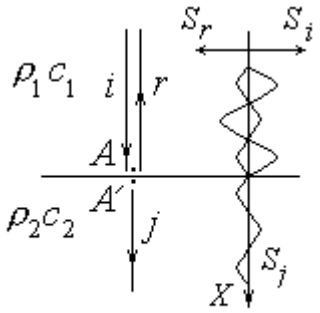

Fig. 7.6.

For the analysis of necessity of the acoustic resistance coordination we shall consider falling of the sound wave from air directly on the liquid medium, fig. 7.6. The index *i* there designate characteristics of the falling wave, *j* – the penetrating, and *r* – the reflected wave.

Let $\rho_1 c_1$ and $\rho_2 c_2$ there are specific acoustic resistances accordingly of air and liquid.

Sound pressure in the point *A*, i.e. in air at interface of two media is equal to sound pressure in the point $A^{/}$ in liquid at interface of two media. If this condition was not observed there would be the difference of pressure between points *A* and $A^{/}$, and the interface of two media would begin to move. Therefore it is possible to write down:

$$P_{A^{/}} = P_A . \qquad (7.3)$$

Hence:

$$P_j = P_i + P_r , \qquad (7.4)$$

where $P_j = P_{A^{/}}$ there is amplitude of sound pressure in the wave penetrated in the liquid medium, P_i - amplitude of sound pressure in the falling wave, and P_r - amplitude of sound pressure in the reflected wave. Sound pressures in the air are sum, since these not vector sizes. Actually the pressures are power characteristics of a wave.

In air due to addition of the falling and reflected waves there is a standing wave. The node of the standing wave is on the interface of two media. On fig. 7.6 curves of displacement of particles in wave *S* are shown. Speeds of oscillations of mediums particles in points *A* and $A^{/}$ from the condition of medium continuity are equal.

Hence:

$$V_{A^{/}} = V_A . \qquad (7.5)$$

As speeds of oscillations of air particles the falling and reflected waves are directed opposite each other:

$$V_j = V_i - V_r . \qquad (7.6)$$

Taking into account interrelation between speeds of the particles oscillations of medium and sound pressure $V = \frac{P}{\rho c}$ and entering the ratio of acoustic resistances of two mediums $\alpha = \frac{\rho_1 c_1}{\rho_2 c_2}$ from (7.6) we shall find:

$$\alpha P_j = P_i - P_r . \qquad (7.7)$$

Solving the system (7.4), (7.7), we find:

$$P_j = \frac{2}{1+\alpha} P_i \quad \text{and} \quad P_r = \frac{1-\alpha}{1+\alpha} P_i . \qquad (7.8)$$

Interrelation between intensity of the sound I and amplitude of the sound pressure P looks like as $I = \frac{P^2}{2\rho c}$. Hence:

$$I_i = \frac{P_i^2}{2\rho_1 c_1}; \qquad I_r = \frac{P_r^2}{2\rho_1 c_1} \qquad I_j = \frac{P_j^2}{2\rho_2 c_2}. \qquad (7.9)$$

The ratio of intensity of the sound penetrated into the medium to intensity of the sound falling on the medium refers to as factor of penetration of the sound wave:

$$\beta = \frac{I_j}{I_i} = \alpha\left(\frac{P_j}{P_i}\right)^2 = \frac{4\alpha}{(1+\alpha)^2}. \qquad (7.10)$$

The received formula for factor of penetration of the sound wave refers to as Rayleigh's formula.

The ratio of intensity of the sound reflected from the interface of two media to intensity of the sound falling on the medium refers to as factor of reflection of the sound wave:

$$R = \frac{I_r}{I_i} = \left(\frac{P_r}{P_i}\right)^2 = \left(\frac{1-\alpha}{1+\alpha}\right)^2. \qquad (7.11)$$

It is possible to see that $\beta + K = 1$.

If acoustic resistances of mediums are equal among themselves, i.e. $\alpha = 1$ from the Rayleigh's formula (7.10) follows that factor of the sound wave penetration $\beta = 1$, and factor of the reflection $R = 0$. It means that reflection of the sound wave is absent. If there is very big distinction in acoustic resistances of mediums, i.e. $\alpha \to 0$ from the Rayleigh's formula follows that the factor of penetration of the sound wave $\beta \to 0$, and $R \to 1$. It means that the sound does not penetrated in more dense medium, and is completely reflected from the interface of two media.

The ratio of the acoustic resistances of air and liquid mediums in the internal ear is $\alpha = 0.00028$. From the Rayleigh's formula we find factor of penetration $\beta = 0.00122 = 0.122\%$, i.e. practically the energy of the sound cannot penetrate in the liquid medium.

Evolution could not allow direct transition of the sound from air in liquid medium of the internal ear. Therefore the middle ear playing a role of the acoustic resistances coordinator was created.

The essence of the acoustic resistances coordination of air in external auditory canal and the liquid medium of the internal ear will be that wave sound process in air is replaced with oscillatory process of the lever mechanism of ear bonds in the middle ear which in his turn passes in wave process in the liquid medium of the internal ear. Oscillations of the liquid medium in the internal ear are carried out lever-mechanical procedure instead there are due to fall the sound on the interface of two media.

Direct transition of the sound from air in the solid or liquid medium in the acoustic analyzer actually is absent. The eardrum very thin, its thickness $\sim 100\ \mu m$, the mass of it, and, hence and inertia are insignificant. Therefore it is impossible to account, the sound falls from air in the solid medium of the eardrum. The eardrum there is oscillated as a unit (in one phase) and reflection of the sound wave from it is insignificant. Therefore energy of the sound wave almost completely is transferred to malleus and further to the lever mechanism of the middle ear.

The stapes plays a role of the handle attached to membrane of the oval window. Moving this handle the lever system ear bonds transfers energy of sound oscillations in the liquid medium of the internal ear with very small losses.

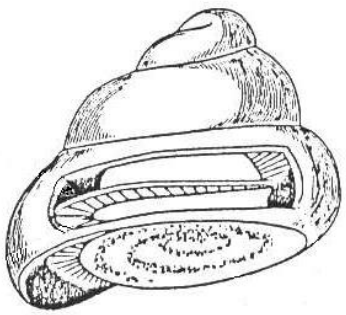

Fig. 7.7.

Let's note that the inflammation of the middle ear (otitis) results in destruction by purulent process of ear bonds and as consequence to development of hearing loss. Destruction of ear bonds lowers hearing in 1000 - 10000 (not in 26) ones that specifies failure of coordination of acoustic resistance in the middle ear.

At the big intensity of the sound falling on the eardrum there is increased reflex contraction of two muscles regulating movement of ear bonds. One muscle at contraction stretching inside of the tympanic cavity the malleus increases of the eardrum tension. The eardrum starts to oscillate

with smaller amplitude. Therefore transfer of oscillations energy from the eardrum to the oval window of internal ear is reduced. Other muscle operates similarly with the first on stapes tensing the membrane of oval window that reduces amplitude of oscillations of this membrane. The reflex tension of muscles can lower transfer of a sound intensity in the middle ear on $30-40\,dB$.

7.3. Internal ear

The internal ear will consist from sound-perceiving system which taking place inside a cochlea 5, fig. 7.2, and the vestibular apparatus 7 is organ of the balance representing three mutual perpendicular semicircular canals. We pay the basic attention to functioning of the cochlea.

The cochlea, fig. 7.7, represents a conical bone spiral approximately 2.5 turns. On fig. 7.8 the internal structure of the cochlea is shown, and for convenience of the analysis the cochlea is shown in the developed kind. Besides there is shown the section of the cochlea, fig. 7.9.

In figures are marked: 1 – cochlear duct or scala media, 2 - scala vestibuli (channel), 3 – scala tympani (channel), 4 - the oval window tightened by a membrane, 5 - the round window tightened by a membrane (its part is visible only), 6 - helicotrema (aperture), 7 – basilar membrane, see also fig. 7.10, 8 – vestibular membrane (membrane of Reissner), 9 – Corti organ, 10 – receptor (hair) cell, see also fig. 7.10, 11 - tectorial membrane, 12 - Corti tunnel filled cortilymph and separated from endolymph by meshed or reticular plate 13, shown on fig. 7.10, 14 - cochlear nerve. The meshed (reticular) plate 13 and basilar a membrane 7 are rigidly connected among themselves so-called by columns of Corti 21, fig. 7.10. These three last rigid structures are original skeleton of Corti organ.

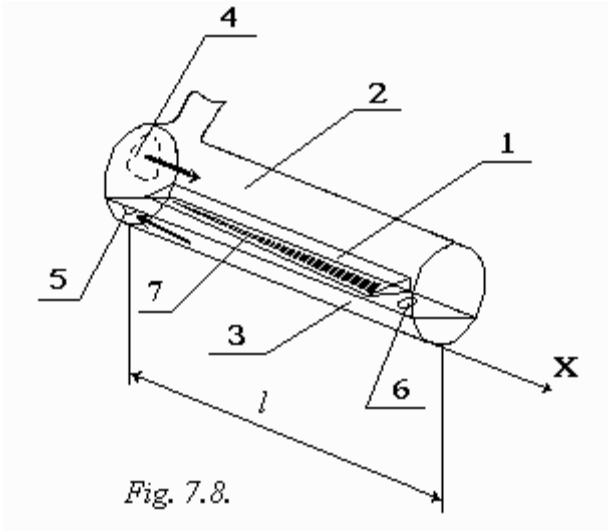

Fig. 7.8.

Length of the basilar membranes of the man is $l \approx 32\,mm$. The scala vestibuli and the scala tympani are connected by the aperture – helicotrema 6 and filled with a liquid - perilymph. Cochlear duct 1 is filled with the endolymph there are on the one side separated from the scala vestibuli 2 by vestibular membrane 8, and on the other side from the scala tympani 3 by the basilar membrane 7.

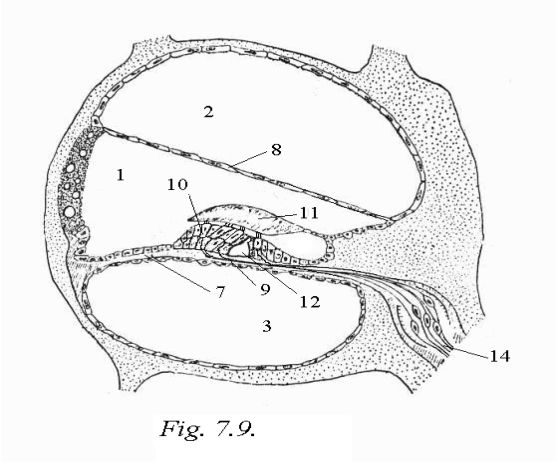

Fig. 7.9.

Endolymph and perilymph have various concentration of ions Na^+, K^+, etc. Perilymph on the ionic structure it is similar to an intercellular liquid and has the big concentration of ions Na^+ and rather small concentration of ions K^+, and endolymph it is similar to cytoplasm. It has small concentration of ions Na^+ and the big concentration of ions K^+.

The basis of the basilar membrane 7 (at the oval window) has width about $0.04\,mm$ (other part of cross section of the cochlea the spiral bone plate occupies) and at helicotrema 6 the width basilar membrane has about $0.5\,mm$.

On the basilar membrane it is located Corti organ - the analyzer of the sound spectrum. Above Corti organ 9 the massive tectorial membrane 11 is located. The somas of the hair cells 10 (see also fig. 7.10) of the Corti organ are submerged in cortilymph which on the ionic structure is similar on perilymph and has with it a free exchange of ions Na^+ and K^+. Cortilymph as well as perilymph has the big concentration of ions Na^+ and small concentration of ions K^+ but in cortilymph there is also plenty of ions Ca^{2+}. The hairs are submerged in endolymph. If hairs cells were completely submerged in endolymph they could not generate action potential since there would be no necessary concentration gradients on their membranes.

The physics of work of Corti organ till now is not absolutely clear.

The first theory of perception of a sound has offered by Helmholtz in 1863. He assumed that waves from the oval window cause oscillations of the perilymph column in the scala vestibuli. Through the helicotrema these oscillations are transferred in the scala tympani. The membrane of the round window is necessary for opportunity of existence of the oscillations since otherwise because of incompressibility of liquids in the bone channel of the cochlea the oscillations cannot arise.

Basilar membrane Helmholtz represented as series of the cross-section tense strings (on type harp) each of which resounds on the certain frequency of a sound. Therefore this theory refers to as resonator's theory. The high sound frequencies believed Helmholtz are perceived by the strings located in area of the oval window, and low frequencies - strings in area of the helicotrema.

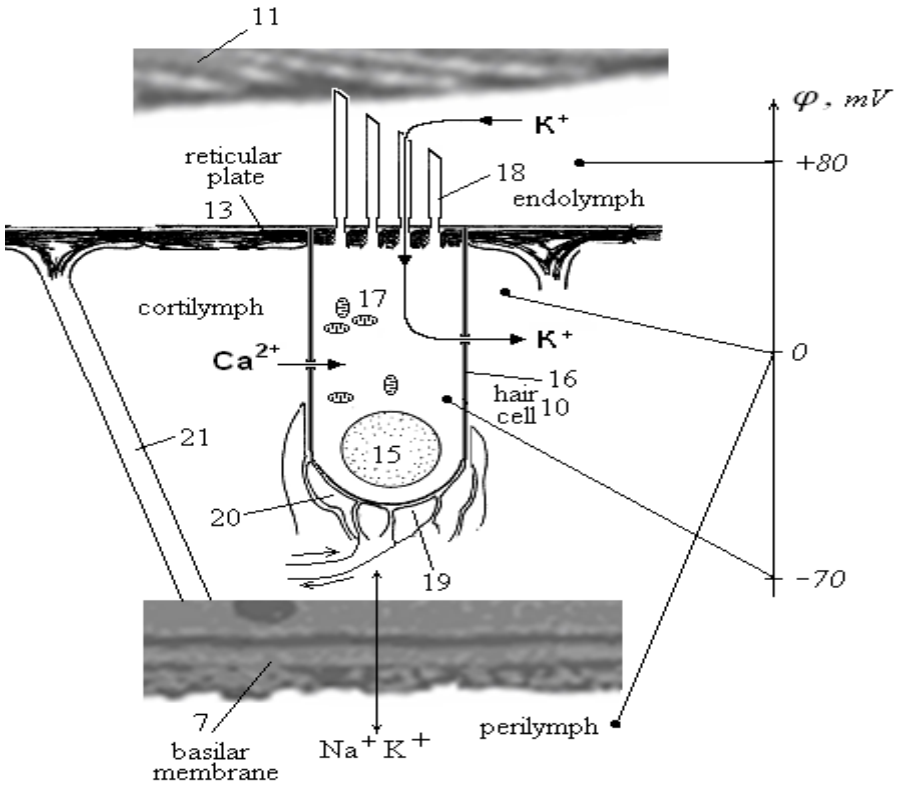

Fig. 7.10.

A series of positions of Helmholtz theory was not correct.

In spite of the fact that the assumption of the various frequencies perception by different sites of Corti organ on basilar membrane has was correct. As a result of histological-morphological researches it was found out that the membrane is not tense also strings on it is not present. The Hungarian scientist the Nobel Prize laureate Bekesy has shown it in 1960.

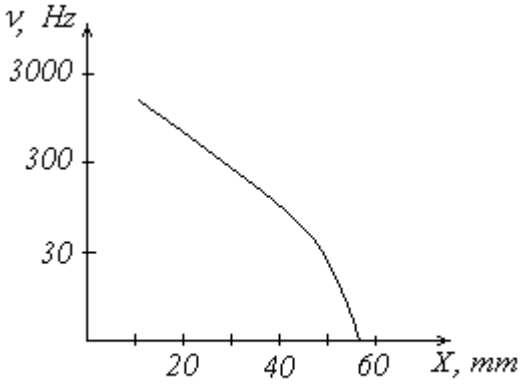

Fig. 7.11.

In experiences on a cochlea of the elephant he has established that dependence of coordinate *X* (*X* is distance from the oval window, fig. 7.8) of the cross displacement maximum of basilar membranes on frequency as corresponds to assumption of Helmholtz. Higher sound frequencies are perceived in area of the oval window, and low frequencies in area of helicotrema. One of experimental curves of Bekesy is shown on fig. 7.11.

Now it is considered that a sound through system ear bonds causes oscillation of the oval window membrane that actuates the perilylymph. Wave movement of perilymph in the scala vestibuli is transferred through the helicotrema to perilymph in scala tympani. There are cross oscillations of basilar membrane. These oscillations shown on fig. 7.10 by arrows excited the receptor cells due to deformation of its hairs in the various sites of Corti organ corresponding to harmonics of the analyzed complex sound wave.

The distance from round window *X* in scala tympani on which the maximal (resonant) amplitude of oscillations of basilar membrane is observed apparently is determined by the elementary mass dm of the membrane site. This mass gradually grows from the round window to the helicotrema due to increase in width of basilar membrane (approximately in 5 ones) there are between two bone formations: the bone spiral plate and the wall of cochlea, i.e. $dm \sim X$. Cyclic frequency of resonant oscillations $\omega = \sqrt{\frac{dk}{dm}}$ (dk it is elasticity of the basilar membrane elementary site in mass dm) is reversely proportional to elementary mass dm and hence is reversely proportional to distance *X* from the round window.

7.3.1. Electrodynamics of the internal ear

On fig. 7.10 the hair cell which soma is fixed by the top part in the reticular plate is shown. In cytoplasm of the cell there are all usual organelles necessary for functioning of the cells: the nucleus 15, mitochondrias 17, etc., and also is the big concentration of ions potassium K^+. The membrane of the cell in rest penetrable for ions K^+ also is impenetrable for ions Ca^{2+} which concentration inside cell is insignificant.

The cell is surrounded with a plasmatic membrane 16 on which internal surface is present potassium resting potential (RP) $\sim 70\, mV$ relative of cortilymph (or perilymph; between cortilymph and perilymph there is no potential difference [15]; perylumph has about the same ionic structure on Na^+ and K^+ as well as cortilymph) and $\sim 150\, mV$ relative of endolymph. Endolymph it is charged positively relative of perilymph (or cortilymph) up to potential $+80\, mV$ - endocochlear potential.

The scale of potentials in the internal ear is shown on fig. 7.10 in the right side. Feature of the hair cells is existence of hair 18 (one kinocilium and sets of stereocilias). Kinocilium longer are in part submerged in the tectorial membrane 11.

Excitation of the receptor cells at development of the wave process on the basilar membrane 7 has the deformation character and is carried out due to a bend of these cells hairs at oscillatory movement of basilar membrane 7 (the direction is shown by arrows) together with the reticular plate 13 concerning the tectorial membrane 11. To relative movement there are promotes an inertia of the massive tectorial membrane 11. Deformation of the receptors cells hairs results in opening albuminous transductive channels in the end of hairs. It causes movement of ions K^+ from the place of their high concentration (in endolymph) inside the hair cells. Concentration of ions K^+ in endolymph exceeds those in cytoplasm of hair cells. Receiption in the cell

cytoplasm of additional ions K^+ reduces endocellular negative potential up to the depolarizing potential *PDep* that results in opening voltage-gates calcium channels. There are begins of the depolarization of the hair cells membrane owing to the current of ions Ca^{2+} through opened calcium channels. On the membrane there is the action potential (AP). As it is usual the potassium channels open with some delay and ions K^+ leave the hair cells in the cortilymph (with low concentration of ions K^+) repolarize cellular membrane.

The passive current of ions K^+ and Ca^{2+} is shown on fig. 7.10. Thus the hair cell has two-ionic (potassium - calcium) system of the action potential (AP) formation that distinguishes it, for example, from a nervous cell, paragraph 2.1.1. Then ionic pumps in the cell membrane due to active transport restore initial concentration of ions K^+ and Ca^{2+} in the hair cell. Biopotentials from the excited cells (so-called afferent impulses) through synaptic contacts 19 propagate on the cochlear nerve in a brain where the information received at sound influence on the acoustic analyzer is analyzed. To the hair cells move also signals through contacts 20 (so-called efferent impulses) from CNS which apparently reduce time of the mechanical trace oscillations of cellular structures after their excitation. Efferent impulses can participate also in adaptable processes of the acoustic analyzer reducing excitability of the hair cells.

As already it was specified earlier now there is no strict biophysical theory in the general use of the spectral analysis of a sound the internal ear. We shall specify only some ambiguities in the theory of functioning of the acoustic analyzer.

1. There are indications that the amplitude of the depolarizing potential of the hair cells (receptive potential) in reply to deformation of hairs is proportional to intensity of sound influence and varies in the range $+10 \div +24\ mV$. Hence it is used both frequency and analog transfer of the information signal. Advantage and the reason of it up to the end it is not clear. We shall notice that in the visual analyzer analog transfer of the information signal is used, see paragraph 8.5.2.

2. The role of Reissner's membrane in realization of the spectral analysis of a sound is not clear. Whether the role of Reissner's membrane only is limited to electrodynamical aspects of functioning of the internal ear?

7.4. The spectral analysis of sound in the acoustic analyzer

Influence of sound waves on the acoustic analyzer causes the compelled oscillatory process in structures of the internal ear.

The internal ear receives the sound information as a sound wave packet, analyzes, processes it, and transfers in a brain as electric (nervous) impulses.

7.4.1. The equations of perilymph oscillations in the scala tympani

We research character of the compelled oscillatory process in perilymph taking place in the scala timpani 3, fig. 7.8.

Viscosity of a liquid we shall not take into account. Its influence we shall note below. The equation of an impulse for the compelled oscillatory process looks like:

$$\frac{\partial V}{\partial t} + V\frac{\partial V}{\partial X} + \frac{1}{\rho}\frac{\partial (PS)}{S\partial X} + f_m \sin(\omega t + \varphi) = 0, \qquad (7.12)$$

where V there is oscillatory speed of the liquid, X - the longitudinal coordinate counted from the round window 5, fig. 7.8, t - time, ρ - perilymph density, P - pressure in perilymph, S - cross section of the scala tympani, f_m - amplitude of the specific compelling force working on perilymph, arising as a result of sound influence, ω - cyclic frequency of the compelled of the perilymph oscillations, φ - initial phase of compelling force.

Change of cross section S of the scala tympani can occur as due to elasticity of the basilar membrane 7 at its cross oscillations, and due to expansion of the membrane to helicotrema 6. The equation of the impulse (7.12) is written down with account of the size S change opportunity. The account of elastic properties of scala tympani one wall – basilar membrane - we shall carry out according to a method submitted in [61].

The compelled oscillations of a liquid in the rigid tube have been investigated, for example, in [62]. However in absolutely rigid tube there is no own frequency of system oscillations (it is equal to infinity),

therefore the resonant phenomena in a stream are not found out. In [62] the harmonious law of the pressure gradient change causing compelled oscillations $-\frac{\partial P}{\partial X}=A\cos(\omega t)$ is offered, where *A* - amplitude of the pressure gradient change.

Substituting in the equation of the impulse (7.12) Hooke's law as $P=-D\frac{\partial(uS)}{S\partial X}$, where *D* is elasticity of basilar membrane, *u* - oscillatory displacement of a liquid in the scala tympani, we receive:

$$-f_m\sin(\omega t+\varphi)+\frac{D}{\rho}\frac{\partial^2(uS)}{S\partial X^2}=\left(\frac{\partial V}{\partial t}+V\frac{\partial V}{\partial X}\right). \qquad (7.13)$$

In case of the small amplitude oscillations the nonlinear convective term in the right part (7.13) it is possible to neglect [51].

Using $V=du/dt$, and also speed of the pressure wave is $c=\sqrt{\frac{D}{\rho}}$ we shall receive:

$$-f_m S\sin\omega t+c^2\frac{\partial^2(uS)}{\partial X^2}=S\frac{\partial^2 u}{\partial t^2}. \qquad (7.14)$$

The two-parametrical wave equation is received. The second equation connecting unknown values *u* and *S* it is a continuity equation:

$$\frac{\partial S}{\partial t}+\frac{\partial(VS)}{\partial X}=0. \qquad (7.15)$$

Let's note that change of the area and flow $Q=VS$ occurs only due to oscillations of speed *V* since the directed movement of the liquid is not present.

We'll find the solving of system (7.14) and (7.15) by method of separation variables of Fourier. Let's take:

$$\begin{aligned} &u=F_1(X)\cdot\Phi_1(t); \qquad S=F_2(X)\cdot\Phi_2(t);\\ &uS=F_1(X)\cdot F_2(X)\cdot\Phi_1(t)\cdot\Phi_2(t)=F(X)\cdot\Phi(t), \end{aligned} \qquad (7.16)$$

where it is designated $F_1(X)\cdot F_2(X)=F(X)$ and $\Phi_1(t)\cdot\Phi_2(t)=\Phi(t)$.

Let's substitute (7.16) in (7.14) and having reduced on $\Phi_2(t)$ we shall separate variables:

$$\frac{1}{\Phi_1}\frac{d^2\Phi_1}{dt^2}=c^2\frac{1}{F}\frac{d^2F}{dX^2}-\frac{f_m}{F_1\Phi_1}\sin(\omega t+\varphi). \qquad (7.17)$$

Let's assume that function Φ_1 varies in time with frequency ω of compelled oscillations under the law:

$$\Phi_1=A_0\sin(\omega t+\varphi). \qquad (7.18)$$

Further A_i and φ_i there are constants $i=0,\ 1,\ 2$.

Substituting (7.18) in (7.17) we shall find:

$$\frac{1}{\Phi_1}\frac{d^2\Phi_1}{dt^2}=c^2\frac{1}{F}\frac{d^2F}{dX^2}-\frac{f_m}{A_0F_1}=-\omega^2. \qquad (7.19)$$

Carrying out the transformations with the account (7.16) we shall receive:

$$\frac{d^2F}{dX^2}+\frac{\omega^2}{c^2}F=\frac{f_m}{A_0c^2}\frac{F}{F_1}=\frac{f_m}{A_0c^2}F_2\,. \qquad (7.20)$$

Functions $\Phi_2(t)$, $F_1(X)$, $F_2(X)$ we shall find from the equation of continuity (7.15). Using (7.16) and taking into account that speed $V=du/dt$ we have:

$$F_2\frac{d\Phi_2}{dt}+\Phi_2\frac{d\Phi_1}{dt}\frac{dF}{dX}=0\,. \qquad (7.21)$$

Hence, the equation of the continuity (7.21) expands to two equations:

$$-\frac{1}{F_2}\frac{dF}{dX}=\frac{1}{\Phi_2}\frac{\partial\Phi_2}{\partial\Phi_1}=-\Theta\,, \qquad (7.22)$$

where Θ there is constant. Solutions of the equations (7.22) look like:

$$\Phi_2=A_2\exp\left(-\Theta\Phi_1\right), \qquad (7.23)$$

$$F_2=\frac{1}{\Theta}\frac{dF}{dX}\,. \qquad (7.24)$$

Substituting (7.24) in (7.20) we have the linear uniformity equation:

$$\frac{d^2F}{dX^2}-2\beta\frac{dF}{dX}+\frac{\omega^2}{c^2}F=0\,, \qquad (7.25)$$

where it is designated $2\beta=\dfrac{f_m}{A_0c^2\Theta}$.

The solution of the equation (7.25) looks like:

$$F(X)=A_1\exp(\beta X)\sin\left(\frac{\omega}{c}X+\varphi_1\right). \qquad (7.26)$$

Using (7.24) we shall find:

$$F_2=\frac{A_1\exp(\beta X)}{\Theta}\left[\beta\sin\left(\frac{\omega}{c}X+\varphi_1\right)+\frac{\omega}{c}\cos\left(\frac{\omega}{c}X+\varphi_1\right)\right]. \qquad (7.27)$$

Let's designate $\tan\delta=\dfrac{\omega}{c\beta}$. Transforming (7.27) we have:

$$F_2=\frac{A_1\exp(\beta X)\beta}{\Theta\cos\delta}\left[\sin\left(\frac{\omega}{c}X+\varphi_1+\delta\right)\right]. \qquad (7.28)$$

Function F_1 we shall find from condition, see (7.16):

$$F_1 = \frac{F}{F_2} = \frac{\Theta \cos\delta \sin\left(\frac{\omega}{c} X + \varphi_1\right)}{\beta \sin\left(\frac{\omega}{c} X + \varphi_1 + \delta\right)}. \qquad (7.29)$$

The system of functions (7.18), (7.23), (7.28) and (7.29) allows receive the solution of system of the equations (7.14), (7.15):

$$S = F_2 \Phi_2 = \frac{A_1 A_2 \exp(\beta X)\beta}{\Theta \cos\delta} \left|\sin\left(\frac{\omega}{c} X + \varphi_1 + \delta\right)\right| \exp(-\Theta A_0 \sin(\omega t + \varphi)), \quad (7.30)$$

$$u = F_1 \Phi_1 = \frac{A_0 \Theta \cos\delta}{\beta} \left|\frac{\sin\left(\frac{\omega}{c} X + \varphi_1\right)}{\sin\left(\frac{\omega}{c} X + \varphi_1 + \delta\right)}\right| \cdot \sin(\omega t + \varphi). \qquad (7.31)$$

At writing (7.30) and (7.31), i.e. solving of the equations (7.14), (7.15), it is necessary to take into account, that these equations have weak nonlinearity. They are linear concerning each of parameters, but they include multiplication of these parameters. This circumstance imposes some restrictions on result of the solving of system (7.14), (7.15). The area of the scala tympani is the value positive therefore in (7.30) it is necessary to use a sign on absolute size. The absolute size according to the continuity equation (7.15) needs to be used and in the equation for displacement (7.31).

Using (7.31) we shall find speed of a liquid in the scala tympani and pressure in it:

$$V = \frac{\partial u}{\partial t} = \frac{A_0 \Theta \omega \cos\delta}{\beta} \left|\frac{\sin\left(\frac{\omega}{c} X + \varphi_1\right)}{\sin\left(\frac{\omega}{c} X + \varphi_1 + \delta\right)}\right| \cdot \cos(\omega t + \varphi). \qquad (7.32)$$

Pressure we shall define proceeding from the ratio $P = -D\frac{\partial(uS)}{S\partial X}$ with use (7.16) and (7.24):

$$P = -D\frac{\partial(uS)}{S\partial X} = -D\frac{\partial(F\Phi)}{F_2\Phi_2\partial X} = -D\frac{\Phi\partial F}{F_2\Phi_2\partial X} = -D\Theta\Phi_1,$$

$$P = -D\Theta A_0 \sin(\omega t + \varphi). \qquad (7.33)$$

As one would expect the gradient of pressure (as approximation of an ideal liquid is used) is equal to zero - pressure does not depend on *X* coordinate. The sign minus in (7.33) specifies to the Hooke's law $P = -D\frac{\partial(uS)}{S\partial X}$ includes not pressure, and the distributed elastic returning force from the wall of basilar membrane and membrane of the round window.

If to accept the maximal relative deformation of basilar membrane $\varepsilon_{\max}$ and to take into account that peak value of pressure oscillations $P_{\max} = -D\varepsilon_{\max}$ from (7.33) follows $\varepsilon_{\max} = \Theta A_0$, and the size $2\beta = \frac{f_m}{\varepsilon_{\max} c^2}$ characterizes the specific compelling force acting on perilymph.

At calculation under formulas (7.30) - (7.33) it is possible to use the following boundary conditions $u = u_{01}\sin(\omega t + \varphi)$, $V = u_{01}\omega\cos(\omega t + \varphi) = V_{01}\cos(\omega t + \varphi)$ where u_{01} is the amplitude value of oscillations of the round window 5, fig. 7.8, ω is frequency of the compelled oscillations of the round window. The area of cross section of the scala tympani is $S = S_{01}$ at $X = 0$. At $X = l$ the area is $S = S_{02}$. Besides the additional boundary condition is necessary: at $X \le 0$ and $X \ge l$ relative deformation ε of the basilar membrane 7 including its maximal value $\varepsilon_{\max}$ there are equal to zero.

7.4.2. Own frequency of oscillations of basilar membrane

Let's carry out the analysis of the basilar membrane oscillations and we shall determine its resonant frequencies.

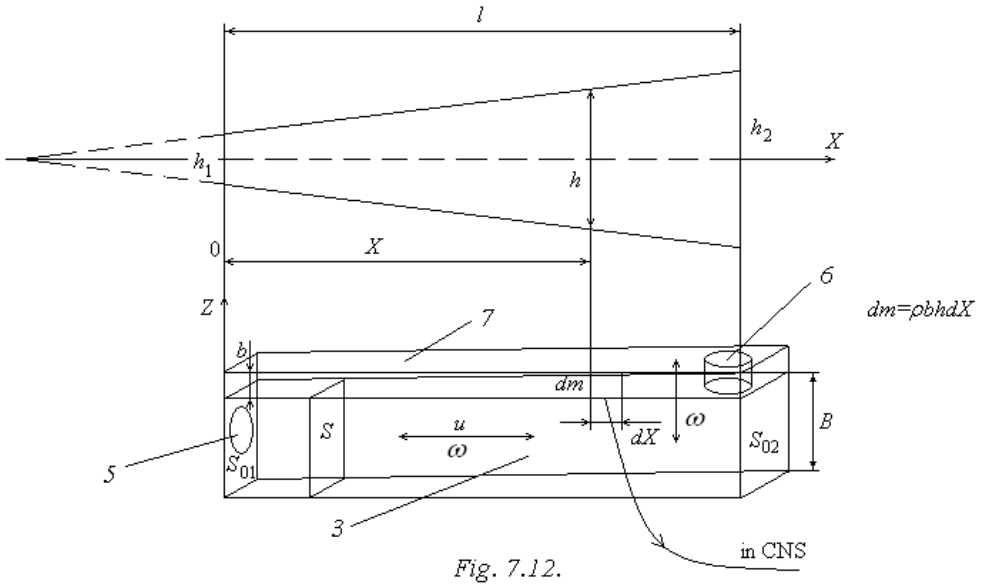

Fig. 7.12.

Let's present the calculate scheme for the analysis of the basilar membrane oscillations as shown in fig. 7.12. Thus digits on fig. 7.12 designate the same structures of the internal ear as in the previous figures.

Let's find as own frequency ω_0 of the basilar membrane oscillations varies depending on its length *X*. 2-nd law of Newton for mass *dm* looks like:

$$adm = df + dF_m \sin(\omega t + \varphi), \qquad (7.34)$$

where df there is the elastic force acting on the site dX in mass dm, *a* - acceleration of mass dm. The second addend in the right part reflects the compelled character of the mass dm oscillations, dF_m - amplitude of the force acting on this mass.

Analyzing the formula (7.30) we assume that linearly varying parameter *Y* in a cross direction, i.e. in the direction of axis *Z*, fig. 7.12, looks like:

$$Y = b\ln\left|\frac{A}{S}\right| = \varepsilon_{\max} b\sin(\omega t + \varphi), \qquad (7.35)$$

where *A* there is amplitude of the scala tympani area oscillations. Thickness of a membrane *b* is used as scaling parameter. We shall note that oscillations of the area *S* have nonlinear character that as already it was specified earlier results in necessity of use of the sign on absolute size. Fluctuations of the area are shifted on the phase relatively of the parameter *Y* oscillations. At $S = A$ there is parameter $Y = 0$, at $S \to 0$ the parameter $Y \to \infty$ that is connected in this case to approximation of zero factor of attenuation.

Transforming (7.34) we shall find:

$$\rho bh(X)dX\frac{d^2Y}{dt^2}=df+dF_m\sin(\omega t+\varphi)=-Ydk+dF_m\sin(\omega t+\varphi),\quad (7.36)$$

where ρ there is density of basilar membrane, $h(X)$ - its width, the mass $dm=\rho bh(X)dX$. The Hooke's law for membrane is used as $df=-Ydk$.

Transforming (7.36) we shall find:

$$\frac{d^2Y}{dt^2}+\frac{k_X}{\rho bh(X)}Y=\frac{dF_m}{dm}\sin(\omega t+\varphi)=f_1\sin(\omega t+\varphi),\quad (7.37)$$

where $f_1=\frac{dF_m}{dm}$ there is specific amplitude of the compelling force acting on the element of mass dm, $k_X=\frac{dk}{dX}$ - the factor describing specific elasticity on a deflection on length of the membrane.

Let's copy the equation (7.37) as:

$$\frac{d^2Y}{dt^2}+\omega_0{}^2Y=f_1\sin(\omega t+\varphi),\quad (7.38)$$

where the square of own frequency of the basilar membrane oscillations is equal:

$$\omega_0{}^2=\frac{k_X}{\rho bh(X)}.\quad (7.39)$$

The solution of the equation of the compelled oscillations (7.38) looks like:

$$Y=A_Y\sin(\omega t+\varphi).\quad (7.40)$$

Substituting (7.40) in (7.38) and comparing (7.40) with (7.35), we shall find amplitude of the compelled oscillations of size *Y*:

$$A_Y=\varepsilon_{\max}b=\frac{f_1}{\left|\omega^2-\omega_0{}^2\right|}.\quad (7.41)$$

Hence, using (7.40) we shall find:

$$Y=b\ln\left|\frac{A}{S}\right|=\frac{f_1}{\left|\omega^2-\omega_0{}^2\right|}\sin(\omega t+\varphi).\quad (7.42)$$

Let's assume, that the width of the basilar membrane changes linearly:

$$h(X)=a_1X+b_1,\quad (7.43)$$

where a_1 and b_1 there are constants. Initial and final width of a membrane are equal $h_1=b_1$ and $h_2=a_1l+h_1$.

Hence, the law of change of the basilar membrane width is:

$$h(X)=(h_2-h_1)\frac{X}{l}+h_1.\quad (7.44)$$

Substituting (7.44) in (7.39) we shall find:

$$\omega_0{}^2 = \frac{k_X}{\rho b\left(\left(h_2 - h_1\right)\frac{X}{l} + h_1\right)}. \qquad (7.45)$$

Let maximal own frequency $\omega_{\max}$ is perceived at the round window, i.e. for $X = 0$, hence $\omega_{\max} = \sqrt{\frac{k_{X\max}}{\rho b h_1}}$. At helicotrema for $X = l$ the minimal frequency $\omega_{\min} = \sqrt{\frac{k_{X\min}}{\rho b h_2}}$ is perceived.

Let's assume that the size k_X varies linearly along of the basilar membrane. Hence:

$$k_X = \left(k_{X\min} - k_{X\max}\right)\frac{X}{l} + k_{X\max}. \qquad (7.46)$$

Thus, from (7.45) follows:

$$\omega_0 = \omega_{\max}\sqrt{\frac{\left(\left(\frac{\omega_{\min}}{\omega_{\max}}\right)^2 h_{21} - 1\right)\frac{X}{l} + 1}{\left(\left(h_{21} - 1\right)\frac{X}{l} + 1\right)}}, \qquad (7.47)$$

where is $h_{21} = \frac{h_2}{h_1}$.

On fig. 7.13 dependence own relative (concerning the maximal value) frequencies of the basilar membrane oscillations from longitudinal coordinate in relative units $\frac{\omega_0}{\omega_{\max}} = f\left(\frac{X}{l}\right)$ is shown. At calculation it is accepted [63]: $h_{21} = 5$, $c = 1700\frac{m}{s}$ - speed of a sound in the basilar membrane, $l = 0{,}035\,mm$ - length of the basilar membrane $\omega_{\min} = 2\pi\nu_{\min}\frac{l}{c} = 0.00207$, $\omega_{\max} = 2\pi\nu_{\max}\frac{l}{c} = 2.587$ - dimensionless minimal and maximal frequencies of the basilar membrane oscillations $\nu_{\min} = 16\,Hz$, $\nu_{\max} = 20000\,Hz$ - boundary frequencies of perception of a sound.

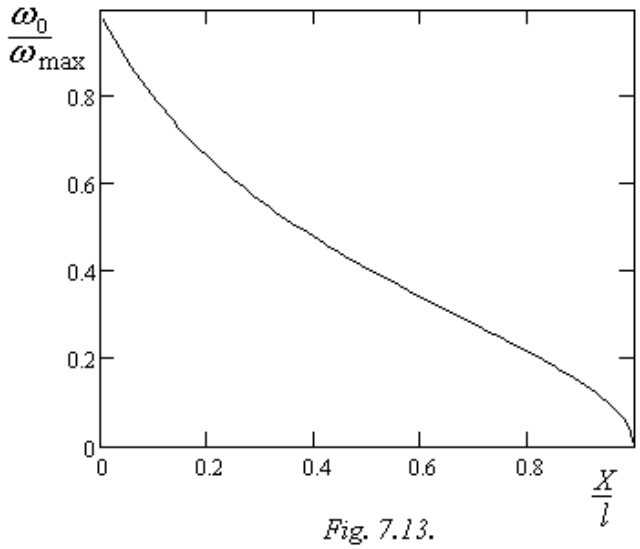

Fig. 7.13.

The received dependence of frequency of the basilar membrane resonance on its longitudinal coordinate is close to results of Bekesy [64, 65], see also fig. 7.11. It specifies validity that frequency of resonance is coordinated by increase in elementary masses of basilar membrane due to its expansion from oval (or round) windows to the helicotrma.

7.4.3. The spectral analysis of sound wave packet in the internal ear

Scanning by the sound wave package of the cochlea of the internal ear causes the resonant answer to corresponding sites of the basilar membrane. We shall examine influence on the cochlea a sound of any one frequency ω.

Let's analyze solutions of the hydrodynamics equations (7.30) - (7.33) on the basis of which the spectral analysis in the acoustic analyzer we shall carry out. Amplitude values of parameters of oscillatory process: the areas of cross section of the scala tympani and longitudinal displacement of the perilymph in it are equal:

$$S_A = \frac{A_1 A_2 \beta}{\Theta \cos\delta}\left|\sin\left(\frac{\omega}{c}X + \varphi_1 + \delta\right)\right|\exp\left(\beta X - \varepsilon_{\max}\right), \qquad (7.48)$$

$$u_A = \frac{\varepsilon_{\max}\cos\delta}{\beta}\left|\frac{\sin\left(\frac{\omega}{c}X + \varphi_1\right)}{\sin\left(\frac{\omega}{c}X + \varphi_1 + \delta\right)}\right|, \qquad (7.49)$$

Using boundary conditions for the cross section area of the scala tympani (7.48) and taking into account that in points $X = 0$ and $X = l$ the size $\varepsilon_{\max} = 0$ we find:

$$S_{01} = \frac{A_1 A_2 \beta}{\Theta \cos\delta}\left|\sin\left(\varphi_1 + \delta\right)\right|. \qquad (7.50)$$

Dividing (7.48) on (7.50) we have:

$$\frac{S_A}{S_{01}} = \exp\left(\beta X - \varepsilon_{\max}\right)\left|\frac{\sin\left(\frac{\omega}{c}X + \varphi_1 + \delta\right)}{\sin\left(\varphi_1 + \delta\right)}\right|. \qquad (7.51)$$

For cross section of the scala tympani in area of helicotrema 6, fig. 7.12, i.e. for $X = l$ we find:

$$\frac{S_{02}}{S_{01}} = \exp\left(\beta l\right)\left|\frac{\sin\left(\frac{\omega}{c}l + \varphi_1 + \delta\right)}{\sin\left(\varphi_1 + \delta\right)}\right| = \exp\left(\beta l\right)\left|\sin\left(\frac{\omega}{c}l\right)\cot\left(\varphi_1 + \delta\right) + \cos\left(\frac{\omega}{c}l\right)\right| \qquad (7.52)$$

Hence:

$$\cot\left(\varphi_1 + \delta\right) = \frac{\frac{S_{02}}{S_{01}} - \exp\left(\beta l\right)\cos\left(\frac{\omega}{c}l\right)}{\exp\left(\beta l\right)\sin\left(\frac{\omega}{c}l\right)}. \qquad (7.53)$$

Substituting (7.53) in (7.51) we have:

$$\frac{S_A}{S_{01}} = \exp\left(-\beta\left(l - X\right) - \varepsilon_{\max}\right)\left|\frac{\frac{S_{02}}{S_{01}}\sin\left(\frac{\omega}{c}X\right) + \exp\left(\beta l\right)\sin\left(\frac{\omega}{c}\left(l - X\right)\right)}{\sin\left(\frac{\omega}{c}l\right)}\right|. \qquad (7.54)$$

Let $S_{01} = Bh_1$ and $S_{02} = Bh_2$ where *B* is the vertical size of the scala tympani 3, fig. 7.12. Hence, with the account (7.41) and $h_{21} = \frac{h_2}{h_1}$ we shall find:

$$\frac{S_A}{S_{01}} = \exp\left(-\beta\left(l - X\right) - \frac{f_1}{\left|\omega^2 - {\omega_0}^2\right|}\right)\left|\frac{h_{21}\sin\left(\frac{\omega}{c}X\right) + \exp\left(\beta l\right)\sin\left(\frac{\omega}{c}\left(l - X\right)\right)}{\sin\left(\frac{\omega}{c}l\right)}\right|. \qquad (7.55)$$

On fig. 7.14 the result of calculation $\frac{S_A}{S_{01}} = f\left(\frac{X}{l}\right)$ is shown. At calculation it is accepted $\beta l = 1; 0.3; 0.001$, the dimensionless frequencies of the compelled oscillations $\omega\frac{l}{c} = 0.5; 1; 1.5$ accordingly for curves 1, 2 and 3. The size is $f_1\left(\frac{l}{c}\right)^2 = 0.0225$.

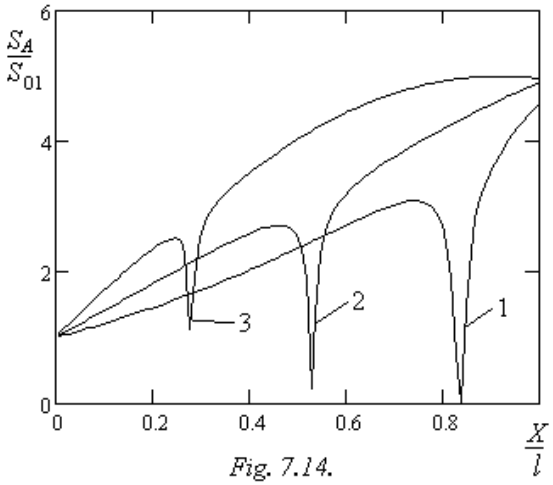

Fig. 7.14.

Let's find amplitude of the perilymph displacement in the scala tympani proceeding from (7.49):

$$u_A = \frac{\varepsilon_{\max}\cos\delta}{\beta}\left|\frac{\sin\left(\frac{\omega}{c}X\right)\cot(\varphi_1)+\cos\left(\frac{\omega}{c}X\right)}{\sin\left(\frac{\omega}{c}X+\delta\right)\cot(\varphi_1)+\cos\left(\frac{\omega}{c}X+\delta\right)}\right|. \quad (7.56)$$

For finding $\cot(\varphi_1)$ we use the formula (7.53) and identity $\cot(\varphi_1+\delta)=\frac{1-\tan\varphi_1\tan\delta}{\tan\varphi_1+\tan\delta}$. We shall receive:

$$\cot\varphi_1 = \frac{\frac{S_{02}}{S_{01}}\cos\delta-\exp(\beta l)\cos\left(\frac{\omega}{c}l+\delta\right)}{\exp(\beta l)\sin\left(\frac{\omega}{c}l+\delta\right)-\frac{S_{02}}{S_{01}}\sin\delta}. \quad (7.57)$$

Substituting (7.57) in (7.56), after rather difficult transformations with the account (7.41) and $h_{21}=\frac{h_2}{h_1}=\frac{S_{02}}{S_{01}}$ we shall find:

$$u_A = \frac{f_1}{\left|\omega^2-{\omega_0}^2\right|}\frac{\cos\delta}{\beta}\left|\frac{h_{21}\sin\left(\frac{\omega}{c}X-\delta\right)+\exp(\beta l)\sin\left(\frac{\omega}{c}(l-X)+\delta\right)}{h_{21}\sin\left(\frac{\omega}{c}X\right)+\exp(\beta l)\sin\left(\frac{\omega}{c}(l-X)\right)}\right|. \quad (7.58)$$

On fig. 7.15 the result of calculation $\frac{u_A}{l}=f\left(\frac{X}{l}\right)$ is shown. At calculation parameters were accepted similarly to calculation fig. 7.14. The angle δ used from the ratio $\tan\delta=\frac{\omega}{c\beta}$.

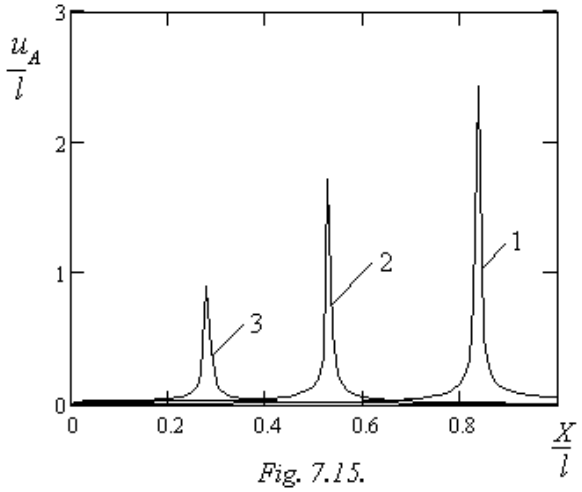

Fig. 7.15.

Thus, the spectral analysis of the complex sound wave by the acoustic analyzer is connected with the resonant answer of the certain site of basilar membrane on frequency of sound. Basilar membrane represents the analyzer of the sound spectrum with own frequency of oscillations decreasing on length due to increase in elementary varying masses at expansion of the basilar membrane.

Calculations show that the greatest amplitude of the basilar membrane oscillations and perilymph is observed at low frequencies in area helicotrma, and at high frequencies in the area of oval (or round) windows.

The solution of the compelled oscillations equations of perilymph in the scala tympani in case of ideal liquid allows calculate both position of the resonance on basilar membrane, and amplitude characteristics of resonant curves. The account of a liquid viscosity can result basically only to reduction of amplitudes values of resonant curves. For example, reduction of amplitude of the cross section area oscillations of the scala tympani in the resonance at low frequencies of a sound, fig. 7.14 (curve 1) obviously should not occur practically up to zero. Quality factor of the resonance of the perilymph displacement, fig. 7.15, at the account of viscosity will be also considerably reduced.

7.5. Interrelation of physical characteristics of a sound and characteristics of acoustical sensation

The man perceives the sound information with the help of the acoustic analyzer through subjective characteristics of acoustical sensation which are formed in CNS.

Characteristics of the acoustical sensation reflect some physical characteristics of a sound wave but they are not identical to these characteristics. In table 1 interrelation of physical characteristics of a sound (sound wave) and characteristics of the acoustical sensation is submitted. From the table it is visible that various physical characteristics of a sound are frequently perceived as the uniform acoustical sensation. There are physical characteristics not perceived by the ear, for example, speed of the sound, the form of wave front which is determined by the form of the sound source.

Table 1

Physical characteristics of a sound wave	Characteristics of acoustical sensation
1. Intensity of wave *I*	Volume of sound *E*
2. Amplitude of wave $A \sim \sqrt{I}$	Volume of sound *E*
3. Sound pressure $P \sim \sqrt{I}$	Volume of sound *E*
4. Frequency of wave ν	Pitch of sound
5. Period of wave *T*	Pitch of sound
6. Harmonic spectrum of sound wave	Timbre of sound
7. Speed of sound *V*	Not perceived

7.5.1. Pitch of sound

Frequency of a sound wave is perceived by the ear as pitch of sound.

The ear of the usual man does not perceive distinction of the frequencies in $1\,Hz$. On the average the frequencies are perceived as various if they differ on 6%.

For estimation of the sound pitch the all range of frequencies is separated into the intervals named octaves, fig. 7.16.

Octave there is interval of the sound pitch in which the ratio of extreme frequencies equally 2.

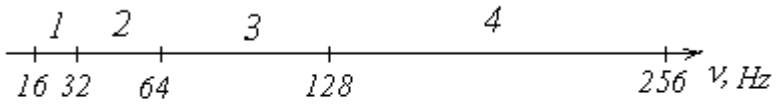

Fig. 7.16.

The ear perceives 10 octaves.

From smaller, than the octave of intervals of the sound pitch we shall note the big third with the ratio of extreme frequencies 1.25 (about 1/3 octaves) and the small third with the ratio of extreme frequencies 1.2 (approximately 1/4 octaves).

7.5.2. Timbre of sound

The timbre of a sound is a qualitative characteristic of acoustical sensation basically caused by the harmonious spectrum of sound.

The timbre is caused by quantity, intensity and a relative disposition of overtones on the frequency scale.

Speech of various people differs by the timbre, i.e. harmonious spectrum of the sound, fig. 7.17. Distinction of the people timbre is defined by the individual distinctions in anatomic structure of vocal chords, larynx and other air cavities - pharyngeal, oral, nasal which play role of resonators, and also features of regulation of the muscles contractions tensing vocal chords.

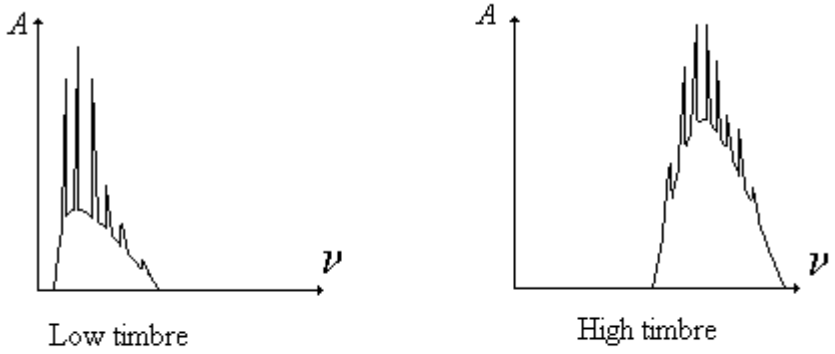

Fig. 7.17.

In air cavities there are the sound resonances amplifying some frequencies. It gives individuality to the speech timbre of people.

Thus the structure of the sound spectrum includes as linear part determined by vowels letters, and the continuous part determined by consonants letters.

Speech of men usually has more low-frequency timbre, than women.

7.5.3. Volume of sound

Volume of sound *E* is the level of acoustical sensation above the threshold of audibility.

Volume of the sound depends on intensity of sound. However, direct proportional dependence between volume *E* and intensity *I* of sound is not present, since the ear adapts for loud and quiet sounds.

Interrelation between volume and intensity of the sound is determined by the law of Weber-Fechner. The Weber-Fechner law determines interrelation between many kinds of irritation and corresponding sensations: acoustical, visual, thermal, tactile, etc.

7.5.3.1. The Weber-Fechner law for hearing

Essence of the Weber-Fechner law it is in the following. The increment of a level of acoustical sensation (i.e. volume of sound) is proportional to increment of the irritation force (i.e. intensity of sound) but due to adaptation in reverse proportion to size (level) of irritation.

$$\Delta E \sim \frac{\Delta I}{I}. \qquad (7.59)$$

Transiting to differentials at $\Delta I \to 0$, and using factor of proportionality *k*, we receive:

$$dE = k\frac{dI}{I}. \qquad (7.60)$$

The ratio of change of output signal for some device to corresponding change of the entrance signal refers to as sensitivity *Z* of this device. For the ear *Y*, fig. 7.18, proceeding from the Weber-Fechner law the size $Z = \frac{\Delta E}{\Delta I} \sim \frac{1}{I}$ i.e. sensitivity of the acoustic analyzer is reversely proportional to force of irritation (intensity of sound).

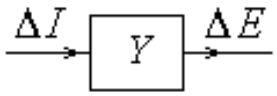

Fig. 7.18.

At small intensity of the sound the ear is more sensitive than at the big intensity. In how many one grows intensity of the sound in as much one the sensitivity of the ear there decreases and on the contrary. The essence of adaptation of the ear consists in it to loud and quiet sounds. Adaptation is carried out basically due to change of the muscles tension of ear bonds, and also due to change of sensitivity of CNS zones responsible for acoustical perception.

Integrating the differential form of the Weber-Fechner law (7.60), we find:

$$\int_0^E dE = k\int_{I_0}^{I}\frac{dI}{I} = k\ln\frac{I}{I_0},$$

where I_0 there is the intensity of the sound corresponding to the threshold of audibility (zero level of audibility). For frequency of sound $\nu = 1000\ Hz$ the average size of the threshold of audibility of the man is $I_0 = 10^{-12}\frac{W}{m^2}$.

7.5.3.2. Units of measurements of volume

Introducing numerical value of factor of proportionality *k* in result of integration of the differential form of the Weber-Fechner law we choose units of measurements of the sound volume. Thus it is convenient transit to decimal logarithms:

$$E = k\ln\frac{I}{I_0} = 2{,}3k\lg\frac{I}{I_0}.$$

For a choice of units of measurements of volume it is accepted that on frequency $\nu = 1000\ Hz$ (since $k = f(\nu)$ - factor *k* it is function of frequency) is $2.3k = 1$, i.e.:

$$E = \lg\frac{I}{I_0}\ [B]\ bel.$$

Bel it is a unit of measurements of the sound volume equal to change of the level of sound volume by frequency $1000\ Hz$ at change of the intensity sound level in 10 ones.

Unit ten ones smaller it is *decibel* $[dB]$. Sometimes the decibel of the volume refers to as phon.

Taking into account that $I \sim P^2$ where *P* it is effective size of the sound pressure is possible to find of the sound volume under the formula:

$$E = 20 \lg \frac{P}{P_0}, \ [dB].$$

Size P_0 it is effective value of sound pressure on the threshold of audibility for the frequency $\nu = 1000\ Hz$. Under normal conditions is $P_0 = 2.06 \cdot 10^{-5}\ Pa$.

In connection with convenience of introduction of a similar logarithmic unit of measurements, in bels and decibels measure for various physical sizes: intensity, capacity, voltage, pressure, etc.

Consider that at increase, for example, intensity of the sound in 10 ones it would grow on 1 *B*.

7.5.3.3. Threshold curves

On fig. 7.19 dependence in norm of the sound intensity which corresponds to the threshold of audibility on frequency (curve 1) is shown. On the threshold of audibility, i.e. on all curve 1 (on all frequencies ν) the volume of sound $E - 0$. From the graph it is visible that the threshold of audibility there is raises on small and big frequencies (the ear becomes less sensitive).

The sound volume at which there is acoustical sensation transit in a pain sensation refers to as the threshold of pain.

On fig. 7.19 curve 2 corresponds to the threshold of pain. On frequency $1000\ Hz$ the threshold of pain corresponds to intensity of sound $I \approx 130\ dB$. On the big and small frequencies the threshold of pain is reduced, i.e. the pain arises at smaller intensity of the sound.

Perforation (destruction) of the eardrum comes at $I \approx 170\ dB$.

The closed curve 3 on the graph marks area of speech.

At frequency $1000\ Hz$ decibels of the volume are equivalent to decibels of intensity.

The incremental threshold of sensitivity of a human ear, i.e. minimally found out change of intensity of a sound above the threshold of audibility at frequency $\sim 1000\ Hz$ is $\Delta I_{\min} \approx 0.59\ dB$.

The differential threshold it is minimally sensible relative increase of the sound intensity $\left(\frac{\Delta I}{I}\right)_{\min}$ depends on intensity of the sound and frequency. For the sound intensity $40 - 50\ dB$ and the frequencies range $500 - 4000\ Hz$ the differential threshold is $\sim 5\%$.

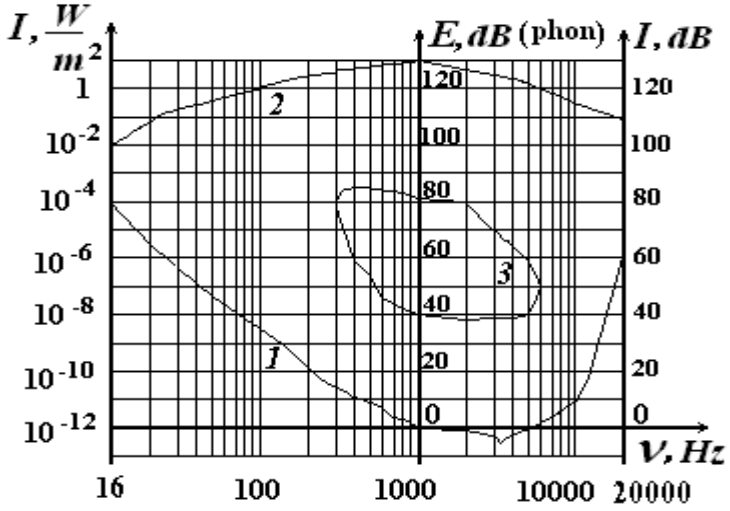

Fig. 7.19.

Chapter 8. The visual analyzer

The visual analyzer or eye is the organ perceiving electromagnetic waves of the seen range ($\lambda = 380 - 760\ nm$) radiated and reflected by subjects, and on the basis of it giving to a brain $\sim 98\%$ of all information about world around.

8.1. Elements of structure of the eye

The eyeball will consist of three layers, fig. 8.1. External layer it is sclera *S* which in a forward part passes in a transparent cornea *C*. Average vascular layers *V* which ahead passes in iris *I* representing aperture diaphragm of the eye. Iris due to a pigment has individual distinctions in painting. This painting involves an opposite sex.

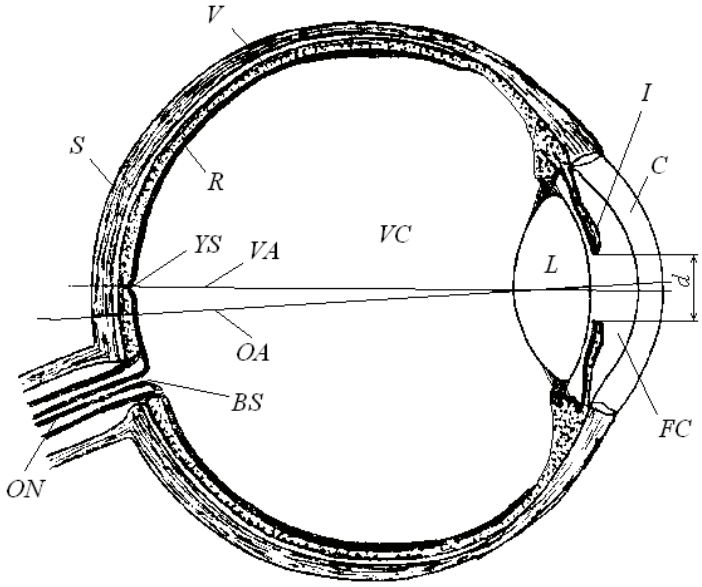

Fig. 8.1.

It forms the aperture or a pupil which diameter can vary in limits $d = 2 - 8\ mm$ that is necessary for avoidance of damage of a retina at too bright light. Thus the light flux proportional to the area of the pupil changes in 16 ones.

The visual analyzer or eye includes light-refractive and light-sensitive apparatuses.

Light-sensitive apparatus of the eye represents internal layer or retina *R* approximately hemispherical form. The maximal light sensitivity there is the area of the retina refers to as a yellow spot *YS* or macula lutea. Near to the yellow spot there is a place of input of the optic nerve *ON* in the eyeball. This area of the retina is absolutely not sensitive for light, so-called a blind spot *BS*. The blind spot was found out in 1666 by the French physicist E. Mariotte.

Light-refractive apparatus of the eye will consist of cornea *C*, the forward chamber *FC* filled with aqueous humor, a lens *L* and transparent vitreous chamber *VC* which a consistence representing gelatinous mass (gel).

The cornea it is transparent complex multilayered structure has thickness $0.8 - 0.9\ mm$ and contains the numerous sensitive nervous terminations. The nervous terminations of the cornea are intended basically for perception of external influence on the cornea at hit on it of various extraneous bodies: the motes, flying insects, etc. This information is transferred in CNS where character of the answer to influence is formed, for example, the blinking, the raised liberation of a lacrimal liquid, etc.

The lens is transparent, colorless, elastic body as a convexo-convex lens in a transparent bag. The lens can change the convexity, i.e. refractive power *D* due to balance of two influences - the force created by circular fibres of a ciliary muscle which weakening a tension of radial suspensory ligament stretching lens do it more

convex owing to elasticity inherent in the lens. Thus refractive power of the eye increases. On the contrary, intraocular pressure and the tension of radial fibres of ciliary muscle stretching the lens does its more flat that reduces refractive power of the eye (thus circular ciliary muscles relax). In norm intraocular pressure has size approximately on $18-20\ mm\ Hg$ is higher atmospheric. It allows an eyeball to keep the spherical form.

On fig. 8.1 are marked also the visual axis of eye *VA* corresponding to a direction of the best sight (passes through the optical center of the eye and the center of yellow spot) and optical axis *OA* of the eye as optical system.

8.2. Refractive powers of the eye medium. Accommodation

Elements of the light-refractive apparatus of the eye have the following refractive power:

1. Cornea $D=42-43\ dptr$.
2. Humor of forward chamber $D=2-4\ dptr$.
3. Vitreous chamber $D=-5\div-6\ dptr$, disperses light.
4. Lens $D=19-33\ dptr$.

General refractive power of all eye is $D=63-74\ dptr$.

The big range of refractive power of the lens is connected to possible physiological change of curvature of its surfaces.

For the analysis of the phenomena connected to sight use the resulted eye or Verbitsky eye. Verbitsky eye, fig. 8.2, is equivalent converging lens *L* with minimal refractive power $D=63\ dptr$ and focal length $F=16\ mm$ in the rest of accommodation.

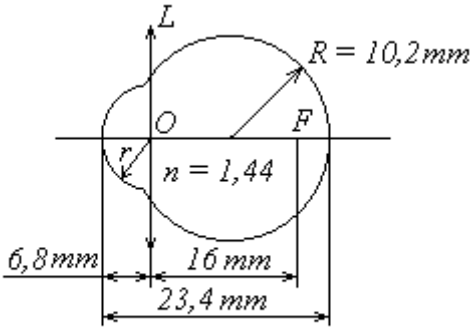

Fig. 8.2.

Construction of the image in the resulted eye is made by the rules of a single lens.

The image there is real, inverted, reduced, taking place between focus *F* and double focus, fig. 8.3.

That the image of subjects taking place on different distances from the eye has got on the retina the eye possesses property of accommodation.

Accommodation is the ability of the eye to formation on the retina of the sharply defined image of variously removed subjects due to change of refractive power of the eye lens.

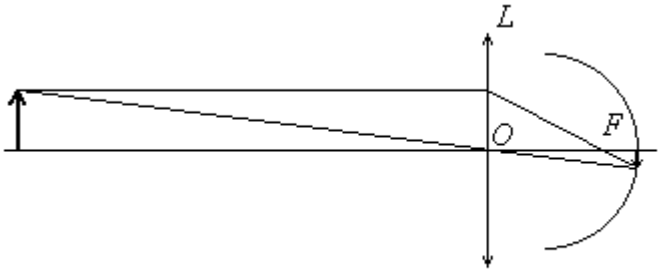

Fig. 8.3.

In rest of accommodation (circular fibres of the ciliary muscle are relaxed, refractive power of eye $D=63\ dptr$, focal length $F=16\ mm$) the lens most flattened due to intraocular pressure and the tension of radial fibres. The sharply define image of the subjects removed on $8-10\ m$ from eyes is on the retina.

In the limits of accommodation (circular fibres of the ciliary muscle intense, $D=74\ dptr$, focal length $F=13.5\ mm$) the sharply define image of a subject is on distance $S=25\ cm$ - distance of the

distinct vision. At this distance the subject is close enough it can be examined well (on the retina the sharply define image) but the excessive stress of accommodation is not, the eye does not get tired. This distance has developed evolutionary since it was necessary attentively and rather long time to examine the subjects which are taking place in hands: food, instruments for work, etc.

The man can well examine a subject and on closer than on distance $S = 25\,cm$ is usual up to $S = 15 - 16\,cm$. In this case the eye is in the condition of the excessive stress of accommodation. Though it is possible to distinguish finer subjects the eyes cannot long time be in this condition.

8.3. Visual angle and visual acuity

For an establishment of interrelation between real size of the subject and distance up to it used the visual angle.

Distance up to the subject, fig. 8.4, it is possible to find under the formula:

$$L = \frac{H}{2tg\,\beta/2}, \qquad (8.1)$$

where β there is visual angle, *H* – the size of the subject. The visual angle a brain estimate on size of the image *h* on the retina actually using the ratio:

$$tg\,\frac{\beta}{2} = \frac{h}{2l}, \qquad (8.2)$$

where is *l* = *const*. The size *l* is the distance from the eye optical center up to the retina is defined by the structure of the eye.

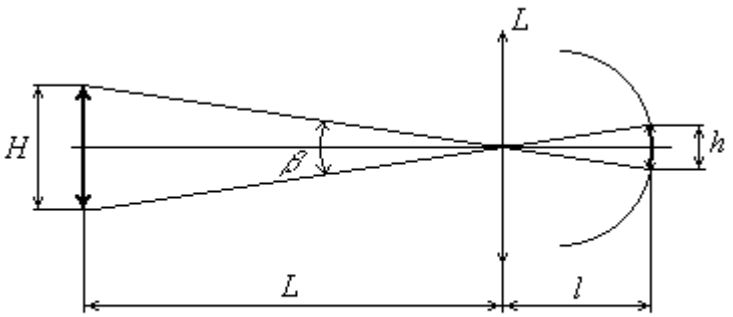

Fig. 8.4.

Hence, if the brain knows size of subject *H* from the last experience he learns distance up to subject *L* having the visual angle β. If the brain knows distance up to the unknown subject he can estimate its sizes.

Accuracy of the estimation of distance up to the subject on small distances there raises due to vision two eyes - binocular vision. Besides binocular vision allows receive the volumetric image of the subject.

Visual acuity characterizes limit of the resolving power of the eye as optical system.

Visual acuity is normal if the man distinguishes extreme points (border) of the subject are taking places under the visual angle $\beta = 1'$. In this case visual acuity is $V = 1.0$. Thus on the retina there is the size of image $\sim 5\,\mu m$.

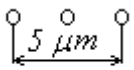

Fig. 8.5.

If the man distinguishes borders of the subject only under the visual angle $\beta = 5'$ the visual acuity is equal $V = 1/5 = 0.2$.

For distinction of the subject extreme points it is necessary on the retina the excitation minimally three rods or cones (visual receptors) so that light rays from the borders of the subject excited the extreme receptors, fig. 8.5. Thus the average receptor can be not excited. If are excited only two beside located receptors the subject is estimated by a brain as a luminous point.

In Sivtsev's table located in $5\,m$ from the eye the man should distinguish letters in the third line from below. Reduction of visual acuity can take place owing to the following reasons:

1. Degeneration of the receptors cells therefore their superficial concentration decreases.
2. Failure of the light-refractive apparatus properties of the eye.

8.4. Glasses

Glasses are the elementary optical devices serving for correction of a vision lacks and protection of the eye from harmful external optical and mechanical influences.

Glasses will consist from the glasses lens and a rim. The rim establishes the necessary position of glasses concerning eyes.

For eyes are typical the following lacks which can arise as a result of diseases or at misuse by the vision organs and also as the age phenomena. First of all it is nearsightedness (myopia), farsightedness (hypermetropia), astigmatism, squint, etc. which are not compensated by the accommodation. Lacks of eyes are corrected with the help of the glasses lenses which possess a series of actions.

Correction of the sight is carried out due to 4 kinds of glasses lenses action.

1. Spherical or stigmatical action (Greek stigme - a point). Such action is provided with lenses with spherical surfaces. This action consists in moving focus of system the lens - eye along the optical axis of the eyeball. Such lacks of the vision as the nearsightedness and farsightedness are corrected.

Let's consider correction of the nearsightedness as a result of which the eye does not see precisely far subjects. Nearsightedness can be connected to excessively high refracting ability of the eye medium or with the lengthened form of the eyeball usually hereditary

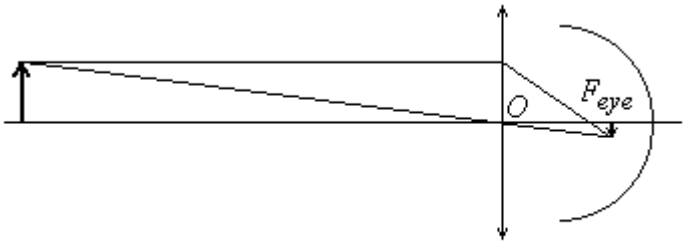

Fig. 8.6.

At nearsightedness focus F_{eye} of the eye refracting system is excessively close to the eye optical center *O*, fig. 8.6. Therefore the image does not get on the retina and settles down before it.

Correction of nearsightedness is carried out with the help of diverging (negative) lens *L* which removes the image on the retina, fig. 8.7.

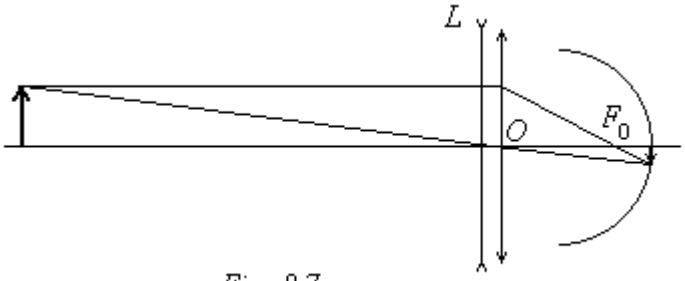

Fig. 8.7.

Let the refractive power of the eye is $D_{eye} = \frac{1}{F_{eye}}$, and refractive power of the glasses lens is negative $D_{gl} < 0$. Selecting glasses it is necessary to reduce the refractive power of system the lens - eye $D_0 = \frac{1}{F_0}$ so that it has reached norm:

$$D_0 = D_{eye} - \left| D_{gl} \right| .$$

Let's consider correction of the farsightedness as a result of which the eye does not see precisely close subjects.

The farsightedness can be connected to insufficient refracting ability of the eye medium which usually arises with the years owing to loss of the lens elasticity (presbyopy) or with the short form of the eyeball.

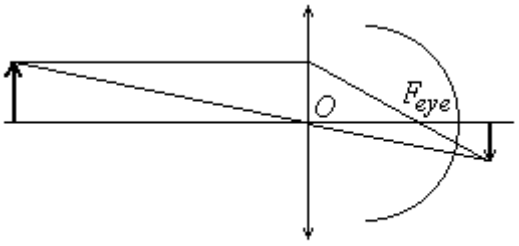

Fig. 8.8.

At the farsightedness focus F_{eye} of refracting system of eye is too far from the optical center *O* of the eye, fig. 8.8. Therefore the image does not get on the retina, and settles down behind it.

Correction of the farsightedness is carried out with the help of converging (positive) lens *L* which approaches the image placing it on the retina, fig. 8.9.

Let refractive power of the eye is $D_{eye} = \frac{1}{F_{eye}}$, and refractive power of the glasses lens is positive $D_{gl} > 0$. Selecting glasses it is necessary to increase refractive power of system the lens - eye $D_0 = \frac{1}{F_0}$ so that it has reached norm:

$$D_0 = D_{eye} + D_{gl}.$$

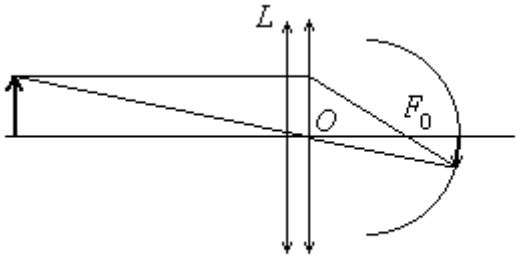

Fig. 8.9.

Powerful converging lenses are used in glasses in case of absence of the lens that takes place, for example, after operation concerning cataract.

2. Astigmatic action (Greek a - negation and stigme - point). Such action is provided with lenses with cylindrical or toroidal surfaces.

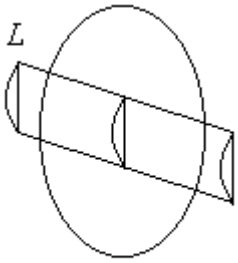

Fig. 8.10.

Astigmatism it is lack of the eye at which the eye differently refracts light in various meridian planes. If in one of two mutually perpendicular planes of the eye the refraction is norm the astigmatism refers to as simple.

Refracting mediums of the eye, first of all cornea, at astigmatism have not spherical, and the ellipsoidal the form. For correction of astigmatism are used the lens *L* possessing mutually perpendicular astigmatism, i.e. lens at which the maximal refractive power is in the meridian plane in which the eye has refractive powers minimal, fig. 8.10.

3. Prismatic action. In the pure state there are typically for a prism with the triangular basis. Prismatic action is consists in turn on the certain angle of the light rays going from the considered subject. Prismatic action of lenses corrects the lack of convergence (unit of images from two eyes). The lack of convergence arises at the squint.

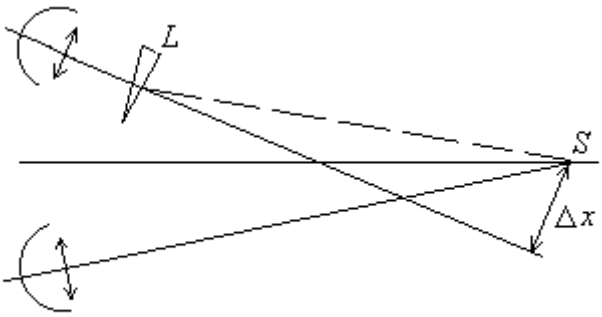

Fig. 8.11.

At the squint the visual axis of one eye is directed on the considered point of subject *S*, and other eye is diverged aside, fig. 8.11, on distance Δx . There is absence of the images convergence. Prismatic lens *L* unit the images from two eyes turning the trace of light rays.

4. Eikonic action (Greek - image). Consists in reduction or increase in the sizes of the image. In the pure state eikonic action the lens with two parallel spherical surfaces possesses.

After passage of rays through eikonic lens *L* the image increases or decreases concerning a subject, fig. 8.12.

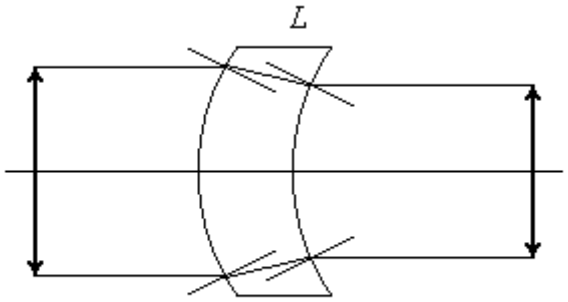

Fig. 8.12.

For the account eikonic actions of lenses such defect of the vision as the unequal sizes of the image received by each eye (aniseikonia) is corrected. Eikonic action is used for increase in the size of the image at disease of the light-sensitive apparatus of the eye (retina), and also at deterioration of the information transfer on the image in CNS on the optic nerve.

All kinds of optical action of glasses as a rule are connected. Spherical actions is connected to the decrease or increase in the image (eikonic action), at the periphery of the glasses lens there is prismatic action.

8.5. Light-sensitive apparatus of eye

Light-sensitive apparatus of the eye is intended for transformation of light energy to the electric signal transferring on the optic nerve in CNS with the purpose of formation of representation about the world surrounding a man.

Light from a subject is focused by the lens of the eye so that the precise image has arisen on the light-sensitive apparatus of the eye - the hemispherical retina.

In the retina there are photosensitive cells or photoreceptors (rods and cones).

Rods are intended for black-and-white twilight sight. They are in regular intervals distributed on the retina, their total in the each eye approximately 125 million.

Cones are intended for color day time sight. They are concentrated in the central part of the retina in the area of yellow spot, their total in the each eye approximately 6.5 million.

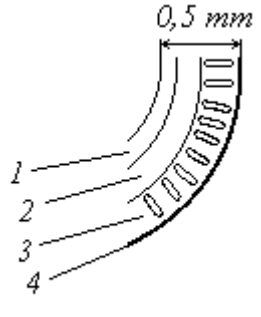

Fig. 8.13.

The retina thickness $\sim 0.5\,mm$ will consist of several layers, fig. 8.13.

1 - a layer of the optic nerve fibres; 2 - a layer of the nervous cells: ganglion, amacrine, horizontal, bipolar, interplexiform cells; 3 - a layer of the photoreceptors; 4 - a black pigmentary layer. In the physiological literature frequently allocate 10 layers of the retina.

At hit of light on the cornea surface:

4% of the light flux are reflected from the cornea,

50% - are absorbed by optical mediums of the eye,

10% - are influence on photoreceptors,

36% - are absorbed in the pigmentary layer.

The pigmentary layer is in very difficult conditions of functioning since by

the light-refractive apparatus of the eye concentrated big light and thermal energy on the small area of its surface. Therefore there is a constant regeneration of a pigment (меланина).

Thus, it is useful only 10% of the light flux falling on the eye cornea.

Before light reach on photoreceptors it passes layers 1 and 2 but these layers are transparent and practically do not absorb light. The pigmentary layer absorbs the quantums of light which are not cooperating with photoreceptors interfering with reflection of light and repeated influence on photoreceptors.

In the photoreceptors and neural network of the retina under influence of the light quantums there are arise impulses of excitation which on nervous fibres transferred in CNS where the visual sensation is formed. It is necessary to note that an environment as a whole is light superfluous for the visual analyzer.

8.5.1. Law of Weber-Fechner for vision

The man sees surrounding subjects due to light which reflected from them and has reached on the retina of the eye or due to light radiated by a subject at heating, a luminescence, etc.

The energy flux of the electromagnetic radiation estimated on visual sensation which it causes in the normal human eye (i.e. the flux of light energy in the range of the waves length perceived by human eye $\lambda = 380 - 760\ nm$) refers to as light flux Φ.

For monochromatic light:

$$\Phi = \mu \frac{W}{t}, \qquad (8.3)$$

where W there is energy of electromagnetic radiation in the range of the waves length perceived by a human eye and passed through pupil, t - time of supervision, $P_S = \frac{W}{t}$, $[W]$ - energy flux of electromagnetic radiation - power of electromagnetic radiation, μ - the factor which is taking into account a photosensitivity of the eye (luminosity factor).

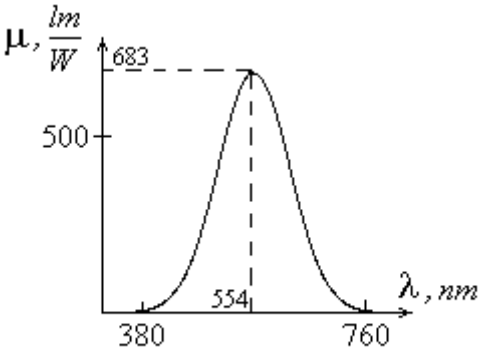

Fig. 8.14.

As unit of measurements of a light flux in SI is lumen $[lm]$ (Latin – light).

Dependence of the luminosity factor on wave length for a normal human eye is shown on fig. 8.14.

The maximal luminosity factor of the eye is marked on length of wave $\lambda = 554\ nm$ $\left(\mu = 683\ \frac{lm}{W}\right)$. To borders of the seen range of wave lengths the luminosity factor falls.

As brightness B refers to superficially - spatial density of the light flux radiating from the surface.

$$B = \frac{\Delta\Phi}{\Delta\Omega \Delta S \cos\theta}, \qquad (8.14)$$

where $\Delta\Omega \Delta S \cos\theta$ there is geometrical factor, ΔS - an element of the area of the radiating or reflecting surface (the surface can have various brightness on different sites), θ - an angle between the perpendicular $\boldsymbol{n}$ to this surface and direction of supervision, $\Delta\Omega$ - a solid angle filled with radiation, fig. 8.15, which basis is the pupil of the eye.

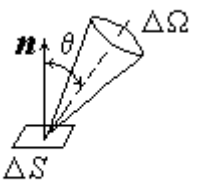

Fig. 8.15.

As unit of measurements of brightness in SI is nit $[nt]$ (Latin – shine).

For brightness there is the principle of superposition i.e. total brightness of the surface illuminated by n light sources is equal to the sum of brightnesses at illumination of this surface by each source separately:

$$B_{\Sigma} = \sum_{i=1}^{n} B_i . \qquad (8.15)$$

The luminosity factor μ does not take into account influence of adaptation of the eye to various levels of brightness; on the graph, fig. 8.14, it is submitted for some average day time illumination.

Adaptation of the eye to conditions of brightness can be carried out: due to change of diameter of the pupil, due to change of the number of participation of photoreceptors in the answer to light influence (at decomposition on light and restoration in darkness of a photosensitive pigment), due to shielding photoreceptors by the dark pigment, etc.

Adaptation of the eye to various levels of brightness submits to the Weber-Fechner law.

Weber-Fechner law for vision can be formulated as follows. The increment of the light sensation ΔL is proportional to the increment of brightness of the considered surface and reversely proportional to the level of its brightness owing to adaptation (i.e. brightnesses of the background).

$$\Delta L = k\frac{\Delta B}{B}, \qquad (8.16)$$

where *k* there is the factor of proportionality dependent on wave length of light.

The eye adapts the brightnesses sensitivity to the conditions of illumination (small, so-called dark adaptation of the eye and big - light adaptation). On the low level brightnesses of the background at change of brightness of some surface the light sensations will be more than at the same change of brightness at the high level the brightnesses of the background.

As against of the Weber-Fechner law for the acoustic analyzer, see paragraph 7.5.3.1, in the same law for vision in the left and the right parts from the equal-sign has the values connected to visual sensation – so-called light sensation *L* and brightness *B*. Therefore the Weber-Fechner law for vision reflects only the phenomenon of adaptation of the eye instead of is interrelation of physical characteristics of light and visual sensation.

Passing in the Weber-Fechner law to the limit at $\Delta B \to 0$, we receive:

$$dL = k\frac{dB}{B}. \qquad (8.17)$$

Integrating the received expression we find the Weber-Fechner law for vision in the integrated form:

$$\int_0^L dL = k\int_{B_0}^{B}\frac{dB}{B}, \quad \to \quad L = k\ln\frac{B}{B_0}, \qquad (8.18)$$

where B_0 there is absolute threshold of sensitivity of the eye, i.e. the minimal brightness perceived by a human eye. It corresponds approximately to $50-150$ the quantums of blue-green light falling on the cornea in second and depends on the frequency of light. Thus cooperate with photoreceptors only $5-10$ quantums of light. However, in connection with absence of validity experimental results about dependence of factor *k* on the wave length or light frequency the transition to the units of measurements of light sensation *L* (bels and decibels) till now in photometry is not worked.

If $B_{\max}$ it is the maximal without big uncomfortable glare perceived limit of brightness then for a normal human eye $\frac{B_{\max}}{B_0} \approx 10^{16}$. We shall note that for the acoustic analyzer the similar size - the ratio of the threshold of pain to the threshold of audibility on frequency of $1000\ Hz$ is equal $\frac{I_{pain}}{I_0} \approx 10^{13}$, i.e. on three degree it is less.

Minimal found out difference of brightnesses of light on a surface refers to as incremental threshold ΔB_{th}.

The ratio of the incremental threshold to the brightness of the background refers to as the differential threshold. For a normal human eye $\frac{\Delta B_{tr}}{B} \approx 1-1.5\%$ (for acoustic analyzer the differential threshold is $\sim 5\%$). The differential threshold defines accuracy of measurement of physical sizes in the optical devices based on equalization of brightness on surface of sight.

In sanitary photometry the concept of illuminance of a surface is used.

Illuminance it is size of the light flux perpendicularly falling on unit of the illuminated surface:

$$E = \frac{\Phi}{S} = \mu \frac{W}{St} \text{ or } E = \frac{d\Phi}{dS}, \qquad (8.19)$$

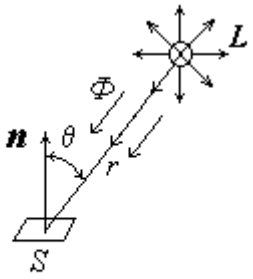

Fig. 8.16.

where *S* there is area of the illuminated, $J = \frac{W}{St}$ - intensity of electromagnetic radiation. A unit of measurements of illuminance in SI is $[E] = \left[\frac{lm}{m^2}\right] = [lx] \to lux$ (Latin - light).

Illuminance of the surface located under the angle to the light flux $E_\theta = E\cos\theta$, where θ it is the angle between the direction of the light flux and the normal ***n*** to surface *S*, fig. 8.16.

German astronomer J. Kepler in 1604 has established that the illuminance falls on the surface in reverse proportion to a square of distance from a dot light source $E \sim \frac{1}{r^2}$ (for example, candles or electric lamp *L*, fig. 8.16).

As well as for brightness, for illuminance the principle of superposition is correct.

Sanitary norms and rules establish sizes of necessary illuminance of working rooms and other places.

On tables in educational rooms illuminance should be not lower $150\ lx$, in drawing - $200\ lx$, in corridors - $20-30\ lx$, in streets - $2-4\ lx$. For household reading it is necessary not less than $30\ lx$. Illuminance a sunny day open-air $\sim 100000\ lx$, at night at a full moon $0.02\ lx$.

8.5.2. Biophysics of photoreceptor work

Let's consider work of one of kinds of photoreceptors which are available in retina of the eye, namely rods.

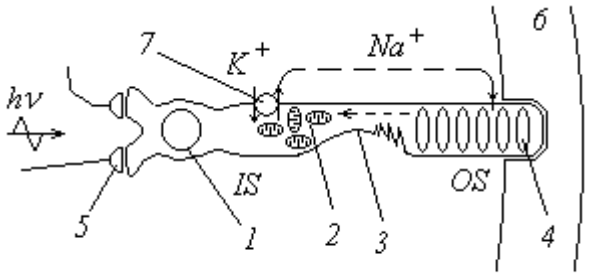

Fig. 8.17.

The rod is the cell which has usual organelles: nucleus 1, mitochondrias 2, etc., fig. 8.17. The rod is divided by a connecting leg 3 into two segments - the outer segment *OS* where there are visual disks 4 (*OS* is directed to the pigmentary layer 6 and in part submerged in it) and inner segment *IS* on which are available synaptic contacts 5. Through these synaptic contacts the excitation transfers from the rod ton a neural network of the retina and further on the optic nerve in CNS.

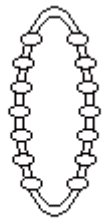

Fig. 8.18.

Quantums of light energy $h\nu$ (*h* it is Planck's constant, ν - frequency of light) get on visual disks through area synaptic contacts and an inner segment of the cell. These areas of the photoreceptor are transparent for light.

Visual disks, fig. 8.18, are the flattened out balls from the double lipids layer which molecules of complex protein - rhodopsin are integrated. The number of visual disks in the rod reaches $500-1000$.

On fig. 8.19 the rhodopsin molecule integrated in lipids bilayers (there are data that the visual disk will consist of lipids monolayers) is shown. It will consist

of protein opsin (or scotopsin) and chromophoric groups - retinal (derivative of vitamin A). The chromophoric group is located in the rhodopsin molecule on the side of the internal surface of the visual disk.

Feature of outer segments *OS* of photoreceptors, fig. 8.17, is that in rest (in darkness) sodium channels of the membrane are open. Therefore in darkness are passes into the outer segment the ions of sodium which then are actively pump out from the inner segment by the sodium - potassium pump 7 ($Na^+ - K^+ - ATPase$). Inside the cell the sodium current flows from the outer segment in inner segment, and outside of the cell as shown in fig. 8.17 from the inner segment to outer segment. It is so-called darkness current.

The general formula for potential on a membrane looks like, see (1.52):

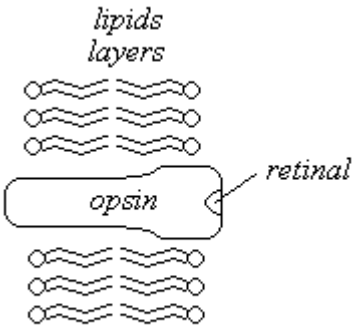

Fig. 8.19.

$$\Delta\varphi = \frac{RT}{zF} \ln \frac{\chi P_K \left[K^+\right]_e + P_{Na} \left[Na^+\right]_e}{\chi P_K \left[K^+\right]_i + P_{Na} \left[Na^+\right]_i}, \qquad (8.20)$$

where P_K and P_{Na} there are factors of permeability of membrane for ions of potassium and sodium, $\chi = \frac{3}{2}$ - stoichiometric factor which is taking into account electrogenic of the sodium – potassium pump.

In rest (in darkness) the ratio of concentration of sodium and potassium on both sides of the membrane, and also permeabilities of membranes of the photoreceptor (rods) for sodium P_{Na} and for potassium P_K is those that on the membrane the potential approximately $\Delta\varphi \approx -40\, mV$ (sign minus inside the cell) is established.

Under influence of the light quantums occur conformable phototransformations of the rhodopsin molecule (retinal): 11-cis-retinal due to rotate of one part of molecule concerning another passes in all-trans-retinal so-called reaction of cis-trans-photoisomerization of retinal. These transformations it is convertible.

Cis-trans-photoisomerization also refers to as geometrical isomerization. Cis-trans-photoisomerization of retinal it is the rotate of one part of the molecule concerning another under action of light quantum by energy $h\nu$ concerning of double carbon bond $C = C$ on the angle 180^0, fig. 8.20.

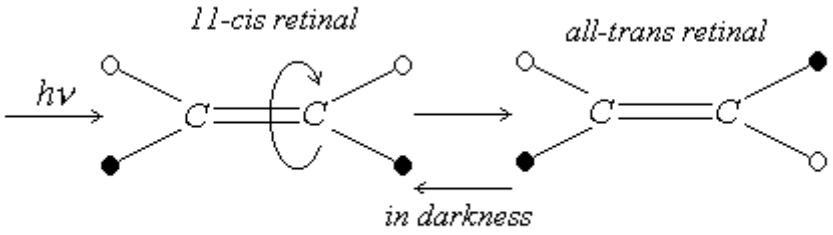

Fig. 8.20.

Concerning the further succession of events there is two hypotheses.

According to the first older hypothesis phototransformations of rhodopsin result to emission from visual disks of ions Ca^{2+} (or ions Ca^{2+} enter into the cell from outside of) which serve mediators (calcium hypothesis), i.e. diffuse transfer the information to the sodium channels of the plasmatic membrane of the photoreceptors outer segment *OS* to their closing.

Permeability of the membrane for sodium is reduced since are closed sodium channels the darkness current stops. However ions of sodium continue are actively pump out from the cell. The ratio of permeabilities of membranes to become $P_{Na} << P_K$. The potential on the membrane not changing the sigh becomes closer to the potassium potential. On light the formula for potential on the membrane of photoreceptor gets the kind (1.10):

$$\Delta\varphi \approx \frac{RT}{zF} \ln \frac{[K^+]_e}{[K^+]_i}. \qquad (8.21)$$

There is a hyperpolarization (be relative of the darkness rest) membranes of the photoreceptor. On a membrane of the rod it is established so-called receptive potential approximately $\Delta\varphi \approx -70 \div -80\, mV$. The impulse of excitation through the neural network of retina is transferred in CNS.

Let's note that in cones the chemical and electric processes occur approximately in 4 ones faster than in rods.

In darkness (for example, at blinking) molecules of rhodopsin undergo return phototransformations the ions Ca^{2+} pump up inside of visual disks, the sodium channels of the membrane of the rods outer segment open, with the help of ionic pumps are restored initial differences of ions concentration on the membrane of photoreceptor.

According to the second hypothesis (the hypothesis of cGMP –mediator; to it share the majority of researchers) in darkness in the outer segment of the rods is present big concentration of molecules of cyclic guanosine monophosphate cGMP. This substance supports sodium channels of the membrane of rods outer segment in the open condition. At phototransformation of 1 molecule of rhodopsin due to the whole cascade of biochemical reactions there is a hydrolysis 10^5 of cGMP molecules. Sodium channels are closed, the potential on the membrane grows (on the module).

In darkness due to biochemical mechanisms concentration cGMP is restored, the sodium channels open. The membrane of the rods outer segment comes back in the resting condition.

In connection with exclusive importance of normal functioning of the visual analyzer for a survival of population probably in photoreceptors both mechanisms of transfer of the information to ionic channels of *OS* from visual disks simultaneously operate.

On fig. 8.21 time dependence of the receptor potential U_{in} (on the entrance in a neural network of the retina) of single cone arising in reply to short light flashes ($10\, ms$) is shown at three various intensities of light [15]. In darkness on a membrane of a photoreceptor there is the resting potential RP which bit more (on the module) of value $-20\, mV$. There are curve 1 corresponds to the weakest intensity I_1, curve 2 – the light intensity $I_2 = 4I_1$, curve 3 – the intensity $I_3 = 16I_1$. Between the intensity of the light flash and the receptor potential analog (logarithmic) dependence $I \sim \ln U_{\max}$ was observed.

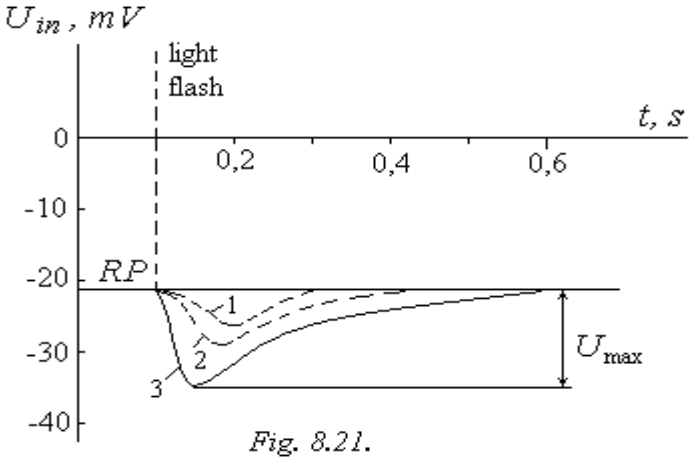

Fig. 8.21.

8.5.3. Neural network of the eye retina

Feature of the photoreceptors is the hyperpolarizing nature of the receptor potential which generated in response to light stimulation, fig. 8.21.

It is known that the brain works with signals in the digital coding.

Therefore analog-digital transformation of the signal from the photoreceptor is necessary. For this purpose the neural network of the eye retina is intended. We shall examine its work.

Receptor potential U_{in} of the photoreceptor PR through synaptic switching there passes at the entrance of the bipolar neuron B, fig. 8.22.

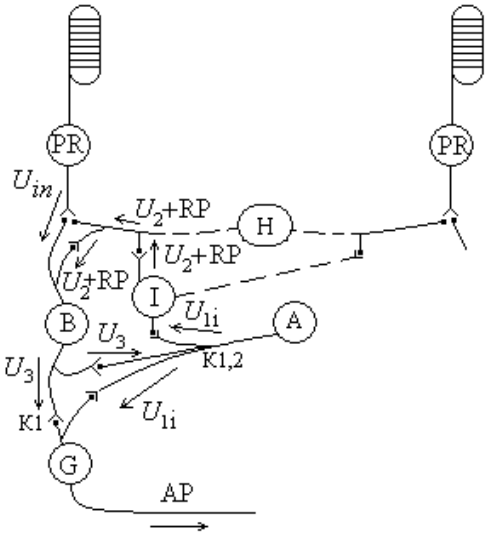

Fig. 8.22.

In fig. 8.22 the distribution of electrical signals in the system retinal neurons are shown. There are shown the following neurons: B - bipolar, A - amacrine, I - interplexiform, G - ganglion, H - horizontal.

The system of the neural network is accepted according to [64] with insignificant simplifications in particular concerning numbers of participating in processing the information of uniformities amacrine neurons.

Neural network of the retina represents a slightly modified circuit of the analog-to-digital converter (ADC) of consecutive calculations [66]. Block-diagram of the ADC corresponding neural network of the retina is shown in fig. 8.23. Each element of the ADC are corresponds to the neuron. In particular the comparator K corresponds bipolar neuron B, generator clock frequency GCF - amacrine neuron A, digital-to-analog converter DAC - interplexiform neuron I, pulse counter PC - ganglion neuron G.

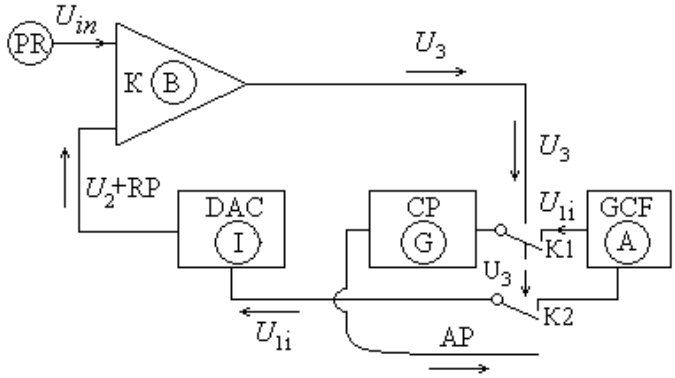

Fig. 8.23.

Horizontal neurons H apparently feebly involved in the analog-to-digital conversion. Their primary function is providing contrast boundaries of visual image in the area of eyesight [65].

Let us consider in more detail the equivalent circuit of the retina ADC, shown in fig. 8.23. Showing items are required for any variety of ADC. There is one of the most important elements the generator of clock frequency GCF which generates a continuous sequence of impulses in the simplest case a constant frequency. This sequence of electrical impulses U_{1i} is shown in fig. 8.24a.

In the neural network of the eye retina continuous sequence of action potentials there are generate amacrine cells A, fig. 8.24c, i.e. they set clock frequency of ADC.

It is known that amacrine neurons A generate action potentials [64] but until now their role is not clear [67]. There are identified by morphological and histochemical methods about 30 species of amacrine neurons [65]. There's also stated that amacrine cells "react to the inclusion and turning off lights, which simply signaling about change of lighting, regardless of its direction." This well correlates with their role GCF in the circuit ADC. A large variety of amacrine neurons indicates about variability of ADC retina parameters.

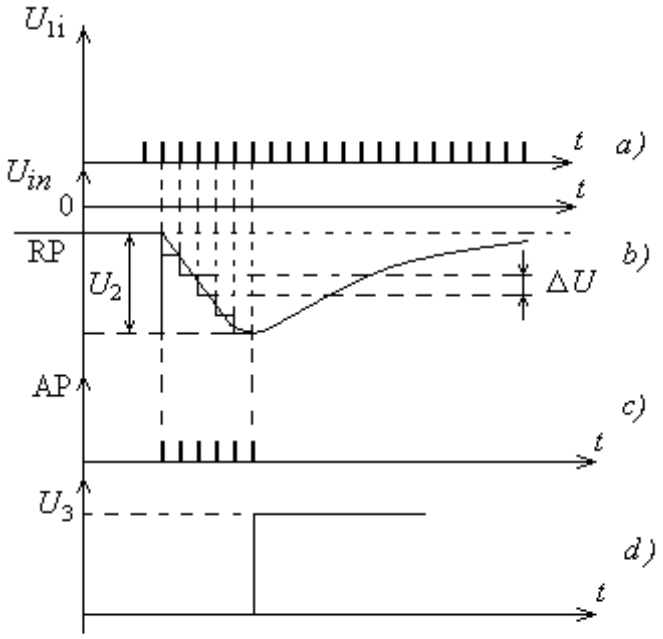

Fig. 8.24.

The important element of the ADC is the comparator K. It does not work with impulsed signals, and compares the two analog signals - the input to the neural network from the photoreceptor U_{in} and the output signal from digital-to-analog converter (DAC) gradually and step increases to size $U_2 + \mathrm{RP}$, fig. 8.24b. This is consistent with the fact that bipolar neurons B do not generate action potentials. Signal on bipolar neurons spreads like electrotonic [15].

In case of equality $U_{in} = U_2 + \mathrm{PR}$ comparator K generates the constant voltage U_3, fig. 8.24d. DAC is the required element of ADC. It is discrete with a step ΔU, fig 8.24b, accumulates potential $U_2 + \mathrm{PR}$ at its output for comparison with the receptor potential U_{in} of photoreceptor PR, fig. 8.23. The interplexiform neuron I of the feedback plays the role of DAC. On the input of this neuron on its impulses branches served impulse voltage U_{1i} and on the output occurs the step-analog potential $U_2 + \mathrm{PR}$ for comparison by comparator K. So far the role and functioning of these neurons were not described. Some authors [65] consider that the role of these neurons is not very important and name them as inter-retinal.

Pulse counter PC in the ADC retina it is the ganglion neuron G, fig. 8.22 and fig. 8.23. Ganglion neurons G direct the signal in the form of action potentials AP to the central nervous system.

Work ADC of retina begins from arise of the receptor potential U_{in} produced by the photoreceptors and transfer it to the entrance of the comparator K. By the closed keys K1 and K2, see fig. 8.23, the impulses from the GCF served on the pulse counter PC where they come out in the form of a sequence of action potentials, and on the DAC, where the potential of comparison $U_2 + \mathrm{PR}$ accumulate, fig. 8.24*b*. If arise the conditions $U_{in} = U_2 + \mathrm{PR}$ the comparator K generates the voltage U_3, fig. 8.24*d*, which breaks the outputs from the GCF by keys K1 and K2. It is also possible input the signal U_3 produced by the comparator K (bipolar neurons B) directly on the ganglion neurons G (pulse counter PC) to stop the generation of impulses of that neuron. Synaptic switching from the B on the G it is another analog of the key K1 in fig. 8.22. Thus, each signal from the photoreceptor the ganglion neuron (or pulse counter) are generates a strictly defined number of impulses *n* – impulse-digital signal.

Hence, the neural network of retina carries out the numeric coding of the analog signal at the output from the photoreceptor with the help of a certain numbers of the impulses to the digital code. In this case the numbers of impulses generated by the ganglion neurons is proportional to the amplitude of the analog receptor potential, $n \sim U_{\max}$.

If we assume that the duration of the signal rise U_{in} (modulo) approximately $0.1\,s$ fig. 8.21, and the duration of the action potential of ganglion neuron is $1\,ms$ (the frequency of pulsation in the optic nerve comes up to 1000 pulses per second [68]) then to one receptor potential of photoreceptor the ganglion neuron generates a spike consisting of approximately 100 action potentials. In fig. 8.24*c* shows the conditional six impulses.

It is noteworthy that the signal $U_2 + \mathrm{PR}$ passage along branches of the horizontal neuron H, fig. 8.22. Some bipolar neurons B (comparators K) receive the signal of comparison $U_2 + \mathrm{PR}$ from DAC (interplexiform neurons I) not directly but through the body of horizontal neurons H [64], fig. 8.22 dotted line. This fact indicates the involvement of horizontal neurons H in work of the ADC of the retina or vice versa the involvement of the ADC in the work of horizontal neurons. There is mutual influence of the analog-to-digital conversion in the retina and the formation process of the visual image contrast. The involvement of interplexiform neurons in work of horizontal neurons also is noted in [64].

It is considered that horizontal neurons H participate in formation of the contrast vision. Taking into account low quality of the image on the eye retina the problem of representation of the information on contrast of border in total information directed in CNS is extremely important. There is formation of the contrast boundary in the area of sight carry out by submitting the brake signal from the horizontal neurons to bipolar neurons in case if the photoreceptors that are connected with these bipolar neurons provide a weak receptor potential. In this case beside located and strongly illuminated photoreceptors can generate the large receptor potential and the brake signal from the horizontal neurons doesn't send on the bipolar neurons connected with them.

It should be noted that the circuit of the neural network retina [64] is somewhat more complicated than that is shown in fig. 8.22. In particular the generator of clock frequency GCF as the amacrine cells A is duplicated apparently to give to ADC a greater reliability. There is a feedback of impulse branch of interplxsiform (DAC) and amacrine neurons (GCF) which is not shown in fig. 8.22 and fig. 8.23. Perhaps it is necessary to stop the pulsation of GCF by achieving equality $U_{in} = U_2 + \mathrm{PR}$, since otherwise by continuous work of GCF happen depletion of amacrine neurons. Perhaps this branch of interplexiform neuron provides more rigid circular connection of two duplicated amacrine neurons in the retinal neural network.

Encoding the analog signal at the output from a photoreceptor to the digital code apparently is the main function of the neural network of the retina. Retinal neurons perform well-defined functions: comparison of analog signals, the generation of clock frequency, digital-to-analog conversion, counting pulses. At the same time horizontal neurons in the retina carry out other important tasks such as staining of the visual image.

8.5.4. Color vision

The maximum of the light absorption by rhodopsin of the rods is on wave length $\lambda \approx 510\,nm$. The rods are intended for black-and-white, so-called achromatic vision. The visions created by rods have grey tone and differed only brightness. In other photoreceptors of the retina - cones instead of rhodppsin there are other proteins - iodopsin (photopsins) (Greek – violet, since iodopsin of cones absorbing red light has violet color).

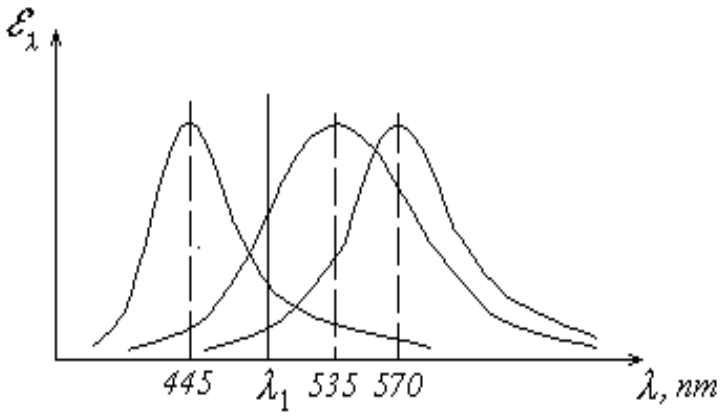

Fig. 8.25.

The cones provide the color vision. The normal human eye distinguishes up to 150 shades - color tones.

There are three cones types and accordingly iodopsins, at which various lengths of the maximums waves of the light absorption. The protein responsible for absorption of red light name also erythropsin, and green - chloropsin.

Maximums of the wave lengths of the light absorption by the iodopsins have the following sizes and colors corresponding to them:

1. 445 nanometers - blue-violet color,
2. 535 nanometers - green color,
3. 570 nanometers - red color.

On fig. 8.25 distributions of the light absorption for three various types iodopsins of cones are shown. On an axis of ordinates the spectral density of light flux absorption of the given wave length $\varepsilon_\lambda = \frac{\Delta\Phi}{\Delta\lambda}$ for three types of photoreceptors - cones is plotted. On the abscissa axis the wave length λ in nanometers is plotted.

For example, on length λ_1 all three kinds of cones are excitated but in different by numbers of the photoreceptors ratio - green is maximum, less blue-violet and even less red. Depending on it the frequency of the action potentials in the optic nerve fibres from various kinds of cones is formed. The action potentials in fibres of the optic nerve arisen owing to excitation various cones are summarized by neurons visual cortex of brain and the frequency of impulsation is analyzed. It determines the color of the observable surface.

The considered theory of the color vision has been offered by English scientist T. Young in 1802 and further is advanced by Helmholtz. Therefore it refers to as theory of Young - Helmholtz.

The sensation of color arises in CNS where signals from three types of cones are summarized. The important role in sensation of color is played also the signals going from rods especially at low illuminance of the subject.

The color sensation from the given monochromatic radiation can be received differently, summarizing light from three monochromatic light sources with various intensities. By mixing of three monochromatic radiations taken in the certain ratio it is possible to receive, for example, white light. The sensation of white light gives a solar spectrum. White light also can be received by addition of two colors (color tones) which in this case refer to as additional.

There are experimentally received curve additions describing sensitivity of the eye as a single whole to the mix of monochromatic radiations, fig. 8.26.

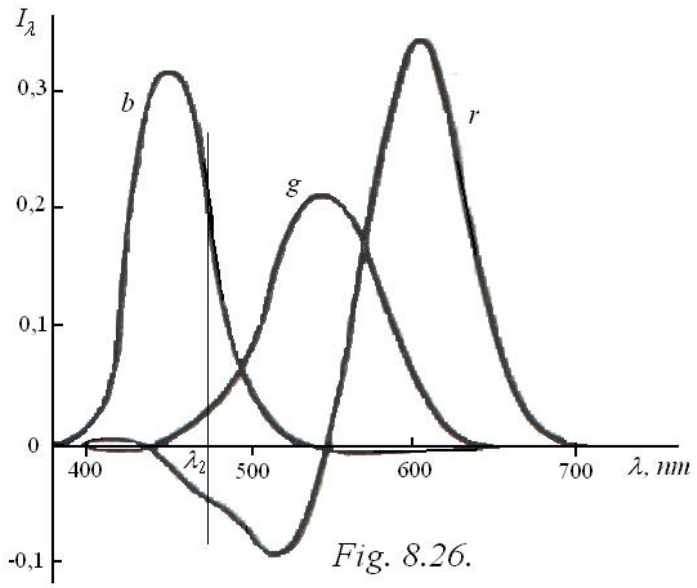

Fig. 8.26.

Essence of the curves it is the following. Standard basic colors are allocated so-called: red with the wave length $700\ nm$, green with the wave length $546.1\ nm$ and dark blue with the wave length $535.8\ nm$. On the axis of ordinates spectral intensity of the basic monochromatic radiations in relative units is plotted. On graphs it is designated b - distribution of blue color, g - green and r - red color. The graphs on fig. 8.26 show what it is necessary to take intensity of the basic colors to receive color sensation identical to the given monochromatic radiation with wave length λ.

Presence on the curves of negative sites pays attention. The negative site at distribution of the red color intensity is especially significant.

Negative sites specify what not for all monochromatic radiations it is possible to receive similar given on color sensation the mix of three basic colors. But if to the given monochromatic radiation, for example, in the wave length λ_2 to add basic red light with the intensity corresponding to the negative part of distribution of basic (red) radiation on coordinate λ_2, fig. 8.26, then the color sensation received from such total radiation always can be received addition of remaining two basic monochromatic radiations - blue and green with intensities corresponding to coordinate λ_2.

Comparison of the curves on fig. 8.25 and fig. 8.26 shows that the color sensation arising at addition of signals from various cones into CNS there is under a little bit other laws than an occurrence of color sensation at direct addition of the monochromatic radiations

Chapter 9. Mathematical genetics

Mathematical genetics is completely special section of biophysics. It enables to understand those or other phenomena in human organism, to explain and predict development of human community as from the point of view of the people health and social processes in community. It is allows to understand the purposes and problems of human community for improvement of the life.

The mathematical genetics is based on Hardy - Weinberg law which was found by English mathematician Hardy and German doctor Weinberg in 1908.

This law in the elementary kind of two alleles of a gene determines that relative frequencies of genotypes in generations correspond to terms of binomial expansion $(p+q)^2$, so $p+q=1$ where *p* and *q* there is alleles frequencies in a population or that is more correct in a family tree. Relative frequencies of genotypes remain constant from generation to generation in case of an ideal population (number of individuals is very large, there is pan-mixing, there is no selection, mutation, migration of individuals, etc.) [34].

The population will consist of set of family trees which periodically contact among themselves.

Allele is one of two or more alternative forms of one gene.

The exponent 2 specifies that two different-sex species are necessary for reception of posterity. At the human are the man and the woman.

Hardy - Weinberg law in genetics has the same fundamental role as, for example, the second Newton law in mechanics. But in the relation to world around of these two laws of genetics and mechanics there is an important distinction. The exponent 2 at the Hardy - Weinberg law reflects concrete conditions of life occurrence in the Earth. It is possible to assume that on other manned planets it exponent can have other value. If three different-sex species, for example, are necessary for reception of posterity at the Hardy - Weinberg law there should be the exponent 3. The second Newton law undoubtedly has the same kind everywhere in Universe.

9.1. Hardy - Weinberg equilibrium

Let's consider essence of the Hardy - Weinberg law.

At crossing opposite-sex individuals at the human the man and the woman in the following generation for autosomal genome (for genes not taking place in sexual chromosomes) frequency balance alleles - so-called Hardy - Weinberg equilibrium is established.

Under this law the genotypes *AA*, *Aa*, and *aa* have the following frequency relation:

$$(AA)\,p^2 : (Aa)\,2pq : (aa)\,q^2, \qquad (9.1)$$

where *p* there is the dominant frequency of allele *A*, *q* - the frequency of the recessive allele *a*, ($p+q=1$) so that:

$$(A)\,p : (a)\,q\,. \qquad (9.2)$$

Dominant alleles define the phenotype of individual, i.e. observable including in the laboratory way attributes, for example, color of eyes, hair, growth, types (groups) of blood, etc. In the ratio (9.1) is present three genotypes but two phenotypes: the first $AA+Aa$ and the second *aa*.

Ratios (9.1) and (9.2) remains unchanged from generation to generation only in the ideal population (number of individuals is very large, there is panmixing, there is no selection, mutation, migration of individuals, etc.) [69].

The Hardy-Weinberg balance is indifferent. For autosoming inheritance it is obvious. Really, using distribution of genotypes (9.1) it is possible to receive, for example, the frequency of recessive allele *a* in the following $(n+1)$ generation. For this purpose it is necessary the summation of the half frequency of heterozygotes *Aa* and frequency of the homozygotes *aa*:

$$q_{n+1} = \frac{1}{2}2p_nq_n + q_n^2 = q_n(p_n + q_n) = q_n\,. \qquad (9.3)$$

In the following generation the same frequency of allele *a* as in previous is received.

Infringement of the ratio (9.1) due to any external influences: mutagenesis, migrations, etc. are resulted only in change in the following generation of the genes frequency ratio (9.2) and to restoration of the ratio (9.1).

In reality, the impact on the population may be related to migration, the emergence of subpopulations, radiation exposure, etc. For a human population essential influence also can be the negative social phenomena connected to the destruction of classes, ethnic and public groups of the population.

Mechanical analogy of three possible types of balance: stable - 1, unstable - 2, indifferent - 3 it is shown on fig. 9.1.

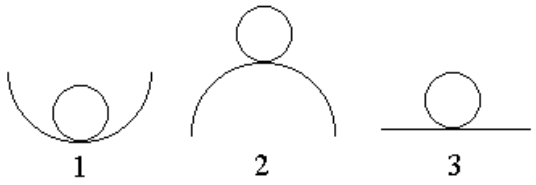

Fig. 9.1.

At influence on a population, for example, the mutagen factors the various natures the Hardy-Weinberg balance is restored, however the population does not compensate it influence there are change frequencies of alleles.

Indifferent character of the Hardy-Weinberg balance results to than the occurrence of the external influence leading to deterioration of the population quality by the population cannot be compensated even if this influence has stopped. Restore of the initial ratio of alleles is possible only due to their receipt from the outside (immigration from the other population).

9.2. Mutations

Extremely important topic of mathematical genetics there are mutations. The mutations explain genetically dependent hereditary diseases. Mutations allow explain process of evolution of organisms. Mutations underlie of animals and plants breeding.

There are allocated [70]:

- genomic mutations resulting in change of chromosomes number;
- chromosomal mutations at which the structure of chromosomes is broken;
- genic mutations which are not resulting in changes chromosomes but breaking normal sequence of the nucleotides in DNA molecule.

Mutations are spontaneous and induced.

During induced mutations there is interaction of the mutagen factor and individual exposed mutation.

Process of a mutation has stochastic character. The individuals under action of the mutagen factor with some probability can be subjected to mutations, and can not be subjected.

During a mutation the mutagen factor has the important role. It is possible classification mutagen factors into two groups: determined and stochastic.

The determined mutagen factors can be constant or functionally time-dependent.

There is pertinently to present the following mechanical analogy.

Let in a room there is an air ball - analogue of the mutagen factor. Molecules of air in the room play a role of the individuals. The model mutation is impact of molecule with the ball.

The probability of the mutation depends on a state of molecule in this case distances from the ball. With the ball can cooperate and the distant molecule, and the near molecule can depart from the ball during thermal movement not having hit on it.

But the probability of mutation depends and on behavior of the ball.

The ball can not change the volume - the constant mutagen factor.

It can increase at blow up and reduce at blow away the volume. The probability of mutations is changes. For example, at full blow away the ball probability of mutations to become equal to zero. The ball can periodically or aperiodically to change the volume. All these processes with the ball are model of the determined mutagen factors.

The ball also can change the volume in completely stochastic it is the model of stochastic mutagen factor.

Further we shall consider variants of genetic inheritance both at absence of action of the mutagen factor, and for mutagen factors of various types.

Let's start with the analysis ABO blood-grouping system at absence of action of the mutagen factor.

9.3. Genetic base of ABO blood-grouping system

For the first time blood transfusion from the man to the man has been carried out in England to 1819 by the professor of obstetrics and gynecology J. Blundell. But only in the beginning of XX century the Austrian pathologist K. Landsteiner has established that blood of people on biological properties can be divided into 4 groups - 4 phenotypes for what he has been awarded the Nobel Prize.

In the further analysis we shall follow German genetics to F. Bernstein who has made it in 1925 [70].

If blood of any group combined with blood of group incompatible for it there is a pasting (agglutination) of erythrocytes, their destruction.

Blood which can be transfused to all people is the group I (O).

Blood which is compatible with blood of IV group is the group II (A).

Blood which also is compatible with blood of IV group is the group III (B).

However with each other the groups of blood II and III are incompatible.

Blood which can be transfused only to people with same group of blood is the group IV (AB).

Groups of blood are inherited and do not vary during a life.

In table 9.1 the distribution of relative frequencies of the blood groups in Berlin is shown.

Table 9.1

Blood groups	O	A	B	AB
Frequencies	0.366	0.4323	0.1415	0.0601

Let there are equilibrium frequencies of genotypes *p*, *q*, and *r* for a locus with three alleles A, B and O so $p+q+r=1$.

Locus it is a site of the given gene on the genetic card of chromosome.

According to Hardy - Weinberg law distribution of the genotypes frequencies looks like similar to decomposition $(p+q+r)^2$:

$$p^2(\mathrm{AA})+q^2(\mathrm{BB})+r^2(\mathrm{OO})+2pq(\mathrm{AB})+2pr(\mathrm{AO})+2qr(\mathrm{BO}). \quad (9.4)$$

Hence, all there are 6 genotypes of blood.

Four phenotypes of blood result of alleles A and B domination above allele O.

In table 9.2 according to distribution (9.4) four classes of phenotypes with their frequencies following from the Hardy - Weinberg law are shown:

Table 9.2

Blood groups	I(O)	II(A)	III(B)	IV(AB)
Blood phenotypes	OO	AA+AO	BB+BO	AB
Phenotypes frequencies	$\overline{\mathrm{O}}=r^2$	$\overline{\mathrm{A}}=p^2+2pr$	$\overline{\mathrm{B}}=q^2+2qr$	$\overline{\mathrm{AB}}=2pq$

Designating frequencies of the blood phenotypes hyphens on top, we have:

$$\overline{\mathrm{O}}+\overline{\mathrm{A}}=(r+p)^2=(1-q)^2 \text{ and } \overline{\mathrm{O}}+\overline{\mathrm{B}}=(r+q)^2=(1-p)^2. \quad (9.5)$$

Hence, frequencies of genotypes are equal:

$$q=1-\sqrt{\overline{\mathrm{O}}+\overline{\mathrm{A}}},\quad p=1-\sqrt{\overline{\mathrm{O}}+\overline{\mathrm{B}}} \text{ and } r=\sqrt{\overline{\mathrm{O}}}. \quad (9.6)$$

Substituting in formulas (9.6) the frequencies of phenotypes from table 9.1, we find:

$$p=0.2876;\quad q=0.1065;\quad r=0.6050. \quad (9.7)$$

For control we summarize frequencies of alleles and it is received $p+q+r=0.9991$ that will very well be coordinated to expected size 1.

9.4. Action of the constant mutagen factor on the coupled with the *X*-chromosome genome

The intensive use of the mobile communication, insufficient protection against electromagnetic radiation of computers on a workplace result to that there is a constant mutagen electromagnetic background which is a source of the changes touching a genofund of a human population. Therefore is the interest to consider existence and development genome in conditions of influence of some constant mutagen factor.

At action of the constant mutagen factor there is probably occurrence of the selection resulting in change of genic frequencies in one direction [70].

9.4.1. Modeling action of the constant mutagen factor on the family tree

Let's consider action of the constant mutagen factor on two-alleles genome coupled with the *X*-chromosome. For this purpose we shall assume, that alleles *A* and *a* are coupled with the *X*-chromosome. The frequency of dominant alleles *A* we shall designate at men p_m and at women p_f. For recessive alleles *a* it is accordingly q_m and q_f.

At crossing in the first generation there is the ratio of genotypes of women according to product $(p_f + q_f)(p_m + q_m)$. Thus:

$$(AA)\, p_f p_m : (Aa)\,(p_m q_f + p_f q_m) : (aa)\, q_m q_f . \qquad (9.8)$$

Men have hemizygous on genes in the *X*-chromosome the frequency ratio determined by that the *X*-chromosome of the woman at crossing passes to the man's descendant:

$$(A)\, p_f : (a)\, q_f . \qquad (9.9)$$

Distribution (9.8) can be used also for the description of blood system ABO. In spite of the fact that to this system corresponds three-alleles ensemble of the genes the two alleles *A* and *B* are dominant and their general frequency can be designated at men p_m and at women p_f. Alleles O has in this case frequency at men q_m at women q_f. The ratio (9.8) for blood system ABO is not frequency distribution of genotypes of blood but the genotype frequency *aa* (or a genotype OO), and also phenotype frequency corresponding to a blood group I it the ratio reflects truly. For example, frequency of alleles O at men and women in Berlin is equal $q_f = q_m = 0.6057$, see (9.7).

The basic demonstration of existence *X*-coupled recessive inheritance for a blood system ABO consists that the destruction at disease of blood, for example, hemophilia are men and daughters phenotypic are healthy [70].

For the first time the mathematical genetics laws has applied Haldane to a problem of hemophilia on basis of Danforth idea about an equilibration of frequency of mutations and selection. Occurrence of hemophilia there is usually concern to spontaneous mutations. However formally meaning balance of mutations and selection, and also a constancy of occurrence of a family tree mutation (otherwise illness quickly would disappear) it is possible to calculate a task of the hemophilia assuming action of some equivalent constant mutagen factor. Action of selection will be appreciated further.

For a finding of recessive alleles *a* frequency in a new generation it is necessary to add frequency of homozygote *aa* and half of frequency of heterozygote *Aa* from a ratio (9.8). It is similarly necessary to act and for alleles *A*. Using this way of calculation of allele frequencies we find that change of alleles *a* frequency in generations of women equally:

$$q_{fn} = \frac{1}{2}[q_{f(n-1)} + q_{m(n-1)}]. \qquad (9.10)$$

Let's assume:

$$\frac{1}{b} q_{m(n-1)} = q_{f(n-2)}, \qquad (9.11)$$

where $b = \dfrac{q_{m(n-1)}}{q_{f(n-2)}}$ it is some constant factor which we shall name the constant mutagen factor. This factor specifies that alleles frequency *a* at the woman of the previous generation not in accuracy is equal to alleles frequency at the man of the following generation. Such situation develops if alleles frequency *a* in a female part of a population during to live before the reproductive period is reduced due to the arisen mutations resulting in impossibility to posterity. [70].

According to (9.11) the equation (9.10) becomes:

$$q_{fn} = \frac{1}{2}[q_{f(n-1)} + bq_{f(n-2)}]. \qquad (9.12)$$

For the solution of the equation (9.12) we shall search as $q_{fn} = a^n$ where *a* there is constant. Substituting this formula in (9.12), we shall find:

$$a^n = \frac{1}{2}[a^{n-1} + ba^{n-2}]. \qquad (9.13)$$

Having divided the both parts of the equation on a^{n-2}, we shall receive some characteristic equation:

$$a^2 - \frac{1}{2}a - \frac{b}{2} = 0, \qquad (9.14)$$

which solutions are two roots $a_1 = \frac{1}{4}(1+\mu)$ and $a_2 = \frac{1}{4}(1-\mu)$ where $\mu = \sqrt{1+8b}$ we shall name the reduced constant mutagen factor. At $b = 1$ or $\mu = 3$ the expression (9.12) describes genome equilibrium condition at absence mutagenesis.

Hence the general solution of the equation (9.12) looks like:

$$q_{fn} = C_1\left(\frac{1}{4}(1+\mu)\right)^n + C_2\left(\frac{1}{4}(1-\mu)\right)^n, \qquad (9.15)$$

where C_1 and C_2 there are constants. The solution (9.15) with account of initial conditions describes change of alleles *a* frequency at women in generations with account of the mutagen factor action.

Constants C_1 and C_2 we shall find proceeding from initial conditions: at $n = 0$, $q_{fn} = q_{f0}$ and at $n = 1$ according to (9.10) $q_{fn} = q_{f1} = \frac{q_{m0} + q_{f0}}{2}$.

We believe that in zero generation of men and women action of the mutagen factor is absent. Thus:

$$C_1 = \frac{2q_{m0} + (1+\mu)q_{f0}}{2\mu}, \; C_2 = -\frac{2q_{m0} + (1-\mu)q_{f0}}{2\mu}.$$

Substituting constants C_1 and C_2 in the formula (9.15), we receive the solution of the equation (9.12) as:

$$q_{fn} = \frac{1}{2\mu 4^n}\left(2q_{m0}\left((1+\mu)^n - (1-\mu)^n\right) + q_{f0}\left((1+\mu)^{n+1} - (1-\mu)^{n+1}\right)\right), \qquad (9.16)$$

where for the further transformations it is convenient to use the function of integer argument:

$$F(n) = \frac{(1+\mu)^n - (1-\mu)^n}{4^n}. \qquad (9.17)$$

In this case the formula (9.16) will be transformed to a kind:

$$q_{fn} = \frac{1}{\mu}\left(q_{m0}F(n) + 2q_{f0}F(n+1)\right). \qquad (9.18)$$

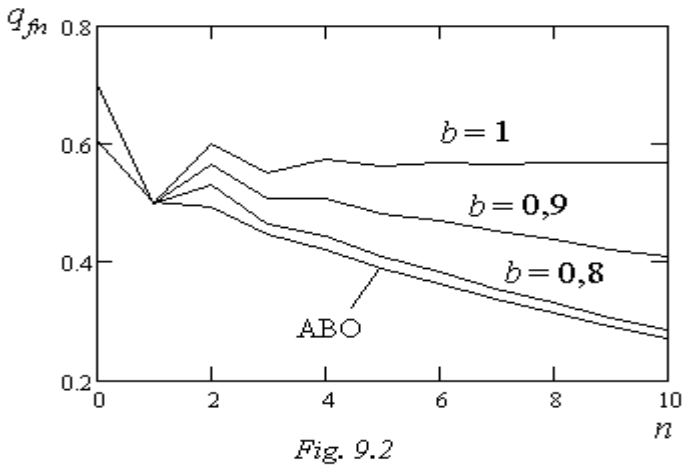

Fig. 9.2

If number of generations there is $n \to \infty$ then at $\frac{1 \pm \mu}{4} < 1$ a limit $\lim\left(\frac{1 \pm \mu}{4}\right)^n \to 0$ if *n* is integer. In this case frequency $q_{fn} \to 0$.

In fig. 9.2 the dependence plotted under the formula (9.18) of alleles *a* frequency at women from number of generation *n* at various values of the mutagen factor *b* is shown. Initial alleles *a* frequency at women was accepted $q_{f0} = 0.7$ at men $q_{m0} = 0.3$.

Curve ABO is plotted for frequency of blood alleles O at women and initial frequencies of it alleles $q_{f0} = q_{m0} = 0.6057$. At the hemophilia the equivalent constant mutagen factor for curve ABO was accepted equal $b = 0.8$.

In fig. 9.2 it is visible that at absence of the mutagen factor influence $b = 1$ the alleles *a* frequency at women gradually drawing near to equilibrium frequency $q_{f\infty} = \frac{q_{m0} + 2q_{f0}}{3} = 0.57$ that coincides with [71]. At occurrence of the mutagen factor there is a decrease in alleles *a* frequency and if all over again are observed jumps of frequency then there is a smooth decrease.

Let's find change of alleles *a* frequency in generation of women:

$$\Delta q_{f(n-1)} = q_{fn} - q_{f(n-1)} = \frac{1}{\mu}\left(\left(q_{m0} - 2q_{f0}\right)F(n) + 2q_{f0}F(n+1) - q_{m0}F(n-1)\right). \quad (9.19)$$

In fig. 9.3 the calculation of change of alleles *a* frequency used under the formula (9.19) is shown depending on generation of women *n* at various values of the mutagen factor *b*.

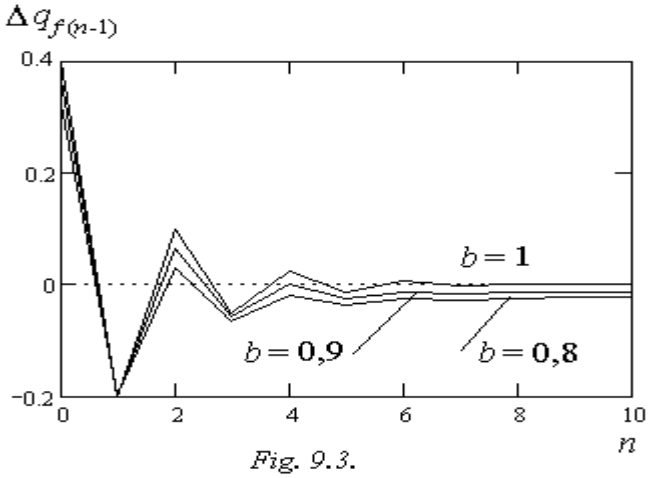

Fig. 9.3.

On fig. 9.3 size $\Delta q_{f(-1)}$ at $n=0$ has rated character. Really, due to action of the mutagen factor in the first generation there is a decrease in frequency of allele *a*, i.e. the curve is correct since $n=1$.

Apparently from fig. 9.3 the approach to equilibrium state of genome $\Delta q_{f(n-1)}=0$ is observed only at absence of the mutagen factor influence, i.e. at $b=1$. Otherwise there is a constant decrease in alleles *a* frequency in generations. And approximately to the seventh generation the constancy of such decrease is established: in 10-th generation at $b=0.9$ the size $\Delta q_{f(n-1)}=-0.014$, at $b=0.8$ the size $\Delta q_{f(n-1)}=-0.021$.

In fig. 9.4 the change of alleles blood O frequency is shown in generations of women at the equivalent constant mutagen factor $b=0.8$.

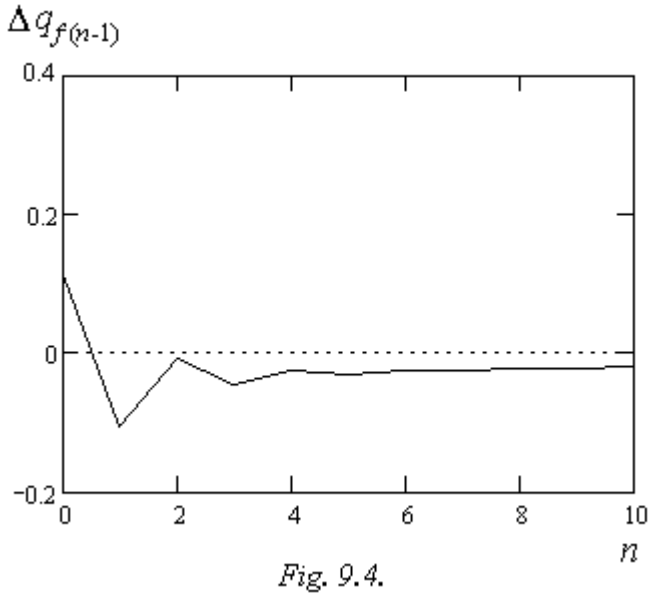

Fig. 9.4.

The mutagen factor acting on alleles O can result, for example, in hemophilia. In 10-th generation size is $\Delta q_{f(n-1)}=-0.02$. It specifies that there is a gradual reduction of healthy alleles O frequency at women and during too time increase at them destructive alleles O frequency.

According to the formula (9.18), fig. 9.2, at the second generation healthy the alleles O frequency at women to become equal $q_{f2}=0.492$. Hence, frequency destructive alleles has increased at them on size $0.6057-0.492=0.113$. Also increase frequency destructive alleles O at men of the third generation since it is transferred to the men. At men destructive alleles O phenotypic it can be shown as hemophilia.

In fig. 9.5 according to [70] the family tree of the European royal houses in which men frequently were ill hemophilia is shown. Distribution of the *X*-chromosome in a family tree is shown also. The circle leads round the *X*-chromosome having destructive alleles O which causes hemophilia. Black squares there are designate men which are sick of hemophilia. From this family tree the gradual increase in number of men which are sick of hemophilia is well visible. The shown family tree not full since on it is possible to conclude that in the third generation all men are sick of hemophilia. Actually it is far from being so. And now in the given royal dynasty the share of sick hemophilia men are not too great.

According to the submitted family tree in the first generation from four men one is sick of hemophilia, and in the second generation from seven men three are sick of hemophilia. Rough calculation of increase in frequency sick of hemophilia in a considered dynasty in the first and second generation at men has size $\frac{3}{7}-\frac{1}{4}=0.178$.

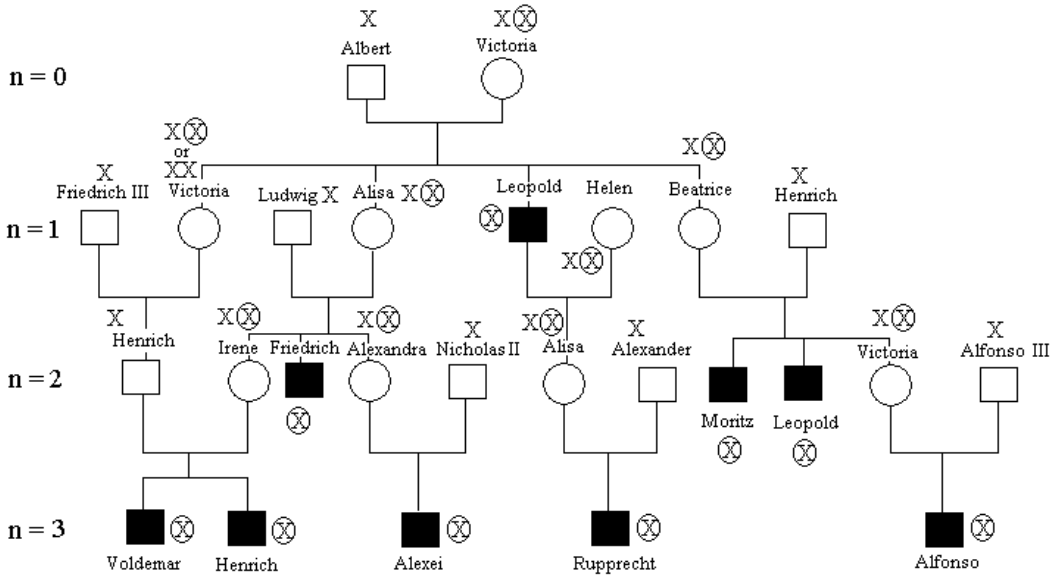

Fig. 9.5.

Corresponding reduction of a share of genotypic healthy women in the zero and first generation, counted up under the formula (9.19) is equal 0.106, see fig. 9.4. If should be more full family tree results apparently should be more close.

9.4.2. Connection between standard parameter of selection and the constant mutagen factor

In a family tree where the hemophilia is observed there is selection resulting in decrease of genic frequencies in particular of alleles O to one direction.

Action of selection there is intensive enough. For example, the life period of the men which are sick of hemophilia makes 1/3 from life period of healthy people [70]. Ability to leave offspring at men in comparison with healthy men is reduced. Therefore, not all men of a family tree take part in reception of offspring and destructive alleles O eliminate from a family tree. However is possible the balance of mutagenesis and selection resulting to preservation of Hardy - Weinberg equilibrium on some level, i.e. ratio of genotypes frequencies (9.4).

The balance at hemophilia mutagenesis and selection allows find connection between the equivalent constant mutagen factor *b* and standard parameter of selection *s* [70].

Let's consider selection against homozygotes *aa*. In [71] there is concrete example of such selection - the phenomenon of industrial melanism, i.e. change of painting of butterfly Biston betularia in industrial regions of England is resulted at the end of XIX century.

Genotypes before selection, for example, in generation $n-2$ are distributed according to (9.8).

We accept fitness of genotypes [70]:

$$1:1:(1-s), \qquad (9.20)$$

where *s* there is reduction of homozygotes fraction of recessive alleles as the result of selection (selection parameter).

Genotypes after selection we shall write down for the following generation $(n-1)$:

$$(AA)\,p_{f(n-1)}p_{m(n-1)}:(Aa)(p_{m(n-1)}q_{f(n-1)}+p_{f(n-1)}q_{m(n-1)}):$$
$$:(aa)\,q_{m(n-1)}q_{f(n-1)}(1-s) \qquad (9.21)$$

Taking into account, that

$$p_{f(n-1)}p_{m(n-1)} + (p_{m(n-1)}q_{f(n-1)} + p_{f(n-1)}q_{m(n-1)}) + q_{m(n-1)}q_{f(n-1)} = \\ = \left(p_{f(n-1)} + q_{f(n-1)}\right)\left(p_{m(n-1)} + q_{m(n-1)}\right) = 1 ,$$

we find the sum of frequencies of genotypes: $1 - q_{m(n-1)}q_{f(n-1)}s$.

Further, using a standard rule of a finding of alleles frequency in the following generation (half of heterozygotes frequency plus of homozygotes frequency) and the formula (9.21) we calculate the frequency of recessive alleles *a* at women in generation *n* it is similar [70] where such calculation is made for autosomal genome:

$$q_{fn} = \frac{\frac{1}{2}\left(p_{m(n-1)}q_{f(n-1)} + p_{f(n-1)}q_{m(n-1)}\right) + q_{m(n-1)}q_{f(n-1)}(1-s)}{1 - q_{m(n-1)}q_{f(n-1)}s} . \quad (9.22)$$

Let's transform the formula (9.22), using $p_{m(n-1)} = 1 - q_{m(n-1)}$ and $p_{f(n-1)} = 1 - q_{f(n-1)}$:

$$q_{fn} = \frac{\frac{1}{2}\left(q_{f(n-1)} + q_{m(n-1)}\right) - q_{m(n-1)}q_{f(n-1)}s}{1 - q_{m(n-1)}q_{f(n-1)}s} . \quad (9.23)$$

At selection all changes in a population occur due to size *s* therefore we believe that alleles *a* frequency at the men is equal to alleles *a* frequency at the woman of the previous generation $q_{m(n-1)} = q_{f(n-2)}$. Hence:

$$q_{fn} = \frac{\frac{1}{2}\left(q_{f(n-1)} + q_{f(n-2)}\right) - q_{f(n-2)}q_{f(n-1)}s}{1 - q_{f(n-2)}q_{f(n-1)}s} . \quad (9.24)$$

As it is underlined in [70] the equation (9.24) has no general solution even for autosomal genome. Especially it is not present for genome linked with the *X*-chromosome. It is essentially complicates the mathematical analysis of the equation (9.24). First of all does not allow is proved that the size *s* remains constant from generation to generation.

Mutagenesis and selection act in one direction. If arisen for the account mutagenesis destructive alleles will be eliminated from a family tree with the same speed due to selection the balance to be kept. A quantity of the destructive genes is kept in a family tree but this quantity will not increase.

We assume in process of mutagenesis in generation *n* at women the quantity of the destructive alleles O has increased in comparison with generation $(n-1)$. We assume generation *n* where the constancy $\Delta q_{f(n-1)}$ was already established, fig. 9.4. Frequency of destructive alleles has increased on $\Delta q_{f(n-1)} = q_{fn} - q_{f(n-1)}$. These alleles due to selection eliminate from a family tree. The balance of mutagenesis and selection will arise in case of equality of frequency q_{fn} in mutagenesis and selection since frequency $q_{f(n-1)}$ up to a mutation is supposed in both cases identical.

Taking into account balance mutagenesis and selection, we equate (9.12) and (9.24). After simple transformations we find:

$$b = 1 - q_{f(n-1)}\left(2 - q_{f(n-1)} - bq_{f(n-2)}\right)s = 1 - 2q_{f(n-1)}p_{fn}s . \quad (9.25)$$

In a case with hemophilia at the equivalent mutagen factor $b = 0.8$ and identical genic frequencies at men and the women equal 0.6057 standard parameter of selection designed under the formula (9.25) $s = 0.27$, and fitness of a genotype $1 - s = 0.73$. The estimation of fitness is enough challenge. One of possible ways to calculate fitness to find it is as the ratio of an average of survived children of the falling one parent which is sick of hemophilia to an average of survived children on one healthy parent. For example, in

[74] the opportunity of calculation is offered (though and with reserves) to fitness at hemophilia $1-s=1.75/2.5=0.7$.

Thus, the opportunity of the accuracy solution of the equation describing change of frequencies in generations with the help of the constant equivalent mutagen factor *b* as against use of the *s*-dependent equation (9.24) apparently specifies preferable of value *b*.

At the analysis of the accuracy solution of process of mutagenesis, for example, in a case with hemophilia, there is an opportunity of more reliable calculation of constant mutagen factor size if there are authentic data on a full family tree with destruct of corresponding allele.

9.5. Development of the genome in the radiation condition of the environment - determined mutagen factor

Emergencies on nuclear installations and result possible application of the nuclear weapon lead to that the raised radioactive background is a source of the mutations touching a genofund of a human population. Therefore is of interest to consider existence and development of the population in conditions of influence on it mutagen ionize radiation which gradually decreases according to the law of radioactive decay of the elements generating radioactive radiation. Thus, action on the population of the determined mutagen factor exponential decreasing in due time is examined.

Failures of the genetic apparatus arisen with it are generally incompatible with the normal functioning of the organism further. Mutations in genes in sex chromosomes can lead either to the disappearance of reproductive function in individuals or to the appearance in the offspring of serious failure.

We will analyze the existence of the population in the radiation environment, and mathematical modeling of changes in the genofund taking as the example changes in both sex-linked allele frequencies and inherited autosomally.

9.5.1. Action of radiation on the autosomal genome

Assume that during the impact on the family tree the frequencies of genotypes changed in the following proportions:

$$(AA)(p^2+Fpq+\alpha):(Aa)[2pq(1-F)+\beta]:\\ :(aa)(q^2+Fpq+\gamma), \quad (9.26)$$

that breaks the Hardy-Weinberg relation (9.1) (or taking into account to inbreeding - Wright). In (9.26) condition of panmixing is weakened. The opportunity of closely-related marriages with inbreeding coefficient *F* there are. This ratio characterizes the decrease in the proportion of individuals in heterozygote $(1-F)$ ones compared with panmixed population.

In the next generation the Hardy-Weinberg equilibrium is restored with the new correlation of allele frequencies. To obtain the dominant frequency of allele *A* in the new balance must sum up the frequency of homozygote *AA* and half the frequency of heterozygote *Aa* from (9.26). Similarly we will do and for the allele *a*. As a result, we obtain:

$$(A)(p+\alpha+\beta/2):(a)(q+\gamma+\beta/2). \quad (9.27)$$

Thus, the ratio of the frequencies of genotypes in the next generation is:

$$(AA)(p+\alpha+\beta/2)^2:(Aa)\,2\,(p+\alpha+\beta/2)(q+\gamma+\beta/2):\\ :(aa)(q+\gamma+\beta/2)^2. \quad (9.28)$$

Let's note that in (9.28) and (9.27) is not an inbreeding coefficient *F*.

In the absence of influences on the family tree, i.e. $\alpha=\beta=\gamma=0$ the ratio (9.28) is identical to (9.1), i.e. we have a well-known position to maintain the frequency of genotypes in a set of generations.

The question of the long gradually reduce of the radiation exposure in which the family tree evolves is of a great interest.

Let's consider a model situation when existence of family tree in the region it is only one element of the radioactive half-life *T*. A was established [70] that the frequency of mutations (usually lethal) is proportional to the power dose of radiation $p = k_1 P$, where k_1 is a constant. As the power dose of radiation is proportional to the activity of radioactive elements scattered in the environment it is possible to record the frequency of mutations using the fundamental of radioactive decay law as the ratio $p \sim \left(\frac{1}{2}\right)^{\left(\frac{t}{T}\right)n}$ where $t \sim 30$ years is the approximate time of one generation [70], *n* is number of the examined generation the existing in conditions of radiation.

As the law of action on the population has functional character the mutagen influence is determined, i.e. on the family tree the determined mutagen factor operates.

Accepting $R = \left(\frac{1}{2}\right)^{\left(\frac{t}{T}\right)}$ and considering the influence of radiation on recessive homozygote *aa* only, i.e. $p = \gamma + \beta / 2$, we obtain:

$$\gamma + \beta / 2 = (k / 2) R^n, \qquad (9.29)$$

where the coefficient 1/2 is taken for the convenience of further transformations. The coefficient *k* characterizes the initial activity of the radioactive elements that affect the family tree. In accordance with [17] $k \sim \frac{N_0}{T}$, where N_0 is the total initial quantity of the radioactive substance that acts on the family tree.

For example, there are recessive genes responsible for the content of catalase in the blood. One can cite as an example of reducing the frequency of recessive alleles of these genes at 15.5 ones for about two generations of people living in Hiroshima and Nagasaki in comparison with the general population of Japan. In this case, the frequency of dominant alleles has not changed [71].

Based on (9.27) the recursive formula for changing the frequency of allele *a* for the generations of the family tree is as follows:

$$q_n = q_{n-1} + \gamma + \beta / 2 = q_{n-1} + (k / 2) R^n, \qquad (9.30)$$

where $k < 0, R < 1$ (at $t = T, R = \frac{1}{2}$).

The solution of this equation is not difficult and it is the sum of a geometric progression:

$$q_n = q_0 + \frac{k}{2}\left(\frac{R(1 - R^n)}{1 - R}\right), \qquad (9.31)$$

where q_0 there is the frequency of allele *a* in the initial generation.

If the number of generations tends to infinity $n \to \infty$ the frequency of allele *a* tends to the value:

$$\hat{q} = q_0 + \frac{k}{2}\left(\frac{R}{1 - R}\right). \qquad (9.32)$$

The possibility of establishing equilibrium is determined by the condition $q_0 > \left|\frac{k}{2}\frac{R}{(1 - R)}\right|$. Taking $q_0 = 0$ we can solve equation (9.31) with respect to *n* a number of generations for which will complete elimination of the allele *a*. It reduces the variability of the population's genofund.

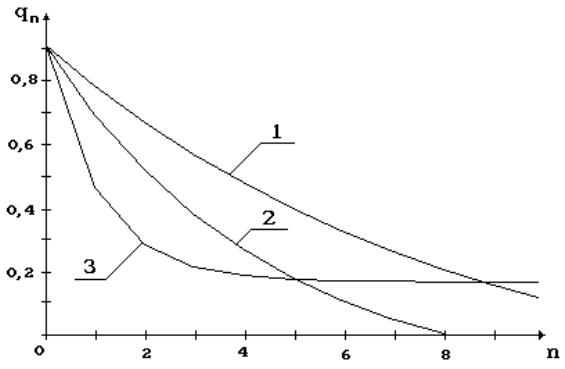

Fig. 9.6.

In fig. 9.6 is graph of the dependence frequency q_n of allele *a* on the number of generations *n*, plotted in accordance with the formula (9.31) for the half-life of radioactive elements in the region accordingly: curve 1 $T = 196$; curve 2 – 93.8 and curve 3 - 22.6 years. For example, half-life of widespread radioactive substances is such as Cs_{55}^{137} – 30.2 years, Sr_{38}^{90} – 28.7 years, and Co_{27}^{60} - 5.3 years [21]. But usually a half-life isotope is considerably smaller.

As can be seen from the graphs for the half-life 93.8 years the allele *a* will be disappears in the eighth generation. For the half-life $T = 22.6$ years after a fifth-generation set a new equilibrium frequency of allele *a* $\hat{q} = 0.17$. In the calculations there are for allele *a* used the initial frequency $q_0 = 0.9; \quad k = -\frac{50}{T}$.

The critical size of the half-life $T = 37.4$ years above which the Hardy-Weinberg equilibrium is not established as a result of complete elimination of the allele *a*.

In fig. 9.6 shows that for small half-life, curve 3, the frequency of alleles *a* at first drops very quickly because high activity radioactive elements. But then equilibrium is established because rapid decrease in the number of highly active substances reduces the effects of radiation. For long half-life the frequency of allele *a* decreases is more slowly but there are completely eliminates the allele at the affect of long radiation exposure, curves 1 and 2.

9.5.2. Action of radiation on genome linked to the X-chromosome

Let's suppose that *A* and *a* alleles and linked to the *X* chromosome. Distribution of genotypes at absence of influence of the mutagen factor corresponds at women (9.8) and at men (9.9). We assume as well as in a case of autosomal inheritance on the family tree the external mutagen factor changing the ratio of frequencies of genotypes at women:

$$\begin{aligned}&(AA)[p_f p_m + (p_m q_f + p_f q_m)F/2 + \alpha]: \\ &:(Aa)[(p_m q_f + p_f q_m)(1-F) + \beta]: \\ &:(aa)[q_m q_f + (p_m q_f + p_f q_m)F/2 + \gamma]\end{aligned} \quad . \qquad (9.33)$$

Assume also that the hemizygous state of men (9.9) is unaffected. Then, using the previous method of calculating allele frequencies, we can find that the change in frequency of alleles *a* generations of women is:

$$q_{fn} = \frac{1}{2}[q_{f(n-1)} + q_{m(n-1)}] + \gamma + \beta/2 . \qquad (9.34)$$

As in the case of autosomal inheritance the inbreeding coefficient of *F* in relation (9.34) is not included.

Take into account that the *X*-chromosome male inherits from his mother it is possible to record $q_{m(n-1)} = q_{f(n-2)}$.

As in the case of autosomal inheritance we consider the effects of ionizing radiation on the recessive homozygote *aa*.

According to (9.29) the equation (9.34) becomes:

$$q_{fn} = \frac{1}{2}[q_{f(n-1)} + q_{f(n-2)}] + (k/2)R^n. \qquad (9.35)$$

Solution of this equation is the sum of the general solution of the homogeneous equation (9.36) and a particular solution of inhomogeneous equation (9.35), [72]:

$$\tilde{q}_{fn} = \frac{1}{2}[\tilde{q}_{f(n-1)} + \tilde{q}_{f(n-2)}], \qquad (9.36)$$

so

$$q_{fn} = \tilde{q}_{fn} + q^*_{fn}. \qquad (9.37)$$

The general solution of homogeneous equation (9.36) $\tilde{q}_{fn}$ will be sought in the form $\tilde{q}_{fn} = a^n$. Substituting this expression into (9.36), we find:

$$a^n = \frac{1}{2}[a^{n-1} + a^{n-2}]. \qquad (9.38)$$

Dividing both sides by a^{n-2} we obtain a quadratic characteristic equation:

$$2a^2 - a - 1 = 0, \qquad (9.39)$$

the solution of which are the two roots $a_1 = 1; a_2 = -\frac{1}{2}$.

So, the general solution of (9.36) has the form:

$$\tilde{q}_{fn} = C_1 + C_2\left(-\frac{1}{2}\right)^n, \qquad (9.40)$$

where C_1 and C_2 there are constants. Solution (9.40) with the initial conditions describes the change of frequency allele *a* women in the generations in the absence of external mutagen factors on the family tree.

A particular solution of equation (9.35) will be sought in the form $q^*_{fn} = LR^n$, where *L* there is yet unknown. Substituting this formula into (9.35) we find:

$$2LR^n - LR^{n-1} - LR^{n-2} = kR^n. \qquad (9.41)$$

Dividing both sides by R^{n-2} we find the value of *L*:

$$L = \frac{kR^2}{2(R-1)(R+1/2)}. \qquad (9.42)$$

Thus, the solution of equation (9.35) in accordance with (9.37) is:

$$q_{fn} = C_1 + C_2\left(-\frac{1}{2}\right)^n + \frac{kR^{n+2}}{2(R-1)(R+1/2)}. \qquad (9.43)$$

Constants C_1 and C_2 we find the basis of the initial conditions at $n = 0, q_{fn} = q_{f0}$ and at $n = 1$ according to (9.34) and (9.29)

$$q_{fn} = q_{f1} = (q_{m0} + q_{f0})/2 + \gamma + \beta/2 = (q_{m0} + q_{f0})/2 + (k/2)R.$$

Consequently the solution of equation (9.35) is:

$$q_{fn} = \frac{2q_{f0} + q_{m0}}{3} - \frac{kR}{3(R-1)} + \left[\frac{q_{f0} - q_{m0}}{3} - \frac{kR}{6(R+1/2)}\right]\left(-\frac{1}{2}\right)^n + \frac{kR^{n+2}}{2(R-1)(R+1/2)}. \quad (9.44)$$

If the number of generations in women tends to infinity ($n \to \infty$) there is an equilibrium frequency of allele *a* (if it is possible):

$$\hat{q}_{fn} = \frac{2q_{f0} + q_{m0}}{3} - \frac{kR}{3(R-1)}. \quad (9.45)$$

Similarly to the case of autosomal inheritance at $q_{fn} = 0$ the number of generations which would completely eliminate allele *a* in women can be found.

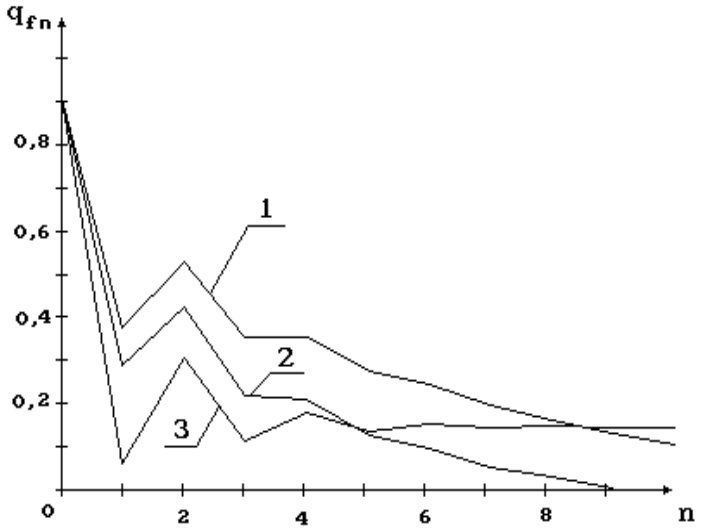

Fig. 9.7.

In fig. 9.7 is a graph of the dependence of the frequency q_{fn} of allele *a* in women and the number of generations *n* plotted by the formula (9.44) for the same half-life as for autosomal inheritance.

As can be seen from the graphs for the half-life $T = 93.8$ years - the allele *a* will be disappears in the ninth generation, the curve 2. For the half-life $T = 22.6$ years since the sixth generation the new equilibrium is established with the frequency of allele *a* in women $\hat{q}_{fn} = 0.14$, curve 3. Curve 1 is designed for the half-life of $T = 176$ years. At the calculations used the initial frequency of allele *a* women $q_{f0} = 0.9$; men $q_{m0} = 0.1$.

The critical size of the half-life above which the Hardy-Weinberg equilibrium is not established as the result of complete elimination of the allele *a* in the case of inheritance of genes linked to the *X* chromosome there is $T = 44.7$ years.

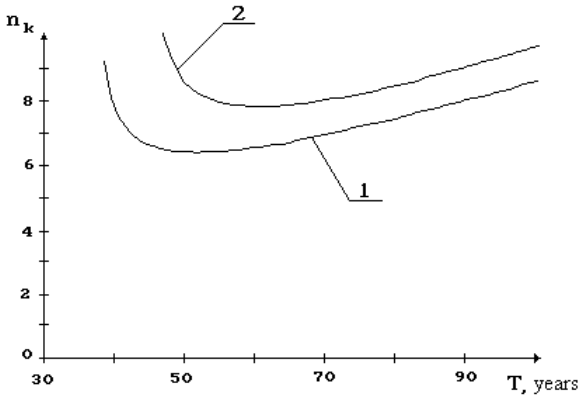

Fig. 9.8.

In fig. 9.8 is a graph of the number of generations n_k of the complete elimination of the allele *a*, and half-life of radioactive element *T* for autosomal genes - 1 and the genes of sex-linked - 2. The graphs are based on the solutions of equations (9.31) and (9.44) at initial conditions accordingly $q_n = 0$ and $q_{fn} = 0$. The graphs show that there are more dangerous radioactive elements to the population. For the given model calculation they are the the elements with half-life $T = 52.2$ years for autosomal genes and $T = 60.2$ years for genes linked to sex. In the first case of complete elimination of the allele *a* it will occur after $n_k \approx 6$ generations, and in the second case - after $n_k \approx 8$ generations. Thus, genes sex-linked are more resistant to radiation than autosomal.

As a result of the family tree analysis we can draw up the following conclusions which can be spread and to the population:

a) When there is the action of radiation on the population 2 outcomes are possible depending on the half-life of radioactive elements in the environment:

- Establishment of the Hardy-Weinberg equilibrium at maintaining the existing in the population genome but at a lower level of the targeted allele frequencies;
- The disappearance of the targeted allele, and consequently the impossibility of preserving the Hardy-Weinberg equilibrium.

b) There is a boundary size of the half-life of radioactive substances in the environment below which the population maintains its genome. Consequently, the outcome of the population depends on the nature of the radiation environment (disaster at nuclear power plants, nuclear explosion, accident at work, natural phenomenon, etc.).

c) Genes that are sex-linked have a somewhat higher resistance to radiation compared with autosomal.

g) Inbreeding does not affect the radiation resistance of the population.

The obtained results allow us to be more cautious at presence the choice to use of radioactive elements with specific half-lives which have a strong mutagenic effect on autosomal genes and genes linked to the *X* chromosome.

Considering in the evolutionary terms that genes linked to the *X*-chromosome have greater resistance we can recall that genes are located in the *X*-chromosome the mutations of which affect the vital functions of the human organism (vision, blood clotting, skin [73]). Therefore, these genes are phylogenetically were better protected against the action of mutagens such as radiation. Greater resistance to radiation of alleles which are localized in 23 pairs of chromosomes again suggests that the female organism is genetically more stable. It plays an important role in maintaining the size of the population.

The obtained results allow us to determine the radiation conditions of the maintaining of the balance of the Hardy-Weinberg in the population as well as conditions of complete elimination of the targeted allele by ionizing radiation.

The above method of analysis of the effects of radiation on the genome can be applied to other types of determined mutagen factors influences. Thus it is necessary only to replace the fundamental law of radioactive decay in (9.29) and (9.35) to another one for the investigated impact.

9.6. Action of the stochastic mutagen factor on the population

Among other kinds of diseases occurrence of malignant newgrowths has some features. First of all, it is the big variability of the site of newgrowths. It can practically arise in any place of an organism. Besides for oncological diseases typically a variety of the cancerigenic factors: poor-quality food, polluted environment, mode of life and professional work, smoking and many other factors.

All these cancerogenic factors finally affect on the mitogenetic function of a cell causing its malignant transformation.

Is generalized we shall consider that set of the reasons resulting to occurrence of the malignant newgrowths is the influence on the organism of some stochastic mutagen factor.

Despite of the stochastic character of influence it is difficult to present a situation at which the given stochastic mutagen factor completely would be absent. It concerns even completely isolated primitive societies. Especially such factor in any kind always is present at a modern civilized society.

As investigated model we shall consider homogeneous and stable in the demographic attitude a human society of very much advanced country with a high level of development of the medicine accessible to all population. In such countries death rate of the population basically should be caused by oncological diseases which start to play a role of the natural factor of inevitable alternation of generations. We shall name such countries demographic stationary

It is possible to assume also that in similar societies the genetic-mathematical laws determining death rate of the population from oncological diseases should operate, i.e. as a result of action of the stochastic mutagen factor.

9.6.1. Dynamics of genome at discrete alternation of generations

Before pass to studying action of the stochastic mutagen factor to the population we shall briefly repeat some mathematical questions of genetic inheritance in case of absence of action of any factor. This repeating we shall carry out from the following positions.

Using distribution of genotypes (9.8), we shall find frequency of allele *a* at women in the following $(n+1)$ generation:

$$q_{f(n+1)} = \frac{1}{2}(p_{mn}q_{fn} + p_{fn}q_{mn}) + q_{mn}q_{fn} =$$
$$= \frac{1}{2}\left[(1-q_{mn})q_{fn} + (1-q_{fn})q_{mn}\right] + q_{mn}q_{fn} = \frac{1}{2}\left[q_{fn} + q_{mn}\right]. \quad (9.46)$$

At the deduction (9.46) the following obvious formulas $p_{mn} = 1 - q_{mn}$ and $p_{fn} = 1 - q_{fn}$ are used. The formula (9.46) can be copied in the following kind:

$$q_{fn} - 2q_{f(n+1)} + q_{mn} = 0. \quad (9.47)$$

For convenience of the further analysis the formula (9.47) we shall write down with displacement on one generation back:

$$q_{f(n-1)} - 2q_{fn} + q_{m(n-1)} = 0. \quad (9.48)$$

At the absent of mutagen influence the frequency of allele *a* at men is equal to the frequency of this allele at women of the previous generation $q_{m(n-1)} = q_{f(n-2)}$. Using the given condition from (9.48) we shall find:

$$q_{f(n-1)} - 2q_{fn} + q_{f(n-2)} = 0. \quad (9.49)$$

The solution of the differencing equation (9.49) we search as $q_{fn} = a^n$ where in this case *a* is constant. Substituting this solution in the formula (9.49), we have:

$$a^{n-1} - 2a^n + a^{n-2} = 0. \quad (9.50)$$

Let's divide the equation (9.50) on a^{n-2}:

$$a - 2a^2 + 1 = 0. \quad (9.51)$$

We find two roots of the characteristic quadratic (9.51):

$a_1 = 1$ and $a_2 = -\frac{1}{2}$. (9.52)

Hence, the general solution of the differencing equation (9.49) looks like:

$$q_{fn} = C_1 + C_2\left(-\frac{1}{2}\right)^n. \quad (9.53)$$

Constants of integration C_1 also C_2 we shall find on the basis of the initial conditions: at $n = 0$, $q_{fn} = q_{f0}$ and at $n = 1$ according to (9.46) $q_{fn} = q_{f1} = \frac{q_{m0} + q_{f0}}{2}$. Thus:

$$C_1 = \frac{2q_{f0} + q_{m0}}{3} \text{ and } C_2 = \frac{q_{f0} - q_{m0}}{3}. \quad (9.54)$$

Therefore the solution (9.53) finally looks like:

$$q_{fn} = \frac{2q_{f0} + q_{m0}}{3} + \left(\frac{q_{f0} - q_{m0}}{3}\right)\left(-\frac{1}{2}\right)^n. \quad (9.55)$$

9.6.2. Populating dynamics of genome at continuous alternation of generations

The Hardy-Weinberg law in the kind considered above there is concerns to a separate family tree. Implicitly this law includes time since alternation of generations occurs through certain time. Average time of the life of one generation $T = 25 - 30\ years$. Thus, Hardy-Weinberg law has the expressed discrete character on time. The population will consist of family trees crossed among themselves and lives in continuous time. Alternation of generations of set of family trees results to the generations vary actually according to continuous time scale.

Let's transit to the continuous time scale *n*. Under size $n = \frac{t}{T}$ in this case we mean time of the population life normalized on average in the population time of the one generation life, i.e. actually dimensionless time.

Let's find out, whether there is the differential equation having the characteristic equation similar (9.51). For this purpose we shall consider the differential equation:

$$\frac{d^2 q_{f(n-1)}}{dn^2} + \eta\frac{dq_{f(n-1)}}{dn} = 0, \quad (9.56)$$

where η is a constant.

Let's transform the equation (9.56) to finite - difference form:

$$\frac{q_{fn} - 2q_{f(n-1)} + q_{f(n-2)}}{\Delta n^2} + \eta\frac{q_{f(n-1)} - q_{f(n-2)}}{\Delta n} = 0. \quad (9.57)$$

Uniting similar members and multiplying the equation (9.57) on -2 we shall find:

$$-2q_{fn} + 2(2 - \eta\Delta n)q_{f(n-1)} - 2(1 - \eta\Delta n)q_{f(n-2)} = 0. \quad (9.58)$$

Let's try to identify the difference's equations (9.58) and (9.49). For this purpose it is necessary to accept:

$$2(2 - \eta\Delta n) = 1 \text{ and } -2(1 - \eta\Delta n) = 1 \quad (9.59)$$

Wonderful feature of the equations (9.59) is that they have one and too the solution:

$$\eta\Delta n = \frac{3}{2}. \quad (9.60)$$

It's means that the difference's equation (9.49) and the differential equation (9.56) can have the same characteristic equation. Taking into account (9.60) the equation (9.56) can be copied as:

$$\frac{d^2 q_{f(n-1)}}{dn^2} + \frac{3}{2\Delta n}\frac{dq_{f(n-1)}}{dn} = 0 . \qquad (9.61)$$

The equation (9.61) can be integrated once:

$$\frac{dq_{f(n-1)}}{dn} + \frac{3}{2\Delta n} q_{f(n-1)} = C_1 . \qquad (9.62)$$

where C_1 is a constant of integration.

Further integrating the equation (9.62) by method of separation of variables:

$$\int_{q_{f0}}^{q_{fn}} \frac{dq_{f(n-1)}}{C_1 - \frac{3}{2\Delta n} q_{f(n-1)}} = \int_0^n dn , \qquad (9.63)$$

we shall find:

$$q_{fn} = \frac{2\Delta n}{3} C_1 - \left(\frac{2\Delta n}{3} C_1 - q_{f0} \right) e^{-\frac{3}{2\Delta n} n} . \qquad (9.64)$$

Identifying the solution (9.64) with the solution (9.55), we shall find:

$$\frac{2q_{f0} + q_{m0}}{3} = \frac{2\Delta n}{3} C_1 \quad \text{and} \quad \frac{q_{f0} - q_{m0}}{3} = -\left(\frac{2\Delta n}{3} C_1 - q_{f0} \right). \qquad (9.65)$$

As it was expected the formulas (9.65) do not contradict each other. Hence, the solution (9.64) can be written down as:

$$q_{fn} = \frac{2q_{f0} + q_{m0}}{3} + \left(\frac{q_{f0} - q_{m0}}{3} \right) e^{-\frac{3}{2\Delta n} n} . \qquad (9.66)$$

The formula (9.66) is correct for frequency of allele only in even generations. This is consequence of transition to the continuous scale of generations *n*.

Comparing (9.55) and (9.66) for even generations we have $2^{-n} = e^{-\frac{3}{2\Delta n} n}$ or $\Delta n = \frac{3}{2\ln 2}$. Hence, (9.66) it will be transformed to a kind:

$$q_{fn} = \frac{2q_{f0} + q_{m0}}{3} + \left(\frac{q_{f0} - q_{m0}}{3} \right) e^{-n \ln 2} , \qquad (9.67)$$

that is identical to the formula (9.55) at even generations.

Taking into account (9.60) and $\Delta n = \frac{3}{2\ln 2}$ we find $\eta = \ln 2$. Thus, the differential equation (9.61) will be written down as:

$$\frac{d^2 q_{f(n-1)}}{dn^2} + \ln 2 \frac{dq_{f(n-1)}}{dn} = 0 . \qquad (9.68)$$

As we used the continuous time the concept of generations actually does not play any role and the formula (9.68) it is possible to write down as:

$$\frac{d^2 q_f}{dn^2} + \ln 2 \frac{dq_f}{dn} = 0 . \qquad (9.69)$$

The formula (9.69) it is Hardy-Weinberg law in case of continuous alternation of generations, i.e. for the continuous time scale. The equation (9.69) defines the time dependence of recessive allele *a* frequency $q_f(n)$ linked with the *X*-chromosome for women in the population.

The differential equation (9.69) as it is determined by the Hardy-Weinberg law reflects indifferent balance of genome, see paragraph 9.1. Really, to the equation (9.69) satisfies the solution $q_f = const$, i.e. any constant value of allele frequency it is stable.

Let's note the important feature of the found form of the Hardy-Weinberg law.

In this law completely there are no reasons of alternation of generations, the reason of the termination of ability to live of the previous generation at occurrence of new generation. It results to that the population numerically indefinitely increases that contradicts the basic biological laws. Thus, there should be a way of correction of the Hardy-Weinberg law with the purpose of more correct description it of the population existence.

9.6.3. Modeling the stochastic mutagen factor

Let's consider existence of a population which the stochastic mutagen factor influences.

The formula (9.69) it is equation of the indifferent equilibrium of genome linked with sex in case of continuous alternation of generations, i.e. for the continuous time scale.

That of it to be convinced we will address to other well investigated physical phenomenon – the Brownian motion [75]. Brownian motion of a particle in a liquid at first sight should not exist. Really, on Brownian particle, for example, flower pollen impacts the molecules of the liquid which operation are counterbalanced from different directions. Therefore, the most probable state of a particle is motionless. The particle should shiver only but should not have some constant displacement from a point of supervision. Einstein and Smoluchowski have shown that physically the Brownian motion is consequence of statistical properties of the second law of thermodynamics. If the researcher has relative small number of the molecules the essential deviation from the most probable state of system should be observed in this case the motionless state of the Brownian particles.

Let's note the main similarity of two phenomena: the Brownian motion and existence of the population in conditions of the stochastic mutagen factor action.

At the Brownian motion on the determined system - particle in the liquid – stochastic force acts from the molecules of a liquid.

In the researched case on the determined system - reproductive genome – some stochastic mutagen factor acts.

At the Brownian motion the equation of movement of the particle looks like:

$$m\frac{d^2S}{dt^2} + r\frac{dS}{dt} = F, \qquad (9.70)$$

where m there is mass of particle, S - displacement of the particle from initial position, r - factor of resistance of medium to movement of the particle, t - time, F - stochastic force acting on a particle from the molecules of the liquid. We shall note absence in the equation (9.70) elastic forces which is determined returned the particle in initial position causing its oscillation around of the balance point.

The equation (9.70) is the equation to which at absence of stochastic function F complies with a solving $S = const.$ I.e. at $F = 0$ the particle can steadily be in any position - indifferent balance. The equation (9.69) is similar to the equation (9.70) at $F = 0$.

If there is some stochastic mutagen factor $D(n)$ randomly time-dependent lives of the population (in conditions of the continuous scale of alternation of the generations) the equation (9.69) by analogy with (9.70) it is necessary to copy as:

$$\frac{d^2q_f}{dn^2} + \ln 2\frac{dq_f}{dn} = D(n). \qquad (9.71)$$

Using the result for the first time received by Einstein [75] for the Brownian motion $\left\langle (\Delta S)^2 \right\rangle \sim t$, we shall note that an average square of a deviation of the allele frequency from norm (9.67) at action on the population of the stochastic mutagen factor proportionally time of the population life $\left\langle (\Delta q_f)^2 \right\rangle \sim n$. Angular brackets are mean averaging on individuals of the population.

Thus, during life of the population at action of the stochastic mutagen factor the mean square deviation of the allele frequency from norm proportionally to a root square from time of the population life

$\sqrt{\left\langle \left(\Delta q_f\right)^2 \right\rangle} \sim \sqrt{n}$. At the certain level of the mean square deviation of the allele frequency from norm can lead to a lethal outcome. For separate individual the lethal deviation is individually.

The received result shows that during of the population life and alternation of generations at action of the stochastic mutagen factor the death rate inevitably grows (similarly to displacement of the Brownian particles from a point of initial supervision). This conclusion has completely general biology-mathematical character also is consequence of the second law of thermodynamics, i.e. consequence of inevitable growth of entropy in the population.

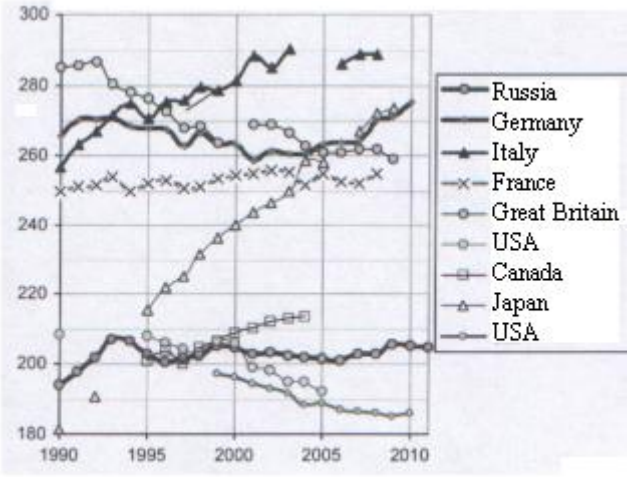

Fig. 9.9.

On fig 9.9 the dynamics death rates (mortality rate coefficient) of the population in the various countries from newgrowths is shown [76]. A mortality rate coefficient this ratio of quantity of died people in the country for the year to an average number of population in the given year multiplied on 1000.

Time interval of 20 years during which death rate was investigated is small term but it is possible to make some conclusions.

In two countries Japans and Canada the law: death rate $\sim \sqrt{n}$ is obviously observed. Distinctive feature of these countries is, first, very high level of medicine second, high uniformity of the population which is almost without exception uses these achievements of medicine. Some other social factors determining as whole a positive psychological climate in these countries influence also. In other words, the situation with detection at the earliest stage and treatment of the newgrowths in these countries has approached to the stationary limit on the given level of development of the country. The not changes in this direction therefore the law - death rate $\sim \sqrt{n}$ therefore is carried out. The further decrease in death rate will take place at occurrence and universal application of essentially new methods of diagnostics and treatment of a cancer that in these countries apparently inevitably. The similar development of a medical science demanding the big financial expenses and intellectual efforts is counteracting against growth entropy in the population.

In the given countries death rate from newgrowths is the basic natural factor of alternation of generations.

For other countries, first, the big heterogeneity of the population, second, high immigration of the population which gradually joins modern medicine that conducts or to decrease in the general death rate from newgrowths (USA, Great Britain), or to its invariance (Germany, Russia, France) is characteristic. Let's note that dynamics of death rate instead of its absolute value is analyzed. As a whole it is possible to speak about the general demographic non stationary in these countries.

The attention an example of Italy for which the law - death rate $\sim \sqrt{n}$ is carried out with periodic fluctuations. Apparently, it is connected by that Italy is basically the transit state for immigrants. However arising due to change of rules the delay of immigrants in the country results in fluctuations of the death rate on a background of the law of death rate $\sim \sqrt{n}$.

In conclusion of the analysis we shall note that occurrence newgrowths occurs at people of old age. Average life expectancy, for example, in Russia is much less than in other countries of Europe and in Japan. The fraction of older humans also is less. Therefore and death rate from newgrowths in Russia is less than in other countries of Europe and Japan, fig. 9.9. It is known that death rate in Russia basically consequence of diseases

of cardiovascular system thus, alternation of generations occurs basically not due to natural, and due to social factors.

Thus, for the description of a population it is necessary to use Hardy-Weinberg law written down for a continuous scale of alternation of generations.

During of the population life at action of the stochastic mutagen factor root mean square deviation of allele frequency from norm proportionally to a root square from time of the population life.

At action of the stochastic mutagen factors resulting in occurrence of the newgrowths death rate of the population in the country is proportional to a root square time of the population life only at demographic stationary, i.e. in case uniformity of the population and the high level of development of medicine accessible to all population. In such countries death rate from oncological diseases has role of the natural factor of alternation of generations.

Demographic non stationary, first of all connected to immigration results or in decrease in death rate of the population from the newgrowths or to its invariance.

9.7. Action of the constant mutagen factor on population

In the paragraph 9.4 action of the constant mutagen factor on of the family tree genome has been considered. Besides it has been marked that spontaneous mutagenesis at balance of mutations and selection (in particular at hemophilia) it is possible to present as action of the equivalent constant mutagen factor.

In the present paragraph we will analyze action of the constant mutagen factor (mobile communication, radiation of office equipment, etc.) on the human population.

The analysis we shall make on the basis of Hardy - Weinberg law written down as formula (9.69):

$$\frac{d^2 q_f}{dn^2} + \ln 2 \frac{dq_f}{dn} = \alpha, \qquad (9.72)$$

where the value α there is characterizes some constant mutagen factor.

The equation (9.72) can be integrated once:

$$\frac{dq_f}{dn} + \ln 2 q_f = \alpha n + C_3, \qquad (9.73)$$

where C_3 there is constant of integration.

The equation (9.73) is integrated in quadratures. The general solution looks like:

$$q_f = \frac{\alpha n}{\ln 2} - \frac{\alpha}{(\ln 2)^2} + \frac{C_3}{\ln 2} + C_4 e^{-n \ln 2}, \qquad (9.74)$$

where C_4 there is constant of integration.

In connection with that the basic results for genetic research of hemophilia have been earlier received at use of discrete alternation generations principle at the given analysis stage, for use of the previous researchers results, it is convenient to return to the discrete scale of generations.

Change of alleles *a* frequency for one generation is equal:

$$\Delta q_{f(n-1)} = q_{fn} - q_{f(n-1)} = \frac{\alpha(n+1)}{\ln 2} - \frac{\alpha}{(\ln 2)^2} + \frac{C_3}{\ln 2} + C_4 e^{-(n+1)\ln 2} -$$

$$-\left(\frac{\alpha n}{\ln 2} - \frac{\alpha}{(\ln 2)^2} + \frac{C_3}{\ln 2} + C_4 e^{-n \ln 2} \right) = \frac{\alpha}{\ln 2} - \frac{1}{2} C_4 e^{-n \ln 2} \qquad (9.75)$$

At increase in number of generations (or time) $n \to \infty$ the change of alleles frequency $\Delta q_{f\infty} = \frac{\alpha}{\ln 2}$

.

Let's address now to the analysis of decrease of alleles blood O frequency at there is hemophilia. As it was specified earlier a spontaneous mutation at hemophilia it is possible to present as action of some constant equivalent mutagen factor in this case α.

Frequency of the mutations at hemophilia in different countries (into the population) changes from $4.4 \cdot 10^{-5}$ (Switzerland) up to $6.4 \cdot 10^{-5}$ (Denmark), i.e. the gene of hemophilia have from 44 up to 64

women on one million [70]. The frequency of the mutations it is ratio of number of cases of anomaly display to the double number of the examined individuals the corrected sizes of frequencies of mutations therefore are used (multiplied on 2).

Let at $n \to \infty$ the size is $\Delta q_{f\infty} \approx -6 \cdot 10^{-5}$. I.e. 60 girls which birth on one million have the gene of hemophilia. In this case the equivalent constant mutagen factor $\alpha = \Delta q_{f\infty} \ln 2 \approx -4.16 \cdot 10^{-5}$.

The uncertain size in dynamics of change of alleles frequencies (9.75) is the constant C_4. According to (9.75) we shall find the law of decrease in genic frequency:

$$q_{fn} = q_{f(n-1)} + \frac{\alpha}{\ln 2} - \frac{1}{2} C_2 e^{-n \ln 2}. \qquad (9.76)$$

We use the initial condition: for $n = 1$ according to (9.10) $q_{fn} = q_{f1} = \frac{q_{m0} + q_{f0}}{2}$.

Hence:

$$q_{f1} = q_{f0} + \frac{\alpha}{\ln 2} - \frac{1}{4} C_4 = \frac{q_{m0} + q_{f0}}{2}. \qquad (9.77)$$

From (9.77) we find constant C_4:

$$C_4 = 2\left(q_{f0} - q_{m0}\right) + \frac{4\alpha}{\ln 2}. \qquad (9.78)$$

Substituting (9.78) in (9.75), we shall find:

$$\Delta q_{f(n-1)} = \frac{\alpha}{\ln 2} - \left(\left(q_{f0} - q_{m0}\right) + \frac{2\alpha}{\ln 2} \right) e^{-n \ln 2}. \qquad (9.79)$$

Believing as well as in case of the family tree (paragraph 9.4.1) $q_{f0} = q_{m0}$ we shall receive:

$$\Delta q_{f(n-1)} = \frac{\alpha}{\ln 2}\left(1 - 2e^{-n \ln 2}\right) = \frac{\alpha}{\ln 2}\left(1 - 2^{-(n-1)}\right). \qquad (9.80)$$

At $n = 0$ we find initial change of alleles O frequency which is equal $\Delta q_{f(-1)} = -\frac{\alpha}{\ln 2}$. Taking into account $\alpha \approx -4.16 \cdot 10^{-5}$ we find $\Delta q_{f(-1)} \approx 6 \cdot 10^{-5}$. We shall note as in case in family tree that the value $\Delta q_{f(-1)}$ has rated character. Change of genic frequency is real at mutagenesis begins from time coordinate $n = 1$ at which according to (9.80) is $\Delta q_{f(n-1)} = \Delta q_{f(0)} = 0$. It concerns to fig. 9.10 and fig. 9.11.

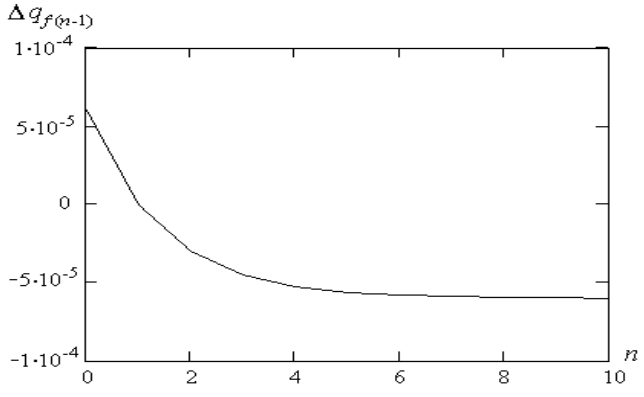

Fig. 9.10.

On fig. 9.10 the dependence of change of genic alleles O frequency $\Delta q_{f(n-1)}$ at women on the time of the population life plotted under the formula (9.80) is shown.

Comparison about fig. 9.4 for change of genic alleles O frequency (under condition of the equivalent constant mutagen factor action) plotted for the separate family tree shows that as a whole dependences are similar. Smoothness of the curve on fig. 9.10 is defined by continuity of the scale of generations alternation or dimensionless time for the population as against discrete time of the separate family tree.

The analysis fig. 9.10 allows to assume that under action of the equivalent constant mutagen factor α acting on the population there is average on individuals of the population the mutation (practically constant after $n > 8$) resulting in average on the population to continuous reduction of healthy alleles O frequency at women and during too time to increase at them of destructive alleles O frequency i.e. to the hemophilia.

The law of decrease in frequency of blood alleles O at mutations (9.74) with the account (9.78) also $q_{f0} = q_{m0}$ can be written down as:

$$q_f = \frac{\alpha n}{\ln 2} - \frac{\alpha}{(\ln 2)^2} + \frac{C_3}{\ln 2} + \frac{4\alpha}{\ln 2} e^{-n \ln 2}. \qquad (9.81)$$

Using the initial condition: for $n = 0$, $q_f = q_{f0}$ we shall find:

$$C_3 = q_{f0} \ln 2 + \frac{\alpha}{\ln 2} - 4\alpha. \qquad (9.82)$$

With the account (9.82) the formula (9.81) we shall write down as:

$$q_f = q_{f0} + \frac{\alpha n}{\ln 2} - \frac{4\alpha}{\ln 2}\left(1 - e^{-n \ln 2}\right). \qquad (9.83)$$

On fig. 9.11 (curve 1, the left scale of the ordinates axis) the graph of dependence of decrease in allele blood O frequency q_f is shown on dimensionless time *n* of the population life at hemophilia, plotted under the formula (9.83) for initial allele frequency $q_{f0} = r = 0.605$ see (9.7).

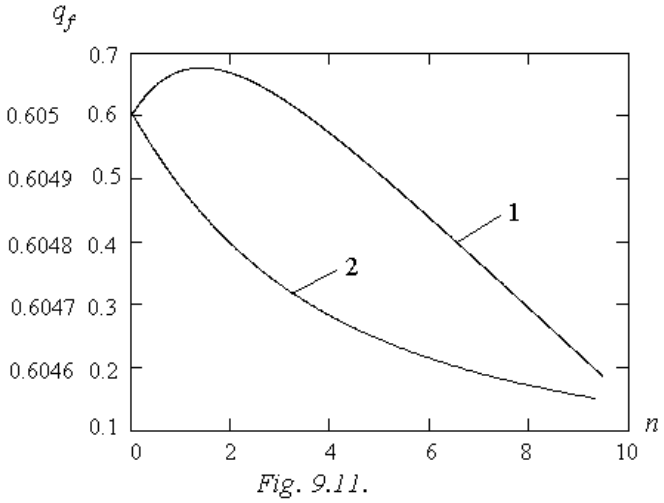

Fig. 9.11.

9.7.1. Action of selection on population

For the analysis of the selection action on the population, with the purpose of the previous researches use, we shall return to the separate family tree. In the family tree where the hemophilia is observed the selection resulting in decrease of genic frequencies in particular of allele blood O operates.

Action of selection is intensive enough. For example, the life duration of the men who are were ill with hemophilia makes 1/3 from the life duration of healthy people [70], male fertility i.e. chances to have posterity in comparison with healthy men is reduced. Therefore not all men of the given family tree participate in reception of posterity and damaged alleles O eliminated from the family tree.

Let's consider selection against homozygotes *aa* (or OO).

Genotypes before selection, for example, in generation $n-2$ are distributed according to (9.8).

We accept fitnesses of genotypes [70]:

$$1:1:(1-s), \qquad (9.84)$$

where *s* there is reduction of the homozygotes fraction of recessive allele as a result of selection (parameter of selection).

For the further analysis we use the formula (9.24).

$$q_{fn} = \frac{\frac{1}{2}\left(q_{f(n-1)} + q_{f(n-2)}\right) - q_{f(n-2)}q_{f(n-1)}s}{1 - q_{f(n-2)}q_{f(n-1)}s}. \qquad (9.85)$$

Mutagenesis and selection operate in one direction. If arisen for the account mutagenesis the damaged alleles will be with the same velocity due to selection eliminated from a family tree the balance to be kept. A quantity of the damaged genes is kept in the family tree but this quantity will not increase.

The change of allele *a* frequency in a family tree using (9.85) it is possible to calculate under the formula:

$$\Delta q_{f(n-1)} = q_{fn} - q_{f(n-1)} =$$

$$= \frac{\frac{1}{2}\left(q_{f(n-1)} + q_{f(n-2)}\right) - q_{f(n-2)}q_{f(n-1)}s}{1 - q_{f(n-2)}q_{f(n-1)}s} - q_{f(n-1)} = \qquad . \qquad (9.86)$$

$$= \frac{\frac{1}{2}\left(-q_{f(n-1)} + q_{f(n-2)}\right) - q_{f(n-2)}q_{f(n-1)}s + q_{f(n-2)}q_{f(n-1)}^2 s}{1 - q_{f(n-2)}q_{f(n-1)}s}$$

At transition to the continuous time scale we believe difference in genic frequencies of two generations following one after another infinitesimal, i.e. $q_{f(n-2)} \approx q_{f(n-1)}$. Hence, the formula (9.86) will be transformed to a kind similar autosomal genome [70]:

$$\Delta q_{f(n-1)} = -\frac{q_{f(n-1)}^2 s\left(1 - q_{f(n-1)}\right)}{1 - q_{f(n-1)}^2 s}. \qquad (9.87)$$

For transition from the family tree to the population we shall take the method offered in [70] for calculation of allele *a* frequency at the big number of generations. We shall copy (9.87) as:

$$\frac{dq_f}{dn} = -\frac{q_f^2 s\left(1 - q_f\right)}{1 - q_f^2 s}. \qquad (9.88)$$

Number of generation in the index of allele frequency for the population we do not write, *n* it is dimensionless time. We shall integrate (9.88):

$$\int_{q_{f0}}^{q_f} \frac{dq_f}{q_f^2 s\left(1 - q_f\right)} - \int_{q_{f0}}^{q_f} \frac{dq_f}{\left(1 - q_f\right)} = -\int_0^n dn. \qquad (9.89)$$

The first integral in the left part (9.89) is found in [70]. Using this result, we receive:

$$\frac{q_{f0} - q_f}{q_{f0}q_f} + \ln \frac{q_{f0}}{q_f}\left(\frac{1 - q_f}{1 - q_{f0}}\right)^{1-s} = sn. \qquad (9.90)$$

For the blood system ABO as before initial allele *a* frequency we shall accept $q_{f0} = 0.605$ see (9.7).

The estimation of fitness $(1-s)$ is enough challenge. As it was specified earlier (see paragraph 9.4.2) one of possible ways to calculate fitness to find it is as the ratio of an average of survived children of the falling one parent which is sick of hemophilia to an average of survived children on one healthy parent. For example, in

[74] fitness calculated thus it is at hemophilia equal $1-s=1.75/2.5=0.7$. But further, proceeding from some supervision, the most comprehensible needs size $1-s=0.29$. For calculation we use size of parameter of selection $s=0.71$.

On fig. 9.11 (curve 2, the right scale of the ordinates axis) the graph of dependence of decrease in blood allele O frequency q_f is shown on dimensionless time *n* at the selection, plotted under the formula (9.90).

Decrease in blood alleles O frequency occurs for the account of the mutants alleles elimination. This process is rather intensive at least it much more intensively mutational process at hemophilia, fig. 9.11 (curve 1, the left scale of the ordinates axis). Thereof concerning Haldane and Danforth ideas some words are necessary to tell about the balance of frequencies of mutations and selection at hemophilia.

Such equilibration is hardly feasible. Physiologically, it is two different processes. The law of occurrence of mutations (9.83) is absolutely not similar to the law of the alleles elimination in population at selection (9.90). But actually equilibrations also it is not necessary. It is necessary only that velocity of mutations occurrence did not exceed the velocity of selection.

Thus, at the first record of the Hardy-Weinberg law the methodical mistake has been admitted connected by that this law was applied to the analysis of a population in the form correct to the family tree, for example (9.1), (9.4) or (9.8). For the analysis of population it is necessary to use continuous time scale and the mathematical section of the differential equations, in particular formulas (9.69), (9.71) or (9.72).

Exception of the given methodical mistake allows to expand the numbers of the problems solved with the help of the Hardy-Weinberg law in particular in the demographic problem it permit to clear genetic-mathematical laws of generations alternation in the countries with a high level of medicine development and the homogeneous population also more clearly to understand the interrelation of mutagenesis and selection, for example, for hemophilia.

Conclusion

In terms of Human Biophysics, you may have raised several questions apparently have collected to give better solution about that. After reading this book you can get your answers.

Firstly, what purpose of the monograph? The human biophysics is closely connected to medicine with treatment of people which ensure their productive longevity. Therefore anyone even small steps in understanding of the human organism functioning will always be cause the maximal interest in people. Finally, first of all, to the person in this world the person is interesting and important.

The purpose of the monograph is the aspiration of the author to induce the reader if the doctor shows great interest to the further independent study about any sections of the book, to cause in the reader desire to penetrate more deeply in this or that phenomenon in the organism, to make the opinion on recommended methods of patients treatment. But even if the reader not the doctor the author hopes for more confident quiet understanding and the attitude of the reader to problems in his organism.

Secondly, why in the monograph there are no, for example, the biophysical sections connected with the respiratory system, kidneys, skeletal system, etc? Where the researches devoted to problems of olfactory sense, touch, thermal reception and many other things? Eventually, where the biophysical questions concerning to the brain? The following is possible to answer it. Biophysics is extremely big science. If to state bases of all questions touched by this science the multivolume composition will appear. Such work to the author is not feasible, therefore he was limited to those questions into which on a sort of the scientific and teaching activity penetrated in detail enough that the questions mentioned in the monograph were interesting to the reader.

Thirdly, where the guarantee of what the concept of the author on this or that question is correct? Validity of this or that law, for example, in physics always is checked experimentally. Anyone, even very beautiful hypothesis should receive experimental acknowledgement before to begin the theory. Though there is necessary to note that recently in physics this principle is sometimes broken.

In biophysics and especially in human biophysics the experimental acknowledgement of the theory frequently happens inconveniently for the various reasons. Therefore the statement of theoretical bases of process in biophysics has independent value. Such statement enables to plan experiment, to understand any supervision, to estimate an opportunity of this or that development of the organism. Plausible theoretical research shows at what level of understanding now there is the functioning this or that organs. This implies, first of all, a necessary level of doctors training, qualifying requirements to them.

It is obvious that books on biophysics do not live for a long time. Development of science goes faster rates. Any concepts are rejected any on the contrary prove to be true. It would be desirable to hope that the given monograph will bring in some contribution to the further development of sciences about the human body.

References

[1] Gennis R.B. “Biomembranes. Molecular Structure and Function.” New York, Berlin, Heidelberg, Tokyo, Springer-Verlag, 1989. 624 p.

[2] Vladimirov Yu.A., Roschupkin D.I., Potapenko A.J., Deev A.I. “Biophysics.” Moscow, Medicine, 1983. 272 p.

[3] Volobuev A.N. “Bases of Medical and Biological Physics.” Manual for students, post-graduate, and doctors. Moscow, Samara Printing House, 2011. 672 p.

[4]. Lehninger A.L. “Biochemistry. Molecular Basis of Cell Structure and Function.” New York, Worth Publishers, Inc., 1972. 958 p.

[5] Musil J., Novakova O., Kunz K. “Biochemistry in Schematic Perspective.” Prague, Avicenum Czechoslovak Medical Press, 1980. 216 p.

[6] Jackson M.B. “Molecular and Cellular Biophysics.” University of Wisconsin Medical School, Cambridge University Press, 2006. 551 p.

[7] Khodorov B.I. “Problem of excitability.” Leningrad, Medicine, 1969. 304 p.

[8] Rubin A.B. “Biophysics.” Volumes 1, 2. Moscow, Higher School, 1987. 624 p.

[9] Hodgkin A.L., Huxley A.F. “A quantitative description of membrane current and its application of conduction and excitation in nerve.” (1952) J. Physiol., **117**, 500-544.

[10] Wolkenstein M.V. “Biophysics.” St. Petersburg, Moscow, Lan, 2008. 608 p.

[11] Wikswo J.P., Branch J.P., Freeman J.A. “Magnetic field of a nerve impulse: First Measurements.” (1980) Science, **208**, 4, 53–55.

[12] Cole K.S., Baker R.F. “Longitudinal impedance of the squid giant axon.” (1941) J. Gen. Phisiol, **24**, 771–788.

[13] Beresovsky V.A., Kholotilov N.N. “Biophysical Characteristics of Tissue of the Man.” Kiev, Naukova Dumka, 1990. 77 p.

[14] Buchachenko A.L., Sagdeev R.Z., Salikhov K.M. “Magnetic and spin effects in chemical reactions.” Novosibirsk, Science, 1978. 296 p

[15] Samojlov V.O. “Medical biophysics.” St. Petersburg, 2004. Speclit, 496 p.

[16] Geletuk V.I., Khasachenko V.N. “Cluster organization of ionic channels.” Moscow, Science, 1990, 224 p.

[17] Yaworsky B.M., Detlaf A.A. “Handbook on Physics.” Moscow, Science, 1990. 624 p.

[18] Volobuev A.N., Ovchinnikov E.L., Trufanov L.A., Pirogov V.P., Koshev V.I. “Influence of the magnetic field on the effective module of elasticity of vascular wall.” Bulletin AMS USSR (1987), 12, 50–54.

[19] Zhukov B.N., Trufanov L.A., Volobuev A.N., Ovchinnikov E.L., Kostenkov A.G. “Mechanisms of biotropic effect of constant magnetic field.” (1987) Electromagnetic therapy in traumas and diseases of the support-motor apparatus. International collection. The Riga medical institute, Riga, 28–33.

[20] Hubel D., Stevens C., Kandel E. “The Brain.” Scientific American, Inc., 1979. 280 p.

[21] Kostuk P.G., Grodzinsky D.M., et al “Biophysics.” Kiev, Higher School, 1988. 504 p.

[22] Hille B. “The permeability of the sodium channel to metal cations in myelinated nerves.” (1982) J. Gen. Physiol., **59**, 637-658.

[23] Lev A.A. “Ionic selectivity of cellular membranes.” Leningrad, Science, 1975, 178 p.

[24] Davidov A.S. “Quantum mechanics.” Moscow, Fizmatgiz, 1963. 748 p.

[25] Levich V.G., Vdovin Yu.A. Mjamlin V.A. “Course of theoretical physics.” Volume 1, 2. Moscow, Fizmatgiz, 1962, 1516 p.

[26] Kamke E. “Differentialgleichungen losungsmethoden und losungen.” Verbesserte auflage, Leipzig, 1959. 576 p.

[27] Stepanov V.M. “Molecular Biology. Structure and functions of albumens.” Moscow, Higher School, 1996. 336 p.

[28] Thomas Y. “Biophysique des solutions. Problemes et exercices resolus.” Breal, 1992. 208 p.

[29] Hodgkin A. “Nervous impulse.” Moscow, World, 1965, 128 p.

[30] Kuznetsov D.S. “Special functions.” Moscow, Higher School, 1965. 424 c.

[31] Purcell E.M. “Electricity and Magnetism.” Berkeley Physics Course, McGraw-Hill Book Co. 1965. 416 p.

[32] Tikhonov A.N., Samarsky A.A. “Equations of mathematical physics.” Moscow, Science, 1972, 736 p.

[33] Dwight H.B. “Tables of Integrals and Other Mathematical Data.” New York, The MacMillan Co. 1961. 228 p.

[34] Libbert E. “Kompendium der allgemeinen biologie.” VEB Gustav Fisher Verlag, Jena. 1982. 440 p.

[35] Hill A.V. “Mechanics of muscular reduction: old and new experiments.” Moscow, World, 1972. 183 p.

[36] Deshcherevsky V.I. “Mathematical models of muscular contraction.” Moscow, Science, 1977. 160 p.

[37] Lilly L.S. “Pathophysiology of heart disease.” Lippincott Williams & Wilkins. Philadelphia, New York, London. 1998. 598 p.)
[38] Magnus K. “Schwingungen.” Durchgesehene auflage, B.G. Teubner Verlagsgesellschaft, Stuttgart. 1976. 228 p.
[39] Zuzenkov M.V. “ Bases of practical electrocardiography.” Minsk, Higher School, 1998. 314 p.
[40] Rashmer R.F. “Dynamics of cardio-vascular system.” Moscow, Medicine, 1981. 600 p.
[41] Ivanitsky G.R., Krinsky V.I., Selkov E.E. “Mathematical biophysics of cells.” Moscow, Science, 1978. 310 p.
[42] Krinsky V.I., Medvinsky A.B., Panfilov A.V. “Evolution of autowaves curls.” Moscow, Knowledge, 1986. 48 p.
[43] Davidov V.A., Zikov V.S. “Spiral autowaves in the round excitable medium.” (1993) JETP, **103**, 3, 844–855.
[44] Fedorova V.N., Stepanova L.A. “Short Course of Medical and Biological Physics.” Moscow, Fizmatlit, 2005. 624 p.
[45] Ponomarenko G.N. “Electromagnetotherapy and light therapy.” St. Petersburg, World and family-95, 1995. 250 p.
[46] Kostukov N.S., Lukichev A.A., Muminov M.I. “ε and $\tan\beta$ at irradiation.” Moscow, Science, 2002. 328 p.
[47] Petrov I.R. “Influence of MW - radiations on human and animals organisms.” Leningrad, Medicine, 1970. 332 p.
[48] Dodd R.K., Eilbeck J.C., Gibbon J.D., et al. “Solitons and Nonlinear Wave Equations.” Academic Press, Inc. London, 1984. 694 p.
[49] Matveev A.N. “Electricity and magnetism.” Moscow, World & Education, 2005. 464 p.
[50] Vinogradova M.B., Pudenko O.V., Sukhorukhov A.P. “Wave theory.” Moscow, Science, 1079. 384 p.
[51] Landau L.D., Lifschits E.M. “Hydrodynamics.” Moscow, Science, 1986. 736 p.
[52] Grawford F.S. “Waves.” Berkeley Physics Course, McGraw-Hill Book Co. 1974. 528 p.
[53] Remizov A.N. “Medical and Biological Physics.” Moscow, Higher School, 1996. 608 p.
[54] Landau L.D., Lifschits E.M. “Electrodynamics of continuous mediums.” Moscow, Fizmatlit, 2003. 652 p.
[55] Hippel A.R. “Dielectrics and Waves.” Moscow, Leningrad, Publishers of the Foreign Literature, 1960. 438 p
[56] Ginetsky A.G., Lebedinsky A.V. “Bases of Human physiology and Animals.” Moscow, Medgiz, 1947. 642 p.
[57] Shmidt R., Tevs G. “Physiology
of man.” Volume 1, Moscow, World, 2005. 323 p.
[58] Bikov K.M., Vladimirov G.E., Konradi G.P., et al. “Textbook of physiology.” Moscow, Medgiz, 1955. 610 p.
[59] Berkinblit M.B., Glagoleva E.G. “Electricity in alive organisms.” Moscow, Science, 1988. 288 p.
[60] Berezina M.P. Vasilevskaja I.E., Averbakh M.S., et al “Big practicum on human physiology and animals.” Moscow, Higher School, 1961. 675 p.
[61] Volobuev A.N., Koshev V.I., Petrov E.S. Biophysical Principles of Hemodynamics. New York: Nova Science Publishers, Inc. 2010. 216 p.
[62] Lojtsansky L.G. “Mechanics of fluid and gas.” Moscow, Drofa, 2003. 840 p.
[63] Begun P.I., Shukejlo Y.A. “Biomechanics.” St. Petersburg, Politekhnika, 2000. 464 p.
[64] Kamkin A., G., Kamensky A.A. “Fundamental and clinical physiology.” Moscow, Publishing center “Academy”, 2004. 1072 p.
[65] Guyton A.C., Hall J.E. “Textbook of Medical Physiology.” New York, Elsevier Inc. 2006. 1296 p.
[66] Prjanishnikov V.A. “Electronics.” St. Petersburg, Crown-century, 2009. 416 p.
[67] Hubel D.H. “Eye, Brain and Vision.” New York, Scientific American Library a division of HPHLP, 1988. 240 p.
[68] Kositsky G.I. “Human physiology.” Moscow, Medicine, 1985. 560 p.
[69] Gunther E., Kampfe L., Penzin H., et al. “Bases of general biology.” Moscow, World, 1982. 438 p.
[70] Vogel F., Motulsky A. “Human genetics.” Volumes 1, 2, 3, Springer-Verlag, Berlin, 1990. 1068 p.
[71] Ayala F., Kiger, J. Jr. “Modern genetics.” Volume 3, The Benjamin/Cummings Publishing Company, Inc. California, 1984. 335 p.
[72] Godunov S.K., Rjabenky V.S. “Differences scheme.” Moscow, Science, 1977. 440 p.
[73] Kozlova S.I., Semenova E.T., Demikova N.S. “Hereditary syndromes and medical-genetic consultation.” Leningrad, Medicine, 1987. 320 p.

[74] Li, C.C. “First Course in Population Genetics.” The Boxwood Press Pacific Grove, California, 1976. 556 p.

[75] Matveev A.N. “Molecular physics.” Moscow, Higher School, 1981. 400 p.
[76] Kalabekov I.G. “Russian Reforms in Digits and Facts.” Moscow, RUSAKI, 2010, 498 p.
[77] Volobuev A.N., Neganov V.A., Zajtsev V.V. “Physical and mathematical nature of the nervous pulse.” (1998) Physics of wave processes and radio engineering systems, **1**, 2-3, 108-110.
[78] Fadeev L.D. “Mathematical Physics. Encyclopedia.” Moscow, Big Russian encyclopedia, 1998. 691 p.
[79] Bogolubov N.N., Shirkov D.V. “Quantum Fields.” Moscow, Fizmatlit, 2005. 384 p.
[80] Volobuev A.N. “Basis of Nonsymmetrical Hydromechanics.” New York, Nova Science Publishers, Inc., 2012. 198 p.
[81] Carola R., Harley J.P., Noback C.R. “Human Anatomy & Physiology.” New York, McGraw-Hill Publishing Company, 1990. 925 p.